The paradox of the plankton:

Investigating the effect of inter-species competition of phytoplankton and its sensitivity to nutrient supply and external forcing.

Thesis submitted in accordance with the requirements of

the University of Liverpool for the degree of Doctor of Philosophy

by

Katarzyna M. Kenitz

December 2014

School of Environmental Sciences, The University of Liverpool

Liverpool, UK

Abstract

"The paradox of the plankton: Investigating the effect of inter-species competition of phytoplankton and its sensitivity to nutrient supply and external forcing."

Katarzyna M. Kenitz

Hutchinson (1961) first posed the paradox of the plankton: Why do so many phytoplankton species coexist while competing for a limited number of resources? High biodiversity has been explained in terms of the phytoplankton system not reaching an equilibrium state. Spatial and temporal variability can be achieved through externally imposed physical variability or internally-induced behaviour including periodic oscillations or irregular, chaotic behaviour. The research presented in this thesis investigates whether the non-equilibrium, chaotic response of the phytoplankton community is a likely outcome within the aquatic ecosystems. The thesis addresses the extent that chaotic behaviour remains a robust response with externally-imposed environmental variability.

The sparsity of long-term time-series data and infrequent sampling inhibits the ability to verify whether marine ecosystems exhibit complex behaviour. The analysis of the time-series records of phytoplankton taxa in the English Channel suggests that chaos might occur within diatom and dinoflagellates abundance time series. However, simulations using a chemostat model for phytoplankton and nutrients suggests that time series sampled every 1-2 days for more than 5 years are required to confidently distinguish deterministic chaos from noise.

The model simulations suggest that the community response depends on the phytoplankton requirement for nutrients and attributed physiological traits allowing each species to be a stronger competitor for a different resource. A wider inter-species specialization increases the likelihood of oscillatory and chaotic responses, with competitive exclusion decreasing from 50% to 20% of the cases. Higher departures from the Redfield ratio in the elemental composition of species favour complex community behaviour and act to increase biodiversity.

Whether chaotic response can be sustained is sensitive to the strength of the diffusive feedback between nutrient supply and ambient nutrient concentration that acts to sustain steady-state nutrient concentrations. Including seasonal and stochastic variability in the nutrient supply reveals that the frequency of chaotic dynamics increases by 20% and 45% respectively. In addition, seasonal forcing leads to temporal variability in the strength of the chaotic response, with chaos becoming more prevalent in the summer.

In contrast to a well-mixed, homogeneous environment, physical dispersal can stir different phytoplankton communities together, which might act to inhibit chaos, but at the same time enhance phytoplankton diversity. Idealised model simulations are conducted to mimic the small and large scale transport processes by including 2 or 3 well-mixed boxes. Locally generated chaotic response is sustained if: 1) there is a low rate of exchange with a strong nutrient competitor that maintains the contrasts in the community structure; 2) a strong competitor is inhibited by a high mortality rate. In addition, if the local community is outcompeted, chaos can be exported through the advection of stronger competitors that exhibit chaotic fluctuations.

This study highlights the importance of understanding the interactions between ambient nutrients and phytoplankton community. The variability in the nutrient supply and connectivity between ecosystems shape the community response to inter-species competition. Complex behaviour arising from inter-species competition is suggested to have a significant contribution in driving biodiversity. Future research on assessing the extent of chaos requires extending and analysing the available time-series data obtained from stable or isolated marine provinces.

Contents

List of Tables

List of Figures

Acknowledgements

First, I would like to acknowledge the patience, guidance and support I have received from my supervisors, Ric and Jonathan. Thank you both for for being such amazing mentors, you have always provided me with thorough advice and our numerous scientific debates posed new and exciting challenges that I have always enjoyed (no matter how taxing!). You have inspired me and kept me focussed whenever I got lost in the detail and needed to be reminded of the wider perspectives. Also, I want to thank you for your assistance and feedback when putting this research thesis together, and I do apologize for all the missing 'a's and 'the's that you had to insert. Ric, I will forever appreciate the effort you put into my development as a young researcher, and time you would always find to give me advice despite your often jam-packed schedule. You have created opportunities for me that not every PhD student is lucky to have, from helping in organising a symposium to developing my networking skills, taking part in writing a REF impact case or a research proposal. I am more thankful than I can write in this!

I am very grateful to Andrew Barton of Duke University for providing time-series data analysed in this thesis, and numerous scientific discussions that have led to new and interesting research ideas. I would also like to acknowledge Vadim Biktashev of the University of Exeter (previously University of Liverpool) for providing me with a better mathematical understanding of complex dynamics and methods for their analysis, and Vassil Roussenov and Alan McCormack of the University of Liverpool for their assistance and help during my first steps with programming in FORTRAN.

I would like to thank my work colleagues who became my great friends, Charlotte, Clare B., Clare D., Nick and Nuala (alphabetical!) and all the other amazing PhD students whose names I cannot list due to the limited space. We have created an amazing PhD support network, celebrating each other's accomplishments as well as sharing an occasional moan and getting one another out of the odd 'PhD trough'.

I am extremely grateful to my loving family, who with their enthusiasm and pride for my successful progress, motivated me to continue with my career aspirations despite having to live at a fair distance away.

And finally, Tom Bailey you have been the greatest support of all - your light-hearted nature and unfaltering humor has always kept my spirits up. Thank you for always making me laugh so hard, those outdated jokes of yours will never become boring. I appreciate your support and patience more than you think. You have been my rock in the stormy sea of the Ocean Science PhD!

Declaration

This thesis is an account of research undertaken between October 2010 and July 2014 at the School of Environmental Sciences, University of Liverpool, Liverpool, United Kingdom. Except where acknowledged in the customary manner, the material presented in this thesis is, to the best of my knowledge, original and has not been submitted in whole or part for a degree in any other university.

Katarzyna M. Kenitz
July 2014

CHAPTER 1

Introduction

1.1 Research motivation: the role of phytoplankton

Marine phytoplankton play a crucial role in the global production of oxygen, contributing 50% of global primary production (Field et al., 1998) with a net primary production of 45-50 Gt C $year^{-1}$ (Longhurst et al., 1995). Primary producers are fundamental components of the oceanic biological pump that is responsible for cycling of the organic matter produced by phytoplankton. Phytoplankton assimilate dissolved inorganic carbon, which acts to lower the partial pressure of CO_2 in the surface waters and facilitates further uptake from the atmopshere. A portion of the carbon fixed into phytoplankton biomass is then exported to the ocean interior at the final stage of phytoplankton life cycle, which contributes to the sequestration of the atmospheric CO_2 (Raven and Falkowski, 1999; Marinov et al., 2006).

Phytoplankton communities display a great diversity, with coexisting species differing in size and physiology that control nutrient requirements and utilization mechanisms. They play a key role in the carbon and energy transfer to the higher trophic levels (Mar-

tin et al., 2006; Dickman et al., 2008). The structure of phytoplankton communities affects the efficiency of carbon export. For example, in comparison to larger phytoplankton with high sinking velocities, picoplankton have a very limited direct contribution to the carbon sinking flux due to their small size and low sinking speeds, which leads to quick remineralization of the particles (Michaels and Silver, 1988). In contrast, aggregation of small particles into larger detrital particles significantly increase the vertical flux of organic matter (Jackson, 2001; Jackson et al., 2005; Richardson and Jackson, 2007).

Primary producers play a key role in biogenic carbon export through indirect pathways such as predation by mesozooplankton (Richardson and Jackson, 2007). Grazing on primary producers significantly contributes to the vertical export of biogenic carbon from the surface layer through production of fast-sinking particles, such as faecal pellets or organic debris, with their high sinking speed inhibiting bacterial reminalization. In addition, biogenic carbon can be transferred up the food web via predators. Large zooplankton species that have an ability to feed on microbial-sized particles, including large phytoplankton and microzooplankton, are found to be most efficient in transferring biogenic carbon to fish and larger predators (Le Fèvre et al., 1998). For example, krill feeding on large diatoms is a main food source for apex predators, such as whales and penguins, and is a key species contributing to the carbon export in the Southern Ocean (Le Fèvre et al., 1998).

Changes in the planktonic communities can affect top predators and have a significant economical implications for human fisheries. Dramatic decline in herring populations in the Baltic Sea was attributed to the long-term failure in feeding success related to zooplankton abundance, a key predator of phytoplankton (Flinkman et al., 1998). Similarly, the variability in the lesser sandeel populations in the North Sea was closely

linked to the climate-driven changes in the abundance in their planktonic prey (Frederiksen et al., 2006). Higher sandeel larval biomass was in turn associated with increased breeding productivity of sandeel-dependent seabirds (Frederiksen et al., 2006).

Each phytoplankton species is characterised by species-specific traits, such as optimum temperature and irradiance, and nutrient requirements that affect their growth (Litchman et al., 2007). Whether or not a species is successful depends on the local environmental conditions that shape the phytoplankton ecological niche. The main drivers of the global phytoplankton distributions are well understood in terms of nutrient requirements and the physical environment (Follows et al., 2007; Follows and Dutkiewicz, 2011; Thomas et al., 2012). Small cells, such as *Prochlorococcus*, are stronger nutrient competitors and thrive in the oligotrophic, nutrient-depleted regions (Fig. 1.1). By contrast, larger eukaryotes, such as diatoms, flourish at higher latitudes where nutrient supply amplifies seasonally, with their chances of survival improved through, for example, the ability of nutrient storing (Verdy et al., 2009), delayed response from predators or lower grazing pressure (Kiørboe, 1993). On spatial scales of order 10 km, phytoplankton community structure can be controlled by variability in

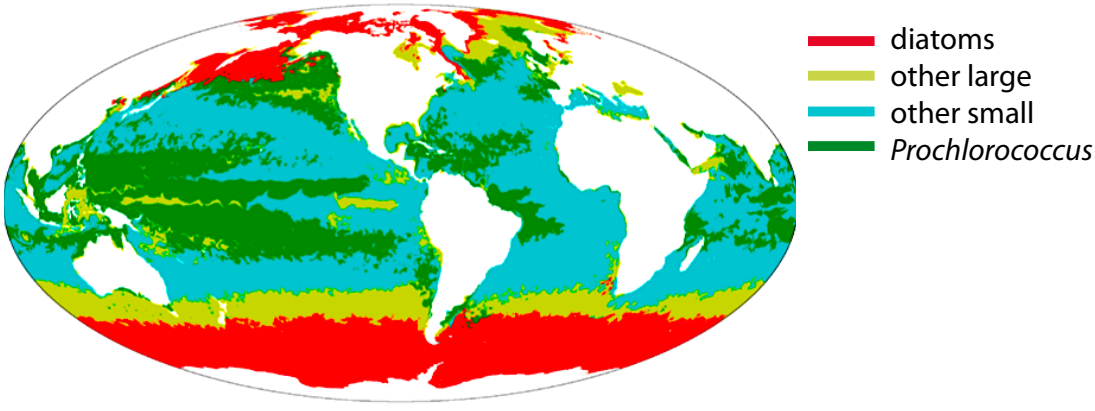

Figure 1.1: Annual mean emergent biogeography from a global ecosystem model seeded with 78 phytoplankton types with randomly assigned growth parameters. Biological provinces are dominated by diatom analogs (red), other large phytoplankton (yellow), other small phytoplankton (blue) or *Prochlorococcus* analogs (green). Figure from Follows and Dutkiewicz (2011).

the physical environment controlling the nutrient supply to the euphotic zone (Sharples et al., 2007, 2009).

Investigation of the processes that control the dynamics of planktonic communities provides an insight into the functioning of marine, and also terrestrial, ecosystems (McCauley and Murdoch, 1987). The dynamics of marine and terrestrial populations are governed by the same key mechanisms: competition, reproduction/growth, mortality-mediated losses and enduring externally-forced, environmental variability. The small temporal timescales of planktonic communities, of the order of tens of days (Sommer, 1985; Reynolds et al., 1993), allow for long-term observations of their life cycle and processes controlling individual populations, within a relatively short time frame. In comparison, seasonal succession of planktonic communities can be viewed as analogous to the response of temperate forests to the last glacial period (Reynolds, 1993).

A primary research question is what drives high taxonomic diversity within marine and terrestrial communities and how potential changes in biodiversity will affect the ecosystem processes. High species richness has been found to increase the population productivity (Tilman et al., 1996, 1997; Worm et al., 2006), which is due to an improved utilization efficiency of essential resources (Tilman et al., 1996; Ptacnik et al., 2008; Cardinale et al., 2006). Also, the analysis of phytoplankton time-series data of Ptacnik et al. (2008) suggested that local biodiversity is reduced by nutrient enrichment caused by pollution-driven processes. A number of studies have suggested that high species richness increases the stability at the community level by decreasing the temporal variance of productivity (Yachi and Loreau, 1999; Tilman, 1999), but increases non-equilibrium fluctuations at the population level (Tilman, 1999). Therefore, increased biodiversity has been suggested to enhance the predictability of some of ecosystem processes, such as ecosystem respiration (McGrady-Steed et al., 1997).

Potential loss of biodiversity would have significant effects on the ability of the ocean to provide food and maintain water quality (Worm et al., 2006). Therefore, it is crucial to understand the factors that influence community diversity and identify the controlling mechanisms.

1.2 The "paradox of the plankton"

Phytoplankton are ubiquitous microscopic primary producers that display great inter-species variability on a global as well as local scale. For example, open ocean and lake surface waters usually contain the order of 1 to 10 dominant phytoplankton species together with many hundreds or more species at very low concentrations. Hutchinson (1961) first posed the paradox of the plankton: Why do so many phytoplankton species coexist while competing for a limited number of resources in a nearly homogeneous environment? This high number of phytoplankton species appears at odds with the competitive exclusion principle (Hardin, 1960). According to this theory, the number of species coexisting at equilibrium is not expected to exceed the number of limiting resources, with each of the coexisting species specializing in the utilization of a different resource (Hardin, 1960; Tilman, 1977).

For phytoplankton, the resources can be viewed in terms of macro nutrients, trace metals and variations in the light and temperature environment, such that if 2 phytoplankton species compete for the same resource, the most successful competitor is the one able to survive on the minimum resource (Tilman, 1977; Tilman et al., 1982). The excess in the number of phytoplankton species has been explained in terms of the phytoplankton system not reaching an equilibrium state due to temporal variability, as first speculated in terms of seasonality by Hutchinson (1961) or spatial variability in the background environment (Richerson et al., 1970).

1.2.1 Competition for essential resources

The rate of photosynthesis and phytoplankton cell growth is strictly controlled by the availability of the essential resources, and these are light, and dissolved organic and inorganic macro- and micronutrients. In addition, phytoplankton metabolic rates are also mediated by ambient temperature.

Energy for the photosynthesis comes from the absorption of components of the visible light spectrum (referred to as photosynthetically available radiation, PAR), where the level of the available radiation exponentially decays with the depth of the water column. The energy from photons is harvested in cell chloroplasts that include photosynthetic pigments. Depending on the intensity of the available radiation, phytoplankton modify the abundance of pigments in a cell. The pigment abundance increases in light limited conditions in order to optimize the light absorption, and reduces in phytoplankton growing at the well-lit surface to avoid photoinhibition (Falkowski et al., 1985). This adaptation can be observed in the vertical structuring of phytoplankton communities through the formation of a deep chlorophyll maximum (Anderson, 1969; Hickman et al., 2010). Light is considered a main limiting factor for the high-latitude phytoplankton communities (Colijn and Cadée, 2003; Harrison and Li, 2007).

The macronutrients essential for phytoplankton growth are carbon, nitrogen, phosphorus and silica. Carbon makes up the majority of the cell by forming major cell components, and controls the fundamental functions such as energy storing for reproduction. Carbon is continuously supplied from the atmosphere and so phytoplankton cell growth is never limited by its insufficient concentration.

Nitrogen is a key element forming proteins that compose over 50% of the cell. Proteins are responsible for the functioning of the structural components of the cell and

facilitating biochemical reactions through enzyme production. Both nitrogen and phosphorus form nucleic acids that hold the genetic information about the cell and control its reproductive functions (Anderson, 1995). Nitrogen is generally found to be the main limiting macronutrient across oceanic environments (Tyrrell, 1999). Limiting nitrogen concentration in the low-latitude regions (Moore et al., 2013) leads to an increase in the rates of nitrogen fixation, that is an enzymatic reaction converting nitrogen gas into organic form, and therefore primary production in the oligotrophic gyres is controlled by the phosphate availability (Mather et al., 2008).

Silica is widely utilized by diatoms for production of the frustule, a hard cell wall composed mainly of silica. Therefore, in low concentrations, silica inhibits diatom blooms and can be an important factor controlling primary production at high latitudes (Jézéquel et al., 2000).

Iron is a pivotal micronutrient that facilitates the enzymatic reduction of oxidized nitrogen compound, nitrate, to nitrite. Iron is often found to be a key factor inhibiting macronutrient uptake in the high-latitude ecosystems (Martin, 1990; de Baar et al., 1995; Boyd et al., 2000; Blain et al., 2007; Achterberg et al., 2013). In nitrogen-limited, oligotrophic gyres, low iron supply can limit the process of nitrogen fixation due to the increased iron requirement for nitrogen-fixing diazotrophs (Berman-Frank et al., 2001).

Additionally, other trace metals, such as manganese, zinc, cobalt, copper, cadmium and nickel, and vitamins are incorporated into some proteins and enable enzymatic reactions and thus control phytoplankton growth (Saito et al., 2002; Morel and Price, 2003; Hassler et al., 2012; Sinoir et al., 2012). The B-vitamins cofactor important cellular processes and can be a co-limiting factor of phytoplankton growth in coastal waters (Gobler et al., 2007) and open ocean habitats (Bertrand et al., 2007; Koch et al., 2011). Also, the biosynthesis of the vitamin B_{12} can be limited by low cobalt

concentrations (Panzeca et al., 2009).

Spatial and temporal variability in essential resources shape global phytoplankton distribution and community structure. In an era of climate change, the environmental conditions that affect phytoplankton communities are predicted to alter through a possible increase of stratification and expansion of the oligotrophic gyres (Sarmiento et al., 2004; Bopp et al., 2005; Irwin and Oliver, 2009). The resulting changes to the availability of essential resources might have crucial implications for the future distribution of phytoplankton biomass and the efficiency of the biological pump (Bopp et al., 2005; Morán et al., 2010).

Diversity of phytoplankton community was found to increase in the environment where many resources limit cell growth simultaneously (Interlandi and Kilham, 2001). Nitrogen, phosphorus, silica and light are key limiting macronutrients. Trace metals and vitamins indirectly inhibit phytoplankton growth through affecting the efficiency of utilization of essential nutrients. Overall, there are maybe few tens of potentially limiting resources that may inhibit phytoplankton growth while there are hundreds of species coexisting throughout the year. There are tens to a hundred of dominant phytoplankton species that make up the majority of the community biomass, found to coexist across oceanic provinces (Cermeño et al., 2013) and freshwater lakes (Stomp et al., 2011). In addition, many background species coexist at very low concentrations which often inhibits the ability of detection.

Therefore, the research presented in this thesis implements the view that the number of species coexisting in aquatic ecosystems exceeds the number of essential resources they compete for, and therefore the paradox remains. In reality, the observational evidence whether the paradox occurs within the real world microbial communities remains challenging to obtain. The techniques applied for sampling of the

planktonic communities entail significant limitations, where a handful of phytoplankton samples taken at a particular location are taken as a representative of the local community. The difficulty in detection of phytoplankton species surviving at low concentrations or sampling at the location where some species are temporarily undetectable, makes the precise estimate of the number of coexisting species unfeasible to obtain. Similarly, verification of how phytoplankton growth and their competitive abilities are affected by climatic factors and availability of micro- and macronutrients, including further implications related to the chemical structuring of molecules, is a continuously developing field of research.

1.2.2 Solutions to the paradox

The paradox of the plankton is formulated from the perspective of species competition for essential resources where the strongest competitor, that is a species with the highest net growth rate, should exclude the less fit species at the final equilibrium. A number of processes that may prevent the system from reaching an equilibrium have been suggested and these include:

- seasonality and stochastic weather events where the modification of environmental conditions prevents the community from reaching competitive exclusion (Sommer, 1986; Reynolds et al., 1993),

- horizontal advection and mixing that continuously (or periodically) introduce new species to the local ecosystem (Richerson et al., 1970; Levin, 1974),

- predation acting to decrease the abundance of the ultimate competitor (Timms and Moss, 1984; Chase et al., 2002),

- internally-induced non-equilibrium, chaotic behaviour generated through species competition for resources (Huisman and Weissing, 1999).

The above-listed solutions to the paradox act to drive higher biodiversity through species immigration driven by transport processes or inhibiting species net growth, where the latter mechanism ultimately determines the success of the species and allows a long-term coexistence. Phytoplankton growth can be constrained through either planktonic interactions or externally imposed environmental factors. As a result, these processes prevent the fittest species from fully utilizing their ecological niche and allow the weaker competitors to thrive through reducing the competitive pressure.

High scientific efforts are invested into quantifying the extent to which each process allows for species coexistence. The potential contribution of the above listed mechanisms to planktonic biodiversity is next discussed in the following sections.

Seasonality and weather-related disturbance

The success of an individual phytoplankton species differs under variable physical and biochemical environments. Species-specific ecological niches are shaped, defining where environmental conditions facilitate the optimal growth of a particular species (Litchman et al., 2007; Litchman and Klausmeier, 2008). Seasonal variability acts to modify the ambient environment and drives the seasonal succession of coexisting species with the timing of the bloom depending on the light availability, and the strength of water column stratification (Reynolds, 1984; Sommer, 1986; Richardson et al., 2000). Additionally, stochastic weather events superimposed on the seasonal fluctuations modify the temperature and light environments through mixing of the water column, which acts to enhance the nutrient supply to the euphotic zone and, at the same time, reduce the light experienced by phytoplankton.

According to the Intermediate Disturbance Hypothesis, first posed by Connell (1978) in the context of biodiversity in tropical rain forests and corals, environmental disturbance of intermediate timescale and intensity is a key factor driving community diversity. Disturbances act to set back the process of competitive exclusion. Relatively high frequency disturbances will have comparable effect to an undisturbed steady state, as any short-lived oscillations will be incorporated into population life cycle. Under low frequency variability only the most effective competitor will survive because it has time to exclude the others (Connell, 1978; Sommer, 1995). The characteristic timescale for phytoplankton to reach competitive exclusion is 35-60 days (Sommer, 1985),

which corresponds to 12-16 generations (Reynolds et al., 1993). The necessary environmental disturbance has to occur at timescales more comparable to the plankton generation timescale (Hutchinson, 1961), to prevent domination by the best-adapted competitor (Reynolds et al., 1993).

Fluctuations in the light and nutrient environment prevent the community from reaching competitive exclusion and enhance phytoplankton diversity (Gemerden, 1974; Sommer, 1985, 1995; Litchman, 1998). Fluctuations in ambient temperature have been found to enhance coexisting abilities of competitive species by modifying their resource utilization abilities (Rhee and Gotham, 1981; Descamps-Julien and Gonzalez, 2005). The numerical study of Ebenhöh (1988) shows that the periodic input of nutrients modifies species growth and mortality, and, depending on the timescale of disturbance, can lead to complex dynamics that act to sustain a greater number of species in the environment. The optimal timescale for the disturbance where the community diversity reaches its maximum was suggested to be 6-10 days (Flöder and Sommer, 1999).

Throughout the year, seasonal variability creates favourable conditions for species adapted to different environmental conditions to thrive. In the meantime, intermediate disturbances generated by stochastic weather events act to interrupt the annual species succession and allow for weaker competitors to be sustained in the environment.

Physical transport processes

Turbulence and mixing are important factors that modify interactions between competing species (Richerson et al., 1970; Kemp and Mitsch, 1979), and can sustain greater diversity through spatial connectivity and interactions with adjacent ecosystems. The heterogeneity of the oceanic environments is affected by a range of physical processes

occurring at a different time and spatial scales, including dispersal through oceanic currents and mesoscale eddies (Smith et al., 1996; Abraham, 1998), to small scale mixing processes through diffusion and turbulence (Richerson et al., 1970).

Dispersal and continuous, large-scale advection of marine ecosystems act to increase local diversity, with the highest number of coexisting species observed at the boundaries of dynamical circulations, such as the extension of western boundary currents separating subtropical and polar environments (Fig. 1.2; Barton et al., 2010). Baroclinic instabilities arising from the large-scale oceanic currents lead to a formation of mesoscale eddies. Eddies and mesoscale vortices can enable the prolonged survival of phytoplankton species that are less fit for the surrounding environment (Bracco et al., 2000). Homogenous environments transported within the eddy core, are gradually mixed into the local environment through the lateral exchange at the boundaries. However, the coexistence of local species and species driven by the mesoscale processes is short-lived (up to several months) and weak nutrient competitors are eventually outcompeted (Bracco et al., 2000).

Mesoscale variability contributes to the generation of 'patchiness' where adjacent eco-

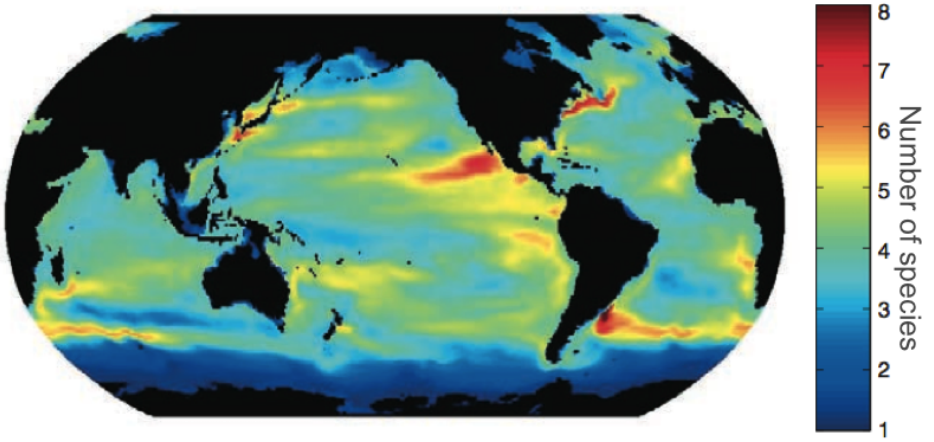

Figure 1.2: Species diversity in the uppermost 260m. Diversity is defined as a number of phytoplankton types that contribute more than 0.1% to the total biomass. Figure from Barton et al. (2010). Biodiversity 'hotspots' found at the boundaries of intensified dynamical circulations.

systems differ in their community structure (Levin, 1974; Tilman, 1994). Coexistence of species with diverse ecological niches is possible when the rate of mixing between the ecosystems corresponds to the phytoplankton generation timescale. The mixing strength of intermediate intensity is argued to favour diversity because it is strong enough to prevent the the ultimate competitor from dominating, but stable enough to sustain the patchiness (Richerson et al., 1970; Levin, 1974; Kemp and Mitsch, 1979). A relatively low mixing rate between different phytoplankton patches can allow species coexistence through continuous exchange, but prevents the exclusive occupation of the environment by the stronger competitor (Richerson et al., 1970).

Physical processes that act to increase the local biodiversity of planktonic communities do not affect the competitive abilities of the species directly, but are a form of an intermediate disturbance that inhibits the ultimate competitor. Transport processes increase local diversity by mixing together different ecosystems, but the coexistence is not sustained in their absence.

Predator-prey interactions

Top-down control on planktonic communities has been found to be a key factor shaping community structure and diversity (Richerson et al., 1970; Chase et al., 2002). Predation has been suggested to inhibit an individual's resource intake and growth, and leads to a reduction in species density (Chase et al., 2002). Increased grazing pressure on the most dominant competitors prevents them from occupying the entire ecological niche, and creates favourable conditions for weaker competitors to become established (Timms and Moss, 1984; Prowe et al., 2012).

Prey preference and the ability of predators to switch to a different food source, in order to optimize their survival, have important implications for planktonic community

structure and functioning (Gentleman et al., 2003; Fasham et al., 1993; Prowe et al., 2012). The modelling study of Prowe et al. (2012) illustrates how the strength of the grazing pressure and the ability of grazers to switch to different food source increases global phytoplankton diversity (Fig. 1.3). Some zooplankton have an ability to switch their feeding strategy which often results in the modification of the prey type (Kiørboe et al., 1996; Kiørboe, 2011). Zooplankton adapt different feeding strategies to optimize their growth and increase feeding opportunities (Visser and Fiksen, 2013). The choice of the feeding mode strongly depends on the physical conditions (Saiz and Kiørboe, 1995; Visser et al., 2001) and the risk of predation (Zaret and Suffern, 1976; Lampert, 1989), and may vary on daily as well as seasonal time scales (Mariani et al., 2013).

The complexity of zooplankton feeding behaviour and continuous variability in the graz-

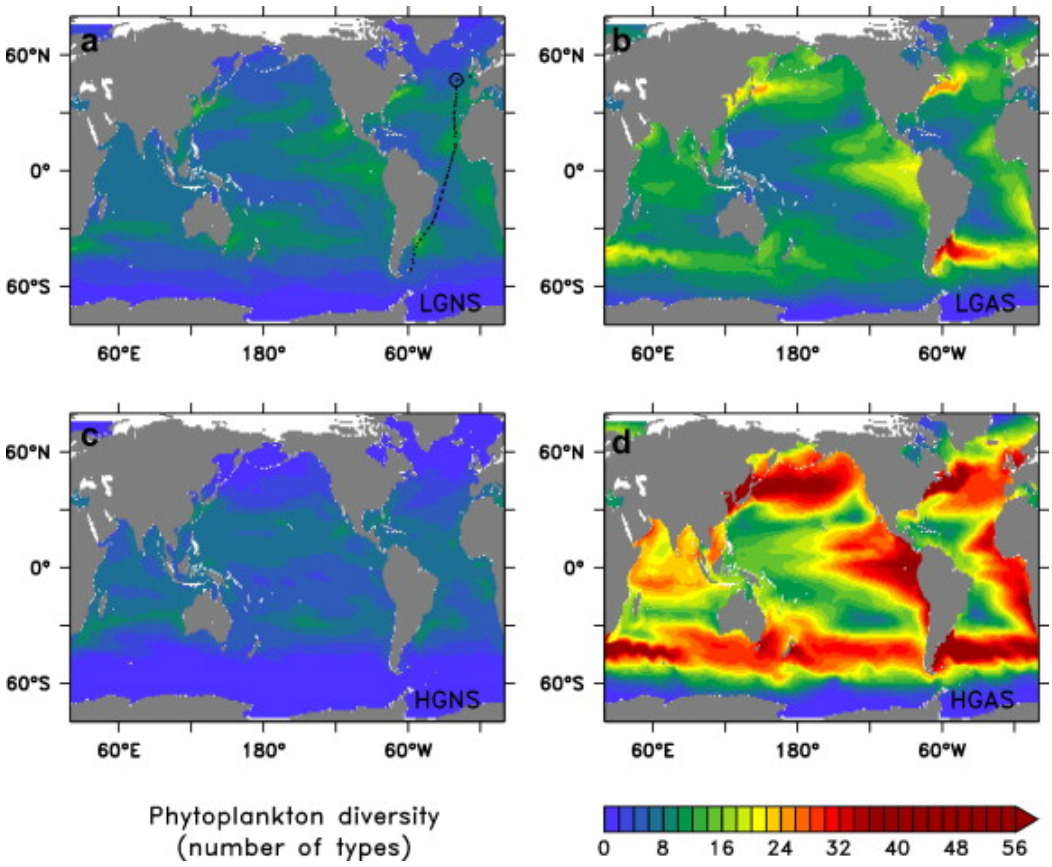

Figure 1.3: Phytoplankton diversity for different scenarios describing zooplankton grazing pressure and ability to switch to a different food source: A) Low grazing and no switching (LGNS), (b) Low grazing and active switching (LGAS), (c) High grazing and no switching (HGNS), and (d) High grazing and active switching (HGAS). Figure from Prowe et al. (2012).

ing pressure is arguably one of the most important factors preventing the planktonic communities from reaching an equilibrium. Grazing inhibits the growth of strong nutrient competitors and creates refuges for less competitive ones, allowing survival of tens of different phytoplankton species (Prowe et al., 2012).

Internally-induced non-equilibrium

Early ecological models suggested that interactions between 3 or more populations or species can lead to unstable equilibria and chaos (May, 1974; May and Oster, 1976; Gilpin, 1979). Deterministic chaos is characterised by irregular fluctuations that do not repeat in time, without stochastic variability being imposed. Chaotic systems are often referred to as 'noise amplifiers', because any small perturbation grows exponentially with time and influences the long-term behaviour of the system (Ellner and Turchin, 1995). This evolution suggests that population behaviour can be predicted on short timescales, but high sensitivity of chaos to initial conditions inhibits the long-term prediction. Note that this feature does not apply for stochastic systems, where there is no skill in prediction.

Early theoretical approaches focussed on investigation of chaotic dynamics within predator-prey models (Gilpin, 1979; Schaffer, 1985; Sabin and Summers, 1993). The possibility of populations exhibiting chaotic fluctuations was also addressed in terrestrial ecology (Turchin and Taylor, 1992; Hastings et al., 1993). Time-series analysis of rodent population dynamics suggested that northern populations may exhibit chaotic behaviour (Turchin, 1993). Similarly, complex behaviour is suggests to drive the variability in insect populations (Turchin and Taylor, 1992; Costantino, 1997).

In the context of phytoplankton communities, predator-prey interactions are analogous

to the species competition for essential abiotic resources. The probability of complex dynamics to occur has been confirmed within modelled microbial ecosystems, such as predator-prey interactions between protozoa and bacteria (Kot et al., 1992), phytoplankton competition for essential resources (Huisman and Weissing, 2001) and interactions between bacterivorous ciliate and two bacterial prey species (Becks et al., 2005). Using an idealized model framework, Huisman and Weissing (1999) illustrated that phytoplankton interspecies competition for nutrients can exhibit a variety of responses including regular and chaotic behaviour. The ecosystem model simulations applied realistic phytoplankton parameterization and the findings suggest that the type of the response depends on the species nutrient requirements (Huisman and Weissing, 2001). Huisman and Weissing (1999) show that introduction of new species leads to more species coexisting than the number of resources they compete for (Fig. 1.4). Application of the trade-off for species competitive abilities, which promotes species specialization in one particular nutrient, can facilitate coexistence of up to a hundred species subject to new species being added to the environment every 50 days (Huisman et al., 2001).

Interactions with higher trophic levels and competition between higher numbers of species increase the complexity of interactions and can easily facilitate chaos (Smale, 1976). In addition, forcing the ecosystem with seasonal variability in light, temperature and nutrient environments is suggested to be a potential driver of chaotic behaviour (Rinaldi and Muratori, 1993). This phenomenon was found to generate strong interannual variability in plankton phenology (Doveri et al., 1993).

Internally-induced non-equilibrium dynamics can potentially contribute significantly to driving planktonic biodiversity, assuming it is a plausible response within the real world environment. Verification whether such behaviour occurs within real microbial com-

munities will provide insight into the complexity of interactions and could at least partially explain the irregular fluctuations of planktonic communities on the inter-annual timescales.

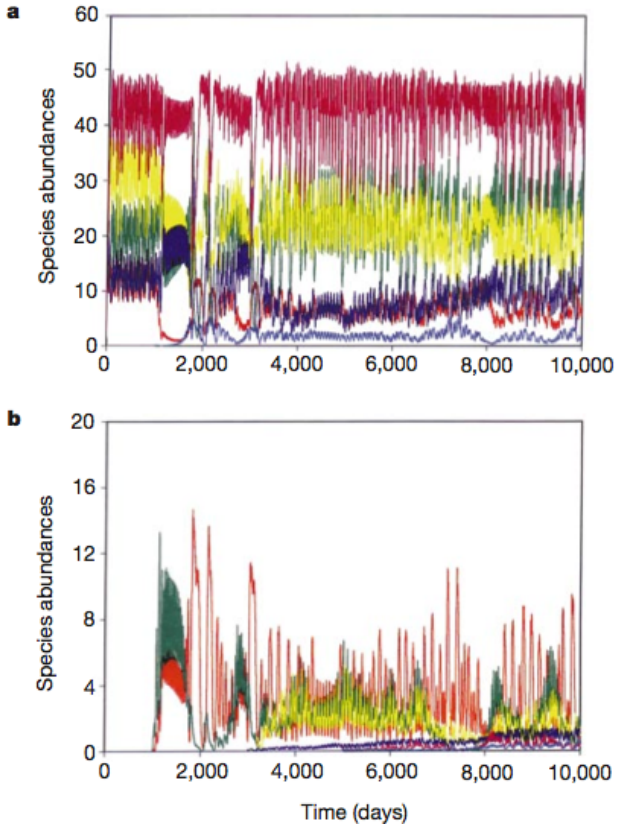

Figure 1.4: Competitive chaos and coexistence of 12 species on 5 resources subject to random addition on new species (species 6-12): (a) abundance of species 1-6, (b) abundance of species 7-12. Figure from Huisman and Weissing (1999).

1.3 Research aims and objectives

Environmental heterogeneity, caused by climatic fluctuations and transport processes driven by ocean circulation, is an important factor preventing marine ecosystems from reaching equilibrium. Alongside the effect of predation, these solutions to the paradox have received a high scientific attention with a number of experimental and modelling studies aiming to address their contribution to biodiversity. On the other hand, a potential role of chaos and non-equilibrium behaviour in driving species diversity has not been fully resolved. Greater understanding of whether variability in species abundance is governed by deterministic or stochastic processes would provide an insight into the stability and predictability of phytoplankton communities (Hastings et al., 1993).

Previous theoretical studies have suggested that complex behaviour and unstable equilibria are a possible outcome of the interactions between organisms for essential resources. Model experiments have shown that the type of the response is highly sensitive to the parameter choices that characterize metabolic functions of an organism. However, there has been no exploration of the parameter space that would shed light on how likely it is for a phytoplankton community to exhibit complex or oscillatory behaviour. For example, Huisman and Weissing (1999) in their model experiments demonstrated how chaotic behaviour can drive biodiversity using a finely-tuned parameter choices. In addition, apart from the laboratory-controlled experiments with real food-webs, there is no scientific evidence that complex behaviour persists in the heterogeneous, marine environment. There has been a limited number of attempts addressing chaos detection within long-term time-series data, and no known studies addressing the predictability of marine ecosystems.

The aim of this research is to establish how likely it is for phytoplankton community to

exhibit non-equilibrium dynamics in the heterogenous marine environment. This work focuses on the contribution of phytoplankton dynamics to biodiversity, and in particular the effect of the inter-species competition for nutrients. The effect of grazer communities is not considered in this work. The research explores whether the prevailing nature of the externally-imposed variability in the physical environment acts to subdue the internally-induced phytoplankton response to the competition for nutrients.

The overarching hypotheses are as follows:

- *(H1) Chaotic behaviour is an infrequent inter-species competition outcome and requires finely-tuned parameter choices.*
- *(H2) Seasonal forcing facilitates a chaotic response within a phytoplankton community, and increases the likelihood of non-equilibrium dynamics.*
- *(H3) Stochastic variability in forcing suppresses chaotic response in marine ecosystems.*
- *(H4) Physical transport processes and connectivity between different ecosystems inhibit internally-induced chaotic behaviour.*

Chapter 3 addresses the inter-annual and seasonal variability observed within time-series phytoplankton and nutrient data. The chapter aims to verify necessary factors that inhibit differentiation between chaotic behaviour from stochastic dynamics.

In chapter 4, model simulations are applied to investigate the range of the parameter space where non-equilibrium dynamics are most likely to occur. The chapter explores the requirements for an idealized phytoplankton community to escape competitive exclusion.

Chapters 5 and 6 focus on the effects of external forcing (periodic and stochastic) and possible effects of the physical transport processes that directly affect phytoplankton

community functioning. The analysis aims to verify whether the chaotic behaviour becomes subdued by the prevailing character of the environmental variability, or whether it persist in the background with significantly inhibited capability of detection.

CHAPTER 2

Model framework and verification of chaos

Rationale:

The objective of the project is to gain a wider insight into how the nutrient environment and species requirements for nutrients shape the real world phytoplankton community. In chapters 3 to 6, a well-mixed box model for phytoplankton competition for nutrients of Huisman and Weissing (1999) is applied in a series of studies. The model simulations investigate the outcome of inter-species competition and the factors that affect the character of the community response. The chapter provides an overview of the model and the assumptions made in its formulation, and explains how different community responses are identified.

2.1 0-D ecosystem model

2.1.1 Model formulation

The model is based on the linear chemostat assumption (Tilman, 1977, 1980; Armstrong and McGehee, 1980; Huisman and Weissing, 1999), where there are n phytoplankton species, P_i, competing for k resources represented as nutrients, N_j, such that:

$$\frac{\partial N_j}{\partial t} = D(S_j - N_j) - \sum_{i=1}^{n} Q_{ji} r_i \gamma_i^N P_i \quad [mmol\ N\ m^{-3}\ d^{-1}] \qquad j = 1,...,k \tag{2.1}$$

$$\frac{\partial P_i}{\partial t} = P_i(r_i \gamma_i^N - m_i) \quad [mmol\ C\ m^{-3}\ d^{-1}] \qquad i = 1,...,n \tag{2.2}$$

$$\gamma_i^N = min\left(\frac{N_1}{K_{1i}+N_1},...,\frac{N_k}{K_{ki}+N_k}\right) \tag{2.3}$$

where the subscripts denote the particular species $i = 1,...,n$ and resources $j = 1,...,k$. In (2.1), the nutrient concentration, N_j, evolves through a competition between a source from a nutrient supply and a sink from phytoplankton consumption: the nutrient supply involves an external supply from nutrient-rich deeper waters, S_j, and a feedback to N_j, for each nutrient j, modulated by the system turnover rate, D, referred to as a dilution rate for a chemostat. The sink from the consumption by the sum of the phytoplankton species depends on the phytoplankton abundance, P_i, and growth rates, γ_i^N, for each species i and the cell quota, Q_{ji}, for each species i and nutrient j. Cell quota represents the amount of nutrient incorporated per unit growth and is interpreted as an elemental ratio used for estimation of the resource uptake during cell growth. In (2.2), each phytoplankton species, P_i, grows exponentially depending on the cell growth rate, $r_i\gamma_i^N$, and the loss term, m_i. The phytoplankton loss term com-

bines the effects of dilution, D, and natural mortality, μ_i, where $m_i = D + \mu_i$. Initially, phytoplankton loss is assumed to be fully controlled by dilution with $m_i = D$ and the effects of natural mortality are neglected. The growth rate depends on the maximum growth rate, r_i, for each species, modified by the abundance of the limiting nutrient relative to the half-saturation coefficient, K_{ji}, for each species and resource in (2.3); note that for simplicity the growth rate does not depend on cell quota (as instead applied by Droop (1973)). The chemostat model emulates steady state conditions where consumption of a resource is balanced by its import, and where maximum growth, resource requirements and external supply remain invariant in time.

The model is usually initialized with the same number of species and resources, $n = k = 5$, and the default parameter settings given in Table 2.1. Note that the majority of model simulations focus on the case when $n = k = 5$, despite the paradox of the plankton addressing the question when $n > k$. Huisman and Weissing (1999) and Huisman et al. (2001) previously illustrated that chaotic response can sustain greater amount of phytoplankton species when new competitors are gradually introduced into the environment. The question that remains, and is the main focus of this thesis, is how likely it is for the phytoplankton community to exhibit chaos and generate conditions facilitating higher biodiversity. Within the modelling framework, chaos occurs when the number of initialized species does not exceed the number of resources they compete for: the presence of additional species is likely to disturb the competition balance where each species is the strongest in the utilization of a different resource, and may favour competitive exclusion. Therefore, for investigation of the likelihood of chaos to occur and its sensitivity to external variability, only the case when $n = k = 5$ is considered.

Any modifications of the model set-up are indicated in the appropriate chapter. The

model Eqs. (2.1) to (2.3) are integrated forward in time using a 4^{th} order Runge-Kutta scheme with a time step of 0.001 d.

Table 2.1: Default parameter settings for the model (Huisman and Weissing, 1999).

Parameter name	**Values**	**Units**
Initial concetration of species i, P_i	$P_i = 0.1 + \frac{i}{100}$	$mmol\ [C]\ m^{-3}$
Supply concentration of resource j, S_j	$[S_j] = \begin{pmatrix} 6 \\ 10 \\ 14 \\ 4 \\ 9 \end{pmatrix}$	$mmol\ [N]\ m^{-3}$
Initial concentration of resource j, N_j	$N_j = S_j$	$mmol\ [N]\ m^{-3}$
System's turnover rate, D	0.25	d^{-1}
Maximum phytoplankton growth rate, r_i	1.0	d^{-1}
Mortality rate, m_i	0.25	d^{-1}
Half-saturation coefficient of species i for resource j, K_{ji}	$[K_{ji}] = \begin{pmatrix} 0.39 & 0.34 & 0.30 & 0.24 & 0.23 \\ 0.22 & 0.39 & 0.34 & 0.30 & 0.27 \\ 0.27 & 0.22 & 0.39 & 0.34 & 0.30 \\ 0.30 & 0.24 & 0.22 & 0.39 & 0.34 \\ 0.34 & 0.30 & 0.22 & 0.20 & 0.39 \end{pmatrix}$	$mmol\ [N]\ m^{-3}$
Cell quota of species of species i for resource j, Q_{ji}	$[Q_{ji}] = \begin{pmatrix} 0.04 & 0.04 & 0.07 & 0.04 & 0.04 \\ 0.08 & 0.08 & 0.08 & 0.10 & 0.08 \\ 0.10 & 0.10 & 0.10 & 0.10 & 0.14 \\ 0.05 & 0.03 & 0.03 & 0.03 & 0.03 \\ 0.07 & 0.09 & 0.07 & 0.07 & 0.07 \end{pmatrix}$	$mol[N]\ /\ mol[C]$

2.1.2 Model approximation of reality

The model simulates the competition of phytoplankton species for 5 arbitrary resources analogous to essential nutrients for phytoplankton growth, for instance nitrate, nitrite, ammonia, phosphate and iron or silica. The concentration of each nutrient is normalized using the Redfield stoichiometric ratio and represented in a form of nitrogen units, $mmol[N]\ m^{-3}$ equivalent in magnitude to $\mu M[N]$ (or $\mu molL^{-1}$).

High departures from the Redfield ratio in the nutrient supply concentration, S_j, might represent the variable rates of bacterial breakdown of organic nutrients or non-Redfieldian atmospheric deposition of nutrients (Baker, 2003; Baker et al., 2007). Similarly, variability in the elemental ratio is applied in the assignment of the physiological traits of modelled phytoplankton species, such as half-saturation coefficient, which is to represent better adaptation (or preference) for utilization of a particular resource. This allocation allows each species to be limited by a different resource (Petersen, 1975; Tilman, 1980). Inter-species variability in cell quota is to resemble the variability in the cellular elemental composition (Arrigo, 2005). Cell quota does not affect the growth rate of a modelled species, but acts as nutrient affinity, denoting the amount of nutrient sequestered during the growth of the biomass.

The ability of the model to accurately capture the resource competition in the chemostat was verified in a number of experimental studies. The chemostat model accurately predicted the biological conditions controlling the competition between freshwater (Tilman, 1977; Holm and Armstrong, 1981) and marine phytoplankton (Sommer, 1986), and competition outcome under variable nutrient supply and temperature (Donk and Kilham, 1990). The model was also applied in theoretical studies investigating the stability of consumer-resource interactions (Armstrong and McGehee, 1976, 1980; Huisman and Weissing, 1999, 2001).

Implementation of the modelling approach has its strengths and weaknesses. An idealized ecosystem model does not incorporate a true food web complexity and interactions related to higher trophic levels. Instead, the approach focuses the experimental efforts on a particular issue by isolating a part of a food chain and inspection of the dynamics and interactions that it entails. The modelled environment is fully controlled, which simplifies the interpretation of the ecosystem sensitivity to a chosen physical or biological variable. In the context of this thesis, the idealized model enables to investigate the role of phytoplankton physiological traits in controlling the frequency of chaotic dynamics, an aspect that would require numerous and time-consuming laboratory experiments.

However, similar to the laboratory experiments, modelling approach does not entail the complexity of the physical and biological forcing controlling the microbial communities in the ocean. An idealized model framework does not capture the real environmental variability incorporating stochastic processes, such as mesoscale vortices, or horizontal and vertical advection, with the latter two processes preventing the phytoplankton community from remaining in the same location in the ocean. A number of sources of inorganic nutrients, direct of indirect, are not considered in the model framework, and neither is the species ability to adapt to the environmental stress, both of which factors may have significant effects on the dynamics resulting from the inter-species competition for nutrients. However, the modelling framework provides a powerful tool to test the theory behind unresolved scientific questions. The work presented in this thesis not only investigates the sensitivity and the likelihood of chaos to occur, but also aims to identify the criteria that need to be considered when detecting chaos within the real world phytoplankton communities.

2.2 Methods of chaos verification

The phytoplankton community in the model exhibits three types of responses: competitive exclusion (Fig. 2.1a), periodic oscillations (Fig. 2.1b) and chaos characterised by irregular, non-repeatable fluctuations (Fig. 2.1c). In order to formally verify the emergence of chaos and differentiate it from stochastic fluctuations, chaotic behaviour is identified through 3 different approaches: phase diagrams, Lyapunov Exponent and 0-1 Test for Chaos.

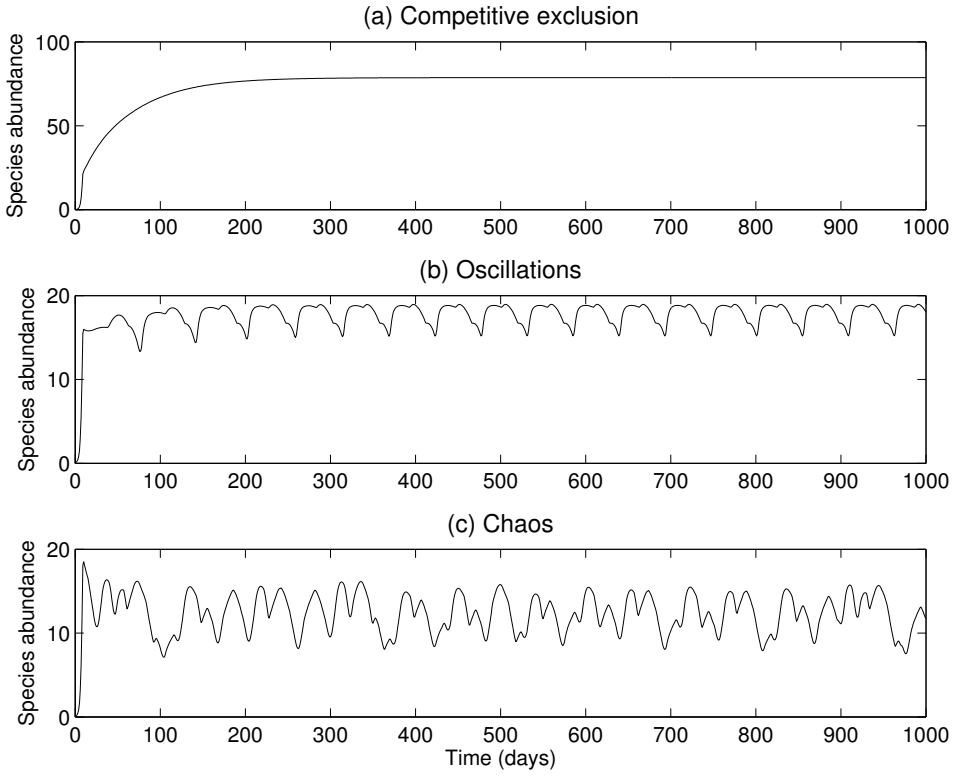

Figure 2.1: Possible types of phytoplankton community response within the ecosystem model: (a) competitive exclusion, (b) oscillations, and (c) chaos.

2.2.1 Phase diagrams and Poincaré sections

The dynamics of the system are commonly illustrated in the form of a 3-dimensional phase diagram, where each dimension represents species abundance (Fig. 2.2, right panels). Oscillatory behaviour is characterised by continuously repeated trajectory in the phase space (Fig. 2.2a). The characteristic feature of chaotic dynamics is an unstable 'strange attractor', where the trajectory appears to fluctuate in a random manner and never repeats in time. This indication of an irregular behaviour inhibits the skill for a long-term prediction (Fig. 2.2b).

(a) Oscillations

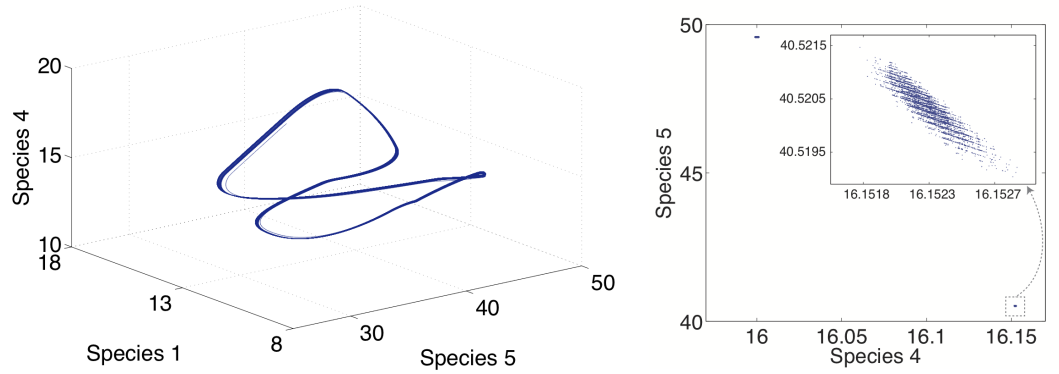

(b) Chaos

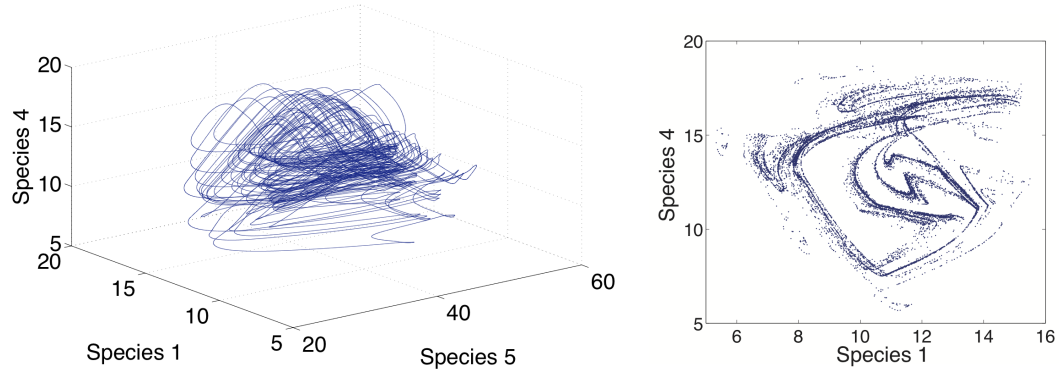

Figure 2.2: The model responses incorporate (a) double period oscillations and (b) chaos, generated with $K_{4,1} = 0.266$ and $K_{4,1} = 0.274$ respectively, with remaining parameters as listed in Table 2.1. The community dynamics are illustrated with phase diagrams for time series from 2000 to 5000 days (left panels) and Poincaré sections over 500 000 days (right panels).

For stochastic systems, the trajectory in the phase space can also resemble a strange attractor despite the system not being chaotic. In such case, further inspection of the phase diagram is necessary by investigating the recurrence map, referred to as a Poincaré section. The Poincaré section is generated by taking a cross-section of the attractor to capture the multiple locations where the trajectory passes through the cross-section plane from the same direction (Fig. 2.2, right panels). Due to the non-repeatable nature of chaotic fluctuations, the trajectory never crosses the cross-section plane in exactly the same location and resulting Poincaré section exemplifies the structure of a Cantor set, a fractal pattern characteristic for chaos (Fig. 2.2b). Generation of the Poincaré section requires long time series sampled at high frequency to accurately capture the fractal structure, which poses severe limitations for application of this method for identifying chaos in observational time-series data.

2.2.2 The Lyapunov exponent

To identify whether chaos is occurring (as suggested by the phase trajectories), the sensitivity to initial conditions can be revealed by estimating the maximal Lyapunov exponent, λ_{max}, which is a measure of the rate at which 2 trajectories diverge over time t:

$$|x(t) - x_\varepsilon(t)| \approx e^{\lambda_{max} t} |x(0) - x_\varepsilon(0)| \tag{2.4}$$

$$\lambda_{max} = \lim_{t \to \infty} \frac{1}{t} \, ln \left(\frac{|x(t) - x_\varepsilon(t)|}{|x(0) - x_\varepsilon(0)|} \right) \tag{2.5}$$

where $x(t)$ and $x_\varepsilon(t)$ are 2 arbitrary trajectories starting at an infinitely small distance between them. Negative λ_{max} indicates the convergence of the time series to a steady state and $\lambda_{max} = 0$ indicates convergence to regular dynamics, i.e. a periodic or quasi-periodic regime. Positive λ_{max} represents an exponential growth in the separation of

trajectories and indicates chaos.

Throughout the series of studies presented in this thesis, the maximal Lyapunov Exponent is estimated using one of the two considered methods: 1) numerical algorithm computation, or 2) the analysis of the observational time-series data or synthetic data generated by the model.

Numerical estimation

The maximal Lyapunov Exponent is estimated numerically during model simulations using the method of Benettin et al. (1976) and Wolf et al. (1985). The test trajectory, $x_\varepsilon(t)$, is initialized at a distance d_0 away from the original trajectory, $x(t)$. The distance d_t between trajectories is measured at every time step using the Cartesian distance formula:

$$d(t) = \sqrt{(\Delta x)^2 + (\Delta y)^2 + (\Delta z)^2} \tag{2.6}$$

For chaotic systems, the trajectory separation quickly saturates and a distance threshold D needs to be specified to accurately capture the rate of divergence. At every time Δt when the d_t exceeds a threshold value D, the ratio $\lambda_I = ln(\frac{d_t}{d_0})$ is computed, where I denotes each of the n moments when threshold value D is exceeded. The test trajectory is then renormalized, that is initialized in the direction of divergence to accurately monitor the continuous increase in trajectory separation,

$$x_\varepsilon(t) = x(t) + d_0 \, \frac{d(t)}{|d(t)|} \tag{2.7}$$

and the calculations for the trajectory divergence are repeated for the entire length of the time series. The maximal Lyapunov Exponent, λ_{max}, is estimated as an average of

the exponents obtained during each rescaling process:

$$\lambda_{max} = \frac{1}{t_n - t_0} \sum_{I=1}^{n} \lambda_I \tag{2.8}$$

For the ecosystem model, the calculations are carried out based on the nutrient concentration trajectory. Each j component of the test trajectory, that is each out of the $k = 5$ considered nutrients, N_j, is initialized as $N_{\varepsilon,j} = N_j + \varepsilon$. The initial distance between original, N_j, and test trajectory, $N_{\varepsilon,j}$, becomes:

$$d_0 = \sqrt{k \times \varepsilon^2} \tag{2.9}$$

For correct λ_{max} approximation, the test trajectory needs to initialized at a sufficiently small distance that would not modify the character of the system. Following the directions of Benettin et al. (1976) and Tancredi et al. (2001), the arbitrary choices for $\varepsilon = 10^{-8}$ and $D = 10^{-3}$ are applied in the numerical calculations.

Time series analysis

To estimate λ_{max} the TISEAN software package is applied (Hegger et al., 1999). The package allows for the calculation of the separation between the trajectories in the phase space, referred to as a stretching factor (CF):

$$e^{\lambda_{max} t} \approx \frac{|x(t) - x_\varepsilon(t)|}{|x(0) - x_\varepsilon(0)|} = CF \tag{2.10}$$

An exponential increase in CF over time indicates chaotic behaviour.

The TISEAN package offers two algorithms for estimation of the maximal Lyapunov Exponent, implementing the methods of Rosenstein et al. (1993) and Kantz (1994).

The algorithms differ in the applied definition of the distance to the test trajectory, with the algorithm of Rosenstein et al. (1993) outperforming when dealing with short and noisy time-series data. Both algorithms generate a 'test' trajectory through applying the method of delays for re-construction of a phase space, where the time series is searched for another data point at which all system variables are in a similar state. The method requires verification of embedding parameters: time series delay and embedding dimension. Embedding dimension, d_{emb}, is indicative of the complexity of the system and denotes the lowest dimension that is necessary to contain the attractor in the phase space. Insufficiently small choice of d_{emb} will lead to an inaccurate estimation of the distance between the original and the test trajectories. Appropriate d_{emb} is a dimension at which the output of the analysis, the rate of exponential increase of CF, is no longer sensitive to a further increase in d_{emb}. The robustness of the results suggests that the distance between the original and the test trajectory is fully captured within the chosen phase space. For example, let's consider the Lorenz equations:

$$\frac{\partial x}{\partial t} = \sigma(y - x) \tag{2.11}$$

$$\frac{\partial y}{\partial t} = x(\rho - z) - y \tag{2.12}$$

$$\frac{\partial z}{\partial t} = xy - \beta z \tag{2.13}$$

where x, y and z are system variables proportional to convective intensity (x), temperature difference between a descending and an ascending flow (y), and a difference in vertical temperature profile (z), t is time, and σ, ρ and β are physical system parameters (Lorenz, 1963). For the Lorenz system $d_{emb} = 3$ is sufficient for accurate approximation of the maximal Lyapunov Exponent. Further increase in d_{emb} does not significantly alter the result and decreases the computational efficiency of the algorithm. The

analysis indicates that for the phytoplankton community generated by the ecosystem model $d_{emb} = 5$ is suitable for the analysis of the model output (Fig. 2.3a).

Time delay, t_{delay}, is estimated using the autocorrelation function, where the appropriate t_{delay} is the time when the autocorrelation function first approaches zero (Fig. 2.3b). The time series is then successively delayed by t_{delay} for each dimension to generate d_{emb}-dimensional trajectory in the phase space.

In order for the stretching factor data to be reliable, the algorithm needs to be iterated at least 10 times for each time series: the time evolution of the stretching factor is calculated for at least 10 sections of the analysed time-series, each of an even length, and subsequently averaged. Thus, the rate of separation can only be calculated for

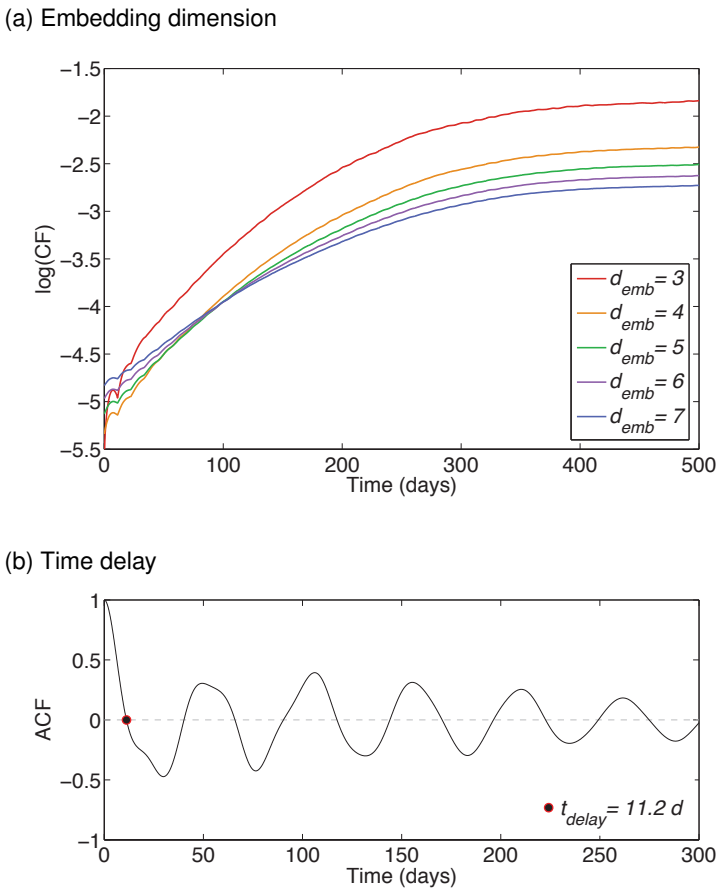

Figure 2.3: Verification of the suitable embedding parameters, (a) embedding dimension, d_{emb}, and (b) time delay, t_{delay}, using an autocorrelation function (ACF), for the modelled phytoplankton community generated with the default parameter settings shown in Table 2.1.

the $\frac{[length\ of\ time\ series]}{10}$ units of time.

The accuracy of the diagnosed λ_{max} is highly sensitive to the length of the time series, as well as the time step and the sampling interval, τ, used for its generation. The analysed time series generated by the model described in Section 2.1 covered 20000 days and was subsampled with $\tau = 0.1$ day, which, when repeated for the classical Lorenz system, gives a relatively accurate prediction for λ_{max}. The obtained λ_{max} range from 0.007 to 0.035 day^{-1} depending on the value of the half-saturation coefficient $K_{4,1}$ (Fig. 2.4), with their small positive values indicating weak chaos. The approximations of λ_{max} using the TISEAN package remain aligned with the estimates obtained numerically (Fig. 2.4).

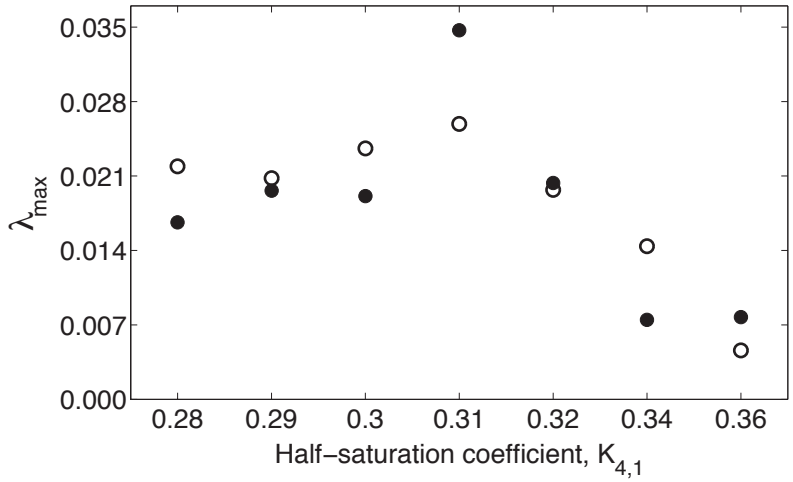

Figure 2.4: Estimation of the maximal Lyapunov exponent, λ_{max}, for the chaotic system generated with varying half-saturation coefficient, $K_{4,1}$. Black dots indicate the estimates obtained using the TISEAN package, and the clear dots are approximations obtained using the numerical implementation of the algorithm.

2.2.3 The 0-1 Test for Chaos

The 0-1 Test for Chaos is applied, a binary test that distinguishes regular from chaotic dynamics, to provide a more efficient identification of chaos (Gottwald and Melbourne, 2004, 2009). The 0-1 Test analyses the time series and returns a scalar value that is used as a determinant of whether chaos occurs.

The time-series data, $\Phi(t)$, is represented in a form of 'translation' variables, calculated for arbitrary constant c where $c \in (0, \pi)$:

$$p_c(t) = \sum_{j=1}^{t} \Phi(j) sin(jc) \qquad q_c(t) = \sum_{j=1}^{t} \Phi(j) cos(jc) \qquad t = 1, 2, ..., T \tag{2.14}$$

Next, the mean square displacement, M_c, and asymptotic growth rate, K_c are computed:

$$M_c(t) = \lim_{t \to \infty} \frac{1}{T} \sum_{j=1}^{T} [p_c(j+t) - p_c(j)]^2 + [q_c(j+t) - q_c(j)]^2 \tag{2.15}$$

$$K_c = \lim_{t \to \infty} \frac{log(M_c(t))}{log(t)} \tag{2.16}$$

The theory behind the test assumes that for regular dynamics $M_c(t)$ is a bounded function in time, and therefore the asymptotic growth rate $K_c \sim 0$ as $t \to \infty$. If the time series is chaotic, $M_c(t)$ scales linearly with time so that $K_c \sim 1$ for any value of c (Fig. 2.5). The above equations describe the main principles of how the 0-1 Test for Chaos works. In practice, further implementation of the test incorporates an improved representation of determining K_c and adjustments necessary to detect weak chaos. More information on the implementation of the test and further adjustments for improved sensitivity are described in more detail by Gottwald and Melbourne (2009).

In simulations with a limited length of the time series, the test indicates chaotic dy-

namics for all values of c only if the series is strongly chaotic. In the case of weak chaos, a longer data series is required. For the data series used in the study, chaos manifests itself initially in a smaller range of values of c, which broadens when a longer time series is analysed (Fig. 2.5 c). Thus, in order for weak chaos to be detected for all values of c, the data series covering at least 10^8 d is needed. For computation efficiency, we generated time series for 50 000 d, and considered the system chaotic when chaos is indicated at the low values of the arbitrary parameter, $c \in (0.2, 0.8)$.

The 0-1 Test for chaos can only be applied to deterministic systems, where no stochastic property interferes with the future evolution of the time series, which is often referred to as dynamic noise. The test does not use the phase space reconstruction method, but works directly with the time series to detect the character of the response (Gottwald and Melbourne, 2009). Random disturbances of the same magnitude can lead to a different response at different point in time, which would result in numerical errors when estimating the mean square displacement, M_c, and could misleadingly indicate chaotic behaviour. Therefore, the method cannot be applied to the analysis of a time-series data affected by the dynamic noise that cannot be extracted from the time series, such as in a phytoplankton concentration record.

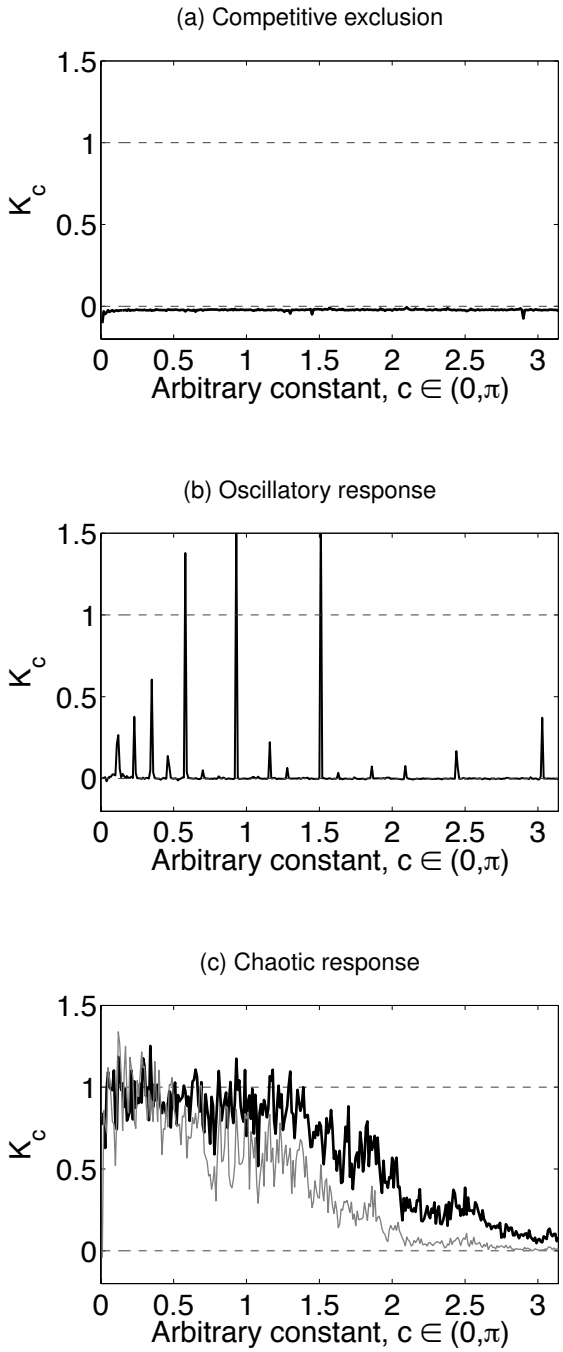

Figure 2.5: The 0-1 Test for Chaos (Gottwald and Melbourne, 2004, 2009) analysis of different characters for the phytoplankton community responses represented for (a) competitive exclusion, (b) oscillations, and (c) chaos from Fig. 4.1. The time series of species abundance used for the analysis is generated for 50 000 d. The grey line in (c) represents the output of the 0-1 Test for the time series of 10 000 d.

2.3 Chapter summary

The chapter provides an overview of the methods for verification of chaotic behaviour applied throughout the series of studies that aim to assess the phytoplankton community dynamics and the outcome of the inter-species competition. The applied methods are:

- phase diagrams and Poincaré sections that allow for a visual inspection of the phase space.
- maximal Lyapunov Exponent that verifies the sensitivity to slight modification of initial conditions
- the 0-1 Test for Chaos that uses statistical properties of the time series to verify the character of the response.

All of the methods can be applied to the analysis of the synthetic data generated by the deterministic model. However an appropriate method needs to be chosen carefully for the analysis of the time-series data, depending on the dynamical properties of the measured variable. Each of the following chapters specifies which set of appropriate methods have been applied.

CHAPTER 3

Chaos in the real-world phytoplankton communities: challenges and limitations when analysing time-series data.

Rationale:

Chaotic behaviour is believed to be a potential solution to the "paradox of the plankton", based on a number of modelling studies (Allen et al., 1993; Huisman and Weissing, 1999; Huisman et al., 2001). The aim of this chapter is to assess whether temporal variabilities in the phytoplankton records are chaotic. The main objectives include identifying difficulties that arise when attempting to analyse time-series data for chaotic behaviour, from limitations arising from insufficient sampling, to noise and seasonality masking the chaotic response. The purpose of the study is to establish the sampling requirements needed for accurate verification of chaos within the marine environment, including the sampling frequency and the length of the time series, as well as suggesting the most suitable sampling region.

3.1 Introduction

Understanding the factors determining ecosystem stability was a main objective of early ecosystem models investigating community interactions. The realization that a community can exhibit non-equilibrium, chaotic behaviour became a research focus of theoretical ecologists (Paine, 1966; May, 1974). In comparison to variability driven purely by the external factors such as weather, the fluctuations of chaotic populations are predictable over short timescales and the ability to forecast the change in a population is essential for efficient management and conservation of natural resources (Lorenz, 1963; Hastings et al., 1993). Also, chaos theory became an explanation for sustaining species coexistence and diversity, posing important implications on community functioning (Huisman and Weissing, 1999). Idealised model experiments reveal that chaotic states enable ecosystem biodiversity and support more species than there are resources, as irregular perturbations allow weaker competitors to be sustained in the environment (Allen et al., 1993; Huisman et al., 2001).

Model approaches are the most common way of investigating the plausibility of chaos to occur in the real world environments. Ecological models of the 1970s revealed unstable equilibria and complex dynamics (e.g. May, 1974; May and Oster, 1976; May, 1976). Complex behaviour arising from species interactions occurs when modelling systems of 3 or more species (May and Leonard, 1975; Price et al., 1980). Early ecological models focussed on investigating how robust the chaotic response is via predator-prey interactions (Gilpin, 1979; Schaffer, 1985; Kot et al., 1992; Hastings and Powell, 1991). Deterministic chaos was shown to be a robust response for modelled bacterial community (Becks et al., 2005), plankton-fish food webs (Doveri et al., 1993; Rinaldi and Solidoro, 1998; Medvinsky et al., 2001; Tikhonov et al., 2001) and

phytoplankton competition for nutrients (Huisman and Weissing, 2001; Huisman et al., 2006).

In order to verify that chaotic behaviour is not an artifact of ecological interactions described in models, and that chaos can occur in reality, analysis of time-series data is required. There are a limited number of possible time-series data to analyse for detection of chaos within the real-world environments. Due to the scarcity of observational time-series records, the efforts of chaos detection within real world communities were directed towards laboratory experiments. In order to optimize the time scale of laboratory experiments for collecting time-series records covering multiple generations, small organisms are preferred due to their short generation time. Chaotic behaviour has been detected previously in the chemostat experiments for insect populations (Costantino, 1997), biological nitrification (Graham et al., 2007), microbial food chains (Kooi et al., 1997; Vayenas and Pavlou, 1999; Becks et al., 2005) and planktonic food web interactions (Ringelberg, 1977; Fernández et al., 1999; Benincà et al., 2008). In particular, in the study of Benincà et al. (2008) a long-term laboratory mesocosm experiment is conducted where a multi-level food web was isolated from the Baltic Sea and cultured under constant external conditions for over six years. Species interactions generated chaotic fluctuations, proving that chaos is a feasible response of marine microbial community under steady environmental conditions.

Chemostat experiments keep the community under strongly-controlled steady state conditions, where the occurrence of chaos often depends on the carefully chosen nutrient conditions (Becks et al., 2005), and do not account for the external variability and multiple stressors shaping the community. These restrictions suggests that as much as the laboratory experiments provide a valuable insight into community behaviour and interactions, they are a crude representation of the real world environment and may

not fully represent its true complexity. There have been a limited number of attempts to verify whether chaos occurs within the observational time-series records due to limitations of short and noisy data, leading to inconclusive findings. In the analysis of the biweekly time-series record of phytoplankton blooms in Lake Kinneret, Sugihara and May (1990) and Stone et al. (1996) confirmed the underlying non-linear dynamics and suggested chaos to be a mechanism driving the irregular fluctuations in the time series. However, Turchin and Taylor (1992) found chaotic behaviour to underly only one out of 36 considered time series of insect and vertebrate populations.

No conclusive observational evidence has been presented to confirm that chaos occurs within marine microbial communities and thus verify its contribution as a potential solution to the paradox of the plankton. Marine communities have the attributes necessary to induce chaotic behaviour: determinism, food web complexity and non-linear, coupled interactions. Yet, imposed external variability interacts with population dynamics and could potentially inhibit the detection of chaotic response.

Here, we apply the maximal Lyapunov Exponent method in the attempt to detect chaotic behaviour in the phytoplankton concentration record from the English Channel, through verification of the sensitivity to initial conditions. The challenges arising from time-series data analysis are discussed, and with the use of environmental reanalysis data and synthetic data generated by a chemostat -based ecosystem model, possible solutions to the limitations are identified. This chapter also investigates how much the time-series data needs to be modified to obscure detection of chaos completely by imposing seasonality or noise, with illustrated cases when the method for chaos detection fails despite the underlying chaotic variability in the system. The aim is to provide an overview of the requirements for the time-series data that would allow determination of chaotic behaviour within the marine ecosystem.

3.2 Methods

In order to determine whether chaos occurs in marine environments, time series analysis techniques and model simulations are applied. First, the observational time-series records from the L4 station in the English Channel are analysed for chaotic behaviour using the maximal Lyapunov Exponent method. The method is then also applied for the analysis of the the SST re-analysis data for investigation whether physical variable characterizing the marine environment exhibits chaos when sampled at the higher frequency. In addition model simulations are included in order to assess the requirements for identification of chaos in a time-series record.

3.2.1 The analysis of the time-series data

Observational records from the L4 station and the SST re-analysis time-series data are processed prior to the analysis for chaotic behaviour. Power spectra are obtained for all of the time series and the slope of the decline in power density towards higher frequency is evaluated. When analysing for chaotic behaviour, the long-term trend at low frequencies, b_k, capturing the seasonal cycle and inter-annual variability are removed from the time series, Γ:

$$\Gamma(t) = \sum_{k=1}^{K} a_k \; sin\,(b_k \; t + c_k) \qquad\qquad k = 1, ..., K \tag{3.1}$$

where amplitude a_k and phase c_k coefficients corresponding to the frequency b_k are determined through harmonic analysis using a non-linear least squares fit. The periodogram is then smoothed using a cosine bell function with the window width covering 7 data points.

3.2.2 The algorithm for chaos verification

Chaotic behaviour is assessed by applying the Rosenstein et al. (1993) algorithm to estimate the maximal Lyapunov Exponent (λ_{max}) using the TISEAN package (Hegger et al., 1999). The algorithm has been successfully applied in the context of population dynamics by Benincà et al. (2008), and it is believed to be superior to the algorithm of Kantz (1994) when analysing relatively short and noisy time series (Rosenstein et al., 1993).

The details of the application of the algorithm application are descibed in Section 2.2.2. The algorithm calculates the separation, or stretching factor (CF), between trajectories initially at some "infinitely small" distance (ε) apart:

$$e^{\lambda_{max}t} \approx \frac{|x(t) - x_\varepsilon(t)|}{|x(0) - x_\varepsilon(0)|} = CF \tag{3.2}$$

where λ_{max} is referred to as the principal Lyapunov Exponent and defines the rate of separation of two trajectories, $x(t)$ and $x_\varepsilon(t)$, in time t.

For chaotic systems, CF exhibits an exponential increase over the initial period of trajectory separation, and (if the time-series record is sufficiently long) approaches saturation when the maximum distance is reached (Fig. 3.1). Here, the calculated CF is presented on a logarithmic scale and thus for confirmation of chaos one expects a linear increase in log(CF) over the initial time period. In this analysis we particularly concentrate on the behaviour of CF, and not the accuracy of the estimate of λ_{max}.

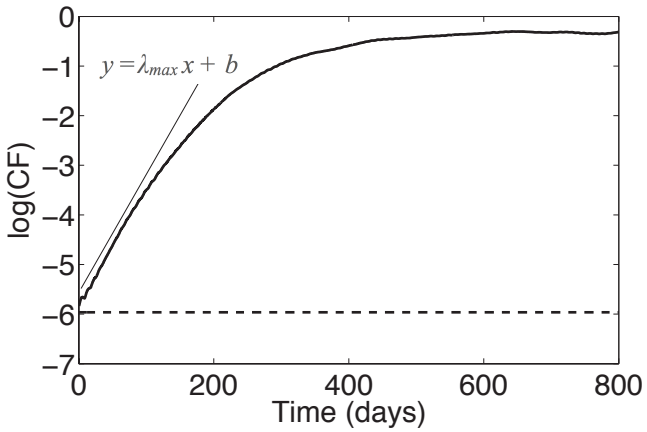

Figure 3.1: The behaviour of the stretching factor, CF, for chaotic (black line) and oscillatory systems (dashed line). The maximal Lyapunov exponent is taken as a slope of the exponential increase in CF.

3.3 Observational data from the English Channel

3.3.1 Time-series data from the L4 station

The time-series data used in the analysis are provided by a record from the L4 station in the English Channel, 50°15.00' N 4°13.02' W, obtained from the Western Channel Observatory by the Plymouth Marine Laboratory. The analysis for chaos is carried out for the concentration time series for individual taxa, phytoplankton groups and total biomass, measured from June 1995 to December 2009. The analysed time series of nutrient concentrations include the measurements of nitrite, nitrate+nitrite, ammonia, phosphate and silicate collected from January 2000 to September 2012. To investigate whether the biological community behaves in the same manner as the surrounding physical environment, the analysis for chaos is also carried out for the salinity and sea surface temperature (SST) time series. Salinity was recorded at the depth of 2 m from January 2002 to December 2011. The SST time series covers the time period from March 1988 - December 2011. In order to obtain a long and continuous SST record, the time series is a compilation of 3 different measuring techniques: bucket temperat-

ure (3/1988 - 12/2007), CTD instrument at 0 m (5/1993 - 2/2000), and SeaBird CTD at 2 m (1/2002 - 12/2011). All time series are sampled predominantly every 1-2 weeks. Time-series data is interpolated onto a weekly grid with any missing data linearly interpolated over.

Phytoplankton community at the L4 station is dominated by phytoflagellates that sustain their high concentrations throughout the year. Strong seasonal and inter-annual variability is observed within the time series of diatoms and dinoflagellates revealing a seasonal succession and decoupling in the timing of the blooms (Fig. 3.2). Non-motile diatoms are well-adapted to turbulent environments and thrive at the initial stage of spring stratification. Motile dinoflagellates benefit in the stratified water column and thrive when the stratification is well established (Margalef, 1978).

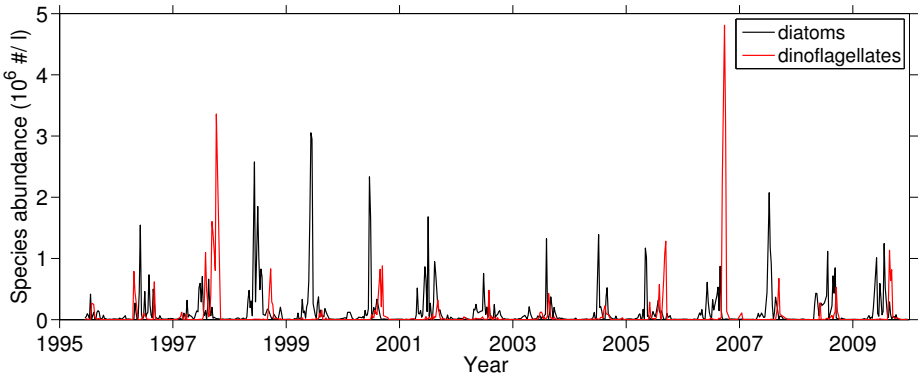

Figure 3.2: Concentration time-series record for diatoms (in black) and dinoflagellates (in red) at the L4 station in the English Channel from June 1995 to December 2009.

3.3.2 Power Spectrum analysis

A normalized frequency power spectrum reveals inter-annual variability in the physical and biological environment and confirms that seasonality is the dominant variability (Fig. 3.3 and 3.4). A gradual decline in power density towards frequencies higher than the frequency of seasonality is detected for each time series. SST responds

to meteorology more rapidly than measured biological quantities and thus exhibits relatively low variability on shorter timescales (Fig. 3.3 a). For biological components, the slope of the decline in power density may reflect the effect of the environmental variability, physical transport processes as well as control from predators (Fig. 3.3 b,c). Large concentrations of phosphate and nitrate supplied from riverine inputs (Fraser et al., 2000) lead to lower variability in those resources at high frequencies (Fig. 3.4 a,b). Additionally, the slope of the decline in power density is affected by the rate of nutrient utilization, e.g. diatoms utilize silica quicker on short timescales leading to a sharper decline in power density (Fig. 3.4c).

A decline in power density towards higher frequencies is characteristic for integral quantities and indicates an internal memory in the system. Such a power spectrum distribution is characteristic for chaotic time series as well as Brownian (red) and flicker (pink) noise. The decline in the power density is proportional to f^{-2} for red and f^{-1} for pink noise, where f denotes a frequency (Timmer and König, 1995; Szendro et al., 2001; Rudnick and Davis, 2003). In comparison, white noise or stochastic variability are characterised by a uniform power spectrum distribution.

3.3.3 Verification of chaos

Seasonal and inter-annual frequencies indicated in Fig. 3.3 and 3.4 are removed from the time series, which are subsequently analysed for chaotic behaviour. The analysis for chaos detects no increase in the stretching factor (CF) for the time series of total biomass and phytoflagellate concentration (Fig. 3.5 a,c). A linear increase in log(CF) is observed for the concentration time series of diatoms and dinoflagellates with estimated $\lambda_{max} = 0.004\ d^{-1}$ for both time series, which indicates the timescale of

predictability of 250 days (Fig. 3.5 b,d). This result suggests the inter-annual variability in the species concentration time series (see Fig. 3.2) is partially driven by the chaotic character of the phytoplankton response.

Similar analysis output is also obtained for the time series for concentration of specific taxa, such as *Nitzschia closterium*, *Pseudo-nitzschia delicatissima* and *Emiliania huxleyi*. Note that the occasional drops in log(CF) are a numerical artifact of the applied algorithm. The oscillatory character of the evolution of log(CF) with time might be an indication of a temporal character to the chaos, however longer time-series data would be essential to confirm this.

Chaos is not detected within the sea surface temperature record (Fig. 3.6 a). The evolution of CF for salinity time series shows a gradual increase over the initial 200 days of algorithm iteration (Fig. 3.6 b). The results look more promising for the time series of ammonia and silicate concentration, and reveal a continuous, linear increase in log(CF) indicting weak chaos with $\lambda_{max} = 0.0006\ d^{-1}$ and $\lambda_{max} = 0.0004\ d^{-1}$ respectively (Fig. 3.6 c,d). Chaotic behaviour is not, though, detected within nitrite, nitrite+nitrate and phosphate concentration time-series data.

(a) Sea surface temperature

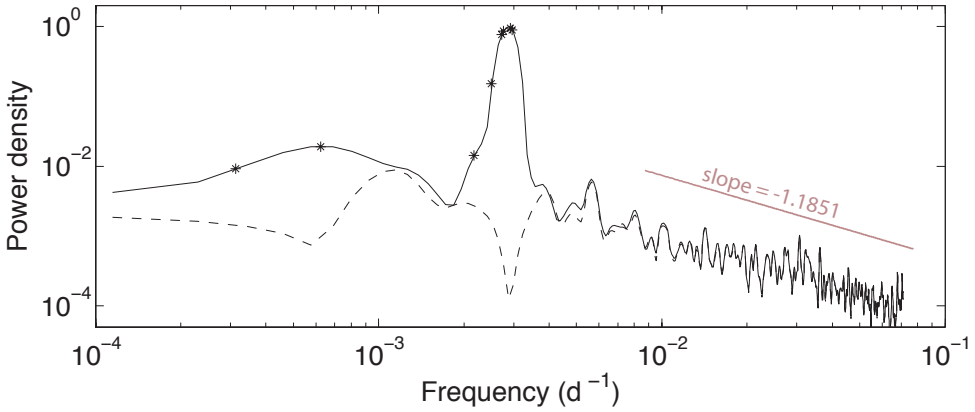

(b) Total phytoplankton concentration

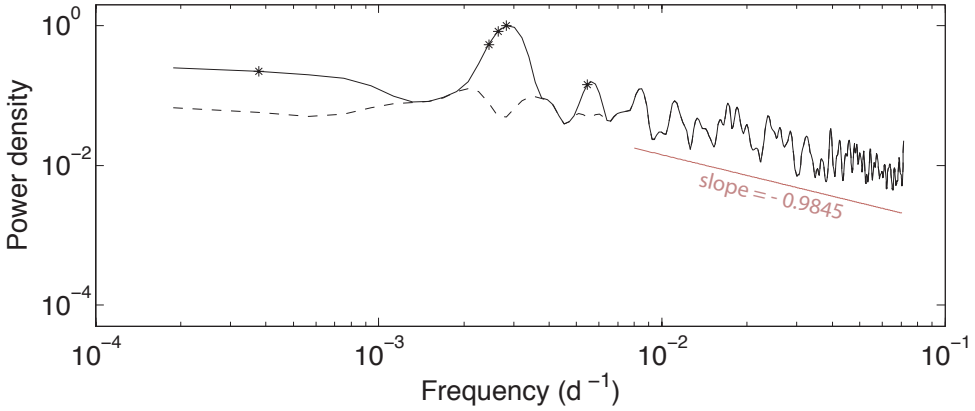

(c) Diatom concentration

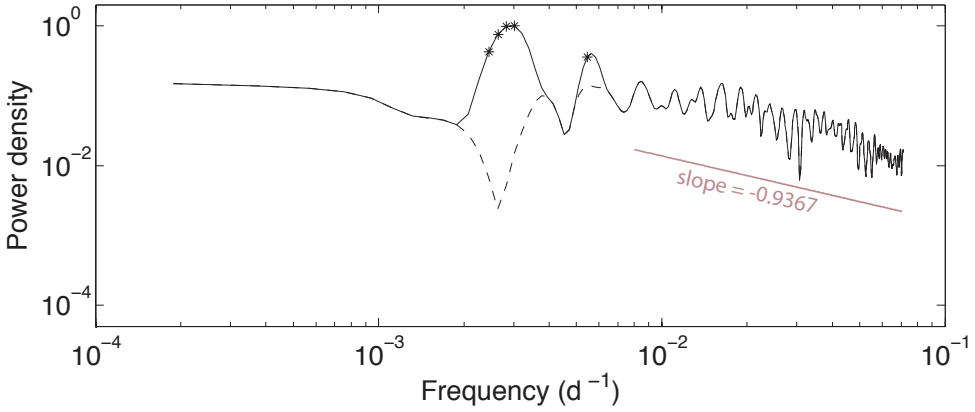

Figure 3.3: Normalized frequency power spectra for the time-series data of (a) sea surface temperature, (b) total phytoplankton concentration, and (c) diatom concentration at the L4 station, English Channel (black, solid line). The long-term trend is removed from the data, and symbol $*$ denotes the frequencies removed from the time series before the analysis for chaos. Power spectra for the data after removal of chosen frequencies are indicated by the dashed lines.

(a) Phosphate concentration

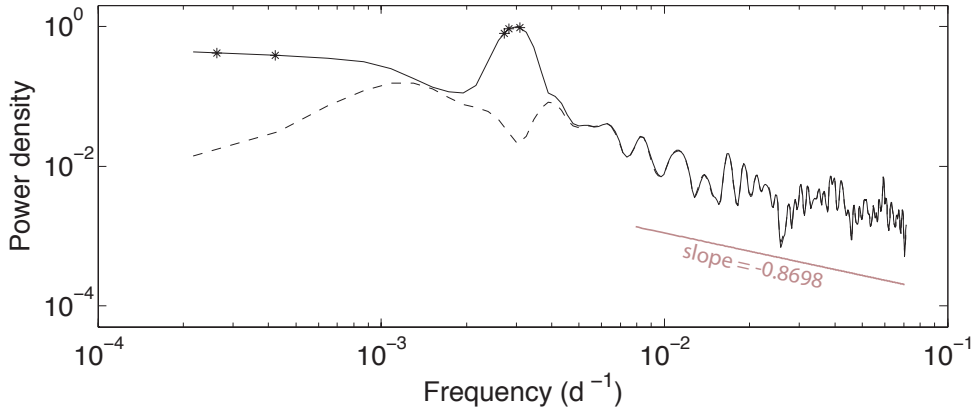

(b) Nitrite + nitrate concentration

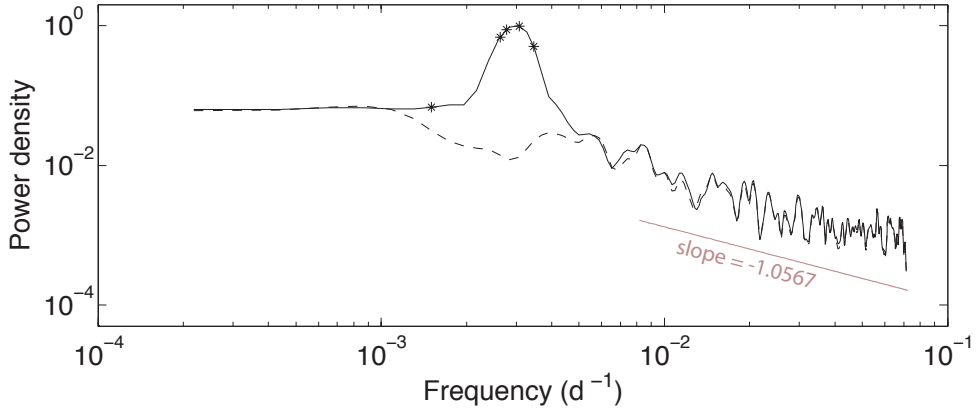

(c) Silica concentration

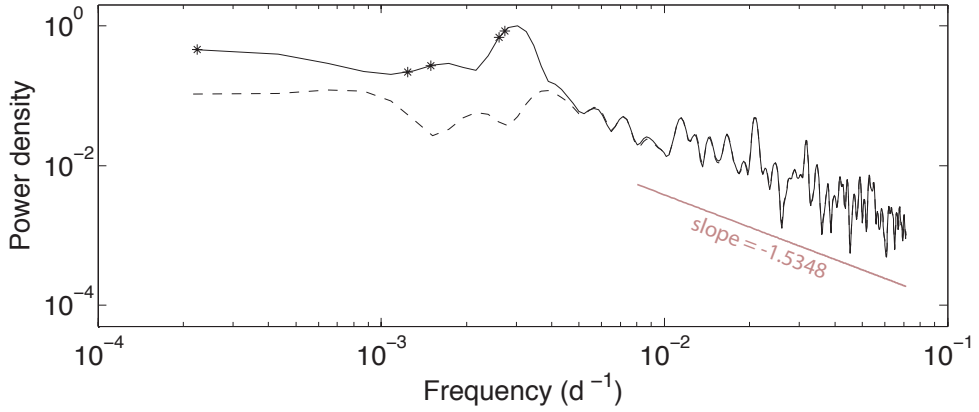

Figure 3.4: Normalized frequency power spectra for the time-series data of (a) phosphate, (b) nitrite + nitrate, and (c) silica concentration at the L4 station, English Channel (black, solid line). The long-term trend is removed from the data, and symbol $*$ denotes the frequencies removed from the time series before the analysis for chaos. Power spectra for the data after removal of chosen frequencies are indicated by the dashed lines.

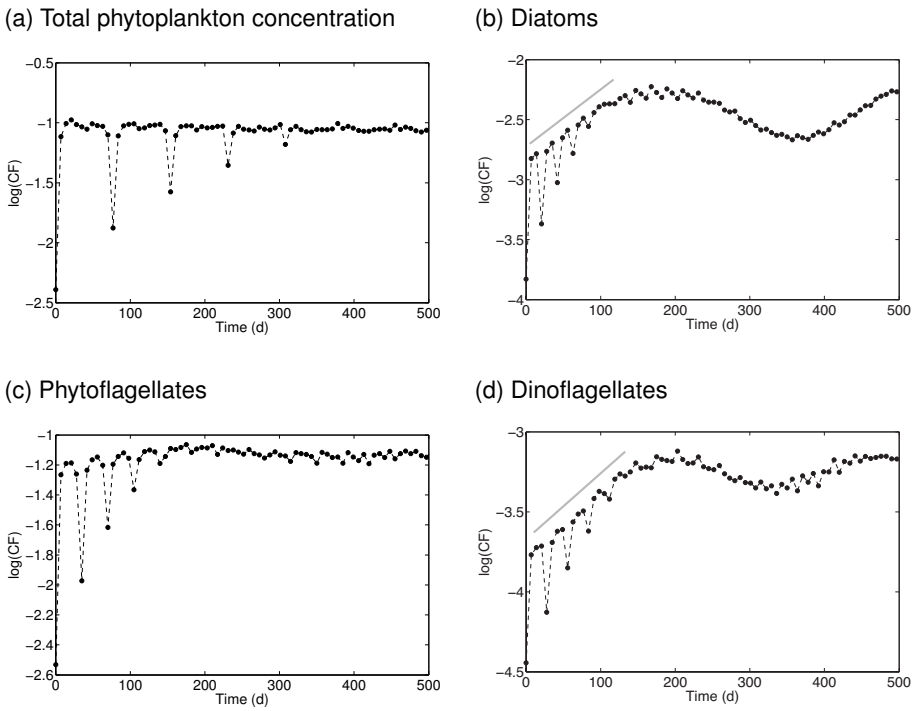

Figure 3.5: The time evolution of the stretching factor (CF) for the weekly concentration time series for (a) total phytoplankton, (b) diatoms, (c) phytoflagellates and (d) dinoflagellates. Time-series data obtained for the L4 station, English Channel.

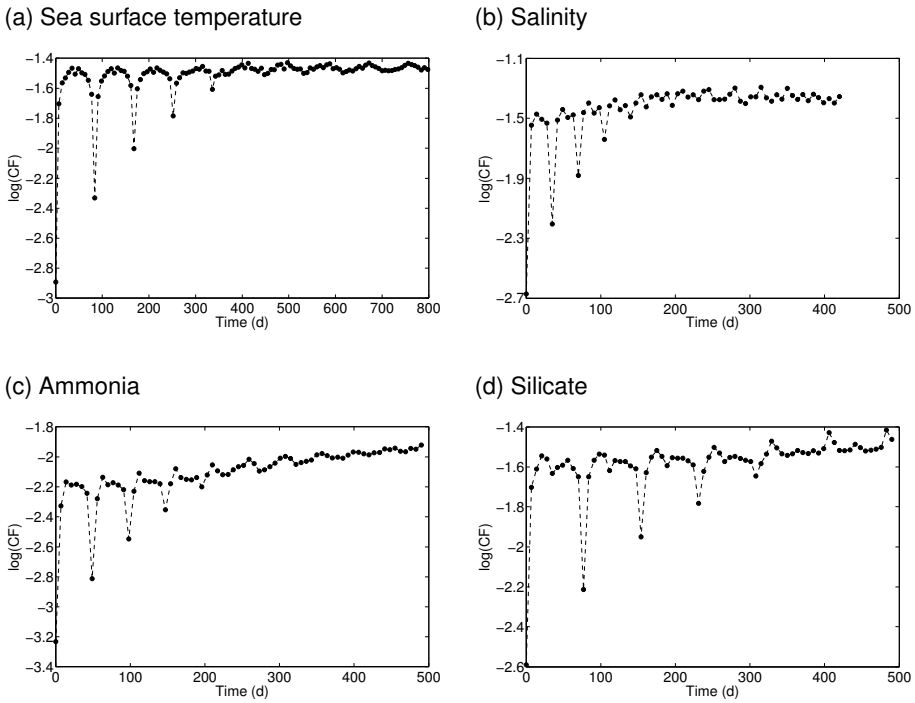

Figure 3.6: The time evolution of the stretching factor (CF) for the weekly time series for (a) sea surface temperature, (b) salinity, (c) ammonia and (d) silicate concentration. Time-series data obtained for the L4 station, English Channel.

3.4 SST re-analysis data from the English Channel

The investigation of the re-analysis data aims to explore whether longer and finely sampled time series allows for detection of chaos within the physical environment. The sensitivity of the chaos detection method to the length of the time series and the sampling frequency is explored. The analysis is then compared to the findings obtained for the observational record from the L4 station in the English Channel.

3.4.1 The SST re-analysis time series

The sea surface temperature re-analysis data are obtained from the European Centre for Medium-Range Weather Forecasts (ECMWF) data server for the location 50°N 4°W, corresponding to the location of the L4 station (Fig. 3.7). The time series covers 34 years, from January 1979 to December 2013, with fields sampled daily at noon to exclude any daily variability that would appear with a higher sampling frequency. The analysis for chaos is carried out for the SST re-analysis record for a range of record lengths, t: 2, 3, 5, 10 or 20 years, and sampling frequencies, τ: data sampled every 1, 2, 3, 5 or 7 days.

3.4.2 Power spectrum analysis

The power spectrum for the SST re-analysis data suggests that apart from inter-annual and annual variability, a semi-annual frequency component is more significant than previously indicated in the analysis of the observational SST record at the L4 station (Fig. 3.8). The decline of power density towards higher frequencies is greater than indicated by the observational records ($slope = -1.8$), and resembles the power density distribution of red noise. For comparison with the observational data sampled approximately every 2 weeks, biweekly sampling of the re-analysis data yields a decline in

power density with $slope = -1.7$, and thus remains significantly higher than that calculated for the observational SST record.

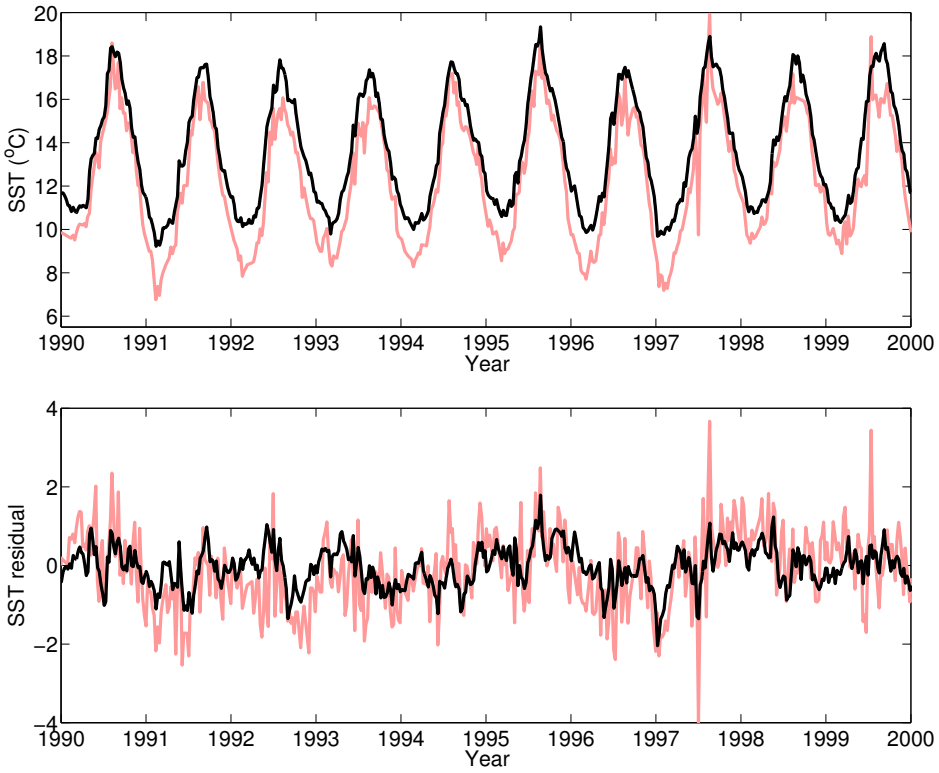

Figure 3.7: Time series for sea surface temperature from 1990 to 2000 retrieved from the ECMWF re-analysis data served for the location of the L4 station in the English Channel (in black; top panel). Observational records from the L4 station obtained by the Western Channel Observatory are indicated in red. The bottom panel illustrates the SST residual after the long-term trend and dominant frequencies in the original time series are removed.

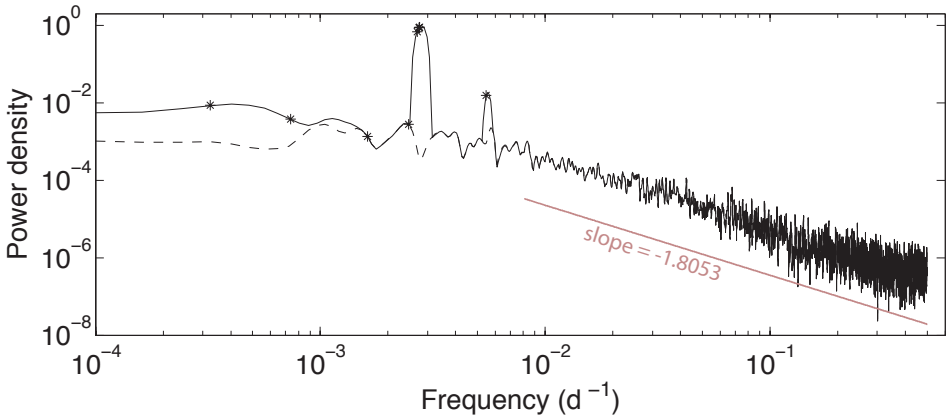

Figure 3.8: Power spectrum analysis for SST time series retrieved from the ECMWF re-analysis data served for the location of the L4 station in the English Channel from January 1979 to December 2013 (solid, black line). The long-term trend has been removed from the data, and symbol $*$ denotes the frequencies removed from the time series before the analysis for chaos. Power spectrum for the data after removal of chosen frequencies is indicated by the dashed line.

3.4.3 Verification of chaos

The algorithm of Rosenstein et al. (1993) is applied to the complete, 34-year record of daily fields of SST after the seasonal variability is removed from the data. The results reveal an exponential dependance on initial conditions with $\lambda_{max} = 0.0002\ d^{-1}$ indicating a weakly chaotic system with predictability timescale of 5000 days (Fig. 3.9).

A minimum of 3 years of daily measurements are essential to indicate the chaotic character of the system (Fig. 3.10 a). Increasing the length of the time series to 10-20 years increases the robustness of the analysis and provides a good estimate of $\lambda_{max} = 0.00015\ d^{-1}$. Weekly sampling is not sufficient to capture chaotic features of the time series and chaos is not detected even for the longest of the time series used (Fig. 3.10 b). The most robust, linear increase in log(CF) is observed for the time series sampled daily or every other day. Further decreases in the sampling frequency increases the variability in log(CF) and further inhibits chaos verification within the time series (Fig. 3.11).

The findings remain consistent with the observations at the L4 station: 23 years of

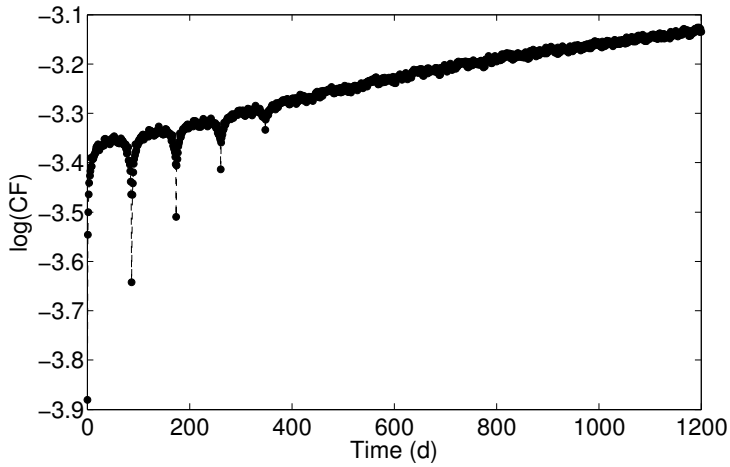

Figure 3.9: The time evolution of the stretching factor, CF, for the sea surface temperature re-analysis data. The time series is obtained from the ECMWF data server, sampled daily from January 1979 to December 2012. Long-term trend, seasonal and inter-annual variability have been removed from the time-series data.

weekly SST measurements at the L4 station is not sufficient to confirm the occurrence of chaos. In this case, the analysis is not limited by the length of the time series, but the insufficient sampling frequency.

(a) Daily fields

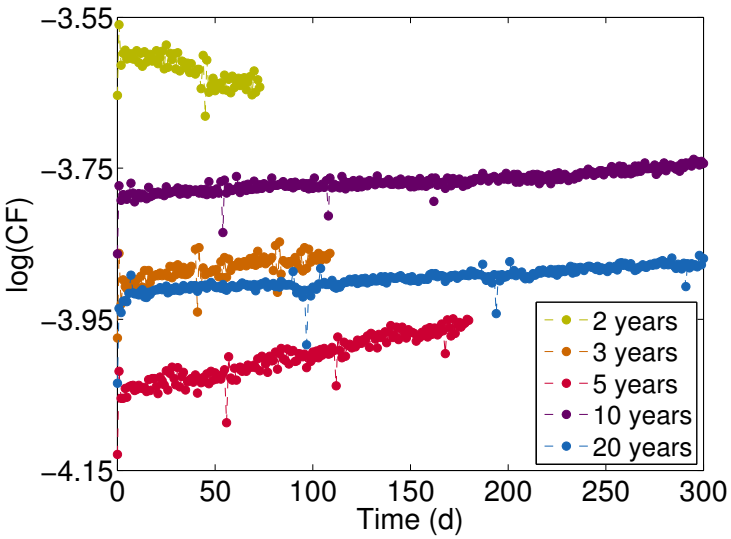

(b) Weekly fields

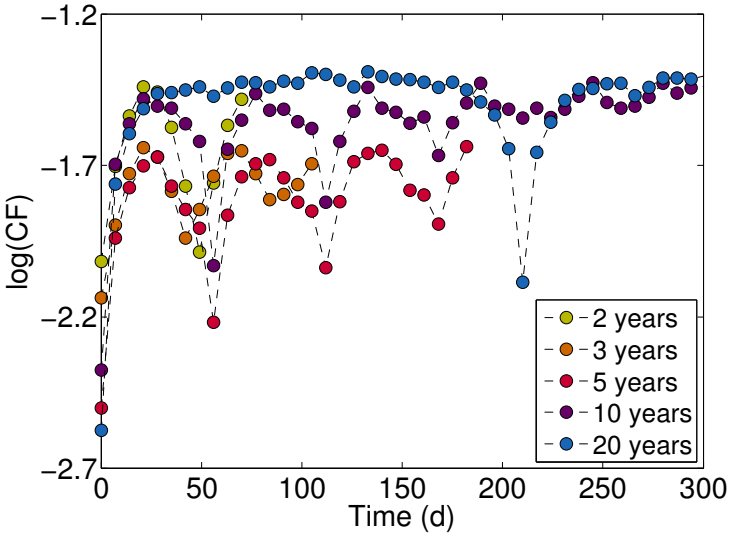

Figure 3.10: The dependance of the length of the sea surface temperature time series on chaos verification. The time-series data is obtained from ECMWF re-analysis data server, ERAinterim. The analysed time series is sampled at (a) daily (at noon), or (b) weekly frequencies with the variable length of the time series: 2, 3, 5, 10 or 20 years.

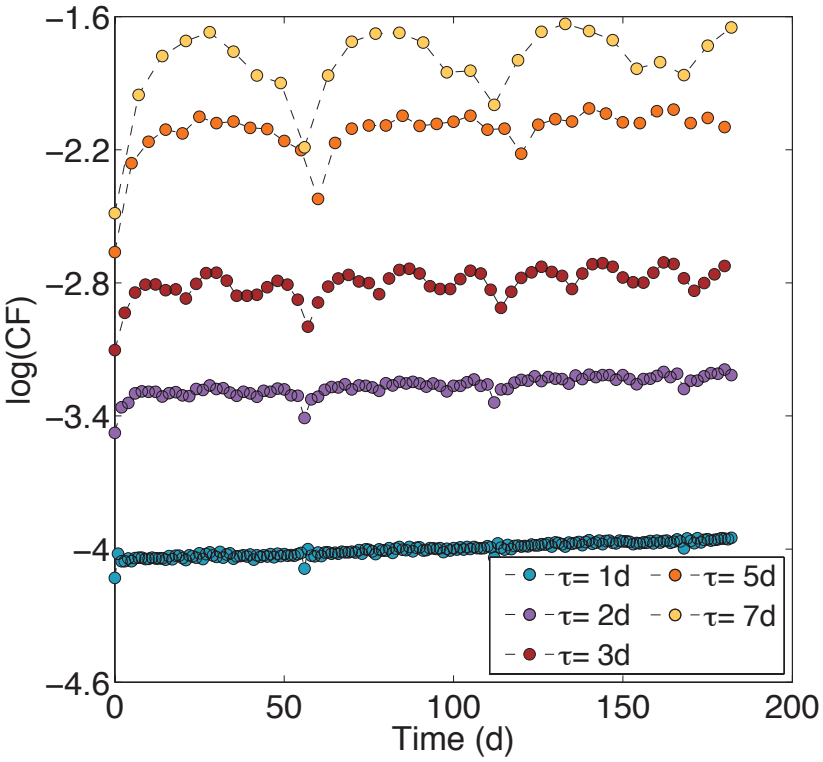

Figure 3.11: The time evolution of the stretching factor, CF, dependent on the sampling frequency. The data used is the 5 year record (1979 - 1984) of sea surface temperatures at 50^{o}N 40^{o}W, obtained from ECMWF re-analysis data server (ERAinterim).

3.5 Model simulations

The skill of the applied algorithm for estimation of the maximal Lyapunov Exponent is now explored using idealized model simulations. The sensitivity of the method is investigated subject to the length of the available time series and its sampling frequency. Additionally, the algorithm is tested against the modelled time-series data with imposed seasonal or stochastic variability.

3.5.1 Model formulation and experiments

A simple well-mixed box model for inter-species competition for nutrients is used for the analysis of how sensitive verification of chaos is to (1) sampling frequency and the length of the time series, (2) imposed seasonal forcing and (3) noise. The applied model is as described in Section 2.1, and generates weakly chaotic behaviour. The modelled phytoplankton community is initiated with 5 species competing for 5 resources and parameterized as described in Table 2.1 (p. 26). The simulations cover 10500 days with the initial 500 days treated as the spin-up time and excluded in the analysis of the time series.

(1) Sampling frequency and the time series length

The model generates a community oscillating at a period of about 38 days. Modelled species concentration time series is subsampled with the sampling period $\tau = 0.1$, $\tau = 1$ and $\tau = 7$ days, and analysed for chaotic behaviour. Monthly sampling is not considered in the analysis as in reality it is used to investigate the seasonal patterns of phytoplankton and would be insufficient to resolve for the irregular fluctuations on

the top of the seasonal pattern. For investigation of the sensitivity to record length, the modelled community is sampled over a range of record lengths: 2, 3, 5, 10 and 20 years, with the analysis outcome then compared between daily and weekly sampled time series.

The results are then compared against the Lorenz system described in section 2.2.2 (p. 31). The Lorenz equations are integrated over 10500 days with the parameters $\sigma = 10$, $\rho = 28$ and $\beta = 8/3$ generating chaos, and again the initial 500 days are excluded from the analysis. The Lorenz system oscillates at a relatively high period of 0.84 day and is subsampled at the same sampling frequencies as discussed above for the ecosystem model.

(2) Seasonal forcing

The nutrient concentration in the model is forced with sinusoidal variation in the nutrient supply of seasonal frequency. The equation for concentration of nutrient j, N_j, now becomes:

$$\frac{\partial N_j}{\partial t} = D(S_j(1 + \alpha sin\left(\frac{2\pi t}{T}\right)) - N_j) - \sum_{i=1}^{n} Q_{ji} r_i \gamma_i^N P_i \qquad j = 1, ..., k \qquad (3.3)$$

where the external forcing period $T = 360$ days, and α denotes the forcing amplitude. The experiment was carried out with a range of forcing amplitudes, $\alpha = 20\%$, $\alpha = 60\%$ and $\alpha = 100\%$, reflecting different impact levels of seasonality. The model output is subsampled with $\tau = 1$ day and analysed for chaotic behaviour.

(3) Noise

Gaussian noise is generated using the TISEAN package (Fig. 3.12). The signal is uncorrelated with independent, daily samples. The algorithm is used to generate a stochastic time series covering 10000 days. The noise time series is then linearly interpolated at $\tau = 0.1$ day, which introduces time-dependence of 1 day. The method for chaos verification is applied to the signal to investigate the behaviour of the stretching factor in noisy data without underlying chaotic behavior. Subsequently, a noisy signal of varying magnitude, referred to as % noise level, is added on top of the chaotic species concentration time series generated by the model in (1), in order to investigate how the level of measurement noise inhibits the capability for chaos detection using the Lyapunov Exponent method. The effect of temporarily correlated stochastic forcing that interacts with phytoplankton community dynamics is explored in Chapter 5.

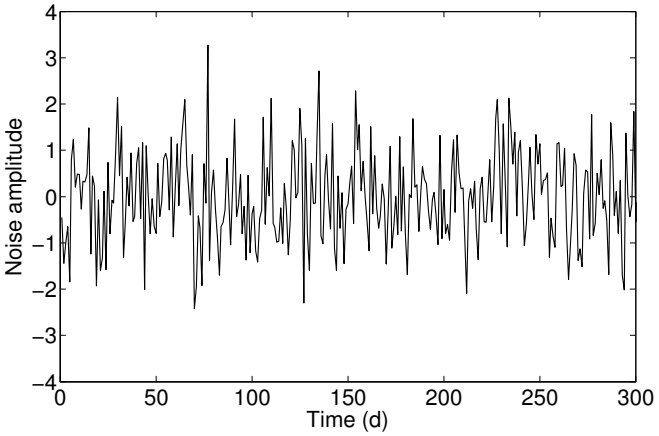

Figure 3.12: Gaussian noise with absolute variance $r = 1$ generated using the TISEAN package.

3.5.2 Sampling frequency and length of the time series

The phytoplankton community generated by the well-mixed box model with realistic parameter values, is sampled at $\tau = 0.1\ d^{-1}$ and yields the Lyapunov exponent estimate of $\lambda_{max} = 0.01\ d^{-1}$. For this relatively low-frequency system, daily and weekly

sampling slightly overestimates the maximal Lyapunov exponent with $\lambda_{max} = 0.014\ d^{-1}$ and $\lambda_{max} = 0.013\ d^{-1}$ respectively, however, it is sufficient to confidently determine the chaotic behaviour within the modelled community (Fig. 3.13 a).

In comparison, the Lorenz system sampled at $\tau = 0.1\ d^{-1}$ is characterized by exponential divergence rate of $\lambda_{max} = 0.72\ d^{-1}$. Sampling the system at 1 day^{-1} aliases the original signal, and introduces some numerical bias during the analysis for chaos. Sampling at lower frequencies, fails to capture key features characterizing this high-frequency system and introduces significant errors when verifying the chaotic behaviour (Fig. 3.13 b).

Sampling frequency has important implications when considering the length of the time series required to confidently verify chaotic behaviour. For the modelled phytoplankton community, 2 years of daily sampled data is sufficient to see an indication

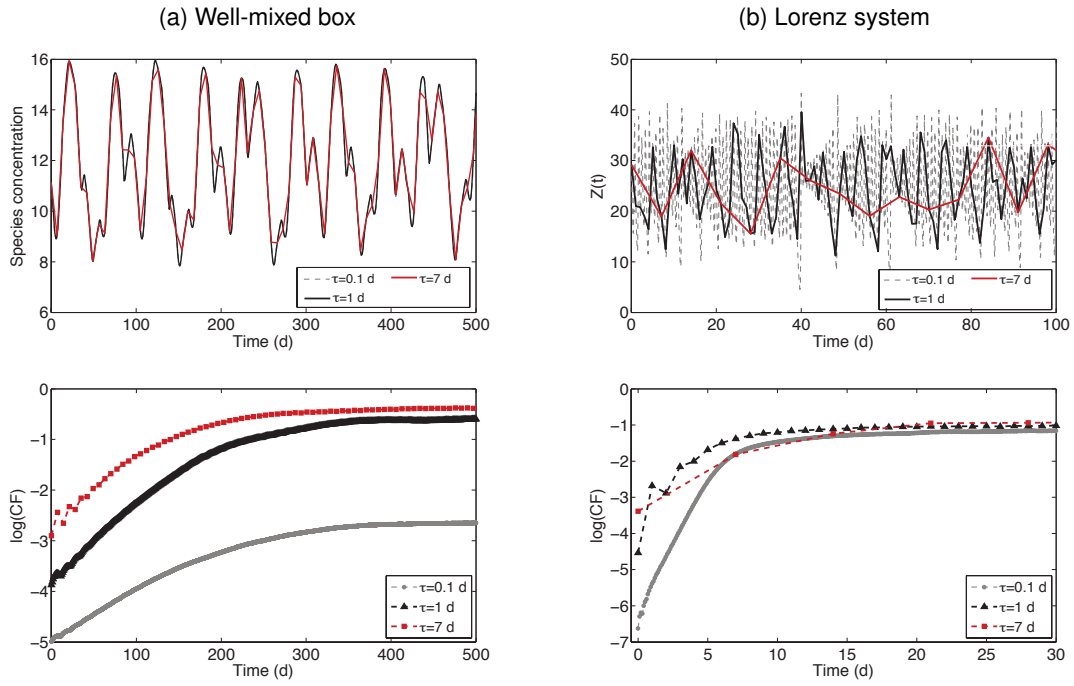

Figure 3.13: The time series for the concentration of species 1 generated by the well-mixed box model (a) and the time-series for variable Z(t) of the Lorenz system (b). Both time-series are subsampled at different sampling frequencies: 10 day^{-1} (grey), 1 day^{-1} (black), and 1 week^{-1} (red), and then analysed for chaotic behaviour. The behaviour of the stretching factor, CF, corresponding to each time-series is indicated in the bottom panels.

of chaotic behaviour (Fig. 3.14 a). For the time series sampled at weekly frequency over 2 to 3 years, an increase in CF is observed, however the initial instability in the stretching factor could introduce some uncertainties (Fig. 3.14 b). The accuracy of verifying chaos increases with the time-series length. For the most robust results, at least a 10 year record is required, and this holds for daily as well as weekly sampled data (Fig. 3.14).

(a) Daily fields

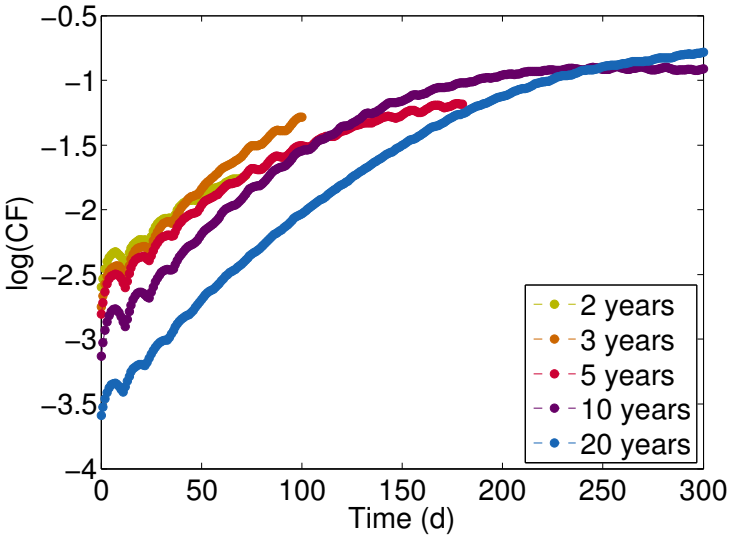

(b) Weekly fields

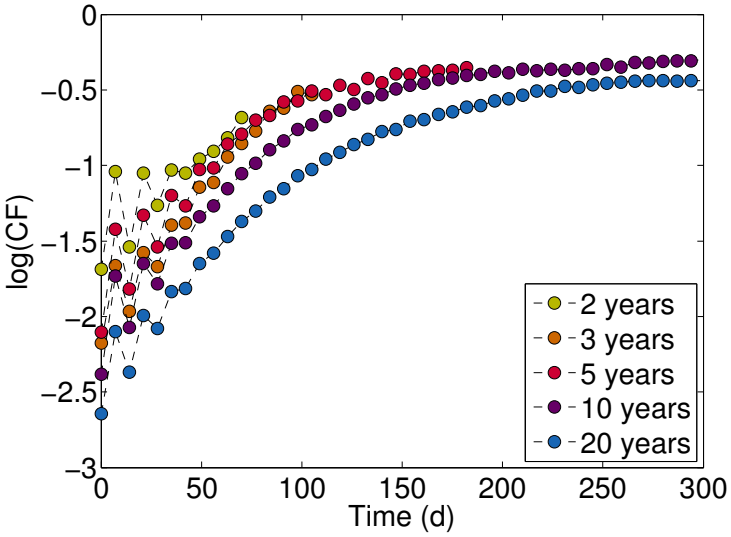

Figure 3.14: The dependance of the length of the model time series on the analysis for chaos. The time-series data is generated using the well-mixed box model. The analysed time series is sampled (a) daily, or (b) weekly with the variable length of the time series: 2, 3, 5, 10 or 20 years.

The comparison to the Lorenz system aims to illustrate how the intrinsic frequency of the system affects the requirements for the length and the sampling frequency of a time series. High frequency system, in this case the Lorenz equations, needs to be sampled more often in order to accurately capture the dynamics, however this allows a shorter time series to be sufficient for chaos detection. This relation illustrated a trade-off between the minimum required sampling frequency and the length of a time series, which is strongly dependent on the intrinsic frequency of the considered system. Extending the time series length decreases the error in the approximation of λ_{max}.

3.5.3 The effect of seasonal forcing

The phytoplankton community at the L4 station is strongly controlled by the seasonal variability in the nutrient environment, which could modify the internally generated response to the competition. Application of the power spectrum analysis and the algorithm of chaos verification aims to reveal the features that chaotic systems may display under imposed seasonal variability. The analysis of the model output is to outline the possible features of the power spectrum distribution for the community exhibiting a chaotic response. This can be then compared with the findings obtained for the observation and re-analysis time-series data. The seasonally-forced, chaotic community is then analysed for chaotic behaviour to verify whether the applied algorithm succeeds to capture chaos underlying seasonality.

Power spectrum

The power spectrum analysis was carried out for the modelled phytoplankton community that exhibits weakly chaotic behaviour and is subjected to the seasonal variability in nutrient supply. Seasonality becomes the dominant frequency and the power density function exhibits a decline towards higher frequencies generated by the modelled ecosystem (Fig. 3.15). For the community forced with weak seasonality, an amplified power density is recorded for the frequency range approximating the frequency of the unforced community, $0.02 - 0.03d^{-1}$ (corresponding to oscillation period of 30-50 days) is still detectable (Fig. 3.15 a). The contribution of this frequency component becomes statistically insignificant as the magnitude of the seasonal forcing increases (Fig. 3.15 b, c).

For daily sampled model data, the rate of the decline of power density towards higher

(a) Weak seasonality

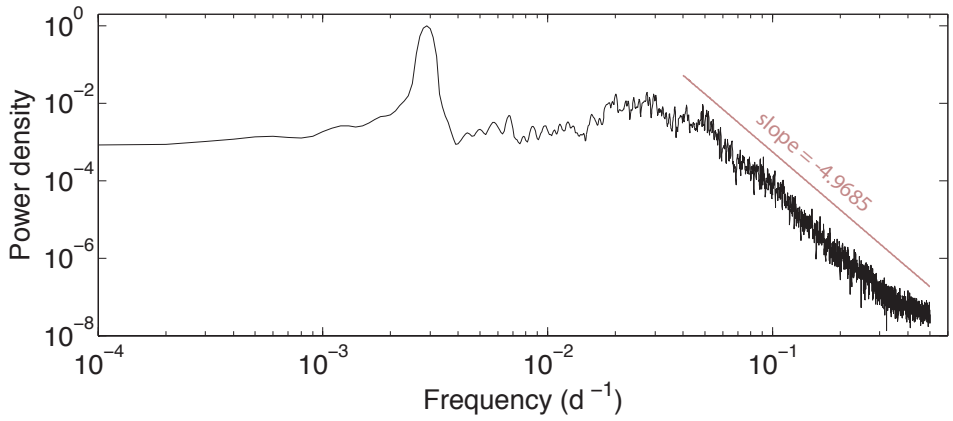

(b) Moderate seasonality

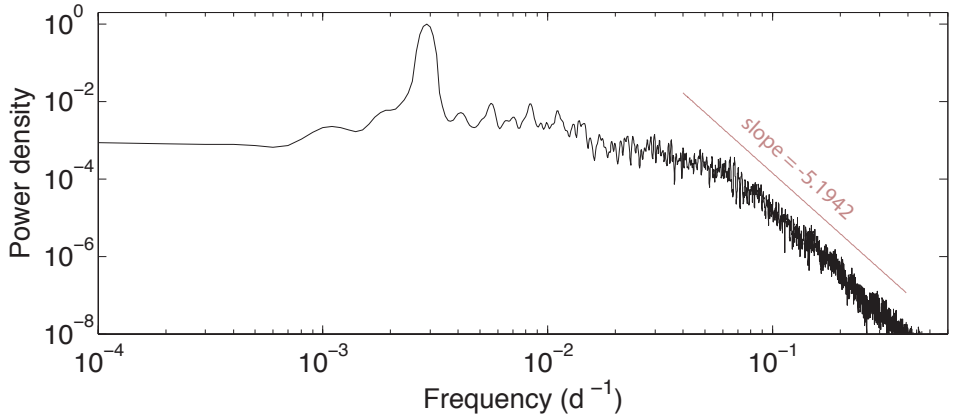

(c) Strong seasonality

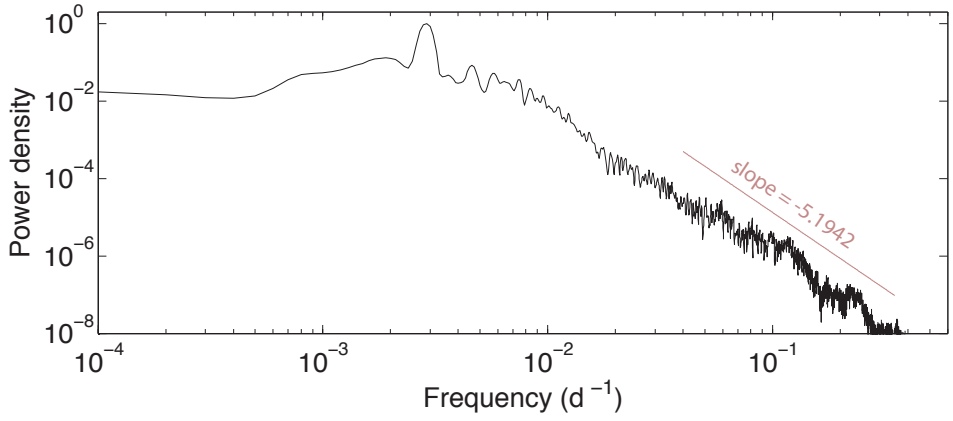

Figure 3.15: Normalized frequency power spectrum for the concentration time series of Species 5 generated by the ecosystem model, with imposed different strength of the seasonal forcing: (a) weak, $\alpha = 20\%$, (b) moderate, $\alpha = 60\%$, and (c) strong, $\alpha = 100\%$. The model output is sampled *daily*.

frequencies is at least twice as high as the rate estimated for observational and re-analysis data. This rapid decline is usually observed for frequencies higher that $0.03\ d^{-1}$ and weekly sampling may not be sufficient to resolve for such feature. For example, for the modelled ecosystem with imposed moderate seasonal forcing, $\alpha = 60\%$ and weekly sampling, the rate of the decline of power density towards higher frequencies is estimated to vary from $-1.10\ d^{-1}$ to $-2.17\ d^{-1}$ (Fig. 3.16 a), which is characteristic of a power spectrum of pink or red noise, and is comparable to the findings of the spectral analysis carried out for the observational and re-analysis data from the L4 station.

Chaotic behaviour is a feature of the modelled ecosystem and therefore can be detected in the time series of modelled nutrient concentrations. The power spectrum for nutrient time series closely follows the distribution obtained for the modelled phytoplankton (Fig. 3.16 b, c). The rate of the decline in power density varies between different nutrients due to the variability in the nutrient requirement and utilization by phytoplankton, which in the model is determined by cell traits, half-saturation coefficient and cell quota, that differ between species.

(a) Abundance of Species 5

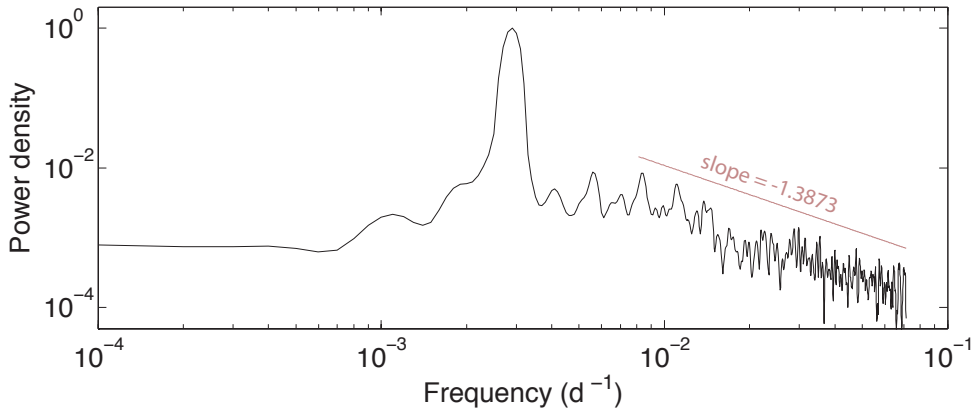

(b) Concentration of Resource 3

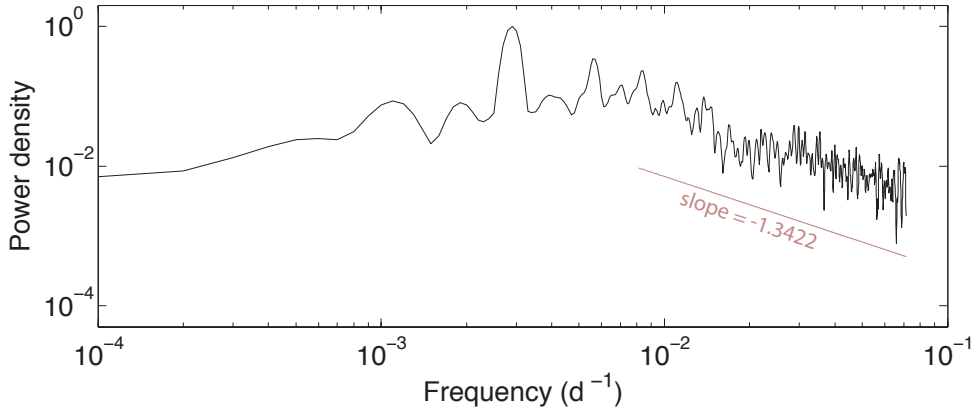

(c) Concentration of Resource 5

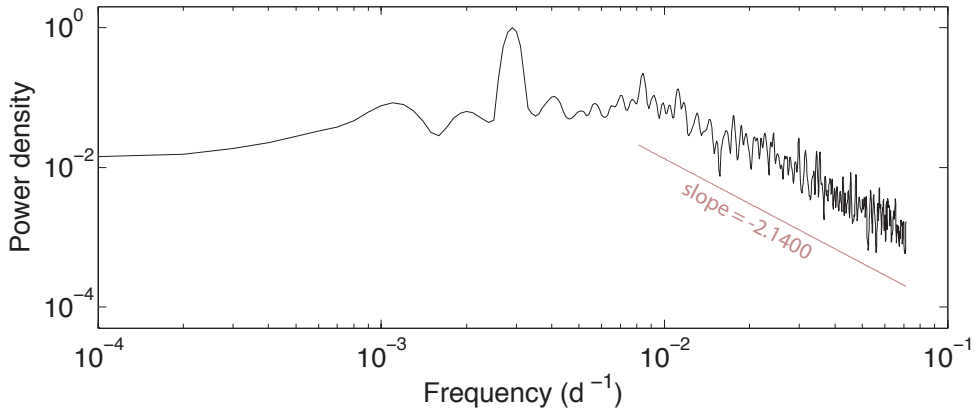

Figure 3.16: Normalized frequency power spectrum for the time-series data generated by the ecosystem model with imposed moderate seasonality ($\alpha = 60\%$): (a) abundance of Species 5, and the concentration time series of (b) Resource 3 and (c) Resource 5. The model output is sampled *weekly*.

Verification of chaos

Imposing a periodic forcing in the ecosystem model changes the character of the system, as when forcing the chaotic community with seasonal variability in the nutrient concentration, seasonality becomes the dominant frequency. At low forcing amplitude the system exhibits oscillations consisting of periodic, seasonal variability and chaotic fluctuations of the unforced community (Fig. 3.17 a). Increasing the forcing amplitude to moderate exhibits similar features, but deviating anomalies indicate an emerging inter-annual variability (Fig. 3.17 b). Inter-annual variability becomes more apparent for strong seasonal forcing: timing and the strength of the phytoplankton blooms vary annually. Although strong seasonality acts to mask chaos, underlying chaotic features pose an important implication for phytoplankton community dynamics (Fig. 3.17 c).

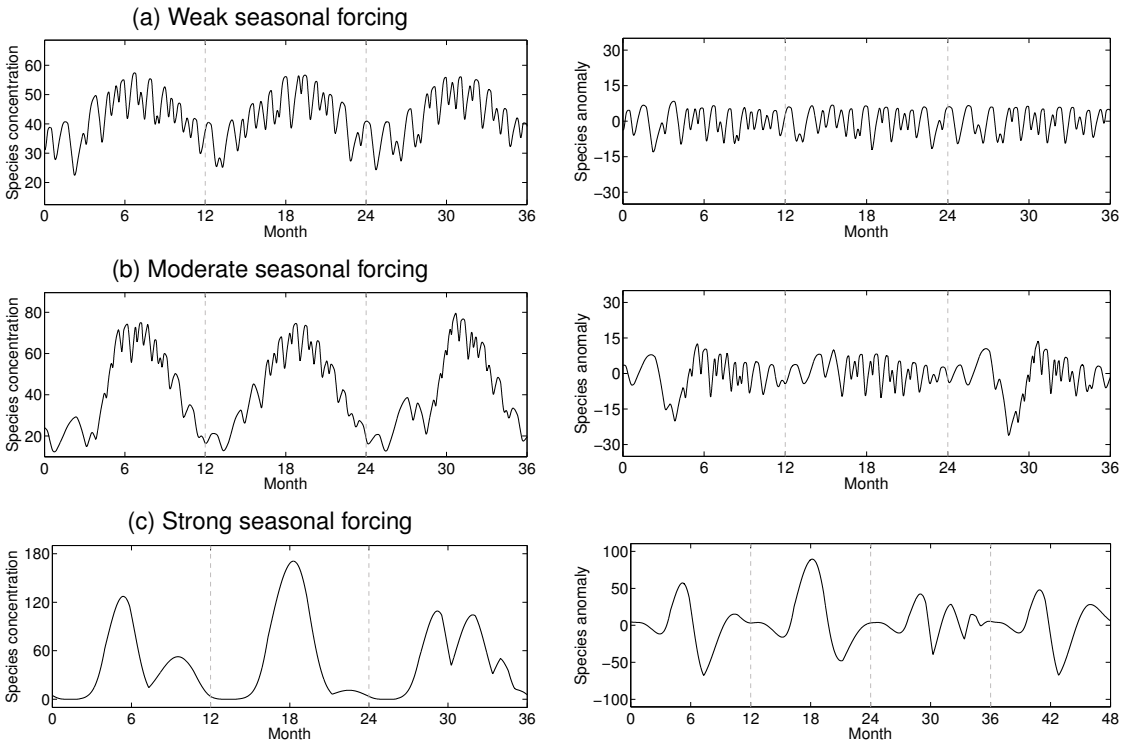

Figure 3.17: Phytoplankton community response to different strength of seasonal forcing: (a) weak with $\alpha = 20\%$, (b) moderate with $\alpha = 60\%$, and (c) strong with $\alpha = 100\%$ (see Eq. 3.3). The concentration of species 5 is indicated in the left panels, and the seasonal anomaly in the right panels. Vertical lines indicate the end of a 12-month period.

Weak chaos can still be detected within the daily-sampled phytoplankton community subjected to weak seasonal forcing. The analysis of the time series clearly shows an exponential increase at a rate $\lambda_{max} = 0.026\ d^{-1}$ and further saturation in the stretching factor (Fig. 3.18 a). Further analysis indicates that more profound seasonal forcing weakens the chaotic response, with $\lambda_{max} = 0.0023\ d^{-1}$ recorded for community under moderate seasonal forcing (Fig. 3.18 b). When forcing the community with strong seasonality, the algorithm fails to detect chaos: the evolution of CF is indicative of regular dynamics and could indicate quasi-periodic behaviour (Fig. 3.18 c).

Additionally, strong seasonality drives the evolution of a long-term trend, ζ, which feature does not prevail within the modelled phytoplankton community exposed to weak or moderate seasonality. Strong seasonal forcing causes 3 species to reveal a significant increase of $0.11 - 0.23\ yr^{-1}$ and 1 species exhibiting a decrease of $\zeta = -0.19\ yr^{-1}$, with remaining 1 species showing less significant long-term change in its abundance of $\zeta = 0.034\ yr^{-1}$ over 29 years of model integration (Fig. 3.19). Under weaker seasonal stress, the community exhibits at least an order of magnitude lower long-term change, ranging between $\zeta = -0.005$ to $\zeta = 0.077\ yr^{-1}$ for moderate and between $\zeta = -0.003$ to $\zeta = 0.029\ yr^{-1}$ for weak seasonal forcing.

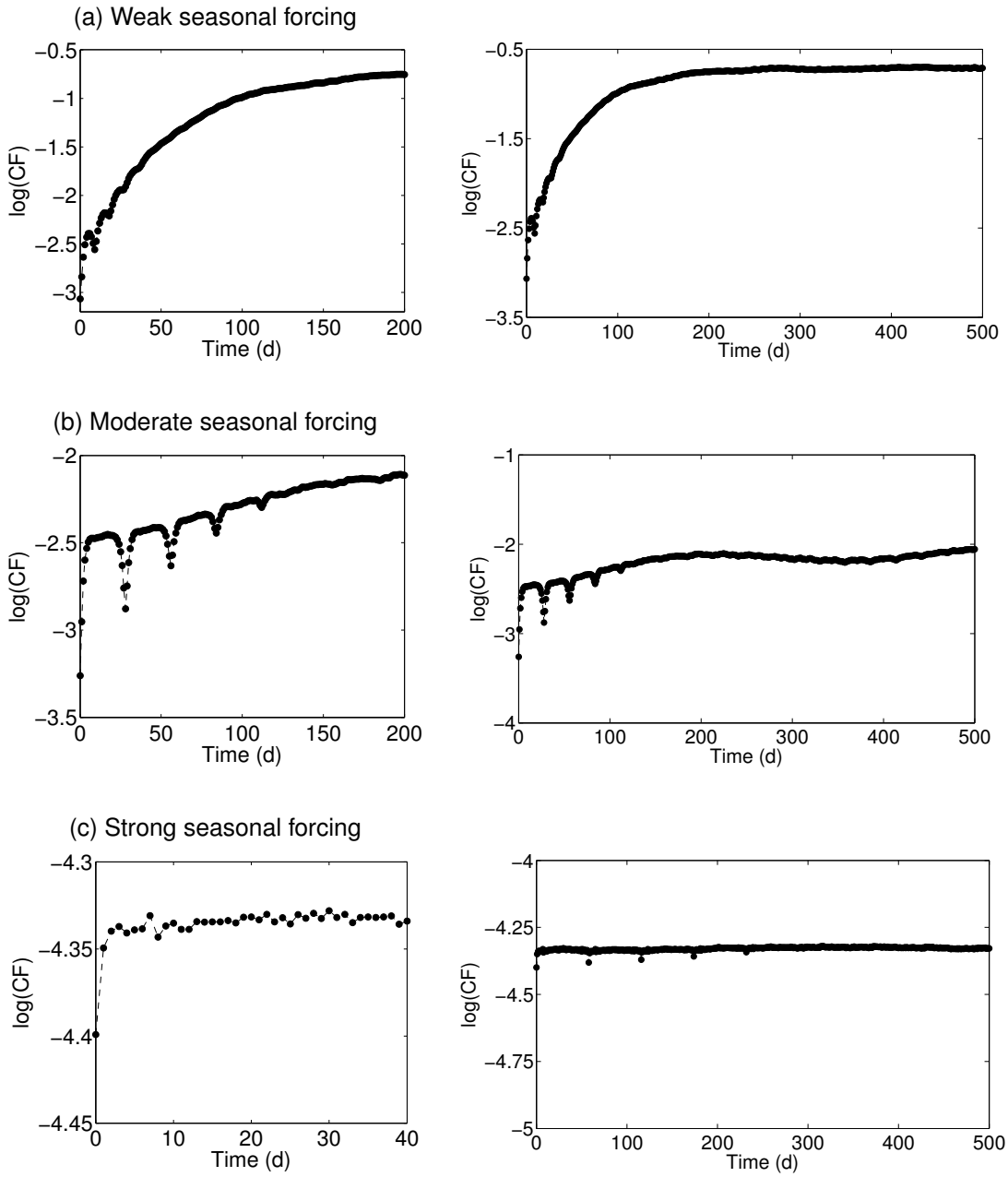

Figure 3.18: The time evolution of the stretching factor, CF, for the time series of concentration of species 5 under seasonal forcing of varied amplitude: (a) weak with $\alpha = 20\%$, (b) moderate with $\alpha = 60\%$, and (c) strong with $\alpha = 100\%$. The analysis is carried out on the data sampled daily, $\tau = 1\ d$.

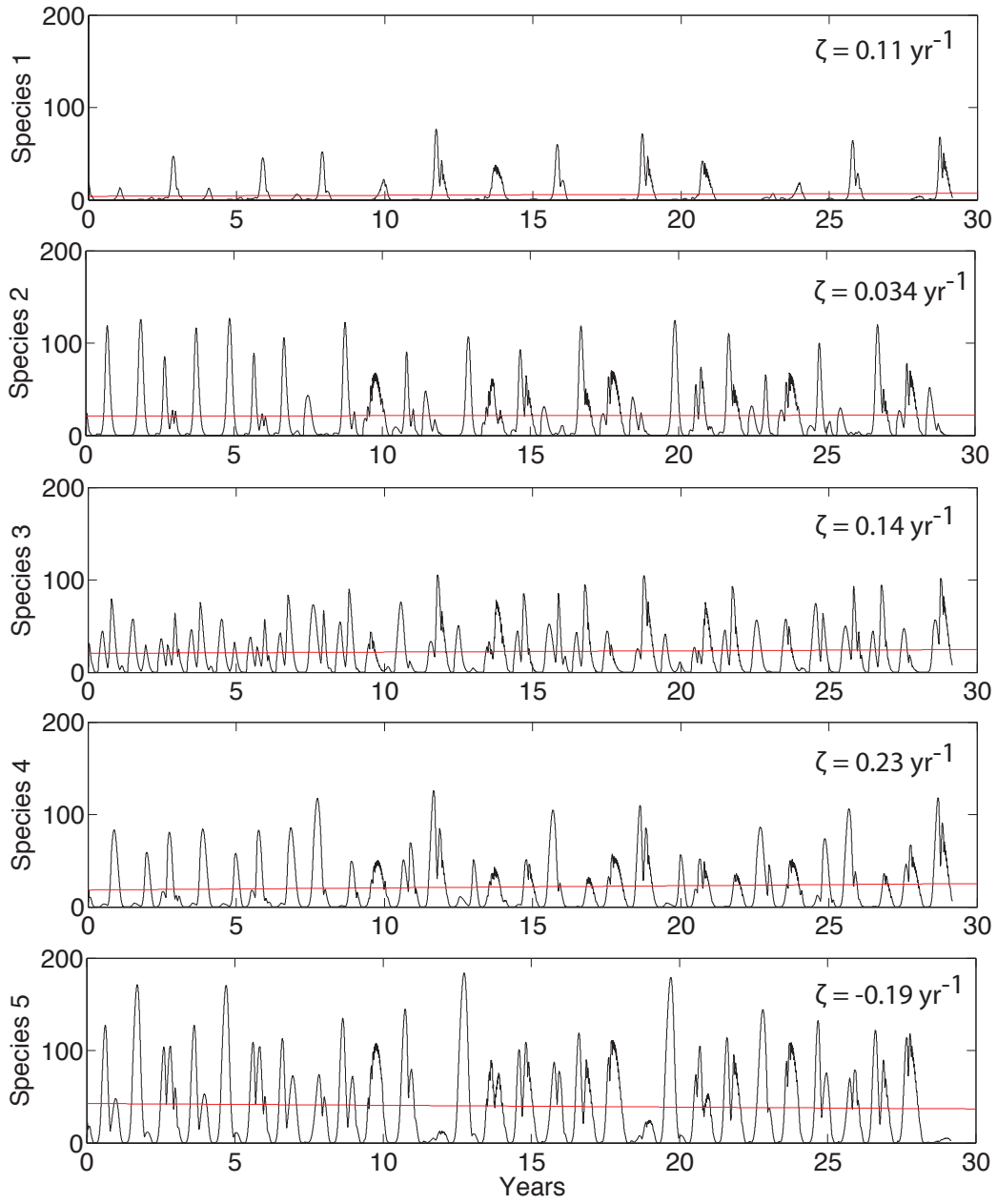

Figure 3.19: Time series of modelled species abundance under strong seasonal forcing ($\alpha = 100\%$, see Eq. (3.3)). Each panel illustrates the variability in abundance of one of the five species initialized in the ecosystem model. The linear, long term trend is indicated in red, with the magnitude of the trend, ζ, specified for each species.

3.5.4 Addition of noise

High levels of noise within the observational time series may significantly obscure the capability of the maximal Lyapunov Exponent method to detect the underlying chaotic dynamics. Here, the focus lies on the effect of the measurement error and the aim is investigate the skill of the algorithm to detect chaos while imposing stochastic variability on the top of the model data.

The application of the chaos detection technique to a purely Gaussian signal (Fig. 3.20) sampled at $\tau = 1$ day produces misleading results: CF exhibits an increase in time and subsequently reaches saturation. However, the resulting $log(CF)$ time series does not exhibit a linear increase over more than two data points (Fig. 3.20a). Thus the requirement of exponential divergence in not satisfied. The time series of $log(CF)$ obtained during the analysis of the Gaussian noise time series interpolated onto a finer grid, $\tau = 0.1$ day, becomes non-monotonic during in the initial stage of CF evolution (Fig. 3.20b). If observed in the analysis of real-world data, such instability could mistakenly be attributed to externally-imposed variability and the linear fit would incorrectly indicate chaotic behaviour.

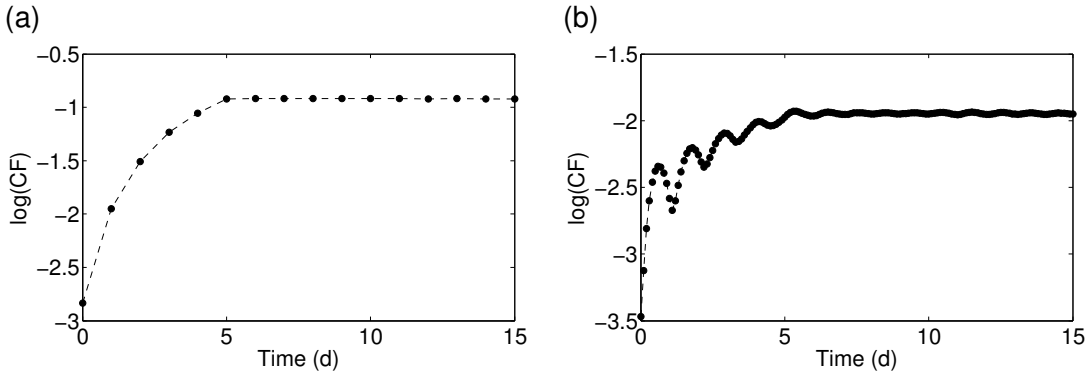

Figure 3.20: Application of methods for chaos verification to the Gaussian noise signal. The analysed time series was sampled at $\tau = 1$ day (a), or interpolated so that $\tau = 0.1$ day (b). Both panels show the evolution of the stretching factor,CF, for the Gaussian time series shown in Fig. 3.12.

Imposing a 5% Gaussian noise level on top of the modelled phytoplankton time series has a noticeable effect on the behaviour of the stretching factor. When compared to the original, noise-free response with $\lambda_{max} = 0.0140\ d^{-1}$, an increase in $log(CF)$ is still observed over the initial 200 days for the noisy time series. However, a gentler slope indicates slight weakening of chaotic behaviour with $\lambda_{max} = 0.0130\ d^{-1}$ (Fig. 3.21 a). Increasing the noise level gradually suppresses an exponential increase in the stretching factor as well as shortening the period over which the increase is observed. The estimate for λ_{max} exhibits further decrease from $\lambda_{max} = 0.0110\ d^{-1}$ at 20% noise level to $\lambda_{max} = 0.0088\ d^{-1}$ at 40% and $\lambda_{max} = 0.0040\ d^{-1}$ at 80% noise level (Fig. 3.21 b,c,d). The capacity of the Lyapunov Exponent method for chaos detection deteriorates as the noise level increases. Imposing noise of a different distribution, such as Pearson, Poisson or noncentral χ^2 distribution, produced results consistent with the above analysis for Gaussian noise.

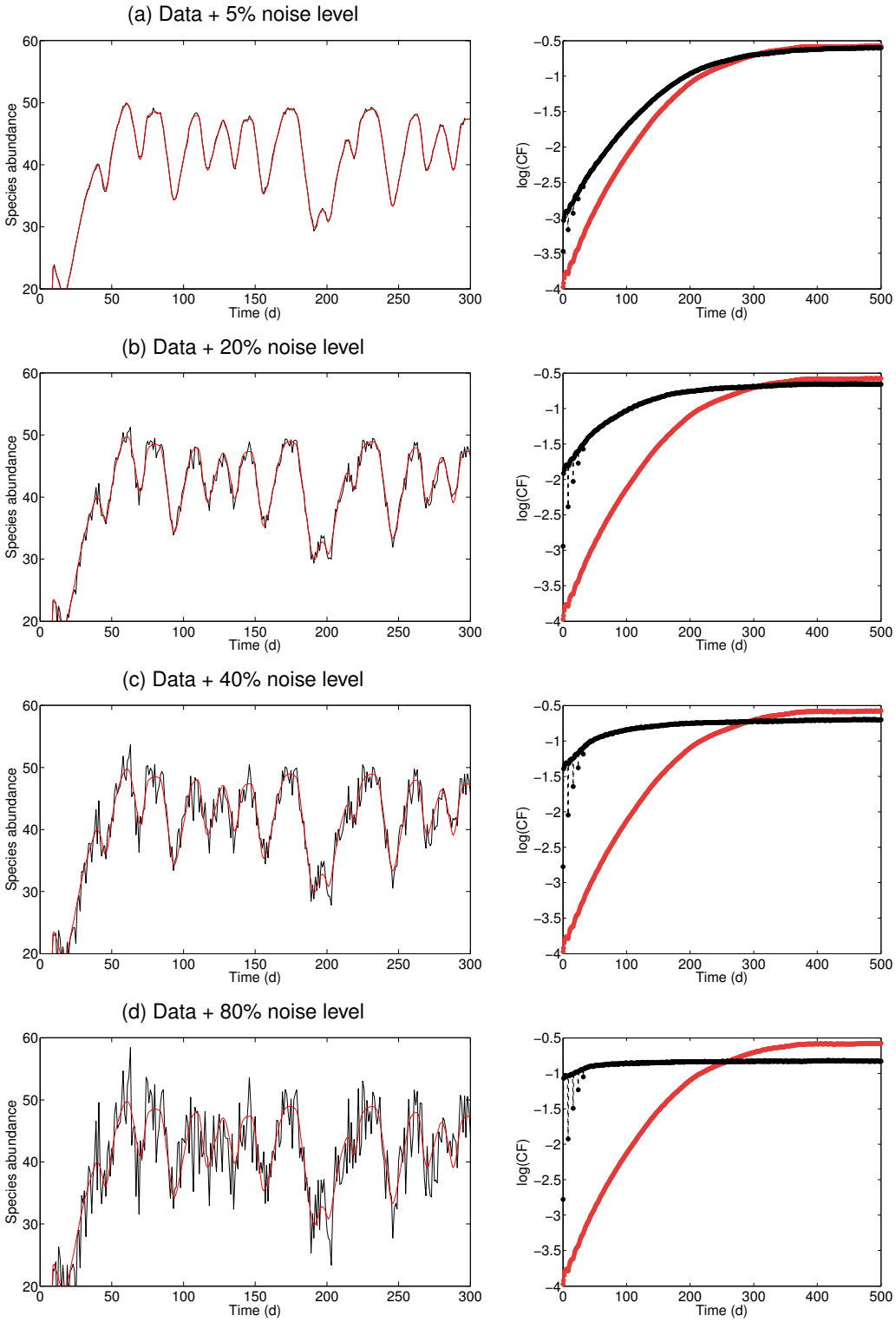

Figure 3.21: The verification of chaos in the modelled phytoplankton time series with imposed Gaussian noise of (a) 5%, (b) 20%, (c) 40% and (d) 80%. In the left panel, the original data is indicated in red and data with added noise is shown in black. The evolution of the stretching factor, CF for each of the time series is illustrated on the right panels: for original, noise-free time series in red, and for noise-contaminated time series in black. Time series are sampled at $\tau = 1$ day.

3.6 Discussion

Chaotic behaviour could potentially be an important mechanism sustaining biodiversity in marine and terrestrial environments, and emphasize the complexity of the natural ecosystems. Verification of whether such a mechanism occurs within real-world communities, currently relies on modelling and short-term laboratory studies. This is due to the limitations of long-term sampling sites that inhibit verification of chaos directly from observational time-series data. The analysis of the observation data measured at the L4 station in the English Channel does not exclude chaos as a phenomenon occurring in nature, and for some of the time-series data (diatoms and dinoflagellates) an exponential dependance on initial conditions is revealed. The time series that suggest underlying chaotic fluctuations include ammonia and silicate concentration, and diatoms and dinoflagellates abundance that exhibit somewhat oscillatory patterns in the exponential sensitivity to initial conditions. The oscillatory character of such behaviour appears on a seasonal scale, where the exponential decline in the stretching factor (suggesting a negative Lyapunov Exponent) followed by another increase occurs after approximately 350 days. This could be an indication of a chaotic response developing at different temporal scales corresponding to the underlying processes controlling the community dynamics, such as the seasonal variability in environmental or nutrient supply conditions. Switching of the microbial community response from regular to chaotic behaviour caused by the temporal variability in the nutrient supply conditions was observed during the chemostat experiments of Becks and Arndt (2008).

The power spectrum analysis reveals similarities between the power density distribution for observational time-series data and weekly sampled synthetic data generated by the ecosystem model. The ecosystem model replicates the power density decline

towards higher frequency with a comparable slope as observed for the in-situ time-series data when weakly chaotic behaviour is forced with seasonal nutrient supply, despite being spatially homogenous. Therefore, the sub-annual variability may not be solely attributed to the environmental forcing and spatial heterogeneity driven by physical mechanisms such as diffusion or horizontal and vertical advection. In addition, the rate of a decline of power density can differ for ecosystem components obtained through both the model and observations. The timescale associated with the instantaneous nutrient uptake or dilution is beyond the high frequency variability of the weekly sampled data. The ability of the model to capture power spectrum differences between ecosystem components suggests that the sub-annual variability within the marine ecosystems may be driven by complex dynamics generated through nutrient-phytoplankton interactions, possibly chaos.

In order to address the question whether chaos occurs in real world environments, it is essential to improve on the sampling resolution to capture variability underlying the seasonal pattern of species abundance and nutrient concentrations. Application of the Lyapunov Exponent method for chaos verification to the daily records of sea surface temperature re-analysis data obtained from the ECMWF data served, reveals that sampling at 2-3 day resolution for 5 years is sufficient to capture chaotic fluctuations. This finding is consistent with the laboratory-based experiment of Benincà et al. (2008), where the ecosystem needs to be sampled every 3.5 days in order to capture chaotic behaviour within the marine food chain isolated from the Baltic Sea. All of the long-term observation time-series sites conduct their measurements at weekly or fortnightly resolution which significantly inhibits the ability to detect chaos.

The detection of chaos shows high sensitivity to the influence of external forcing and noise imposed on the time-series data. The analysis of the synthetic data gener-

ated by the ecosystem model reveals that although the irregular oscillations underlying seasonality are clearly chaotic, the capability of the method to detect chaos is significantly inhibited. It appears that strong seasonality weakens the chaotic response by increasing the predictability of the system. Pronounced seasonal pattern in the SST re-analysis time-series data could be the reason why the predictability within the physical environment is estimated for as much as 5000 days. On the contrary, noise imposed on the chaotic time series introduces numerical 'instability' into the calculations and moderate to large noise level acts to obscure the analysis.

The investigation of the sensitivity of the chaos detection algorithm to the strength of seasonal and stochastic variability provides an insight into the requirements for the sampling location that would greatly improve the ability of chaos detection within real world ecosystems. For example, the phytoplankton community in the English Channel is highly influenced by the vigorous physical regime: periodic advection of new waters by tides and currents, and sporadic eddy transport resulting from the instabilities at the interface between open ocean and the shelf. Additionally, the mid-latitude location means that the considered environment is greatly influenced by seasonal variation in the nutrient supply. Such environmental features can significantly mask underlying chaotic behaviour and amplify the level of noise in the time-series data. Thus, the analysed observational data is considered to be collected at a challenging location where ability to detect the dynamics of the resident species is significantly inhibited. An ideal sampling site should be located in the region subjected to no extreme or sudden fluctuations in atmospheric conditions and physical environment, such as the central part of a subtropical oligotrophic gyre. Such a stable environment is most likely to reveal a chaotic response within marine environment. This conclusion was previously suggested by Huisman et al. (2006) in the modelling experiment where chaos is considered to be a possible competition outcome at the level of the deep

chlorophyll maximum in the oligotrophic waters.

A number of practical issues and limitations need to be considered when choosing a sampling location for verification whether chaos occurs within the marine ecosystem. Challenges arise when selecting an appropriate sampling depth: thermocline assures for a stable environment but at a potential cost of relatively low phytoplankton abundance, while at the level of biomass or chlorophyll maximum community can be susceptible to the atmospheric variability that could inhibit the detection of chaotic behaviour. Special precautions need to be taken when considering the seasonal variability in the depth at which those features are detected. In addition, sampling in a stationary location entails a risk that, due to the continuous advection, different phytoplankton communities that are transported through the site would be measured, which would amplify the stochastic variability within a time series. Therefore, sampling location should follow a water column and investigate the phytoplankton community within it, assuring for a sufficiently long residence time within the boundaries of the subtropical gyre. Alternatively, the physical transport control on microbial communities would suggest that chaos must occur over a wide area in order to be detected. Averaging over spatially sampled data entails a risk that chaotic signal may diminish if phytoplankton exhibit out of phase synchronization on a spatial scale. The spatial resolution should be limited to a region where climatic and physical variability of the same magnitude has an equivalent impact on the biological environment.

The Lyapunov Exponent can fail in distinguishing chaos from noise, and thus for reliable results, a long time series with no or low-amplitude noise is required. Here, chaos is successfully detected for the re-analysis time series of sea surface temperature. This suggest that if chaos is a governing mechanism, it could be successfully verified within the marine microbial community due to comparable timescales of variability,

and provided that the community was sampled at sufficient frequency. In comparison, atmospheric systems are believed to be chaotic due to inhibited skill for long-term predictability and potentially significant impact of initially tiny disturbances. This posed a context of early investigations of chaotic dynamics (Lorenz, 1963, 1965). However, when applied to the 6-hourly re-analysis data of atmospheric pressure or wind speed, the algorithm failed to detect chaos. This failure may be due to much smaller timescales of variability that require finer sampling frequency. Additionally, the noise level observed in the atmospheric time-series data is much greater. This limitation undermines the application of the Rosenstein et al. (1993) algorithm for identification of chaos within meteorological time-series data.

In conclusion, the analysis of the observational time-series data from the L4 station provided some promising results indicating that chaos could potentially occur in nature. The analysis suggests that diatoms and dinoflagellates in the English Channel may be exhibiting chaotic response that could be a key factor driving the inter-annual variability in species phenology. Still, it is essential to improve on the sampling frequency for more precise verification whether chaotic response governs the marine community. Sampling in the region influenced by a vigorous physical regime poses great challenges and implications for the data analysis, and thus investigating the community in the stable environment is recommended.

3.7 Chapter summary

The analysis of phytoplankton concentration time-series data obtained from the L4 station in the English Channel provides encouraging results as to whether chaos can be observed to occur within marine community. Further analysis based on time-series (re-analysis) data and model simulations show that:

- detection of chaos is highly sensitive to the length of the time series and the choice of appropriate sampling frequency.
- the analysis of sea surface temperature (SST) fields retrieved from the ECMWF re-analysis data server, suggests chaotic variability, subject to the record being sampled daily and covering 34 years.
- sensitivity analysis to sampling frequency and the length of the SST time series implies that a time series sampled every 1-3 days for 5 years is required to confidently detect chaos
- strong seasonality and noise are factors that can significantly inhibit the skill of chaos detection for the applied methods.

This analysis suggests that low-latitude, stable environments are most suitable regions where underlying chaotic behaviour would be most evident. Insufficient sampling frequency, strong seasonality and vigorous physical regime at the L4 station could all be potential causes for the failure of the TISEAN algorithm to detect chaos within the phytoplankton time-series data. Finer sampling resolution is essential for more robust and elucidative analysis.

CHAPTER 4

Investigating how species competition and nutrient feedback sustain modelled phytoplankton diversity [†]

Rationale:

Using an idealized model framework this chapter provides an insight into whether complex behaviour generated through inter-species competition for nutrients is plausible within an aquatic plankton community. The main result identifies how different choices in fundamental ecosystem model closures influence the outcome of the inter-species competition. The ecosystem model outcomes are defined in terms of whether competitive exclusion, oscillations or chaos are most likely to occur. The study addresses the sensitivity of the chaotic response to the strength of the coupling in the model related to nutrient supply. The implications for biodiversity are also explored, including how chaos and oscillations facilitate survival of new species and enhance biodiversity, when compared to competitive exclusion.

[†]Published in Marine Ecology Progress Series: Kenitz, K., Williams, R.G., Sharples, J., Selsil, Ö., Biktashev, V.N. (2013), 'The paradox of the plankton: species competition and nutrient feedback sustain phytoplankton diversity', *Mar Ecol Prog Ser* **490**,107-119.

4.1 Introduction

Hutchinson (1961) first posed the paradox of the plankton: why do so many phytoplankton species coexist while competing for a limited number of resources in a nearly homogeneous environment. It has been suggested that the high biodiversity is a result of the ecosystem never reaching an equilibrium (Hutchinson, 1961) which can be achieved through the temporal and spatial variability within the environment (Kemp and Mitsch, 1979; Reynolds et al., 1993; Bracco et al., 2000), but which can also arise as an internally-induced response formed by the species interactions (Armstrong and McGehee, 1980; Huisman and Weissing, 1999; Scheffer et al., 2003). The latter is the focus of this study.

The response of the phytoplankton community to the surrounding environment is a key factor that determines the number of coexisting species in a homogenous environment. According to the competitive exclusion principle, species of similar ecology cannot coexist at equilibrium (Gause, 1934). The axiom of inequality assumes that there are no two species with identical competitive traits, so that the strongest, best-adapted competitor for a resource will ultimately dominate the environment over either short or a long time periods (Hardin, 1960). While competitive exclusion acts to decrease community diversity, the community can also exhibit internally induced cyclic behaviour that allows more species to be supported than the number of resources (Armstrong and McGehee, 1980). In particular, Huisman and Weissing (1999, 2001) demonstrate that phytoplankton species consuming an abiotic resource can have a chaotic response; the phytoplankton abundance of each species does not reach an equilibrium, but instead continually evolves in a non-repeating sequence. Alongside this irregular behaviour, chaos is characterised by a high sensitivity to initial condi-

tions; any differences in initial conditions exponentially increase in time and inhibit any predictability. With respect to the paradox of the phytoplankton, the number of phytoplankton species can exceed the number of resources in these chaotic solutions, subject to there also being a random injection of species into the environment (Huisman and Weissing 1999, henceforth HW; Huisman et al. 2001).

Within model ecosystems the occurrence of chaos exhibits high sensitivity to the choices for the species growth rate (May, 1974; Hastings et al., 1993), the strength of trophic interactions (McCann et al., 1998), the resource availability (Doveri et al., 1993) and the nutrient requirement (Huisman and Weissing, 2001). Similarly, a number of laboratory experiments found that the type of the community response can change depending on the experimental set up related to the chemostat dilution rate controlling the supply of resources (Kooi et al., 1997; Becks et al., 2005; Becks and Arndt, 2008, 2013).

In the study of HW a claim is made that the complex behaviour within microbial communities solves the paradox of the plankton. However, the robustness of chaos and sensitivity to the finely-tuned model parameters was not discussed. Schippers et al. (2001) challenged the idea of increased diversity driven by non-equilibrium dynamics and found that it is an unlikely outcome within a modelled phytoplankton community. The study investigated the likelihood of 'supersaturated coexistence', when the number of species exceeds the number of resources, by randomly introducing new species, but also modifying the initial community structure. The design of the experiments has been criticized for inappropriate model choices (Huisman et al., 2001). Schippers et al. (2001) overlooked the importance of the internal structuring of planktonic communities and the condition relating the resource consumption and requirement that allows for chaos to occur (Huisman and Weissing, 2001). However, the study emphasized the

importance of the internal hierarchy within the phytoplankton community that prevents a single competitor from dominating the environment.

Here, the conditions for the phytoplankton community to exhibit chaotic, oscillatory and competitive exclusion solutions are investigated by addressing the dependence on the nutrient source. The role of niche differentiation in generating non-equilibrium behaviour is examined and the likelihood of competitive exclusion to occur is established. Finally, the role of phytoplankton community behaviour in sustaining greater diversity is investigated by estimation of how long an intermittent addition of new species persists in the phytoplankton community.

4.2 Model Formulation

In this study, the coupled phytoplankton (P_i) and nutrient (N_j) model of HW is applied for a well-mixed box, as described in Section 2.1:

$$\frac{\partial N_j}{\partial t} = D(S_j - N_j) - \sum_{i=1}^{n} Q_{ji} r_i \gamma_i^N P_i \qquad j = 1,...,k \tag{4.1}$$

$$\frac{\partial P_i}{\partial t} = P_i(r_i \gamma_i^N - m_i) \qquad i = 1,...,n \tag{4.2}$$

$$\gamma_i^N = min\left(\frac{N_1}{K_{1i}+N_1},...,\frac{N_k}{K_{ki}+N_k}\right) \tag{4.3}$$

We firstly consider cases with the same number of species and resources ($n = k = 5$; Figs. 4.1 to 4.5) and secondly where the number of species exceeds the number of resources ($n > k = 5$; Figs. 4.6 to 4.8). The model parameters and initial conditions follow those of HW unless otherwise stated (see Table 2.1, p. 26).

The broad types of the relationship between the abundance of phytoplankton species and nutrients are characterised, extending experiments by HW. The model solutions for the abundance of phytoplankton species reveal 3 different characteristic regimes: (1) competitive exclusion, when a long-term equilibrium is reached where one or more species dominate and drive the others to extinction (Fig. 4.1 a); (2) repeating oscillations, when there is a repeating cycle in the abundance of each species (Fig. 4.1 b); or (3) chaotic solutions, when there are non-repeating changes in species abundance (Fig. 4.1 c). These differences start to become apparent over the first 100 d (Fig. 4.1, left panel). The character of the different responses is also reflected in the nutrient response in the well-mixed box: competitive exclusion leads to steady-state nutrient concentrations sustained by their nutrient source, while oscillations or chaos within the phytoplankton community are associated with periodic or irregular fluctuations in the

ambient nutrient concentrations.

In terms of the "paradox of the phytoplankton", both the repeating oscillations and chaotic solutions are of interest as a long-term equilibrium is not reached, part of the explanation suggested by Hutchinson (1961). Taking that view further forward, HW argued that a chaotic state enables the number of species to exceed the number of resources.

(a) Competitive exclusion

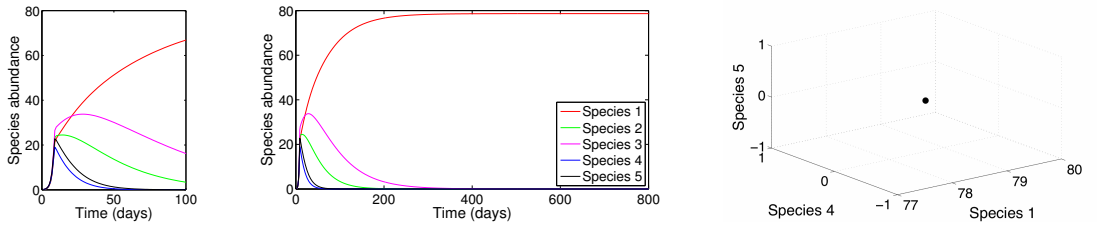

(b) Oscillatory response

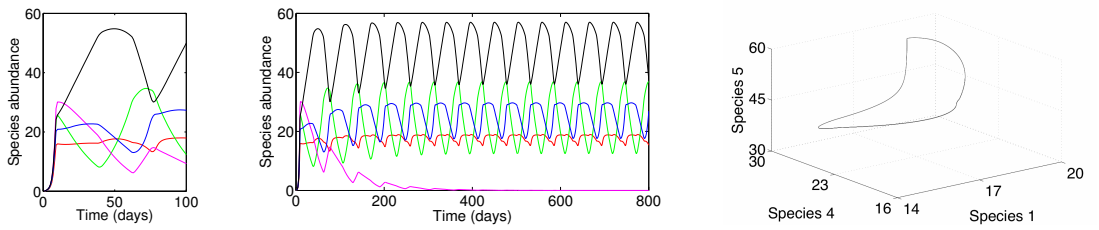

(c) Chaotic response

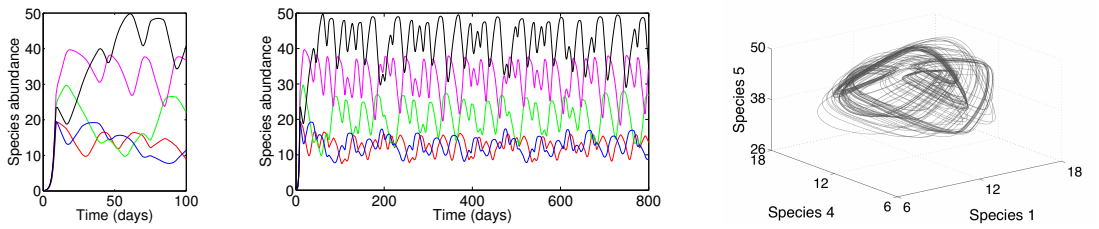

Figure 4.1: Phytoplankton community response generated by the model of Huisman and Weissing (1999). The model responses incorporate (a) competitive exclusion, (b) oscillations and (c) chaos, generated with $K_{4,1} = 0.20$, $K_{4,1} = 0.40$ and $K_{4,1}$ = 0.30 respectively, where K is the half-saturation coefficient. The species responses are shown for the initial period of 100 d and over 1000 d (left and central panels), and their phase diagrams are from 500 to 5000 d (right panels).

In our model diagnostics, whether chaos is obtained is formally identified using the following approaches, described in detail in Chapter 2. Firstly, the temporal changes in phytoplankton abundance are illustrated by a trajectory in a phase space, where each dimension represents the abundance of a particular phytoplankton species. For example, consider the evolution of 3 arbitrary species in a 3-D phase diagram (Fig. 4.1, right panels): competitive exclusion is represented by a single point; repeating oscillations by repeating closed trajectories; and chaotic solutions by irregular and continually changing trajectories. Secondly, the sensitivity to initial conditions can be estimated by evaluating the rate at which 2 points in phase space, initially close together, subsequently diverge away from each other. This diagnostic, referred to as the maximal Lyapunov Exponent (Kantz, 1994), is often used to define chaos, identifying when there is an exponential increase in the separation of 2 trajectories. Thirdly, we employ a binary test distinguishing chaos from non-chaotic dynamics, referred to as the 0-1 test for chaos, adjusted to detect weak chaos (Gottwald and Melbourne, 2004, 2009). This technique is the most efficient approach when there are many repeated model integrations. Detailed explanation of these methods is provided in Section 2.2.

4.3 Model sensitivity experiments

Sensitivity experiments are now performed to understand the different ecosystem response in the well-mixed box, focussing in turn on the environmental control via the nutrient supply, the physiological control of each species via the cell quota and K_{ji} coefficient, and the effect of random injections of different phytoplankton species.

4.3.1 Environmental control by nutrient supply

The nutrient supply in Eq.(4.1), includes an external supply, DS_j, and a feedback term, DN_j, to ambient nutrient concentrations. The external supply and feedback together act to restore nutrient concentrations, which can be viewed as a crude way of replicating how physical processes act to supply nutrients and sustain biological productivity. For example, in a vertical water column, phytoplankton consume inorganic nutrients in the euphotic zone, and these inorganic nutrients can be resupplied by vertical diffusion, acting to transfer nutrients down gradient from high concentrations in the nutricline to the surface. This diffusive nutrient supply is given by $\frac{\partial}{\partial z}(\kappa\frac{\partial N}{\partial z})$, which, applying scale analysis, is typically $-\frac{\kappa}{\Delta z^2}(N_{surface}-N_{nutricline})$, where κ is the vertical diffusivity, $N_{surface}$ and $N_{nutricline}$ are the nutrient concentrations at the surface and nutricline, separated by a vertical spacing Δz. Thus, when $N_{surface} < N_{nutricline}$, diffusion acts to restore the surface nutrients towards the value in the nutricline, reducing the contrast between $N_{surface}$ and $N_{nutricline}$, so acting in a similar manner to DN_j in the nutrient supply in Eq.(4.1).

To assess the effect of the nutrient feedback in Eq.(4.1), model experiments are performed with the nutrient supply taking the form $D(S_j - \alpha N_j)$ where α ranges from 0 to 1 (and otherwise default model parameters are used; Table 2.1 in the Appendix). The factor α controls the net amount of nutrient supplied into the environment, and measures the strength of feedback to the nutrient resource. At weak to moderate feedback ($\alpha < 1$), there are repeating cycles of a single species dominating, switching later to a different single species, and this pattern is progressively repeated (Fig. 4.2 a). Increasing the feedback leads to a reduction in the period of each cycle (Fig. 4.2 a,b).

For strong feedback ($\alpha \sim 1$), there are always time varying changes in the abundances of the 5 species and a chaotic response, when the sequences for the abundances of phytoplankton species do not exactly repeat in time (Fig. 4.2 c), as evident in their trajectories not repeating in phase diagrams. Thus, the presence of DN_j in Eq.(4.1) fundamentally affects the nature of the phytoplankton solutions.

While some form of nutrient feedback is plausible given how diffusion acts to supply

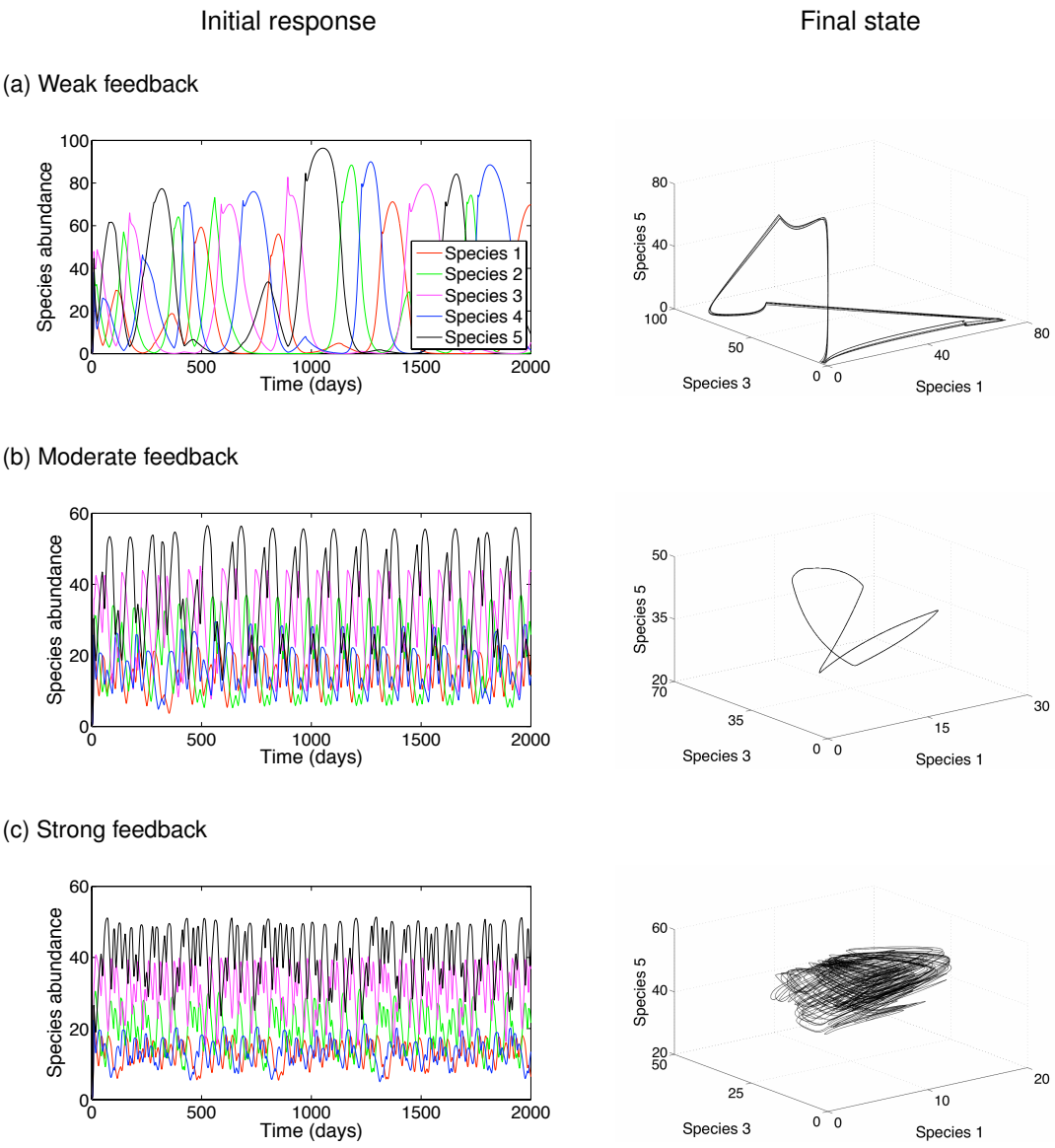

Figure 4.2: Phytoplankton community response to the nutrient supply, $D(S_j - \alpha N_j)$ (for abbreviations see Section 2.1, p. 24), with varying levels of feedback: (a) weak ($\alpha = 0.2$), (b) moderate ($\alpha = 0.6$), and (c) strong ($\alpha = 0.8$). Time series plots are for the initial 2000 d (left panels) and phase plots over the later 7000 to 10 000 d (right panels).

nutrients to the surface, other physical transport processes often dominate over this diffusive supply, such as entrainment at the base of the mixed layer, and the horizontal and vertical transport of nutrients (Williams and Follows, 2003). Hence, the nutrient feedback acting to restore surface nutrients is unlikely to hold all the time, possibly varying in an episodic manner, and probably depending on the physical forcing and background circulation operating on a long timescale. Accordingly, we now consider the effect of introducing slight modifications in DN_j in model experiments using the default chaotic parameters.

(1) Interactive feedback with intermediate disturbance

The nutrient supply, $D(S_j - N_j(t))$, is now interspersed by intermittent periods when there is no feedback, such that the supply temporarily increases to DS_j for short periods ranging from 10 min to 8 wk (Fig. 4.3 a, shaded). During the intermissions, the phytoplankton solutions move towards a single species dominating at any single time (Fig. 4.3 a, upper panel), rather than 5 species being sustained; this response is more apparent for prolonged periods without relaxation. After the intermissions, the nutrient supply returns to including the nutrient feedback, and the phytoplankton solutions return to being chaotic (Fig. 4.3 a). In terms of the nutrient forcing, the nutrient sources for this case with intermissions and the default case without intermissions (Fig. 4.1 c) are initially identical, but then differ after the first intermission due to the different evolution of the nutrients (Fig. 4.3 a, lower panel).

(2) Non-interactive feedback with intermediate disturbance

The model solutions are altered if the nutrient supply is adjusted to $D(S_j - \tilde{N}_j)$, where $\tilde{N}_j$ represents the past record of forcing based upon the default $N_j(t)$ record (shown to trigger the chaotic response in Fig. 4.1 c with $\alpha = 1$), but now including prescribed intermissions. After the first intermission, the lack of any interactive nutrient feedback leads to the phytoplankton solutions changing from being chaotic and evolving to a single species dominating (Fig. 4.3 b); the dominant species can alternate in time with a period lengthening with every cycle, referred to as heteroclinic cycles (Huisman and Weissing, 2001). The nutrient source in this case and the default are nearly identical (Fig. 4.3 b, lower panel), but the lack of any interactive adjustment prevents the chaotic solutions being sustained. Thus, the presence of the interactive feedback allows for the chaotic solutions to emerge and persist in a chemostat model. However, for the models incorporating higher level of complexity, nutrient feedback may not be crucial for generation of chaotic behaviour as long as other non-linear interactions control the evolution of the system.

(3) Lagged interactive feedback

Given the importance of the nutrient feedback, the effect of a slight delay is now introduced into the nutrient supply (an arbitrary lag of 1 day), so that the supply term becomes $D(S_j - N_j(t - 1day))$. The nutrient supply retains the interactive feedback, although the lag implies that the nutrient supply is not exactly the same as in the chaotic case (1) (Fig. 4.3 a). However, including the temporal lag does not significantly alter the character of the solutions: chaos is either sustained or moves to multiple-period oscillations (Fig. 4.3 c) with all 5 species persisting and varying in time.

In summary, the chaotic nature for the abundance of the phytoplankton species is reliant on there being a feedback to the nutrient concentration: an absent or too weak feedback leads to competitive exclusion or oscillatory changes in the dominant phytoplankton species, which sustain fewer species at any particular time. In partial accord with this viewpoint, chemostat laboratory experiments find that the community response is sensitive to nutrient supply rates (Becks et al., 2005), where the nutrient supply is modelled with feedback terms as in Eq.(4.1).

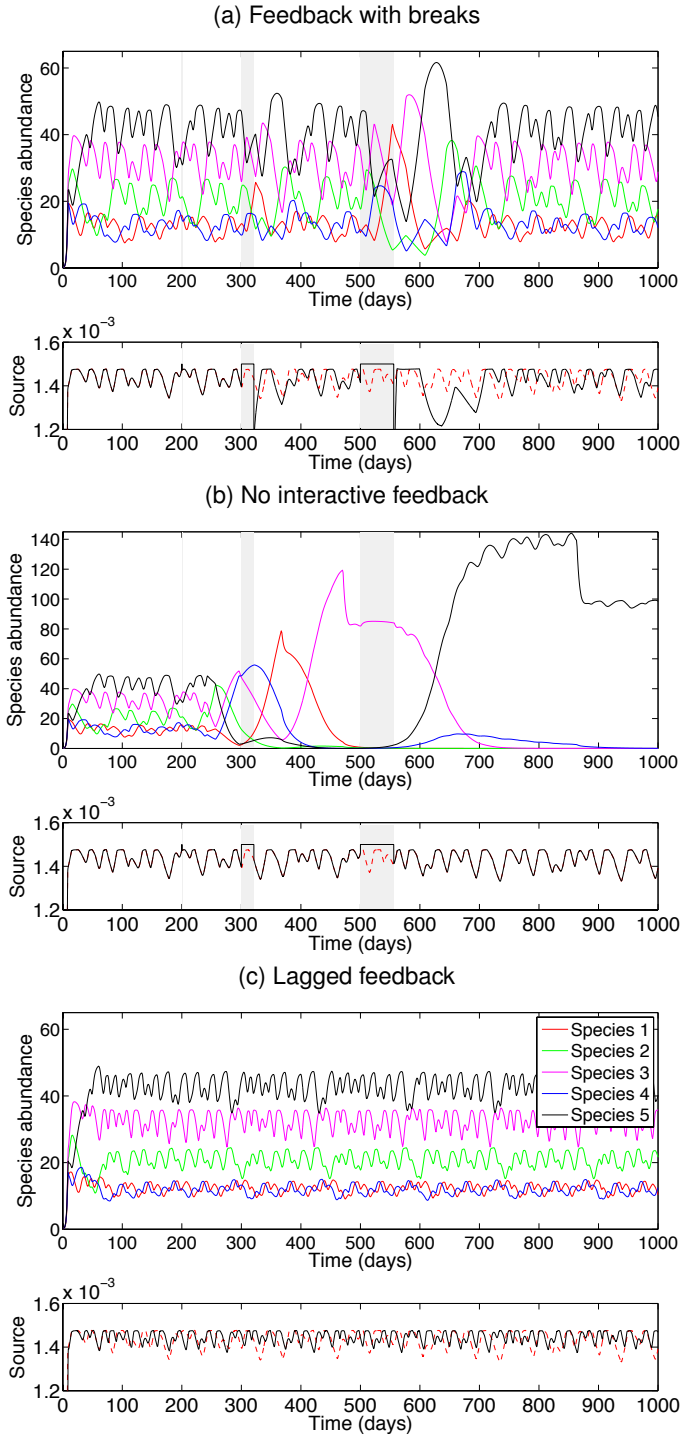

Figure 4.3: Phytoplankton species abundance (upper panels) and nutrient source (lower panels) versus time with the modified nutrient supply: (a) nutrient source with feedback and intermittent disruptions (grey shading) lasting 10 min (Day 200), 3 wk (Day 300) and 8 wk (Day 500), when the default nutrient feedback is temporarily removed, DS_j; (b) nutrient source without feedback defined by the record of the default nutrient source (as in Fig. 4.1 c) including intermissions (as in Panel a); (c) nutrient source with lagged feedback, where nutrient supply depends on the nutrient concentration from the previous day, $D(S_j - N_j(t - 1day))$. In each case, the time series of the nutrient source for resource 1 (black line) is compared with that for the default source term (dashed red line) in the bottom panels. For abbreviations see Section 2.1.

4.3.2 Physiological choices

Physiological traits and related trade-offs define the ecological niche of species and affect their survival ability. The effect of modifying the choice of cell quota and K_{ji} is now assessed on the phytoplankton community structure.

Cell quota

In a similar manner to the way the nutrient relaxation is investigated, the cell quota, Q_{ji}, is assumed either (1) to be the same for all species and alter in the same manner for each resource, or (2) to vary in a different manner for each species and resource (following HW):

$$Q_{ji} = \begin{pmatrix} 0.04 & 0.04 & 0.04 & 0.04 & 0.04 \\ 0.08 & 0.08 & 0.08 & 0.08 & 0.08 \\ 0.10 & 0.10 & 0.10 & 0.10 & 0.10 \\ 0.03 & 0.03 & 0.03 & 0.03 & 0.03 \\ 0.07 & 0.07 & 0.07 & 0.07 & 0.07 \end{pmatrix} + \beta \begin{pmatrix} 0.0 & 0.0 & 0.03 & 0.0 & 0.0 \\ 0.0 & 0.0 & 0.0 & 0.02 & 0.0 \\ 0.0 & 0.0 & 0.0 & 0.0 & 0.04 \\ 0.02 & 0.0 & 0.0 & 0.0 & 0.0 \\ 0.0 & 0.02 & 0.0 & 0.0 & 0.0 \end{pmatrix} \quad (4.4)$$

where the values in the matrix for Q_{ji} are for each resource j in the rows and for each species i in the columns, and β varies from 0 to 1; other model parameters, including K_{ji} and nutrient relaxation, are the default (Table 2.1). A choice of $\beta = 0$ represents the same cell quota for all species, while $\beta = 1$ is representative of HW with an increase in the contrast in cell quota for a particular resource for each species.

When the cell quota is identical for each species, there is competitive exclusion (Fig. 4.4 a) and the fittest species has the lowest requirement for the limiting resource (Tilman,

1977). When moderate changes in cell quota are chosen, there are oscillations in the phytoplankton response (Fig. 4.4 b). When large contrasts in cell quota are chosen for each species, there are chaotic fluctuations in the concentrations of each phytoplankton species (Fig. 4.4 c), allowing the coexistence of all 5 species. Comparable results are obtained when the contrasts in Q_{ji} occur through lowering the cellular nutrient content with preserving the default requirement that species with intermediate K_{ji} for a particular resource has the highest Q_{ji} for that resource.

(a) Nearly uniform cell quota, Q_{ji}

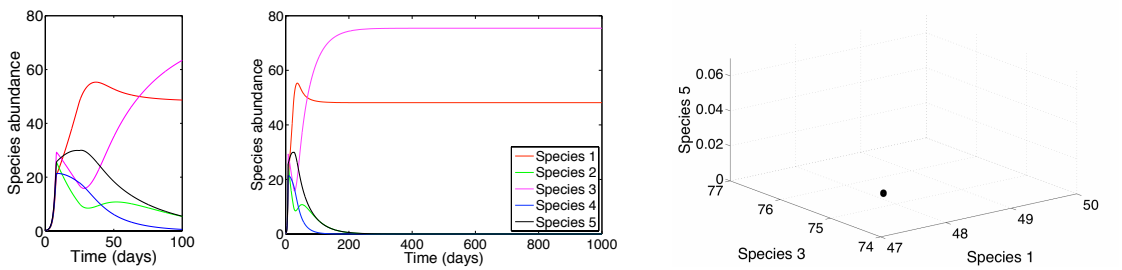

(b) Moderate changes in cell quota, Q_{ji}

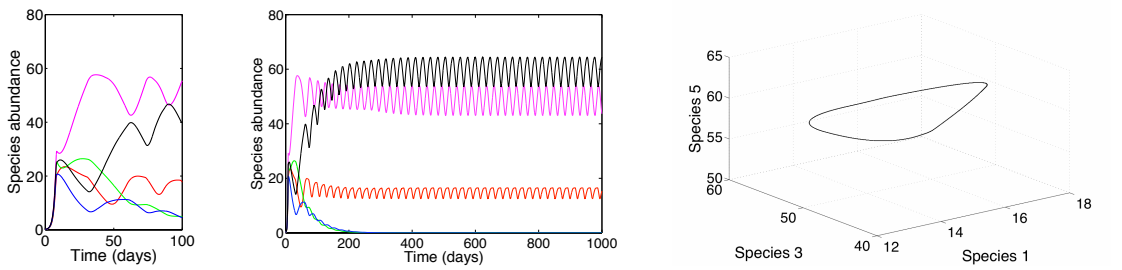

(c) Large changes in cell quota, Q_{ji}

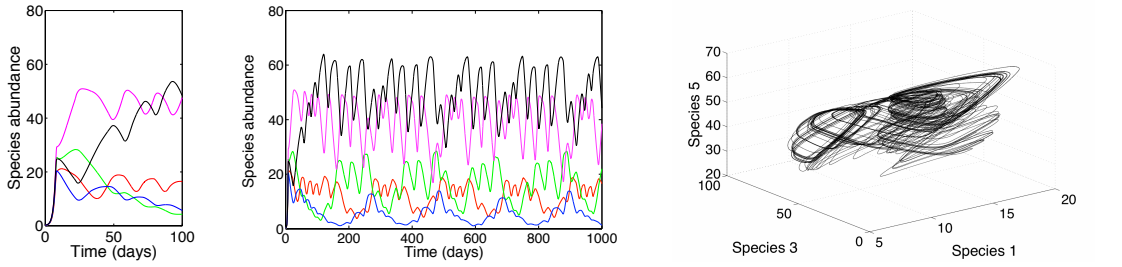

Figure 4.4: Phytoplankton community response to changes in cell quota, Q_{ji}: (a) nearly uniform cell quota for each species, $\beta = 0.2$; (b) moderate contrasts in cell quota for each species, $\beta = 0.6$; and (c) strong contrasts in cell quota, $\beta = 0.7$. The temporal adjustment is shown over the first 100 and 1000 d (left and middle panels) and corresponding phase plots (right panels) for abundance of species 1, 3 and 5 for 500 to 5000 d.

The findings suggest that the complex behaviour is most likely to occur where competing species exhibit contrasts in their cellular stoichiometry, which can be achieved through either decreasing or increasing their nutrient quota.

Half-saturation coefficient

The sensitivity to the half-saturation coefficient, K_{ji}, is investigated by varying the values for each species and resource, but in an ordered manner so that each of the species is the optimal competitor for one of the resources:

$$K_{ji} = \begin{pmatrix} k_5 & k_4 & k_3 & k_2 & k_1 \\ k_1 & k_5 & k_4 & k_3 & k_2 \\ k_2 & k_1 & k_5 & k_4 & k_3 \\ k_3 & k_2 & k_1 & k_5 & k_4 \\ k_4 & k_3 & k_2 & k_1 & k_5 \end{pmatrix} \tag{4.5}$$

where k_i are randomly generated numbers, such that $k_1 < k_2 < k_3 < k_4 < k_5$, denoting the strongest (k_1) and the weakest (k_5) competitor, and the values in the matrix are for each resource j in the rows and for each species i in the columns. Coexisting phytoplankton species that are characterised by comparable maximum growth rates exhibit contrasts in their competitive abilities thought the variability in nutrient uptake abilities arising from physiological differences between phytoplankton classes or genera (Edwards et al., 2012). Three separate sets of simulations are included, with k_i randomly chosen (retaining the above structure and ordering) within the intervals 0.2 to 0.23, 0.2 to 0.5, and 0.1 to 1. The simulations aim to investigate the role of in-between species variation in nutrient requirement in driving non-equilibrium dynamics. In each set, the model was integrated 1000 times over 50000 days and all solutions were identified using the 0-1 Test for Chaos.

At any particular time, the solutions take the form of either competitive exclusion involving a single dominant species (Fig. 4.5, blue), oscillations with a repeating cycle in species abundance or irregular chaos, both involving all 5 species (Fig. 4.5, green and red respectively). For competitive exclusion, the dominant species might alter and be replaced by another species, taking the form of heteroclinic cycles (as shown earlier in Fig. 4.3 b); the resulting ordered sequence is a consequence of each species being the optimal competitor for a different resource.

A pattern in the different model responses is evident when comparing the competitive ability of the intermediate species with the other competitors (Fig. 4.5). For the intermediate competitor, k_3, compared with the 2 strongest competitors, k_1 and k_2, competitive exclusion is the most likely response when species are of comparable fitness, but alters to chaos and then oscillations with greater contrasts in the strength of these competitors (Fig. 4.5, left panels). Hence, the more competitive the intermediate competitor, the more chance of there being an optimal competitor and obtaining competitive exclusion, while a weaker intermediate competitor encourages chaos or oscillations.

The other side of this response is that comparing the intermediate competitor, k_3, with the 2 weakest competitors, k_4 and k_5, leads to the reversed pattern (Fig. 4.5, right panels): a similar fitness of the 3 species favours oscillations, while increased contrasts generally lead to chaos and eventually are more likely to lead to competitive exclusion. Indeed, the more similar the intermediate competitor is to the weaker species, the more the intermediate competitor differs from the strong competitors, which explains the reversed pattern. No regular structure is evident when K_{ji} are compared for strong versus weak competitors.

When the perturbations in K_{ji} are in a very narrow range (0.2 to 0.23), competitive ex-

clusion is the dominant response, occurring over 47% of the parameter space, while oscillations occur in 17% and chaotic solutions in 14% of parameter space (Table 4.1); the remaining 22% of solutions are not distinguished between oscillations and chaos. When the perturbations in K_{ji} are in a larger range (0.1 to 1.0), competitive exclusion reduces to 19% of parameter space and instead oscillations increase to 45% and chaos to 17% of parameter space. Hence, when K_{ji} of intermediate and strong competitors are close together, there is more chance of identifying the optimal competitor and obtaining competitive exclusion.

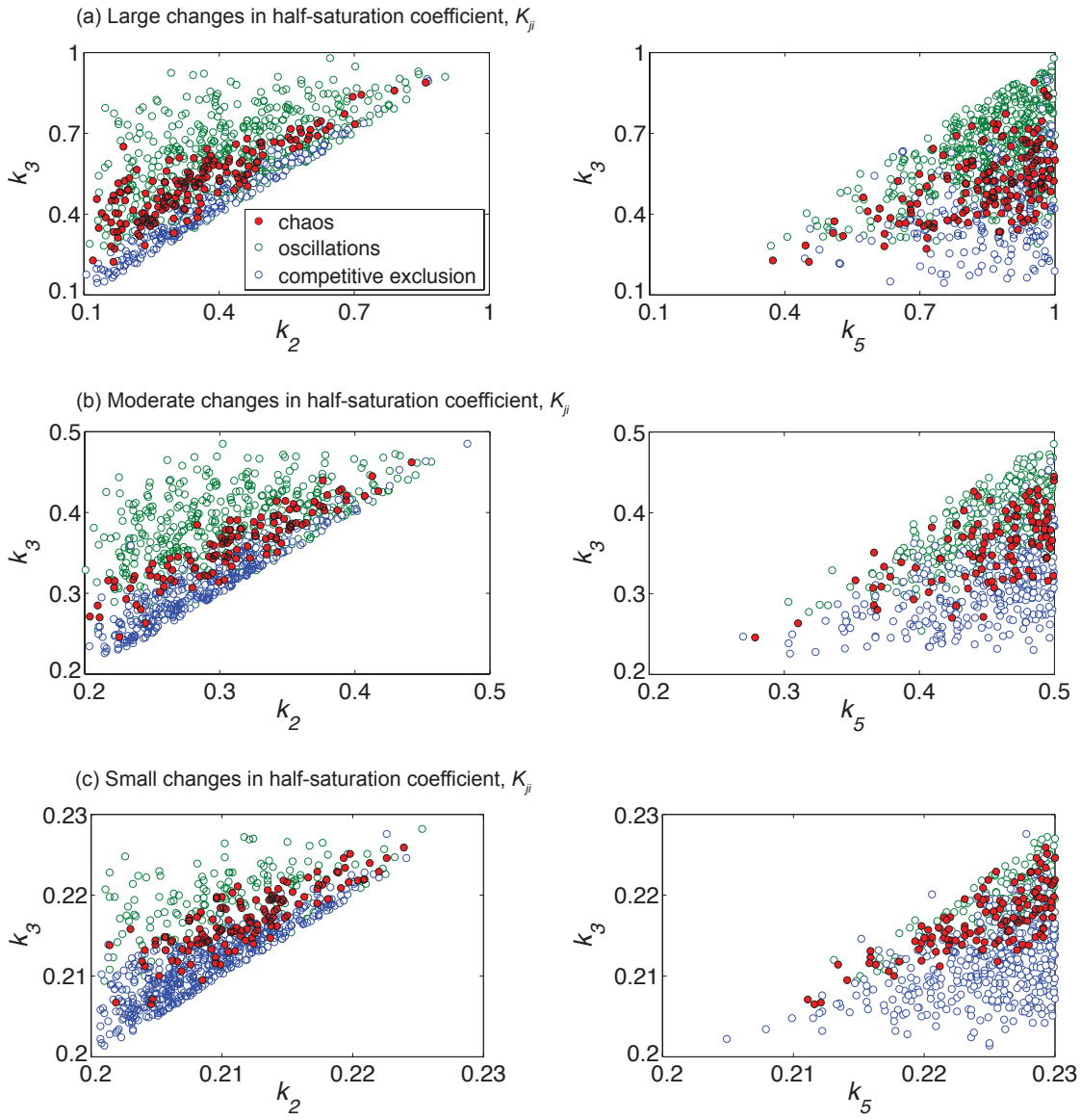

Figure 4.5: The phytoplankton community response to randomly assigned half-saturation coefficient, K_{ji}, within prescribed bounds for 1000 model integrations, each lasting 50 000 d. The model responses include competitive exclusion with 1 dominant species at any time (blue), oscillations (green) and chaos (red). Illustrated are the relationships between different K_{ji} for (a) large, (b) moderate and (c) small contrasts. The model solutions for a strong versus intermediate competitor, k_2 versus k_3 are shown in the left panels, and a weak versus intermediate competitor, k_5 versus k_3 in the right panels.

Table 4.1: Different phytoplankton community responses (%) for 3 separate sets of 1000 model integrations, each with a different range of randomly generated half-saturation coefficient, K_{ji}. For a proportion of model simulations, community behaviour could not be distinguished between oscillations and chaos.

K_{ji} range	Competitive exclusion	Oscillations	Chaos	Oscillations or chaos
0.2 - 0.23	47	17	14	22
0.2 - 0.5	32	40	12	16
0.1 - 1.0	19	45	17	19

4.3.3 Random injection of phytoplankton species

Physical transport processes, in a form of horizontal and vertical advection, are key factors driving the exchange between adjacent environments and introducing new species to the local ecosystem. Here, the response of the model to an intermittent injection of new species is investigated, replicating how ocean circulation leads to the transport and dispersal of phytoplankton species.

To investigate this species injection and the longer term community response, an invasion approach is applied broadly following Huisman et al. (2001): additional species are introduced with 3 new species with initial abundance $P_i = 0.1$, typically introduced every 30 d (with random deviations of a maximum of 10 d), starting at Day 90 and persisting for 1 yr. No new species are added after 1 year, and the model results are used to assess how many species co-exist, and how the number changes in time.

The additional species have their cell traits stochastically determined for each model integration, with K_{ji} chosen within the interval 0.2 to 0.5, and Q_{ji} within the interval 0.01 to 0.1. These biological parameters were assigned for each species and resource either in a random manner, or assuming a negative relation between fitness and cell quota (scenarios 1 and 3 of Huisman et al. (2001), respectively); however, the longterm character of the model results turned out not to be sensitive to these scenarios.

The model state prior to the invasion is our default choice: 5 species competing for 5 resources, so that competition theory predicts that up to 5 different species should be sustained for a long-term equilibrium. To sample the different characteristic regimes, the model experiments are repeated for a range of choices for K_{ji}: obtaining (1) chaos with the default K_{ji} matrix, (2) single-period oscillations with $K_{5,4} = 0.37$, and (3) competitive exclusion with $K_{2,4} = 0.20$; with otherwise default choices for the rest of K_{ji} for all 3 cases.

In the chaotic case, the number of phytoplankton species exceeds the number of resources over the length of the integration of 2500 d (Fig. 4.6 a, panel [i]). Chaotic fluctuations then allow the number of species to exceed the number of resources, referred to as supersaturation, in our integrations supporting 20 to 30 species within 3 months from the last input of new species (Fig. 4.7 a). The number of coexisting species gradually reduces to 10-15 surviving species after 1 yr, and decreases further to less than 5 after 2 yr for the majority of the model compilations. The chaotic fluctuations can sometimes abruptly diminish (Fig. 4.6 a, panel [ii]), without any intermittent disruption prior to the event. Thus, the fittest competitors persist, while the weaker species progressively become extinct. During the process of introducing more species, there is more chance for an optimal competitor to be identified and so there is less chance for chaos and oscillations to emerge. The stability of model solutions decreases as additional species are introduced. In the model simulations, a large amount of added species finally leads to a break down of instability and subsequent convergence to a steady state.

Oscillatory solutions lead to a broadly similar response to chaotic solutions: there is a supersaturation in the number of species, which gradually declines in time, as illustrated for 1-period oscillations (Figs. 4.6 b and 4.7 b) and also obtained for 2-

period oscillations (not shown). In the case of competitive exclusion, the community is already dominated by an optimal competitor and so there is a very weak, short-lived response to an injection of additional species (Fig. 4.6 c). Supersaturation is only sustained for a brief 6-month period after the last input of additional species, swiftly returning to fewer than 5 coexisting species (Fig. 4.7 c). Hence, none of the species

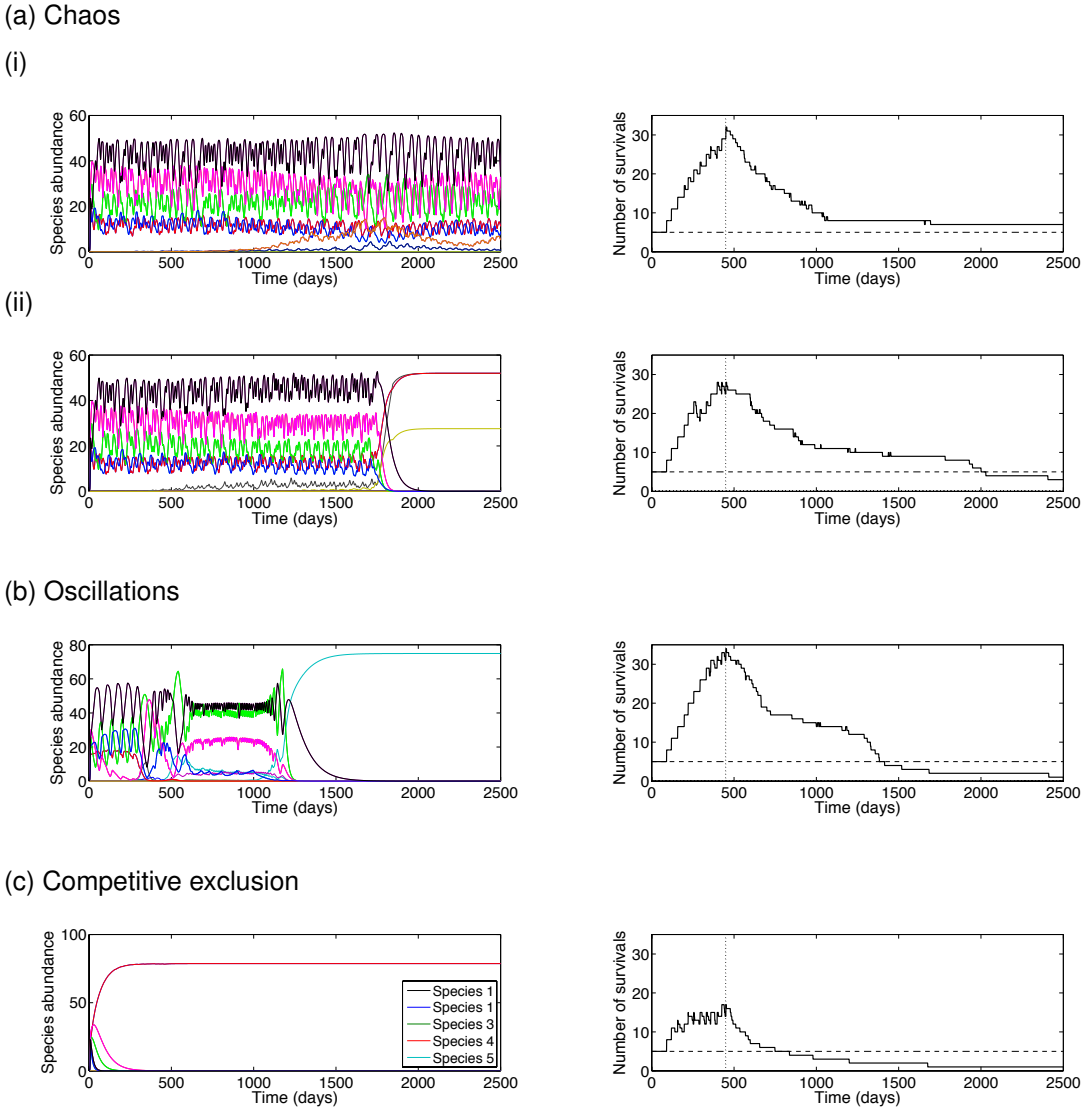

Figure 4.6: Phytoplankton species abundance (left panels) and number of survival species (right panels) versus time after 12 intermittent injections of 3 additional species (starting from Day 90 to Day 450, vertical line), depending on whether there is (a) chaos, shown for 2 examples (i) and (ii) with different randomly generated species, (b) oscillations or (c) competitive exclusion. For all cases, there is the same timing of species injections, with the final input indicated by the vertical dotted line. Survival species are defined by the abundance greater than an arbitrary small value of 0.0001. The horizontal dashed line shows the maximum species number predicted from resource competition theory for an equilibrium state.

added to the system are fit enough to outcompete the optimal competitor once it is strongly established in the community.

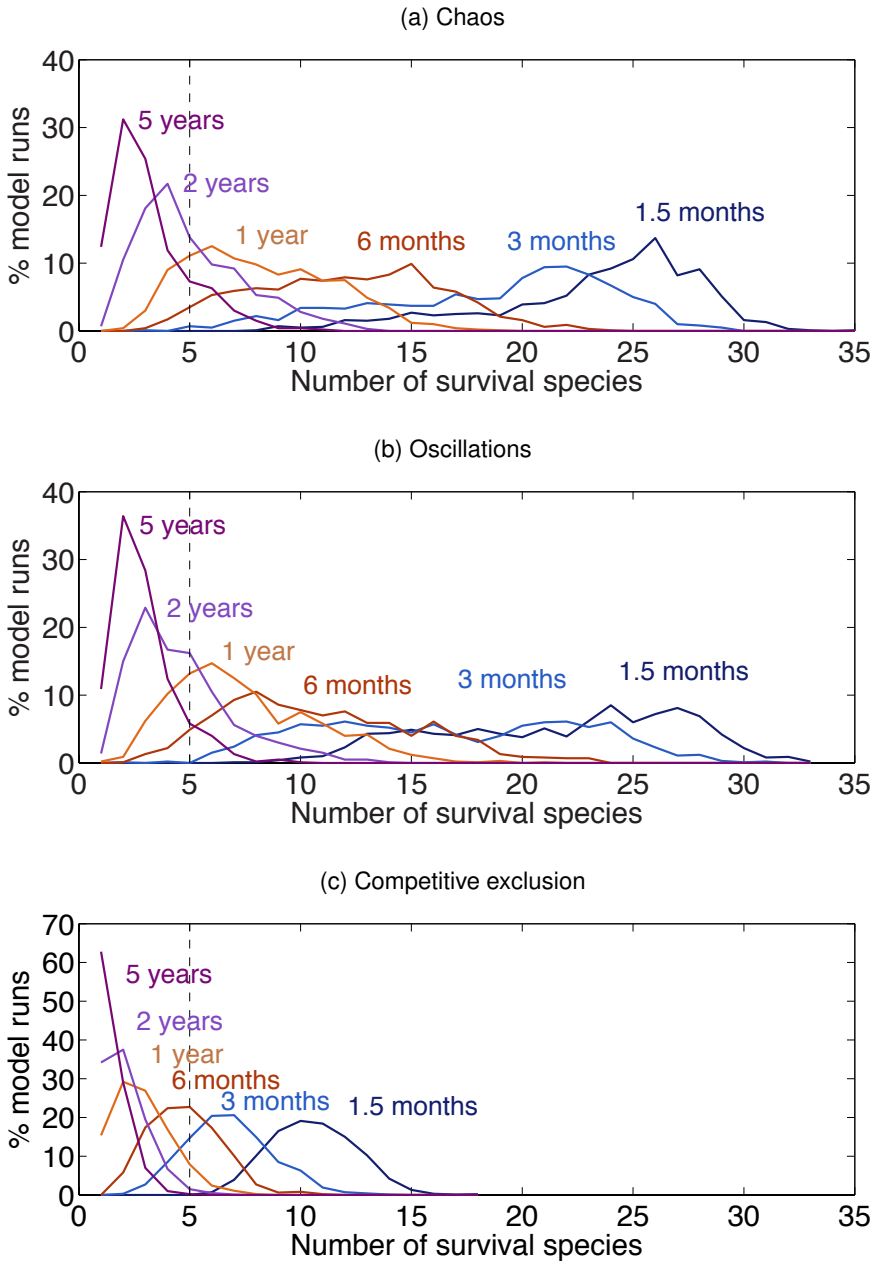

Figure 4.7: Number of species sustained at a particular time after the last injection of species, for 1000 model integrations, with each model compilation generated with a different set of random cell traits of injected species. Each set of 1000 runs is induced with different choices of the half-saturation coefficients, K_{ji} for the initial 5 species, which leads to (a) chaos (with default K_{ji}), (b) 1-period oscillations (with $K_{5,4} = 0.37$) and (c) competitive exclusion (with $K_{2,4} = 0.20$). The dashed line indicates the maximum of 5 species surviving on 5 resources predicted for equilibrium by the resource competition theory.

In summary, chaos and oscillations support a comparable number of species, exceeding the number of resources for as long as 2 yr after the last input of new species, while competitive exclusion usually sustains a lower number of species than expected from the resource competition theory (Fig. 4.8).

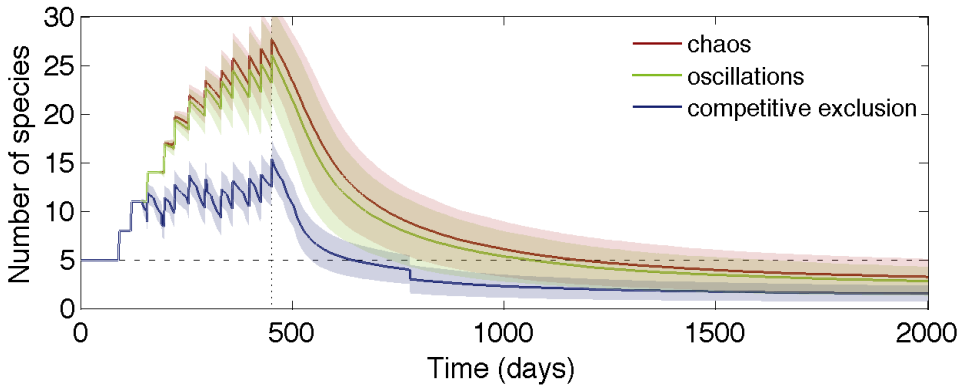

Figure 4.8: Mean number of species sustained throughout 1000 model integrations after the last pulse of extra species (indicated by vertical, dotted line). Each set of 1000 runs is induced with different choices of the half-saturation coefficients, K_{ji}, for the initial 5 species, which leads to (a) chaos (red line, with default K_{ji}), (b) 1-period oscillations (green line, with $K_{5,4} = 0.37$ and (c) competitive exclusion (blue line, with $K_{2,4} = 0.20$). Standard deviation is indicated by the corresponding shaded regions. The horizontal dashed line specifies the maximum of 5 species coexisting on 5 resources based on the resource competition theory.

4.4 Discussion

Hutchinson (1961) first questioned why so many different phytoplankton species persist, given competition theory predicting that at equilibrium the number of species cannot exceed the number of limiting resources. He suggested that this paradox of the phytoplankton and inconsistency with competition theory might be reconciled by the phytoplankton community not being at equilibrium. One of the proposed solutions to the paradox is that variability within planktonic communities can be generated as a result of inter-species competition for resources, as advocated by Huisman and Weissing (1999, 2001). Rather than a single or a few species dominating as in competitive exclusion, the phytoplankton community can continually vary in the form of repeating oscillations or chaotic changes in the abundance of different species.

Whether the model solutions lead to competitive exclusion, oscillations or chaos turns out to be sensitive to assumptions on the modelled nutrient cycling, the cell physiology and nutrient requirements. Competition between species of similar fitness is most likely to lead to competitive exclusion, with the optimal competitor having the lowest requirement for a resource (Tilman, 1977). Including competition between species with variability in nutrient requirement and cell physiology via cell quota does not lead to an optimal competitor emerging, and instead favours oscillatory or chaotic behaviour. The findings suggest that greater differentiation and niche separation between individual species introduce greater complexity to the inter-species interactions which may lead to oscillatory or chaotic behaviour. Specialization on a different resource has been suggested as a key factor allowing for species coexistence (Tilman et al., 1982). Whether chaotic response can emerge is controlled by the internal variability in the cell nutrient quota which suggests that higher departures from the Redfield ratio in the

elemental composition of species favour complex community behaviour and act to increase biodiversity. Departures from the Redfield ratio have been widely documented within microbial community (Arrigo et al., 1999, 2000; Pahlow and Riebesell, 2000; Sweeney et al., 2000; Veldhuis et al., 2005). It has been previously suggested that implementation of variable stoichiometry may improve the ability of ecosystem models to capture species coexistence and biodiversity (Göthlich and Oschlies, 2012), which is confirmed by the findings of this study.

Model simulations suggest that the detailed response turns out to be controlled by the nutrient requirement of the intermediate species compared with that of the other species. In our sets of 1000 model experiments with different ranges in half-saturation coefficient (Table 4.1), competitive exclusion occurs for 19% of the integrations if there are large contrasts in half-saturation coefficient, and increases to 47% of the integrations if there are small contrasts in half-saturation coefficient (Table 4.1), reflecting the increased chance of identifying an optimal competitor with small contrasts in half saturation. In turn, a combination of oscillations and chaos then occur for at least half of the model integrations.

A particular criticism of whether inter-species competition explains the paradox of the plankton is that chaotic solutions might be an unusual occurrence, as suggested by model experiments initialised with randomly assigned characteristics for the phytoplankton (Schippers et al., 2001). However, this conclusion is challenged by Huisman et al. (2001) who argue that a different response is obtained if additional phytoplankton species are injected at different times and a wider range of physiological choices are made. Here, the model diagnostics support the view of Huisman and Weissing (1999, 2001) that chaos can emerge in a well-mixed box through inter-species competition for phytoplankton communities. Indeed, a long-term laboratory mesocosm experiment

which monitored the plankton community twice a week for 2300 d revealed chaotic fluctuations in phytoplankton species abundances (Benincà et al., 2008), consistent with a lack of predictability beyond 15 to 30 d.

With respect to how many phytoplankton species are supported when transport and dispersal are included from the wider environment, a short-term injection of species leads to a long-term sustenance of more species than resources if there are oscillations or chaotic solutions. In both cases, there is a very similar response with supersaturation in the number of species, and in a limited number of cases ($< 8\%$) we observed supersaturation of the community until the final stage of model simulations. In contrast, when there is a competitive exclusion, an additional injection of species only leads to a short-lived excess of species, which quickly die away. Thus, given a random injection of species, both oscillatory and chaotic solutions help sustain more phytoplankton species than resources. For an observational time series data, it may be challenging to determine whether a species is gradually becoming extinct or whether the negative net growth rate is sustained due to the low frequency variability that is not captured within the sampling period. Chapter 3 (see Fig. 3.19) illustrates that imposing seasonal variability in the nutrient supply on a stable phytoplankton community exhibiting chaotic behaviour, can lead to a long-term trend emerging, with an overall loss indicated for some of the coexisting species. Physical transport through mesoscale vortices can further inhibit verification of species fitness through periodically re-introducing the declining species to the unfavourable environment.

In the model experiments conducted in this study, the emergence of chaos versus oscillations is very sensitive to whether a nutrient feedback is included. When the feedback is strong, chaotic solutions emerge, but when the feedback is weak or absent then the solutions switch to oscillations or competitive exclusion. A choice of

strong feedback acting to restore nutrients is appropriate for the way a chemostat operates or for a simple 1-dimensional problem, such as how vertical diffusion acts to supply nutrients down-gradient to the euphotic zone and sustain productivity. However, there is a question as to the extent that the nutrient feedback always holds in the open ocean. The nutrient supply to the euphotic zone is affected by a wide range of physical processes, including convection, entrainment at the base of the mixed layer, and horizontal and vertical transport by the gyre, eddy and basin scale overturning circulations (Williams and Follows, 2003). These processes can either enhance or inhibit biological productivity. For example, wind-driven upwelling induces productive surface waters over subpolar gyres, while wind-driven downwelling induces oligotrophic surface waters over subtropical gyres. These physical processes are unlikely to always provide a nutrient feedback to sustain inter-species driven chaos. There may be some regimes, particularly physically isolated cases, when species competition might induce chaos, such as in the deep chlorophyll maximum in oligotrophic gyres during the summer when there is weak mixing (Huisman et al., 2006). Elsewhere, phytoplankton diversity is probably determined by a combination of inter-species competition and the effects of spatial and temporal variations in physical forcing. For example, phytoplankton diversity is enhanced in western boundary currents and gyre boundaries by the combination of transport, lateral mixing and dispersal, as shown by Barton et al. (2010) and Follows et al. (2007). In stable environments, stochastic mixing events or passing eddies may temporarily disturb the nutrient feedback and inhibit chaos, however, the phytoplankton community has an ability to recover and switch back to its initial, long-term response. The temporal variability in the availability of abiotic resources has been previously suggested to lead to intrinsic transitions in dynamic behaviour when the phytoplankton community can switch between equilibrium and chaotic response (Becks and Arndt, 2008).

The sensitivity of our phytoplankton solutions to the coupling between phytoplankton species and the abiotic resource is perhaps analogous to how predator-prey cycles and their chaotic solutions are sensitive to the nature of their coupling. For example, coupling of the predator-prey cycles through competition between predators for all prey species leads to predator abundance increasing in phase with the prey, while coupling the cycles of specialist predators leads to the opposite response of prey species declining with increasing predator abundance (Vandermeer, 2004; Benincà et al., 2009). The strength of predator-prey interactions also affects whether competitive exclusion, oscillatory or chaotic responses occur (Vandermeer, 1993, 2004). Overabundant prey can even destabilize the ecosystem, leading to large amplitude cycles of predator populations (Rosenzweig, 1971; May, 1972). Chaotic dynamics thus emerge as a response to a coupling of multiple, non-linear oscillators. For an idealized chemostat model used in this thesis, nutrient feedback introduces the non-linearity to a nutrient equation and therefore is crucial for generating chaos. In the absence of a nutrient feedback, implementation of another variable with non-linear interactions may be necessary for chaos to occur.

Returning to the question of how the diversity of the phytoplankton community is sustained, as originally posed by Hutchinson (1961), there are 2 apparently contrasting views: the effect of spatial and temporal variability in forcing, and the inter-species competition view. However, both viewpoints involve mechanisms preventing the optimal competitor dominating and leading to an equilibrium state, either achieved via the physical disturbance of the environment or by a transient flourishing of suboptimal competitors as part of oscillatory and chaotic solutions. The timescale of species extinction is estimated for 3 to 6 months and can further increase to 1-2 years if the resident community exhibits non-equilibrium behaviour. This suggests that disturbances occurring at an approximately monthly frequency, such as weather events, should be

sufficient to significantly delay species extinction for community initially exhibiting competitive exclusion. In case of the oscillatory and chaotic behaviour, where species extinction is already reduced, disturbances occurring at lower frequencies should be sufficient to further increase the persistence of weaker nutrient competitors, and these will now incorporate physical transport processes such as mesoscale eddies that can re-occur 4-5 times a year (Schouten et al., 2003; Palastanga et al., 2006) and re-introduce new phytoplankton species. The role of the intermediate disturbance on phytoplankton community dynamics and diversity is further examined in Chapter 5.

4.5 Chapter summary

The diversity of phytoplankton species and their relationship to nutrient resources are examined using a coupled phytoplankton and nutrient model for a well-mixed box. The phytoplankton community either reaches a competitive exclusion state, where there is an optimal competitor, or the abundance of each phytoplankton species continually varies in the form of repeating oscillations or irregular chaotic changes:

- oscillatory and chaotic solutions make up over half of the model solutions based upon sets of 1000 separate model integrations,
- the oscillatory or chaotic states allow a greater number of phytoplankton species to be sustained in the environment.

The chaotic response turns out to be sensitive to particular model choices:

- the strength of the feedback between nutrient supply and ambient nutrient concentration, which can be viewed as mimicking the diffusive nutrient supply from the nutricline,
- physiological differences among species, including cell quota and K_{ji}.

Inter-species competition might be important in generating chaos when the diffusive nutrient transfer is important, but less likely to be significant when other transport processes sustain surface nutrient concentrations. Further investigation will aim to assess how robust is the locally generated community response under the externally-induced variability in nutrient supply, and how continuous horizontal advection of new communities modifies the response of the resident community.

CHAPTER 5

The role of externally-imposed variability in shaping the phytoplankton community response

Rationale:

This chapter focuses on the role of externally-induced environmental variability in shaping phytoplankton community dynamics, and explores whether chaotic response of phytoplankton to competition for nutrients can persist under environmental heterogeneity. The study focuses on two distinct forcing mechanisms that directly affect the competition between phytoplankton species: intermediate frequency disturbances and seasonal fluctuations in the nutrient availability. The applicability of the Intermediate Disturbance Hypothesis (Connell, 1978) is tested by including stochastic, weather-related variability leading to enhanced nutrient supply to the surface waters as a result of irregular mixing events. The objective is to establish whether chaos is enhanced or inhibited by periodic and stochastic variability in the resource availability.

5.1 Introduction

A number of idealized model experiments have confirmed that interactions and competition within biological populations can lead to non-equilibrium dynamics and chaos (May, 1974; Hastings and Powell, 1991; Huisman and Weissing, 2001). Irregular fluctuations prevent the community from exhibiting competitive exclusion and can support a greater number of species, thus making a significant contribution to diversity (Allen et al., 1993; Huisman and Weissing, 1999; Huisman et al., 2001). However, marine ecosystems are subject to random and periodic environmental fluctuations, in the form of stochastic weather conditions or the seasonal cycle. Such environmental variability could potentially modify the internally-induced response of the phytoplankton competing for nutrients, which in turn might have important implications for local biodiversity.

According to the Intermediate Disturbance Hypothesis (Connell, 1978), environmental perturbation in the physical environment could prevent the best-adapted competitor from dominating the community. The necessary disturbance needs to be of an intermediate timescale relative to the generation timescale of affected population (Connell, 1978; Reynolds et al., 1993). For phytoplankton communities, the generation timescale is about 2-3 days and environmental perturbations occurring every 5-15 days might be sufficient for species to respond to the disturbance and effectively prevent the progression of the community towards competitive exclusion (Reynolds et al., 1993).

In the context of microbial communities, laboratory experiments have confirmed that the number of coexisting species increases as a result of intermittent variability in light (Gemerden, 1974; Sommer, 1985; Litchman, 1998), temperature (Rhee and Gotham, 1981; Descamps-Julien and Gonzalez, 2005) or nutrient environment (Ebenhöh, 1988). In particular, the model study of Ebenhöh (1988) investigated the competition of phyto-

plankton for a single resource in a well-mixed box and suggested that the optimal timescale of intermediate disturbance is between 6 to 10 days. For real world ecosystems, this timescale is comparable to the timescale of weather-related variability and storm intensification, or the spring-neap cycle in the tidal forcing. Such physical variability leads to an enhanced vertical mixing and nutrient supply to the upper mixed layer, and temporarily fuels phytoplankton growth. The applicability of the Intermediate Disturbance Theory has been tested in a model simulating phytoplankton dynamics in a stratified lake, where the intermediate disturbance was introduced through variations in the mixed layer depth (Elliott et al., 2001). The model experiments of Elliott et al. (2001) suggested that the highest biodiversity is sustained under imposed mixing events of intermediate frequency, every 12 to 45 days, and intermediate intensity, lasting of 3 to 7 days. The community reaches competitive exclusion when mixing events occur less frequently or of a too low intensity to affect the population, or for the mixing to be so strong that extinction is facilitated (Elliott et al., 2001).

Alongside the Intermediate Disturbance Hypothesis, seasonal variability in environmental conditions is the main driver of annual species succession. Summer stratification stabilizes the water column, which enhances the available light experienced by phytoplankton at the surface and inhibits nutrient supply across the thermocline, whilst winter deepening of the upper mixed layer entrains high amounts of nutrients in the surface waters. The modification of the physical environment allows the dominant phytoplankton groups to change as the environmental conditions become more beneficial. Seasonality is the most profound forcing controlling the functioning of marine ecosystems and shaping the community structure (Letelier et al., 1993; Habib et al., 1997). However, according to the principles of the Intermediate Disturbance Hypothesis, seasonality is of a too low frequency to result in an increased number of coexisting species and prevent the competitive exclusion from occurring. All the same, periodic forcing is

an important factor for controlling population dynamics and can reduce species extinction rates by driving a non-equilibrium community response (Dakos et al., 2009). The effect of regular seasonal forcing on modelled populations have been explored through predator-prey models (Rinaldi and Muratori, 1993), multi-species plankton community models (Dakos et al., 2009), plankton-fish food webs (Doveri et al., 1993), and ecosystem models with implemented variability within the upper mixed layer (Popova et al., 1997). The above examples of model simulations confirm that chaos is an inherent response within a seasonally forced environment. However, some of the studies have emphasized the narrow range of forcing parameters for which chaotic behaviour is predominant. For example, Popova et al. (1997) applied a 4-component ecosystem model (nitrogen, detritus, phytoplankton and zooplankton) with implicit representation of upper mixed layer depth and seasonality, and found that chaos is only prevalent under environmental conditions corresponding to the low latitude regions of strong upwelling. The model simulations of Doveri et al. (1993), where a 4-level marine food-web (phosphorus, phytoplankton, zooplankton and fish) is simulated in a well-mixed box, suggest that chaos is a phenomenon occurring in high-light, high-phosphorus regions, such as low latitude eutrophic lakes.

Chaos under imposed seasonal variability manifests itself in the form of a strong inter-annual variability in species succession through variations in phytoplankton phenology (Doveri et al., 1993; Rinaldi and Solidoro, 1998; Dakos et al., 2009). Indeed, large inter-annual variability is detected in seasonally varying marine ecosystems across a wide latitudinal range (Talling, 1993; Smayda, 1998; Philippart et al., 2000; also see Fig. 3.2, p. 48, illustrating inter-annual variability in the blooms of diatoms and dinoflagellates in the English Channel), as well as within terrestrial populations (Berg et al., 1998).

There are two prevailing types of climate-related variability that shape the marine environment and prevent the ecosystem from reaching an equilibrium: seasonality and weather-related variability. Both types of variability have the potential to modify significantly the phytoplankton community response generated through inter-species competition for nutrients. This study focuses on the effect of external variability in controlling phytoplankton community dynamics and shaping biodiversity. Through implementation of periodic and stochastic forcing in nutrient supply, we examine how phytoplankton response and number of surviving species change subject to the externally-imposed variability, and therefore test the applicability of the Intermediate Disturbance Hypothesis and the effects of seasonal forcing. In particular, the sensitivity of chaotic phytoplankton response is examined. While previous studies have investigated the validity of the Intermediate Disturbance Hypothesis, this study focuses on the interactions between the imposed forcing and the outcome of the interspecies competition. The aim is to verify the potential contribution of periodic and stochastic environmental variability in driving complex behaviour within aquatic ecosystems.

5.2 Model experiments

An idealized chemostat model for phytoplankton competition for essential resources is applied, where n phytoplankton species, P_i, compete for k limiting nutrients, N_j (see Chapter 2). Phytoplankton growth, γ^N, is controlled by the availability of the limiting nutrient:

$$\frac{\partial P_i}{\partial t} = P_i(r_i\gamma_i^N - m_i) \qquad i = 1,...,n \tag{5.1}$$

$$\gamma_i^N = min\left(\frac{N_1}{K_{1i}+N_1},...,\frac{N_k}{K_{ki}+N_k}\right) \tag{5.2}$$

where r_i and m_i denote the maximum growth rate and mortality rate respectively. Each phytoplankton species is attributed species- and resource-specific half-saturation coefficient, K_{ji}, and cell quota, Q_{ji}. Unless otherwise stated, the model parameters and initial conditions follow those of Huisman and Weissing (1999) as described in Table 2.1 (p. 26).

Model simulations aim to test the sensitivity of the community response to modified nutrient supply conditions. The effects of periodic nutrient variability and stochastic, weather-related nutrient inputs are considered. Enhanced mixing generated by the two processes act to amplify the background nutrient supply, S_j. In order to lower the minimum level of the background nutrient supply in the absence of physical forcing, the default S_j is decreased to $\frac{1}{2}S_j$, so that $S_j = [3.0, 5.0, 7.0, 2.0, 4.5]$.

The necessary modifications in the nutrient supply for both cases are discussed in sections 5.2.2 to 5.2.3. The variability in the nutrient supply is first imposed on example phytoplankton communities exhibiting different types of responses, discussed in section 5.3.1.

The final stage of the analysis involves investigation of the effects of the externally-

induced variability on the occurrence of chaos in particular. Seasonal and stochastic fluctuations in the nutrient supply of variable amplitude are applied to a set of 1000 model integrations, with each simulation initialized with a different phytoplankton community generated through randomized choices for K_{ji}, described in section 5.4.1.

Every model simulation under a different nutrient supply scenario is analysed for chaotic behaviour, diversity and dominant oscillation frequency, and compared against the unforced community. The model simulations cover 11000 days with the initial 1000 days treated as the spin-up time and excluded in the analysis of the time series. Diversity is measured as (i) a number of species with a non-zero abundance, and as (ii) a number of species that constitute at least 5% of the total community biomass, which is calculated as a contribution average over the last 2000 days of the model simulation in order to account for species annual succession. The dominant frequency is obtained through Fast Fourier Transform analysis of the concentration time series for the most abundant species. In the experiments, periodic and stochastic variability in nutrient supply are imposed within the first day of model simulations, before the phytoplankton community is established.

5.2.1 Verification of chaos

Complex dynamics are determined by numerical estimation of the maximal Lyapunov Exponent, λ_{max}, that verifies the sensitivity to initial conditions:

$$\lambda_{max} = \lim_{t\to\infty} \frac{1}{t}\ ln\left(\frac{|x(t) - x_\varepsilon(t)|}{|x(0) - x_\varepsilon(0)|}\right). \tag{5.3}$$

The algorithm calculates the rate of exponential separation, λ_{max}, with time t, between two trajectories, x and x_ε, initially at some small distance apart. Details on the numer-

ical implementation of the method are discussed in Chapter 2.

5.2.2 Periodic forcing

The nutrient supply concentration, S_j, is now controlled in a form of a periodic, sinusoidal variability, σ, of variable amplitude, A:

$$\frac{\partial N_j}{\partial t} = D(\sigma S_j - N_j) - \sum_{i=1}^{n} Q_{ji} r_i \gamma_i^N P_i \qquad j = 1, ..., k \tag{5.4}$$

$$\sigma = 1 + 0.5\, A\, \left(sin\left(\frac{2\pi t}{T} \right) + 1 \right), \tag{5.5}$$

where D is the system's turnover rate, T is the forcing-specific oscillation period and A is the amplitude of the oscillations.

The impact of periodic nutrient input of variable frequency, is investigated for a range of forcing amplitudes: 0.5, 2.0, 6.0, 10.0 (Fig. 5.1a).Chosen periods range from semi-diurnal ($T = 0.5$ d) to annual ($T = 365$ d). Different forcing amplitudes aim to represent regional or meridional variability in the intensity of the enhanced mixing events that occur regularly. For example, seasonal nutrient supply is weaker in the low latitudes where the sea surface temperature range is of the order of a few ^oC. This contrast increases to tens of ^oC in the higher latitudes where the effects of seasonal variability are more profound. Similarly the amplitude of spring-neap tidal cycle varies regionally depending on the local bathymetry.

5.2.3 Stochastic weather-related variability

Wind speed data is used as a proxy for the strength of the weather events that lead to an enhanced nutrient supply. The data is taken as an approximation of the an-

nual relative variability in the level of erosion of the mixed later depth, resulting in the entrainment of inorganic nutrients in the upper mixed layer.

Wind speed time-series data is retrieved from the European Centre for Medium-Range Weather Forecasts (ECMWF) re-analysis data for the location 50°N 4°W. The time series is sampled every 6 hours and covers 30 years, from January 1980 to December 2009. The long-term trend is removed from the data. Analysis of the time series for chaotic behaviour yielded non positive Lyapunov Exponent and suggested stochastic variability.

The study assumes that the external forcing is composed of repeated annual cycle and stochastic variability. An annual time series of wind speed variability is taken from a 30-year climatology, and the seasonal cycle is removed. The annual time series of the stochastic component is then normalized, where 0 represents calm weather conditions and no mixing, and 1 denotes the strongest recorded storm and, therefore, highest possible nutrient input resulting from enhanced mixing. The time series now exhibits irregular oscillations with a dominant oscillation period of about 25 days.

The normalized wind speed time series, ws_{norm}, is linearly interpolated to align with the time step applied in the model simulations ($dt = 0.001$), and replicated every 365 days. The stochastic variability, ε_s, is implemented in the nutrient supply term so that:

$$\frac{\partial N_j}{\partial t} = D(\varepsilon_s S_j - N_j) - \sum_{i=1}^{n} Q_{ji} r_i \gamma_i^N P_i \qquad j = 1, ..., k \tag{5.6}$$

$$\varepsilon_s = 1 + A\ ws_{norm} \tag{5.7}$$

The impact of stochastic weather events is investigated for a range of forcing amplitudes, A: 0.2, 0.5, 1.0, 3.0, 5.0 and 10.0 (Fig. 5.1b) in order to account for regional variability in the intensity of the weather events.

(a) Periodic nutrient supply

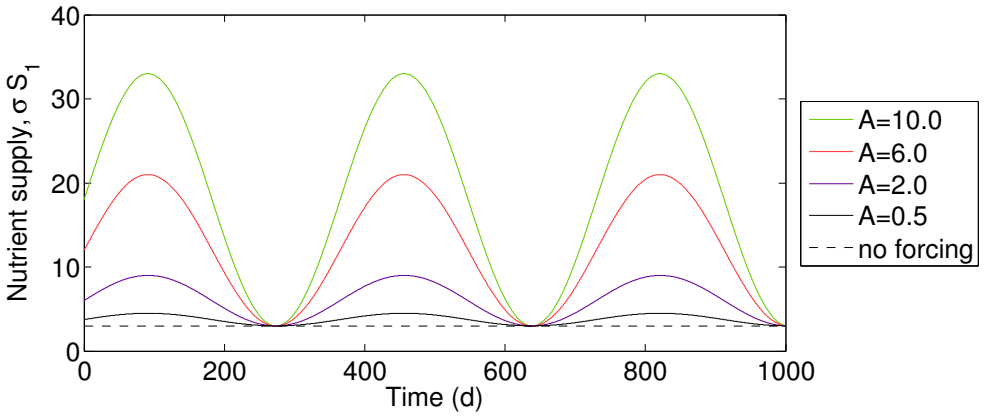

(b) Stochastic variability

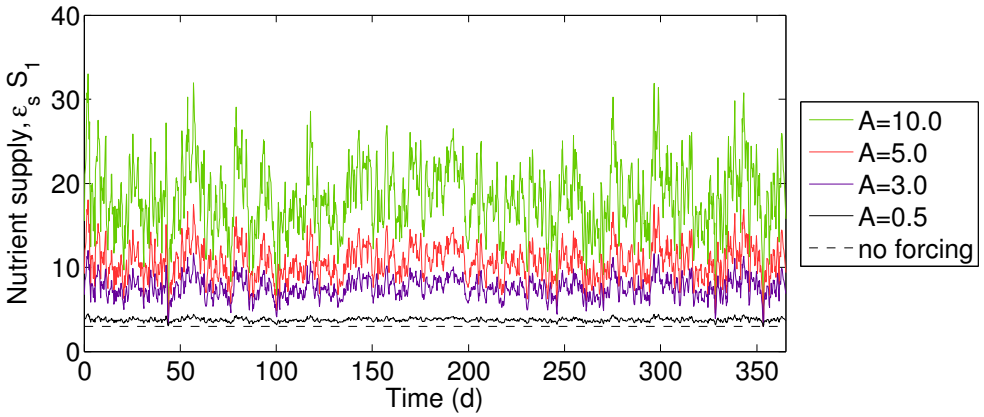

Figure 5.1: Variability in the modelled nutrient supply as a result of (a) periodic forcing, such as, for example, seasonal variability generated with $T = 365$ days, and (b) stochastic weather events.

5.3 The effect of external forcing - community examples

5.3.1 Considered phytoplankton communities

Variability in the nutrient supply in a form of periodic pulses and stochastic variability is imposed on 5 different, modelled phytoplankton communities exhibiting various levels of diversity and different types of community response. Example phytoplankton communities are generated through modification of a particular half-saturation coefficient, K_{ji}, with the rest of the parameters remaining unchanged, as in the default model set up.

Here, the considered phytoplankton communities exhibit: (1) regular oscillations of 4 species with $K_{4,1} = 0.40$ (Fig. 5.2a), (2) regular oscillations of 3 species with $K_{1,4} = 0.40$ (Fig. 5.2b), (3) competitive exclusion with 2 survival species with $K_{3,3} = 0.29$ (Fig. 5.2c), (4) competitive exclusion with 1 dominant species with $K_{4,1} = 0.20$ (not shown; see Fig. 4.1a, p. 88) (5) chaotic fluctuations of 5 species with the default K_{ji} (not shown; see Fig. 4.1c, p. 88).

(a) Oscillations of 4 species

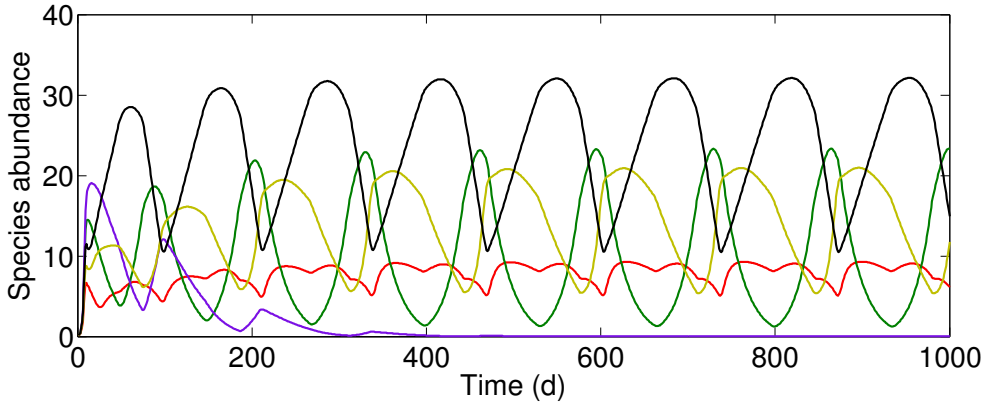

(b) Oscillations of 3 species

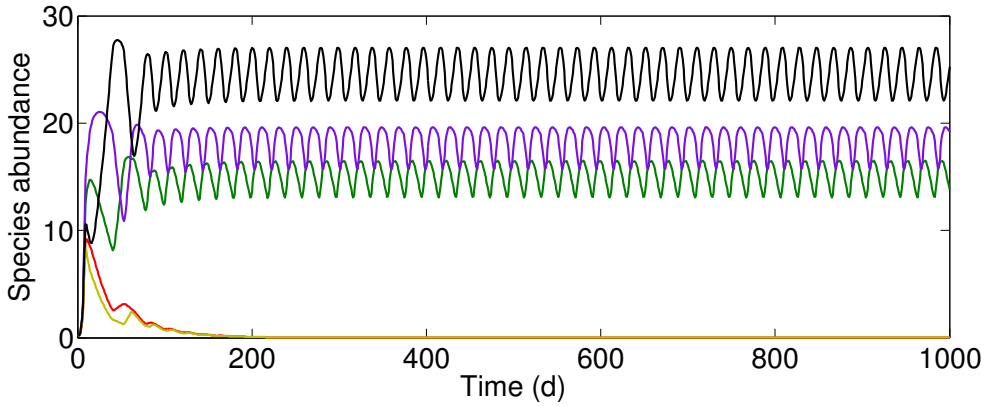

(c) Steady coexistence of 2 species

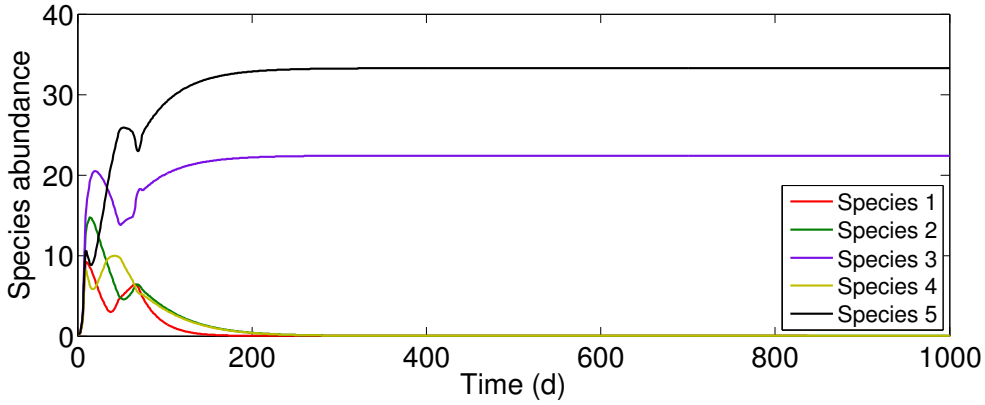

Figure 5.2: Example community behaviour under no externally-induced variability: regular oscillations of (a) 4 and (b) 3 species, and (c) steady coexistence of 2 species.

5.3.2 Periodic forcing

The response of the phytoplankton community to periodic forcing depends on the community structure. For all of the considered community examples, the number of species contributing to community diversity is calculated as a number of species with a non-zero abundance. All of the species contribute at least 5% to the total community biomass and, therefore, defining biodiversity as a minimum percentage contribution does not alter the findings.

The community exhibiting regular oscillations with 4 survival species (Fig. 5.2a), exhibits greatest sensitivity to imposed periodic forcing. High frequency oscillations in the nutrient supply lead to the community response switching to a chaotic regime, with highest recorded $\lambda_{max} = 0.038$ d^{-1} (Fig. 5.3a). The number of coexisting species increases to 5 species when imposing the variability of the oscillation period of up to $T_{forcing} = 40$ days for all considered amplitudes. Lower frequency forcing leads to a decline in species diversity coinciding with lower λ_{max}, or $\lambda_{max} = 0$ for forcing variability of low amplitude (Fig. 5.3b). Under imposed high frequency forcing, the community oscillates at half the oscillation period set by the inter-species competition under no forcing variability (133 days), of about $T_{community} = 60$ days. When the forcing oscillation period $T_{forcing} =$ 2 to 6 days is imposed the phytoplankton community begins to oscillate at the frequency of the external forcing, a phenomenon referred to as frequency locking (Fig. 5.3c).

In contrast, the phytoplankton community initially having regular oscillations with 3 survival species (Fig. 5.2b), exhibits much less sensitivity to the external forcing. The community exhibits chaotic behaviour when imposing forcing with an oscillation period $T_{forcing} =$ 2 to 10 days, with positive λ_{max} recorded (Fig. 5.4a). However, the diversity

level of the community remains unchanged under imposed periodic variability for all considered frequencies and amplitudes (Fig. 5.4b). Similarly to the previously discussed cases, the phytoplankton community under high frequency variability oscillates at twice the frequency of the unforced community, with the oscillation period decreasing from $T_{community} = 20$ to 10 days for low amplitude forcing (Fig. 5.4b).

For communities initially showing competitive exclusion, the responses to periodic forcing vary depending on the species interactions. In case of competitive exclusion with 2 dominant species (Fig. 5.2c), imposing external variability leads to regular oscillations of the community ($\lambda_{max} = 0$) with up to 4 coexisting species (Fig. 5.5a,b), but with only a handful of cases where external variability leads to a chaotic response ($\lambda_{max} = 0.04$ d^{-1}). In contrast, for the pre existing case of competitive exclusion where only one species dominates, no external forcing frequency generates complex dynamics and increases the number of coexisting species. For both cases, phytoplankton species experiencing high frequency forcing exhibit oscillations of $T_{community} = 2$ to 20 days, with frequency locking occurring when the forcing of at least $T_{forcing} = 2$ days is imposed (Fig. 5.5c).

In a chaotic community, for the vast majority of the cases, external forcing generally acts to enhance the chaotic response by increasing λ_{max} from 0.013 d^{-1} for the unforced community, up to 0.067 d^{-1} for a community experiencing periodic variability of a strong amplitude. There are only a few cases where periodic variability is imposed and $\lambda_{max} = 0$ indicates non-chaotic behaviour. The number of survival species remains 5 for all simulations. High frequency forcing leads to the community oscillating at approximately twice the frequency of the internally-set pace of community oscillations, decreasing the oscillation period from $T_{community} = 85$ days to $T_{community} = 40$ days. Lower frequency forcing, of a period greater than about $T_{forcing} = 2$ days, leads to frequency

locking within the phytoplankton community.

The point at which the frequency of the external forcing becomes the dominant frequency of the phytoplankton community appears to be sensitive to the internally set pace of the phytoplankton community. Taking the discussed chaotic community as an example, increasing the mortality rate to $m_i = 0.35$ d^{-1} for the modelled community, leads to a decrease in the actual growth rate, γ_i^N (since in a homogenous environment $\gamma_i^N \approx m_i$) and results in the dominant oscillation period of 133 days. In this case, frequency locking occurs when periodic variability of 8-day period is imposed. In contrast for decreased mortality rate $m_i = 0.15$, a community growing at higher $\gamma_i^N \approx 0.35$ d^{-1} generates oscillations of 12.8-day period. For the frequency locking to occur for this case, the required variability needs to be of a lower oscillation period of 2 days. This analysis suggests that for high frequency systems, forcing of a higher frequency drives the community to synchronize their oscillation frequency. In contrast, communities oscillating at a lower frequency appear slightly more resilient. This relation is also illustrated on the example of the two considered communities exhibiting periodic oscillations (community (2) in Fig. 5.2a and community (3) in Fig. 5.2b): frequency locking for the community oscillating at a 133-day period (community (2)) occurs under imposed forcing of longer period, of 6 days, whilst for the community exhibiting oscillations of 20 day period, frequency locking occurs under imposed forcing of slower period, of 2 days (community (3); Fig. 5.3c and 5.4c).

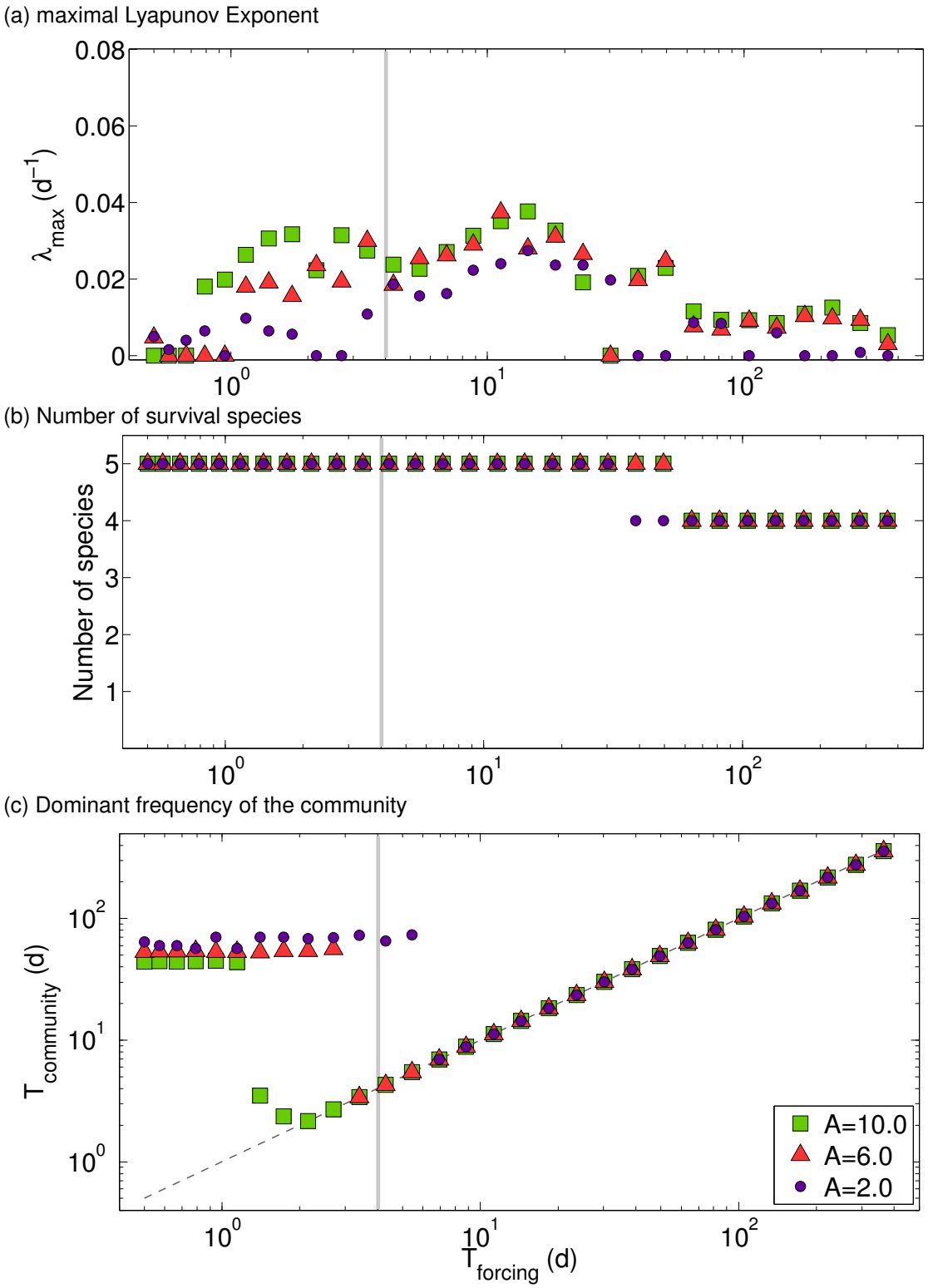

Figure 5.3: The effect of imposed periodic variability in the nutrient supply on the modelled phytoplankton community that exhibits periodic oscillations of 4 species, illustrated in Fig. 5.2a. The imposed forcing is of the variable frequency, ranging in oscillation period, $T_{forcing}$, from 0.5 to 365 days. Panels illustrate changes in (a) the estimated maximal Lyapunov exponent, λ_{max}, (b) number of coexisting species, and (c) dominant oscillation period, $T_{community}$, of the modelled community. Vertical grey line denotes the generation timescale of the unforced community. Dashed line indicates when the frequency locking occurs where $T_{community} = T_{forcing}$.

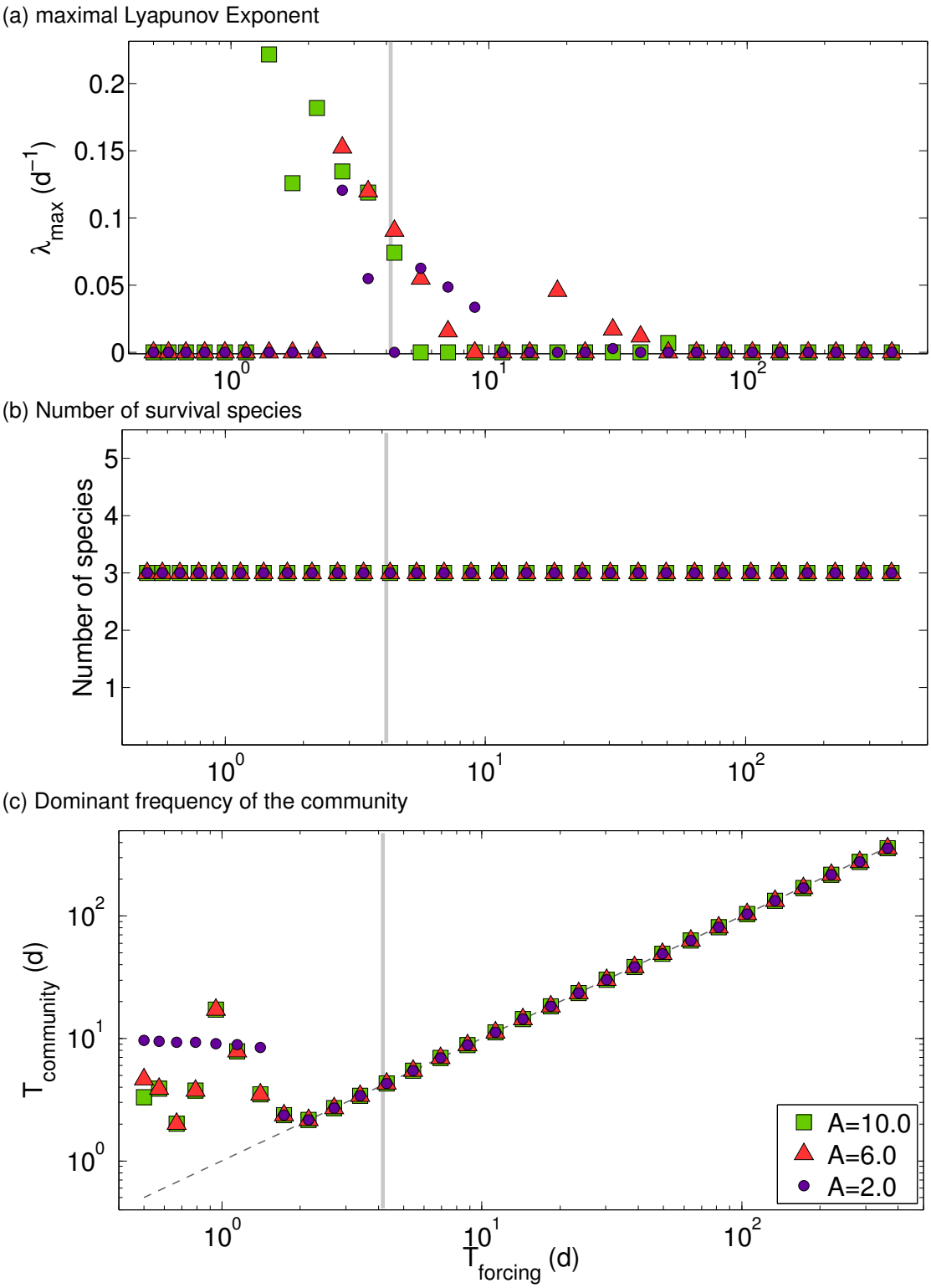

Figure 5.4: The effect of imposed periodic variability in the nutrient supply on the modelled phytoplankton community that exhibits periodic oscillations of 3 species, illustrated in Fig. 5.2b. The imposed forcing is of the variable frequency, ranging in oscillation period, $T_{forcing}$, from 0.5 to 365 days. Panels illustrate changes in (a) the estimated maximal Lyapunov exponent, λ_{max}, (b) number of coexisting species, and (c) dominant oscillation period, $T_{community}$, of the modelled community. Vertical grey line denotes the generation timescale of the unforced community. Dashed line indicates when the frequency locking occurs where $T_{community} = T_{forcing}$.

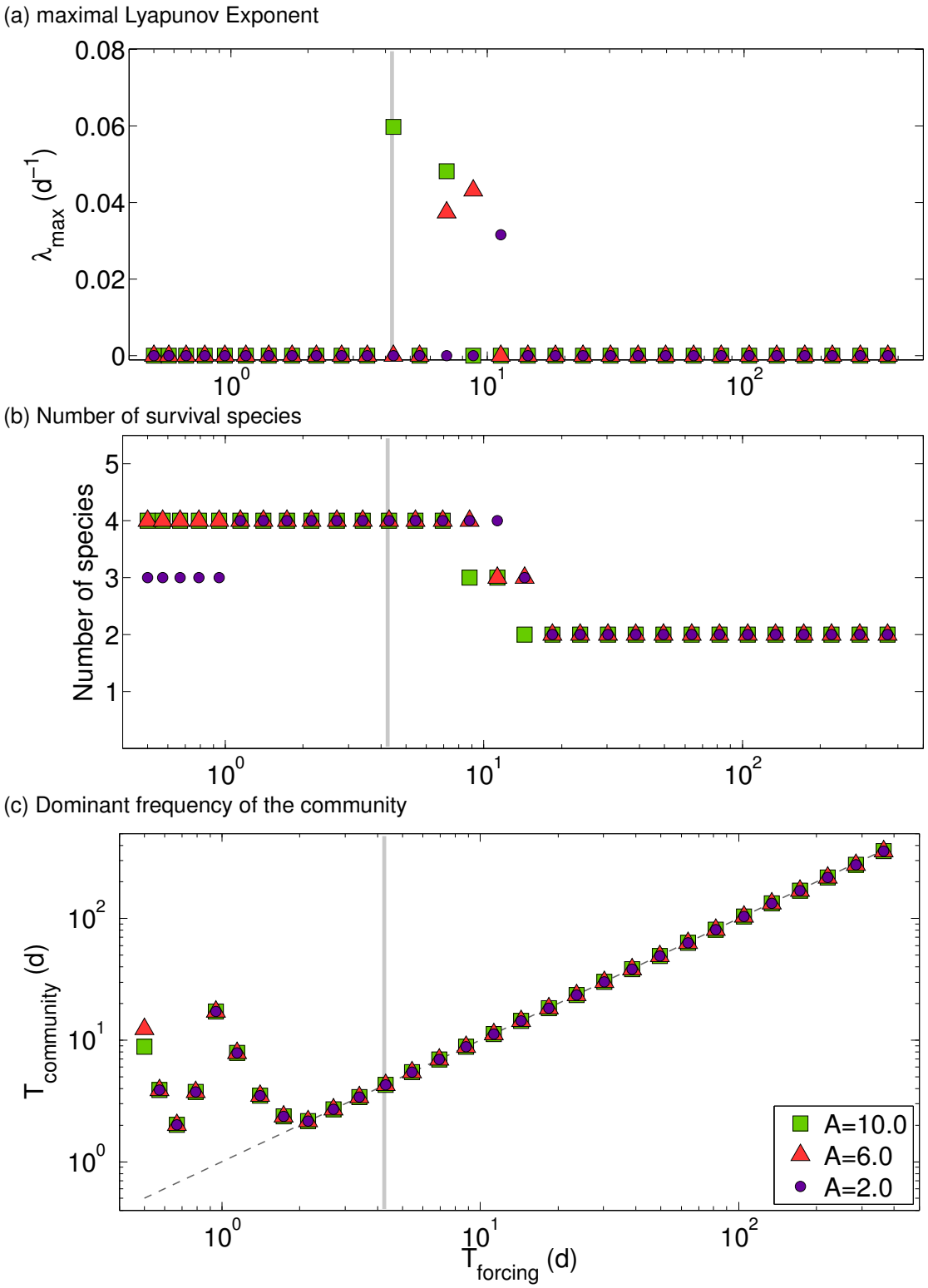

Figure 5.5: The effect of imposed periodic variability in the nutrient supply on the modelled phytoplankton community that exhibits steady coexistence of species, illustrated in Fig. 5.2c. The imposed forcing is of the variable frequency, ranging in oscillation period, $T_{forcing}$, from 0.5 to 365 days. Panels illustrate changes in (a) the estimated maximal Lyapunov exponent, λ_{max}, (b) number of coexisting species, and (c) dominant oscillation period, $T_{community}$, of the modelled community. Vertical grey line denotes the generation timescale of the unforced community. Dashed line indicates when the frequency locking occurs where $T_{community} = T_{forcing}$.

5.3.3 Seasonality and chaos

In order to verify the potential effect of seasonality on the evolution of the maximal Lyapunov Exponent, λ_{max}, the variability in the 'local' Lyapunov Exponents, λ, is considered. Each λ measures exponential separation between the trajectories over a corresponding predictability timescale $\sim \frac{1}{\lambda}$, which means that there is a new λ calculated for each part of the time series of a specific length. An estimation of λ_{max} is obtained through averaging of all λ (see section 2.2.2 on Numerical Estimation of λ_{max}).

The annual variability in the rate of exponential divergence of the trajectory increases as the concentration of the available nutrient starts to decline (Fig. 5.6). This relation suggests that the chaotic response is enhanced over the summer and subdued over the winter period. Indeed, this temporal character of the predictability timescales has been revealed in the seasonally forced upper mixed layer model of Popova et al. (1997).

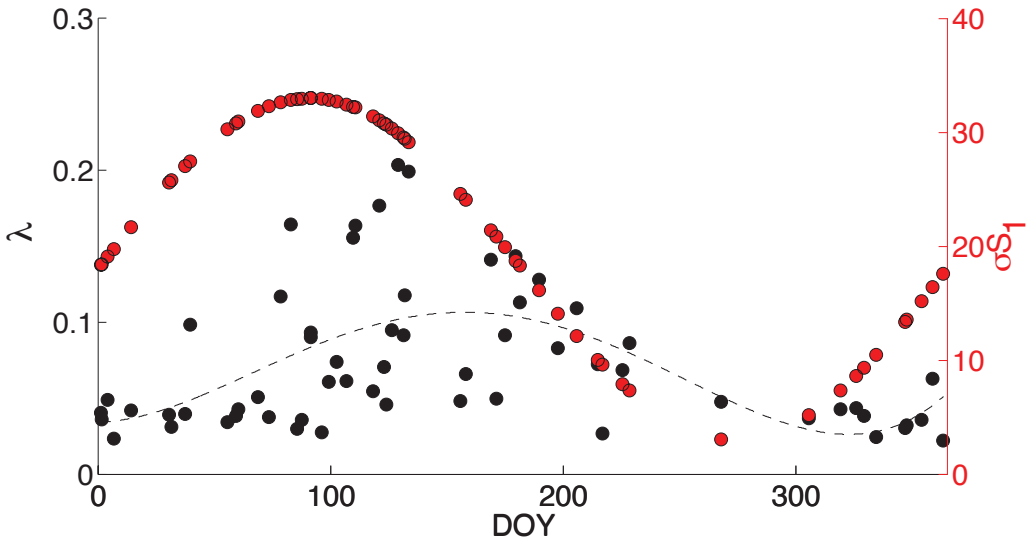

Figure 5.6: Annual variability in the Lyapunov Exponents (λ, in black) and seasonally forced nutrient supply (σS_1, in red) from a 30-year model simulation (11000 days). The dashed line indicates the general pattern of variability in λ versus a day of the year (DOY).

Such a pattern is not observed for the seasonal forcing of low amplitude due to the design of the λ calculation. A lower λ_{max} estimated for phytoplankton community under mildly seasonal conditions suggests higher predictability timescales for the ecosystem, and thus longer time intervals between each calculation of λ. There are an insufficient number of data points distributed throughout the year to be able to establish accurately an annual pattern.

5.3.4 Stochastic variability

In this section, the availability in the nutrient concentration is forced with the stochastic time series obtained from the wind speed re-analysis data in order to mimic the irregular amplification of the nutrient supply driven by weather-related mixing. The analysis investigates how the intermediate frequency disturbances modify the community diversity and response for the example phytoplankton communities.

Environmental disturbance in the form of stochastic weather events do not initially inhibit chaotic dynamics. Increasing the intensity of the variability leads to an increase in λ_{max} which suggests an increased sensitivity to initial conditions and a decline in the timescale for short-term predictability to under 13 days (for $\lambda_{max} = 0.0807\ d^{-1}$; Table 5.1). For the community initially exhibiting regular oscillations of 4 species (Fig. 5.2a), imposing stochastic variability leads to a chaotic response emerging. Although the number of survival species has increased by 1 for high amplitude forcing ($A = 10.0$), the contribution to diversity of the extra species is negligible.

For other examples of community behaviour, imposing stochastic variability does not affect the character of the community response or the number of coexisting species. Increasing the intensity of the weather events modifies the dominant oscillation fre-

quency of the community, with frequency synchronization occurring at higher forcing amplitude (amplitude $A = 5.0$ or above) for oscillatory and chaotic responses.

Table 5.1: The effect of stochastic variability in the nutrient supply for the example phytoplankton communities described in section 5.3.1. Considered community responses incorporate: chaos, oscillations and competitive exclusion.
* see Fig. 5.2a; ** see Fig. 5.2b; ***see Fig. 5.2c.

	Community response	**No forcing**	**A=0.2**	**A=0.5**	**A=5.0**	**A=10.0**
Maximum Lyapunov Exponent, $\lambda_{max}\ (d^{-1})$	chaos	0.0112	0.0123	0.0154	0.0495	0.0807
	oscillations *	0	0	0.0009	0.0265	0.0607
	oscillations **	0	0	0	0	0
	exclusion ***	0	0	0	0	0
	exclusion	0	0	0	0	0
Number of coexisting species	chaos	5	5	5	5	5
	oscillations *	4	4	4	4	5
	oscillations **	3	3	3	3	3
	exclusion ***	2	2	2	2	2
	exclusion	1	1	1	1	1
Dominant oscillation period, $T = \frac{1}{f}\ (d)$	chaos	84.7	33.8	77.5	27.9	27.9
	oscillations *	133.3	119.0	90.1	72.0	27.9
	oscillations **	19.6	17.7	15.8	13.0	27.9
	exclusion ***	-	27.9	27.9	27.9	27.9
	exclusion	-	27.9	27.9	27.9	27.9

5.4 Wider implications of external forcing on chaos and diversity

5.4.1 Investigation of the parameter space

In order to investigate whether externally-imposed periodic or stochastic forcing act to diminish or enhance chaotic response, the forcing is imposed on 1000 separate model simulations. In each model simulation the phytoplankton community is randomly generated through random selection of half-saturation coefficients, K_{ji}, for each species i and resource j. The attribution of K_{ji} is carried out in an ordered manner so that each of the species is the optimal competitor for one of the resources:

$$K_{ji} = \begin{pmatrix} k_5 & k_4 & k_3 & k_2 & k_1 \\ k_1 & k_5 & k_4 & k_3 & k_2 \\ k_2 & k_1 & k_5 & k_4 & k_3 \\ k_3 & k_2 & k_1 & k_5 & k_4 \\ k_4 & k_3 & k_2 & k_1 & k_5 \end{pmatrix} \tag{5.8}$$

where k_i are randomly generated numbers, such that $k_1 < k_2 < k_3 < k_4 < k_5$, denoting the strongest (k_1) and the weakest (k_5) competitor. The values for k_i are chosen (retaining the above structure and ordering) within the interval 0.1 to 1.0. Other parameters characterizing phytoplankton community remain unchanged.

The stochastic and periodic forcing is implemented as described in previous sections with prescribed variations in the amplitude. In the case of the periodic variability, only effects of the seasonal frequency are examined, with $T = 365$ days, because it is the dominant forcing frequency driving the annual variability and seasonal succession in the aquatic plankton communities. Therefore, the analysis investigates the effects of the long-term, seasonal variability and then short-term, stochastic fluctuations.

The phytoplankton community is initiated with 5 species competing for 5 resources, $n = k = 5$. Note, in order to investigate the role of environmental variability in driving higher phytoplankton biodiversity, it is necessary to allow for super-saturated community where $n > k = 5$.

5.4.2 Chaos and community diversity under no external forcing

Out of the entire set of model simulations with generated phytoplankton communities through random assignment of K_{ji}, nearly 60% of model solutions already sustain all 5 species in the environment, with all chaotic solutions composing a half of these cases (33%, indicated by dark purple diamonds in Fig. 5.7a, left panel). For a vast majority of the modelled community 4 species contribute over 5% to the annually-averaged community biomass (indicated in light purple in Fig. 5.7b, left panel; Table 5.2).

Table 5.2: The number of coexisting species (where abundance $P_i > 0$) and the number of species dominating the community (where $P_i > 5\%$ total biomass) in the 1000, unforced model simulations with randomly assigned half-saturation coefficients for phytoplankton species. The proportion of communities characterized by a particular diversity and structure is reported as % of all model simulations and only chaotic solutions. Chaotic solutions compose 33% of all model solutions.

	Number of species, n				
	1	2	3	4	5
All model simulations					
$P_i > 0$	7.5	7.8	6.4	19.7	58.6
$P_i > 5\%$ biomass	9.4	8	14.4	42.2	26
Chaotic solutions					
$P_i > 0$	0	0	1.2	4.5	94.3
$P_i > 5\%$ biomass	0	0	2.4	68.2	29.4

5.4.3 The effect of seasonality

The majority of model simulations, 71.3±0.6%, show no change in the number of survival species under imposed seasonal variability of a range of amplitudes. In the remaining model solutions seasonal forcing tends to increase the number of coexisting species (Table 5.3). A decrease in the number of coexisting species occurred only in a handful of model simulations (Fig. 5.7).

Seasonal forcing turns out to have a profound role in increasing the number of cases where community exhibits chaos from 33% to 55±3% (Fig. 5.7b). There appears to be no relation between the forcing amplitude and the number of emerging chaotic responses. Almost all of initially chaotic cases remain chaotic (28.3±1.1% of all model

Table 5.3: Changes in the number of coexisting species (where abundance $P_i > 0.0$) and the number of species dominating the community (where $P_i > 5\%$ total biomass) under imposed **seasonal** forcing of variable amplitude A, expressed as a % of all model simulations and, in brackets, all of the chaotic solutions.

	Forcing amplitude	Change in the number of species, Δn			
	A	< 0	no change	$+1/+2$	> 3
Biodiversity, $P_i > 0.0$	A=0.5	5.1 (1.7)	72.5 (73)	22.3 (25.2)	0.1
	A=1	5.3 (1.7)	71.1 (71.2)	23.3 (26.6)	0.2
	A=3	5.1 (1.1)	71.6 (73.7)	23.2 (25.1)	0.1
	A=10	4.2 (1.3)	71.7 (73.8)	24 (24.7)	0.1 (0.1)
$P_i > 5\%$ *biomass*	A=0.5	5.7 (3.6)	65.6 (63)	28.6 (33.2)	0.1
	A=1	4.8 (1.3)	51.8 (47.2)	43.1 (51.5)	0.3
	A=3	4.2 (0.9)	40.2 (32.2)	55.3 (56.9)	0.3
	A=10	3.5 (0.9)	40 (34.7)	56.3 (64)	0.2 (0.3)

simulations). Seasonal variability in the nutrient supply leads to the chaotic response emerging in the additional 26.7$\pm$3.4% of randomly generated communities. Solutions that remained chaotic (60% of all chaotic cases) show no change in the number of survival species, as they already support a maximum of 5 species. A vast majority of newly emerged chaotic solutions exhibit an increase in the number of survival species under imposed seasonal variability (illustrated by yellow and red circles in Fig. 5.7b, left panel). This pattern prevails for the cases where the assigned half-saturation coefficients for a strong and moderate nutrient competitor exhibit moderate to large contrasts in their magnitude.

The amplitude of the forcing turns out to have an impact on the species annual contribution to the total community biomass. For low amplitude forcing, A=0.5, a majority of model simulations show no change in the number of species dominating the community. However, higher forcing amplitude leads to an increase in the number of species that constitute the vast majority of the total community biomass (Table 5.3). Communities that exhibit a chaotic response are responsible for over a half of the cases where species contribution to the annual community biomass is enhanced (illustrated by yellow and red in Fig. 5.7b, right panel).

Overall, seasonal forcing can increase the number of species coexisting in a community and acts to enhance the chaotic response. Cases when chaos emerged are responsible for only a half of the increase in the number of survival species mainly because the response emerged for the communities already sustaining 4-5 species (see Fig 5.7a and b, right panels). Strong seasonality acts to enhance the number of species that significantly contribute to the total annual community biomass. In the vast majority of cases when a community exhibits chaotic response, chaos leads to all 5 species making a significant contribution to the total community biomass. Chaotic

solutions that were previously characterized by community controlled mainly by 3 or 4 species (in dark pink and light purple in Fig. 5.7a, right panel), experience an increase of 1 or 2 species that significantly contribute to the total biomass under imposed seasonal forcing (in yellow and red in Fig. 5.7b, right panel). The greatest changes in the community diversity and structure occur when the phytoplankton community is composed of species that differ in their nutrient requirements which is implemented by greater contrasts in the assigned half-saturation coefficients for a strong, k_1 or k_2, and intermediate, k_3, nutrient competitor (Fig. 5.7b,c).

5.4.4 The effect of weather-related disturbances

For all considered forcing amplitudes, a majority of stochastically generated phytoplankton communities exhibit no change in the number of coexisting species due to the 60% of unforced model solutions already supporting the maximum of 5 species (in dark purple in Fig. 5.8a, left panel). Similarly to the effect of seasonal forcing in the nutrient supply, stochastic variability leads to an increase in community diversity recorded in approximately 60% of model solutions that could experience a further increase in the number of coexisting species (21.5$\pm$1.5% of all model solutions; yellow and red circles in Fig. 5.8b, left panel).

Chaos remains for the majority of all modelled communities that exhibit complex behaviour under no external variability. At low amplitude of stochastic forcing (A=0.5), an additional 29% of model simulations reveal chaotic behaviour, and this proportion increases with forcing amplitude. Overall, depending on the intensity, externally-imposed stochastic variability leads to chaos emerging in 60-74% of model simulations. Chaotic solutions emerge when there are already 3-5 species surviving under unforced conditions and therefore increasing the amplitude of mixing events tends to

have no significant effect on further enhancing the number of survival species (Table 5.4).

Increasing the amplitude of the stochastic forcing reveals an effect on the structure of the communities in terms of the species contribution to biodiversity. For low amplitude forcing, A=0.5, there is no change for the majority of model solutions, with only a quarter of cases where the number of species with significant contribution to the total community biomass increases. Increasing forcing amplitude to A=3.0 and higher, doubles the percentage of cases where species increase their contribution to the total community biomass. Communities exhibiting chaotic behaviour represent over a half of the cases when the number of species composing the majority of community biomass increases (in yellow and red in Fig. 5.8b, right panel).

Table 5.4: Changes in the number of coexisting species (where abundance $P_i > 0.0$) and the number of species dominating the community (where $P_i > 5\%$ total biomass) under imposed **stochastic** forcing of variable amplitude A, expressed as a % of all model simulations and, in brackets, all of the chaotic solutions.

	Forcing amplitude	Change in the number of species, Δn			
	A	< 0	no change	$+1/+2$	> 3
Biodiversity, $P_i > 0.0$	A=0.5	5.2 (1.1)	72 (75.2)	22.7 (23.7)	0.1
	A=2	5.2 (0.6)	71 (79.2)	23.7 (20.2)	0.1
	A=6	5.1 (1.1)	70.7 (78.1)	24 (20.8)	0.2
	A=10	4.2 (0.5)	71.7 (78.2)	23.9 (20.9)	0.2 (0.4)
$P_i > 5\%$ *biomass*	A=0.5	6 (3.5)	67.8 (67.5)	26.2 (29)	0
	A=2	4.5 (0.6)	44.1 (39.6)	51.2 (59.8)	0.2
	A=6	4.6 (0.5)	39.6 (38.5)	55.5 (61)	0.3
	A=10	3.9 (1.1)	39.9 (39.4)	45.8 (59.3)	0.4 (0.2)

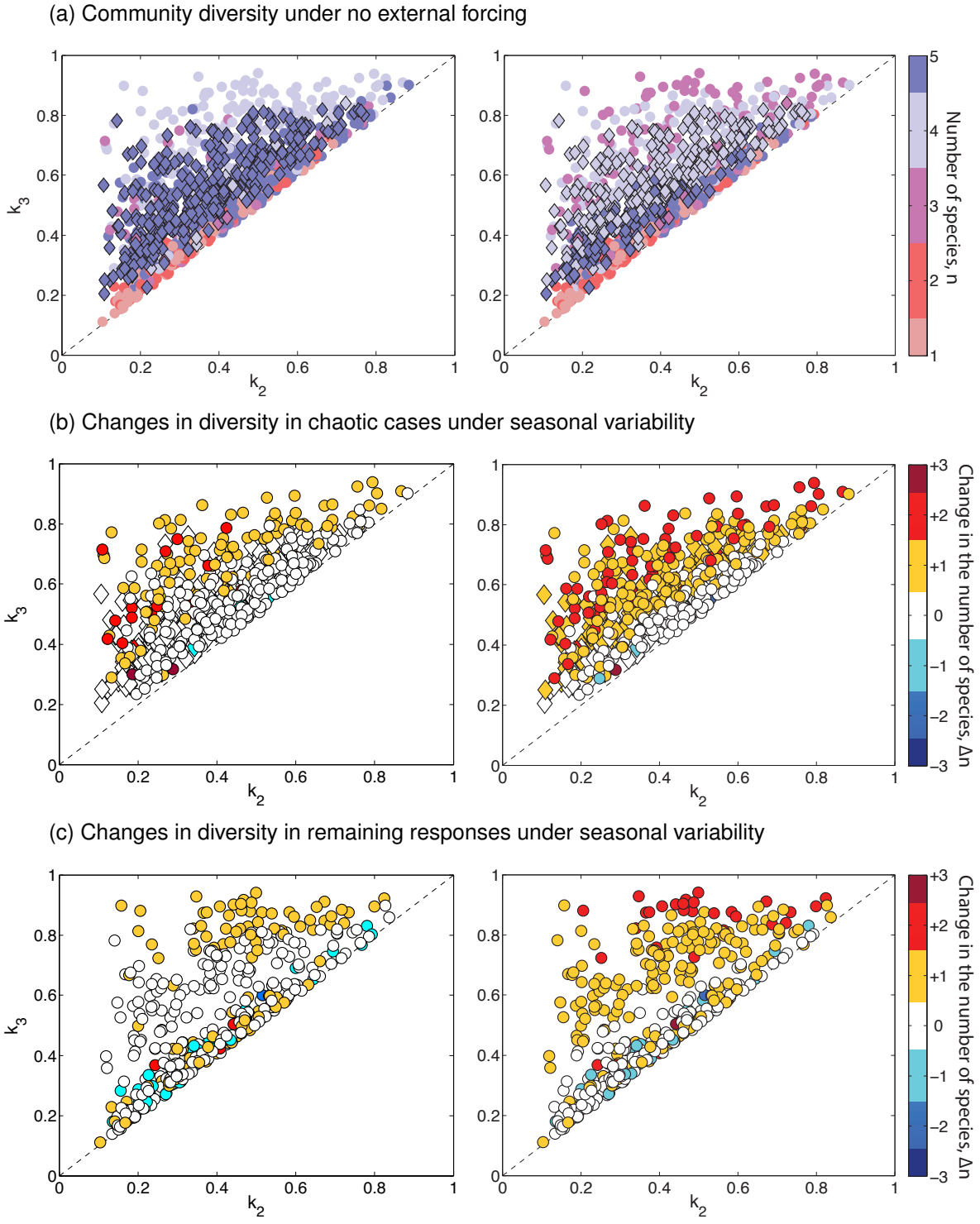

Figure 5.7: The effect of seasonal variability in nutrient supply (amplitude $A = 10.0$) on driving chaotic response and community diversity: (a) number of species, n, recorded for generated communities under no external forcing, with chaotic response indicated by $\diamond$, and (b) changes in relation to the unforced community in the number of species, Δn, for model simulations that remained chaotic ($\diamond$) and turned chaotic ($\circ$) under the imposed forcing and (c) the rest of the responses. Left panels indicate changes in the number of coexisting species, estimated as a number of species of the abundance greater than 0. Right panels show changes in the number of species contributing more than 5% to the annually-averaged community biomass over the last 5 years of model simulations. Phytoplankton community was randomly assigned half saturation coefficient, K_{ji}, within prescribed bounds for 1000 model integrations. Illustrated are the relationships between different K_{ji} for a strong versus intermediate competitor, k_2 versus k_3. Dashed line indicates $k_2 = k_3$.

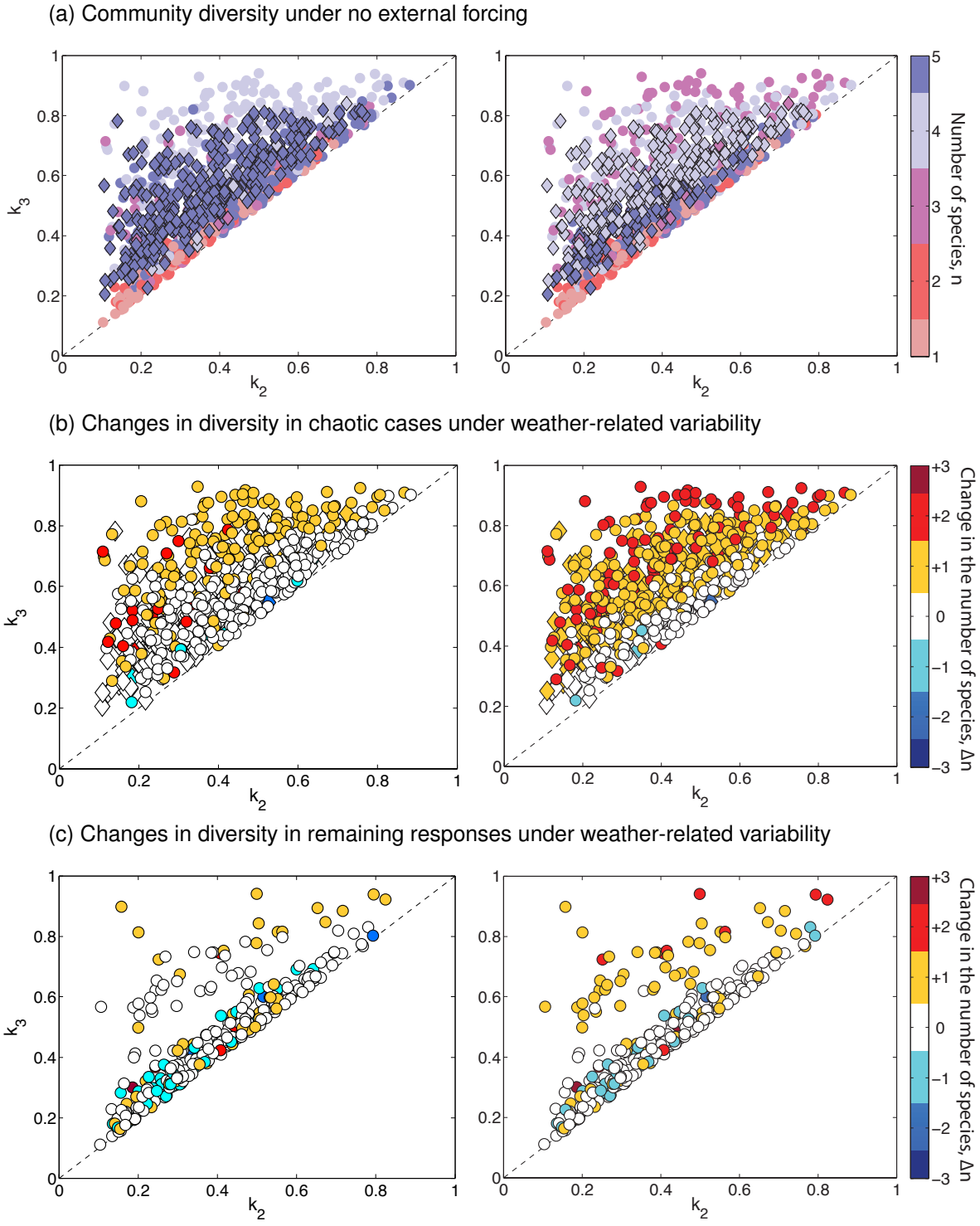

Figure 5.8: The effect of stochastic, weather -related variability in nutrient supply (amplitude $A = 3.0$) on driving chaotic response and community diversity: (a) number of species, n, recorded for generated communities under no external forcing, with chaotic response indicated by $\diamond$, and (b) changes in relation to the unforced community in the number of species, Δn, for model simulations that remained chaotic ($\diamond$) and turned chaotic ($\circ$) under the imposed forcing and (c) the rest of the responses. Left panels indicate changes in the number of coexisting species, estimated as a number of species of the abundance greater than 0. Right panels show changes in the number of species contributing more than 5% to the annually-averaged community biomass over the last 5 years of model simulations. Phytoplankton community was randomly assigned half saturation coefficient, K_{ji}, within prescribed bounds for 1000 model integrations. Illustrated are the relationships between different K_{ji} for a strong versus intermediate competitor, k_2 versus k_3. Dashed line indicates $k_2 = k_3$.

Communities that switch to a chaotic regime when subjected to stochastic or seasonal forcing, in general do not show a decline in the number of coexisting species nor the number of species contributing more than 5% to the total community biomass, with only few exceptions. Similarly to the effect of the seasonal forcing, chaos emerging as a result of stochastic variability in majority leads to all 5 species significantly contributing to the total community biomass averaged over the year.

5.5 Discussion

The work in this chapter has addressed two contrasting views as to how externally-induced variability in nutrient supply drives species coexistence and community diversity: intermittent variability through weather events and steady, periodic modification of the physical environment in the form of seasonality.

According to the Intermediate Disturbance Hypothesis (Connell, 1978), environmental disturbances of intermediate intensity and frequency on the timescale of days to weeks, can potentially prevent the phytoplankton community from reaching an equilibrium. The intermediate disturbances modifies the surrounding environment so that the ultimate competitor cannot become established (Reynolds et al., 1993; Sommer, 1986). The intermittent disturbance in nutrient supply acts as a 'reset' process and allows the community to be restored to the state before the exclusion begins. Lower frequency, intermittent modifications in the physical environment may only act to delay the processes of phytoplankton community converging towards competitive exclusion.

In contrast, seasonal variability gradually modifies the physical environment and creates favourable conditions for particular species to flourish at different points of the year. This annual succession of species and related changes in the community structure allow the temporarily weaker competitors to be sustained at background concentrations at one time of the year to flourish at another.

Thus both seasonal fluctuations and weather-related variability both have potential to drive species coexistence. For the majority of the randomly seeded model simulations that is 60%, the phytoplankton community was already composed of 5 species in the absence of an external forcing in the nutrient supply, and therefore no further increase in community diversity was possible under imposed stochastic or seasonal variability.

Out of all remaining model simulations where further increase in the number of coexisting species was possible, implementation of the seasonal forcing led to an increase in community diversity in 60% of those cases. These proportions turn out to be insensitive of the forcing amplitude, which suggests that seasonality enhances chaos in weakly and strongly seasonal environments equally. Similar findings are recorded when stochastic variability in the nutrient supply is imposed, however, an increase in the amplitude of stochastic forcing further increases the likelihood of complex dynamics to occur. Extinction of species was recorded for under 5% of all model simulations and occurs in the parameter regime when competing species are of comparable fitness and share the same nutrient requirements.

The initial objective of the study was to investigate the importance of the frequency at which the nutrient environment is perturbed. However, the effect on community behaviour and diversity is comparable for both seasonal and stochastic variability despite their contrasting mechanisms. An isolated environmental disturbance occurring annually is not sufficient to significantly prevent the phytoplankton community from converging towards competitive exclusion, according to the Intermediate Disturbance Hypothesis. The duration at which a seasonal 'perturbation' operates, i.e. 1 year, turns out be crucial in preventing phytoplankton from reaching a stable growth rate as the environmental conditions never stabilize for long enough to allow for species extinction. On the contrary, weather events that last up to a few days need to occur more frequently in order to revert the consequences of the competitive exclusion that proceeds in-between isolated, weather-related perturbations. The Intermediate Disturbance Hypothesis refers to the intermittently occurring phenomenon and therefore the findings presented in this chapter are in support of the theory and outline the importance of both the duration and the frequency of environmental perturbations.

The model analysis suggests that the Intermediate Disturbance Hypothesis applies in the aquatic communities and that the number of coexisting species is enhanced when there are differences in nutrient requirements between competing species. Imposed periodic and stochastic forcing causes no change in community diversity and structure when communities are composed of species of comparable physiology. On contrary, environmental variability appears to have greatest effects in enhancing species diversity for phytoplankton communities composed of species exhibiting contrasts in nutrient requirements between strong and intermediate nutrient competitors. The strongest competitor for the most limiting nutrient may dominate the community and drive other species to extinction in a homogenous environment. However, sudden perturbations in the available nutrients allows the weaker competitors to temporarily flourish due to their advantage in utilizing other resources. Chapter 4 illustrates that competitive exclusion is the most likely outcome when strong and intermediate competitors are of a similar fitness, with the frequency of non-equilibrium solutions increasing with higher differentiation in nutrient requirement. Therefore, seasonal as well as weather-related variability in the nutrient supply is unlikely to benefit phytoplankton community exhibiting competitive exclusion. Species of similar nutrient requirements exhibit a comparable response to the environmental perturbations so that competitive exclusion will proceed. Phytoplankton community consisting of species with contrasting nutrient requirements allows for each species to respond differently to perturbations and facilitates seasonal succession.

Seasonal forcing acts to enhance the chaotic response of the phytoplankton community by increasing the probability of chaos to occur in 50% of the modelled phytoplankton communities (Table 5.3, Fig. 5.7). Again, this proportion turns out to be insensitive of the forcing amplitude. In contrast, a model study of Dakos et al. (2009) suggested that the amplitude of seasonal forcing controls the frequency at which chaotic

responses emerge. This discrepancy may be due to higher food web complexity implemented in the multi-species ecosystem model of Dakos et al. (2009), and, to a lesser extent, the differences in implementation in the seasonal forcing. In the study presented in this thesis, seasonality leads to an enhanced supply of nutrients with the same minimum level of nutrient supply for all forcing amplitude scenarios. In comparison, representation of seasonality implemented by Dakos et al. (2009) suggests that an amplified nutrient supply entails a greater level of nutrient depletion in periods of inhibited nutrient supply, a scenario which is arguably less plausible for the real environment.

The strength of chaos, and thus the timescale for predictability, turns out to be sensitive to the seasonal variability in nutrient supply. The chaotic response becomes more prevalent and the predictability timescale decreases in the summer period, when the concentration of essential resources begins to decline. In contrast, chaos tends to diminish in the winter, which suggests that variability in phytoplankton abundance can be predicted on slightly longer timescales. This temporal sensitivity of chaos was also previously suggested by Popova et al. (1997), who simulated seasonality through variability in temperature, irradiance and the upper mixed layer depth (controlling nitrogen supply) in a 4-component microbial food web. Temporal variability in the non-equilibrium dynamics may have significant implications for phytoplankton community diversity. Microbial ecosystems exhibit an ability to switch between different types of community responses subject to the temporal variability in the nutrient supply (Becks and Arndt, 2008). The amplification of the chaotic response or phytoplankton switching to the complex behaviour in the summer, may contribute to an increase in community biodiversity at that time of the year. Indeed, an enhancement in phytoplankton diversity that occurs over the summer period has been previously reported for phytoplankton in isolated freshwater basins (Sommer, 1993; Nuccio et al., 2003).

Stochastic variability in the nutrient supply acts to increase the frequency at which chaos occurs within randomly seeded model simulations, with higher amplitude forcing enhancing the prevalence of the response by almost 45% (Table 5.4, Fig. 5.8). The question remains whether the reason for chaos to emerge within the forced model simulations is either the dominant period of the forcing of a monthly frequency or the stochastic fluctuations. A chaotic response could emerge as a result of the monthly variability being the dominant forcing frequency within the wind speed time series. In such a case, the stochastic forcing drives a chaotic response due to the remaining periodicity within the data, and not the irregular fluctuations. Otherwise, the phenomenon of noise-induced chaos has been previously reported for mathematical systems (Crutchfield and Huberman, 1980; Crutchfield et al., 1982), where irregular fluctuations themselves can drive complex dynamics. However, dynamical noise can overestimate the maximal Lyapunov Exponent if the standard methods for chaos verification of deterministic systems are applied (Gao et al., 1999; Dennis et al., 2003). In such case, the proportion of chaotic solutions might be falsely classified as chaos, when the irregular fluctuations are a result of purely stochastic processes.

This study confirms that amplification of environmental variability does not act to diminish chaos, but instead can enhance non-equilibrium dynamics. It is therefore suggested that higher latitude environments with seasonally controlled nutrient supply and more vigorous meteorology are more likely to exhibit chaotic behaviour. However, in strongly seasonal environments, chaotic response manifest itself in a form of inter-annual variability in phytoplankton abundance (Doveri et al., 1993; Rinaldi and Solidoro, 1998; Dakos et al., 2009).

In Chapter 3, an attempt was made to verify whether chaotic fluctuations could be detected within the phytoplankton abundance time series from a strongly seasonal

English Sea. The analysis turned out to be inconclusive and model simulations were implemented in order to investigate the sensitivity of the chaos detection technique applied in the analysis of the time series data. The findings presented in Chapter 3 illustrate that the method fails to detect chaotic behaviour in a strongly seasonal environment. The investigations of seasonal fluctuations in nutrient supply discussed here, may be a potential reason for the difficulty of detecting chaos.

Both seasonality and stochastic weather events show a large potential for driving complex behaviour within phytoplankton communities. The findings suggest that chaos is more likely to occur in the high latitude provinces due to the more vigorous weather patterns. However, the type of the community response can change on a temporal scale in strongly seasonal environments at high latitudes and the ability to accurately detect complex behaviour from a time series of data is limited. Methods for chaos detection are most reliable if applied to the phytoplankton community under weak seasonal variability (illustrated in Chapter 3) where the internally induced variability is most prevalent and where the microbial community is most likely to sustain the same type of response throughout the year. The analysis of chaos is recommended using a time-series data from oceanic provinces characterized by stable phytoplankton community structure with less profound seasonal species succession, such as previously reported for the phytoplankton community in the Sargasso Sea (Goericke, 1998). The limitations for detecting chaos will be returned to in the final chapter of this thesis.

5.6 Chapter Summary

The chapter investigates the effect of periodic and stochastic forcing in driving community diversity and enhancing complex behaviour. The effect of externally-imposed variability is investigated for specific community examples as well as a set of 1000 model simulations with randomly generated phytoplankton community. The key findings are:

- seasonal and weather-related stochastic variability in the nutrient supply enhance local community diversity in 20% of model simulations, with only 5% of modelled community experiencing a decline in biodiversity.
- phytoplankton communities consisting of species with inter-species differences in nutrient requirement experience an increase in community diversity and structure under environmental variability.
- externally-imposed variability enhances the probability of chaos to occur by about 25% under seasonal and 30-45% under stochastic variability in relation to the unforced model simulations.
- the strength of the chaotic response varies temporarily under imposed seasonal fluctuations, with more persistent chaotic response observed in the summer.

Therefore, the likelihood of chaotic behaviour increases in regions where nutrient supply is controlled seasonally and via vigorous weather events. The temporal variability in the strength of the chaotic response in strongly seasonal provinces, decreases the predictability of the ecosystem during summer, which may contribute to an increase in local biodiversity.

CHAPTER 6

The effects of lateral exchange on phytoplankton community structure and species diversity

Rationale:

This chapter investigates potential changes in the phytoplankton community biodiversity and response to nutrient competition, when subjected to dispersal and lateral exchange driving the spatially heterogeneous environment. Marine populations are spatially connected, and continuous exchange can act to modify the response that the ecosystem would otherwise exhibit in a homogenous, isolated environment. The study aims to explore the conditions for chaos to be sustained when there is lateral exchange with a contrasting ecosystem. The objective is to verify how the strength of the exchange affects the final competition outcome between connected ecosystems. The role of dispersal is examined using an idealized model framework, first simulating the exchange between two adjacent phytoplankton patches and, second, a simple depiction of advection in a western boundary current and dispersal of a low-latitude community.

6.1 Introduction

Multi-species food webs can display a variety of behaviours from competitive exclusion, through regular oscillations, quasi-periodicity and chaos (May, 1974; Gilpin, 1979; demonstrated also in the earlier chapters). Laboratory and theoretical experiments suggest that internally-induced chaotic behaviour is a prevalent response within marine communities in a homogenous environment (Huisman and Weissing, 2001; Becks and Arndt, 2008; Benincà et al., 2008). In turn, the generation of non-equilibrium dynamics, including chaos, can then enhance local biodiversity (Huisman and Weissing, 1999; Huisman et al., 2001).

In reality, marine populations are spatially linked and interact with other communities to form metapopulations. The connectivity between different phytoplankton communities may have important implications on shaping local community dynamics. Holt and McPeek (1996) suggested that chaos alone can drive density-dependent dispersal that controls species emigration from a high-density site, because high sensitivity to initial conditions of chaotic systems may lead to contrasts in community structure between adjacent ecosystems and generation of patchiness. However, it has been suggested that even for weakly inter-connected systems, chaotic populations tend to evolve towards stable, cyclic equilibria (Allen et al., 1993; Gonzalez-Andujar and Perry, 1993; Hastings, 1993; Ruxton, 1994).

Early ecological studies have shown that dispersal is a key mechanism controlling community structure and diversity of terrestrial populations (Gleason, 1917; Shmida and Ellner, 1985) and has been explored using theoretical models (Levins and Culver, 1971; Horn and Arthur, 1972; Hastings, 1980). The connectivity between populations in the marine environments is driven by dispersal on a variety of scales of motion, from

vertical mixing to mesoscale eddies and large-scale, horizontal currents. The effect of the physical transport on the biodiversity can vary depending on the spatial scale of the ecosystem processes (Fig 6.1).

Lateral stirring and mixing driven by passing oceanic eddies and fronts (Abraham, 1998; Martin, 2003) leads to generation of patchiness on smaller spatial scales, where adjacent ecosystems are characterized by contrasting phytoplankton community structure (Therriault and Platt, 1981; Gower et al., 1980; Strass, 1992).

On a local scale, intermediate rates of introduction of new species are thought to enhance species richness within a community (Mouquet and Loreau, 2002, 2003). The process of biodiversity enhancement can occur via the 'mass effect' where immigrating species are poor nutrient competitors, but are not excluded from the local community due to the continuous emigration from the regions where they are the fittest (Shmida and Ellner, 1985; Loreau and Mouquet, 1999; Mouquet and Loreau, 2003). The process of the mass effect is not possible in a closed systems (Loreau and Mouquet, 1999), such as freshwater lakes. Within the marine environment, transport of new species within mesoscale vortices is an example of a closed system: local biodiversity

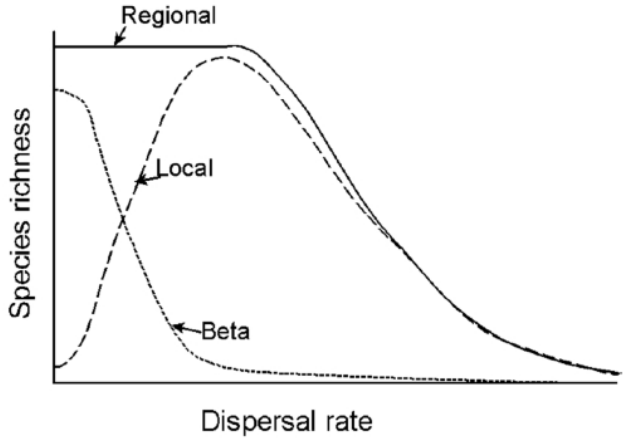

Figure 6.1: Hypothetical relation between the strength of dispersal and the number of species coexisting at different spatial scales: within community ('local'), in-between communities ('beta'), and regional. Figure from Cadotte (2006) (adapted from Mouquet and Loreau (2003)).

is increased, but this is only a short-term phenomenon as a lack of a continuous inflow of weaker competitors will gradually lead to their extinction (Bracco et al., 2000). Alternatively, too high a dispersal acts to homogenize the community and inhibits the ability of species to coexist and, in the open systems, invasion of new species may displace the local community.

When considering the contrasts in the community structure in the adjacent ecosystems, increased levels of dispersal act to inhibit the diversity between the neighbouring communities as the environment becomes more homogenous. In-between community biodiversity is the highest at low exchange rates when the environmental conditions allow for the patchiness and contrasts in the community structure to remain in the ecosystem (Richerson et al., 1970; Levin, 1974; Mouquet and Loreau, 2003).

The decline in species diversity on a local scale leads to a decline in biodiversity on a regional scale (Mouquet and Loreau, 2003). Global ecosystem model simulations suggest that the highest phytoplankton diversity occurs in the equatorial and subtropical regions, with biodiversity hotspots associated with the areas of coastal upwelling and western boundary currents (Barton et al., 2010; Clayton et al., 2013). Clayton et al. (2013) suggested that intensified biodiversity recorded downstream of the dynamical circulations is sustained due to the influx of less-adapted species.

In this chapter, the effects of spatial heterogeneity and connectivity between marine phytoplankton communities are explored using an adaptation of the idealized model framework developed in Chapter 2. The aim is to identify how the inflow of new species affects the local biodiversity and the internally-induced response of the community to compete for nutrients. First, the role of mixing on small spatial scales is explored, such as representing in-between community exchange through patch dynamics. In particular, we focus on whether the introduction of stronger or weaker nutrient competitor

allows for an initially chaotic response of the local community to persist, and how this response is affected by the strength of the exchange. The second set of idealized model experiments simulates large-scale circulation and continuous transport of species in the western boundary currents. The role of the mass effect in driving biodiversity is explored. We investigate whether the inflow of better nutrient competitors from low-latitudes to the local community can sustain or generate a chaotic response at the mid latitudes.

6.2 Methods

6.2.1 Model experiments

This study explores the effect of lateral exchange between phytoplankton communities, and investigates the role of this connectivity in shaping the community response. The chemostat model applied in this study simulates the inter-species competition for nutrients in a homogenous environment, as represented by a well-mixed box (Armstrong and McGehee, 1980; Huisman and Weissing, 1999); for model equations see section 2.1.

Ecosystem experiments are conducted using a set of well-mixed box models to mimic the effect of lateral exchange and dispersal. Each box is initially occupied by a phytoplankton community in a range of initial states, either competitive exclusion, regular oscillations or chaos. Two physical transport processes are investigated that determine the type of connections between each chemostat: (1) in-habitat, two-way exchange between two adjacent ecosystems, and (2) poleward transport in a boundary current followed by an exchange with the local community. The specifics of the model design are expanded upon in later sections.

6.2.2 Verification of chaos

Chaotic behaviour is determined through verification of the sensitivity to initial conditions. The maximal Lyapunov Exponent, λ_{max}, is diagnosed throughout the model simulations and measures the rate of exponential divergence of the nearby trajectories, with positive values indicating chaos. The diagnostic is implemented online within the ecosystem model and calculates the rate of divergence for the nutrient concentration trajectory; for more details see section 2.2.2.

6.3 Two-way exchange between communities

On a local scale, biodiversity can increase through environmental patchiness or through an eddy bringing in a new water mass, where there is a two-way, continuous exchange between two distinct ecosystems. Here, the study examines the effect of the interaction between communities in shaping local biodiversity and modifying the community response. The objectives are to assess the diversity in the connected communities and verify the necessary conditions when the chaotic response can be sustained in the environment subject to the exchange with stronger or weaker nutrient competitors.

6.3.1 Model formulation

The model represents two chemostat environments, B1 and B2, with a two-way continuous exchange between them. The total of $n = 10$ species is initialized in both environments and compete for $k = 5$ resources. Initially species 1 to 5 occupy B1 and species 6 to 10 reside in B2. Each community response develops in isolation over the initial 1000 days, after which period the two-way exchange, β, of phytoplankton species, P_i, and nutrients, N_j, is initiated:

$$\frac{\partial P_{B1,i}}{\partial t} = P_{B1,i}(r_i\gamma_i^N - m_i) + \beta(P_{B2,i} - P_{B1,i}) \qquad i = 1,...,n \tag{6.1}$$

$$\frac{\partial N_{B1,j}}{\partial t} = D(S_j - N_{B1,j}) + \beta(N_{B2,j} - N_{B1,j}) - \sum_{i=1}^{n} Q_{ji} r_i \gamma_i^N P_{B1,i} \qquad j = 1,...,k \tag{6.2}$$

Equations describing interactions in B2 follow the same principles as in the equations for B1 illustrated above. The rate of exchange β varies from 0 to 1 d^{-1}, and is related to the timescale of the exchange, T_x. The horizontal diffusivity timescale can be estimated from the diffusive flux of a tracer, c, where $\frac{\partial c}{\partial t} \sim \kappa \frac{\partial^2 c}{\partial x^2}$. An order of magnitude estimate for the diffusive timescale, T_x, is given by $T_x \sim \frac{L^2}{\kappa}$ with L and κ representing

the length scale and horizontal diffusivity respectively. In reality, the patches can range in size from 100 m up to 100 km, equivalent to the size of geostrophic eddies. Horizontal diffusivity, κ, ranges from 10^3 m^2s^{-1} in the regions of intensified stirring and can decrease down to 10^2 m^2s^{-1} at the surface waters where the exchange is inhibited (Visbeck et al., 1997; Marshall et al., 2006; Abernathey et al., 2010). Assuming the length scale $L = 100$ km, a maximum timescale for horizontal diffusion in the ocean is estimated for about $T_x = 3$ years. The exchange rate β represents the proportion of the community exchanged per day, where $\beta = \frac{1}{T_x}$. Therefore, the estimate for $T_x = 3$ years corresponds to $\beta = 9 \times 10^{-4}$ d^{-1} in this model study. For comparison purposes, the analysis involves the exchange rates as low as $\beta = 10^{-8}$ d^{-1} for arbitrary low κ and high L, which is to represent almost completely isolated ecosystems.

Both well-mixed boxes are initialized in the same manner, following the model parameters described in Table 2.1 (p. 26). Communities in both chemostats are assigned the same rates for maximum growth, $r = 1\ d^{-1}$, and mortality, $m = 0.25\ d^{-1}$. Similarly, the assignment of cell quota, Q_{ji}, is the same for both communities. Contrasts in community structure and type of the phytoplankton response are achieved by modification of the default half-saturation parameters, K_{ji}, of species i for resource j.

This study considers 4 different scenarios of phytoplankton community exchange, with modification for each community, as described in Table 6.1:

(1) exchange between communities exhibiting competitive exclusion,

(2) exchange between a community dominated by a stronger competitor and a weaker, chaotic community,

(3) exchange between a weaker competitor and a stronger, chaotic community, and

(4) exchange between stronger nutrient competitors exhibiting regular oscillations and a weaker, chaotic community.

The simulations of all 4 scenarios under a variable strength of horizontal exchange between ecosystems aims to reveal conditions for chaotic response to be sustained in the environment.

Table 6.1: Specification for the half-saturation coefficients, K_{ji}, for phytoplankton communities exchanged between well-mixed box 1 (B1) and box 2 (B2). There are 4 different cases for the exchange experiments that are illustrated in Figures 6.2 to 6.5. Gray shading indicate species (in columns i) that became extinct and '$-$' denote species that were not initialized in the model. Underlined values are the modifications of the default model parameters.

Scenario	**Half-saturation coefficients, K_{ji}**		**Comments**
	B1 (species 1-5)	***B2 (species 6-10)***	
(1) Exclusion - Exclusion: *stronger (B1) vs weaker (B2) competitor*	$K_{ji} = \begin{pmatrix} 0.39 & 0.34 & 0.30 & 0.24 & 0.23 \\ 0.22 & 0.39 & 0.34 & 0.30 & 0.27 \\ 0.27 & 0.22 & 0.39 & 0.34 & 0.30 \\ \underline{0.20} & 0.24 & 0.22 & 0.39 & 0.34 \\ 0.34 & 0.30 & 0.22 & 0.20 & 0.39 \end{pmatrix}$	$K_{ji} = \begin{pmatrix} 0.39 & 0.34 & 0.30 & 0.24 & 0.23 \\ 0.22 & 0.39 & 0.34 & 0.30 & 0.27 \\ 0.27 & 0.22 & \underline{0.29} & 0.34 & 0.30 \\ 0.20 & 0.24 & 0.22 & 0.39 & 0.34 \\ 0.34 & 0.30 & 0.22 & 0.20 & 0.39 \end{pmatrix}$	- Species 1 wins because is a better competitor for 2 resources; in B2 species coexist due to specialization on different resources
(2) Exclusion - Chaos: *stronger (B1) vs weaker (B2) competitor*	$K_{ji} = 0.02 + \begin{pmatrix} 0.39 & 0.34 & 0.30 & 0.24 & 0.23 \\ 0.22 & 0.39 & 0.34 & 0.30 & 0.27 \\ 0.27 & 0.22 & 0.39 & 0.34 & 0.30 \\ \underline{0.20} & 0.24 & 0.22 & 0.39 & 0.34 \\ 0.34 & 0.30 & 0.22 & 0.20 & 0.39 \end{pmatrix}$	$K_{ji} = \begin{pmatrix} 0.39 & 0.34 & 0.30 & 0.24 & 0.23 \\ 0.22 & 0.39 & 0.34 & 0.30 & 0.27 \\ 0.27 & 0.22 & 0.39 & 0.34 & 0.30 \\ 0.30 & 0.24 & 0.22 & 0.39 & 0.34 \\ 0.34 & 0.30 & 0.22 & 0.20 & 0.39 \end{pmatrix} = default$	- Species 1 wins because it drives species 10 to extinction, the balance between the chaotic community is disturbed and competition progresses
(3) Exclusion - Chaos: *weaker (B1) vs stronger (B2) competitor*	$K_{ji} = 0.02 + \begin{pmatrix} \underline{0.37} & 0.34 & 0.30 & - & - \\ 0.22 & \underline{0.37} & 0.34 & - & - \\ 0.27 & 0.22 & 0.39 & - & - \\ 0.30 & 0.24 & 0.22 & - & - \\ 0.34 & 0.30 & 0.22 & - & - \end{pmatrix}$	$K_{ji} = default$	- Species 3 loses to species 8 due to the imposed offset in K_{ji} (+0.02)
(4) Oscillations - Chaos: *stronger (B1) vs weaker (B2) competitor*	$K_{ji} = -0.02 + \begin{pmatrix} - & 0.34 & 0.30 & - & 0.23 \\ - & 0.39 & 0.34 & - & 0.27 \\ - & 0.22 & 0.39 & - & 0.30 \\ - & 0.24 & 0.22 & - & 0.34 \\ - & 0.30 & 0.22 & - & 0.39 \end{pmatrix}$	$K_{ji} = default$	- Species in B1 are stronger competitors due to the imposed offset in K_{ji} (-0.02)

6.3.2 Competition and exchange between patches

Horizontal exchange between ecosystems occupied by phytoplankton communities of contrasting structure can modify the community response and biodiversity. Whether biodiversity is sustained depends on the interactions between competing species and the strength of the exchange.

In scenario (1), two communities exhibiting competitive exclusion are considered. In this example, exchange at a sufficiently low rate can prevent the strongest competitor from dominating the environment, and higher biodiversity can then be sustained (Fig. 6.2a,b). A higher exchange rate instead leads to the ultimate competitor taking over the community (Fig. 6.2c).

This exchange mechanism carries over to communities exhibiting chaotic behaviour. In scenario (2), consider a stronger nutrient competitor introduced into the community which already exhibits a chaotic response. A sufficiently low exchange allows the chaotic response to continue as the well-established local community remains resistant to the limited influx of the ultimate competitor. In this process, higher biodiversity is achieved due to the contrasts remaining between the ecosystems in the two patches (Fig. 6.3a,b). Increasing the exchange rate to above $\beta = 10^{-4}$ d^{-1} leads to a more homogenous environment dominated by 2 species (Fig. 6.3c). The coexistence is possible due to the species specializing on different resources (Table 6.1). However, a very slow and gradual increase in the concentration of the stronger competitor under low β may lead to the process of exclusion occurring over much longer timescales than considered in the model simulations. The threshold for the rate of exchange necessary to sustain chaos strongly depends on the strength of the optimal competitor. Here, the introduced offset to K_{ji} of +0.02 acts to weaken the strongest competitor so

that it does not remain the optimal competitor for the resources it is least specialized in utilizing. Therefore low exchange rates between communities allow chaos to be sustained. Without this offset, the ultimate competitor takes over the community even at the lowest exchange rate.

In contrast, exchanging a chaotic community with a relatively weak nutrient competitor (scenario (3)) does not modify the initially chaotic response. Chaos eventually becomes a robust response in both patches even at low exchange rate, and the level of diversity remains unchanged as the weaker competitors are outcompeted (Fig. 6.4). A low rate for horizontal exchange, lower than $\beta = 10^{-4}$ d^{-1}, generates transient dynamics in the patch initially occupied by the weaker competitor, and it may take up to 1000 days before the community in that patch converges to chaotic behaviour.

However, introduction of a stronger nutrient competitor into the chaotic community can lead to chaos persisting if the members of the dominant community do not specialize in the utilization of all the nutrients. In this case, species from the chaotic community that are able to utilize the available niche, persist and drive the chaotic response within the ensemble community (Fig. 6.5a). Such responses exploiting an available niche turn out to be independent of the strength of the horizontal exchange (Fig. 6.5b,c).

The model simulations suggest that a chaotic response can be sustained in three cases: (i) if introduced phytoplankton species are weaker nutrient competitors and the local community remains unaltered,(ii) if there is a weak exchange with a strong competitor where the community contrasts and patchiness are maintained, and (iii) if the exchange occurs with a community consisting of stronger nutrient competitors, where there is an unoccupied niche for specialization of a particular nutrient. Transfer of chaos into the non-chaotic patch then increases the local diversity within that patch.

(a) Initial response to the exchange with $\beta = 10^{-3}$ d^{-1}

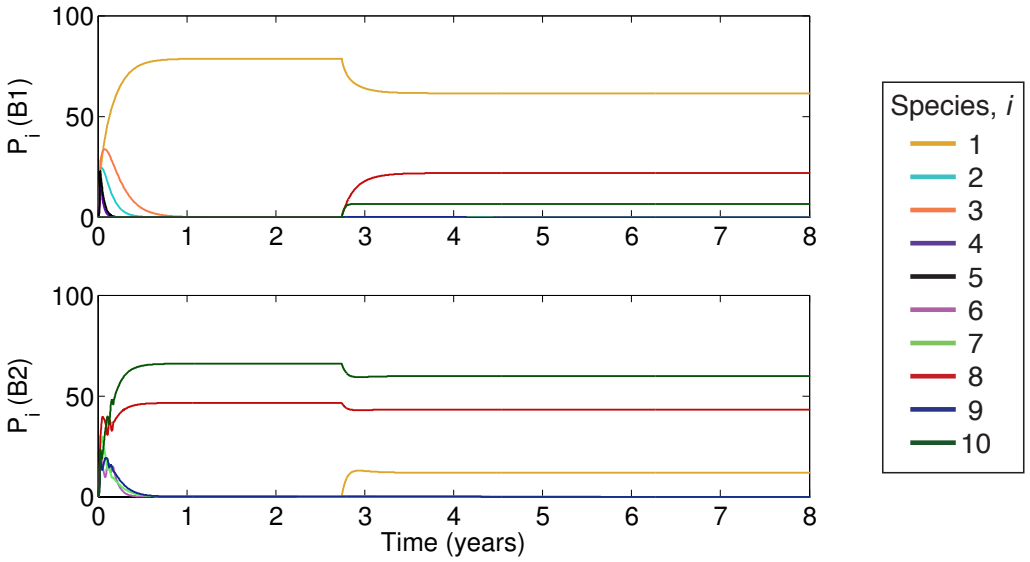

(b) Community structure 25 years after the exchange with $\beta = 10^{-2}$ d^{-1}

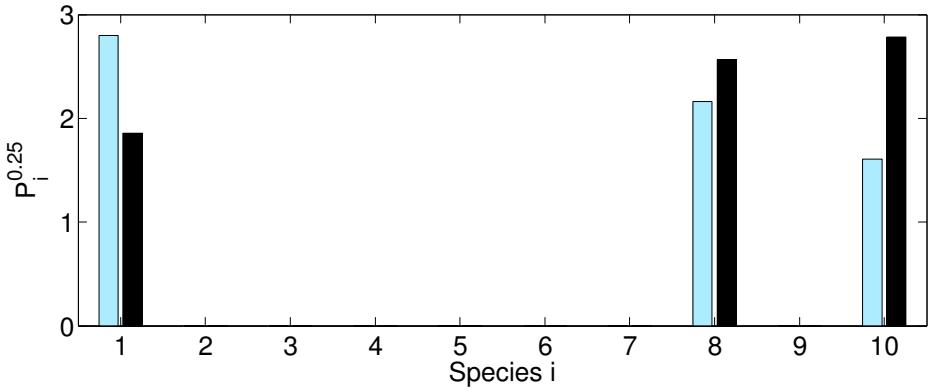

(c) Community structure 25 years after the exchange with $\beta = 10^{-1}$ d^{-1}

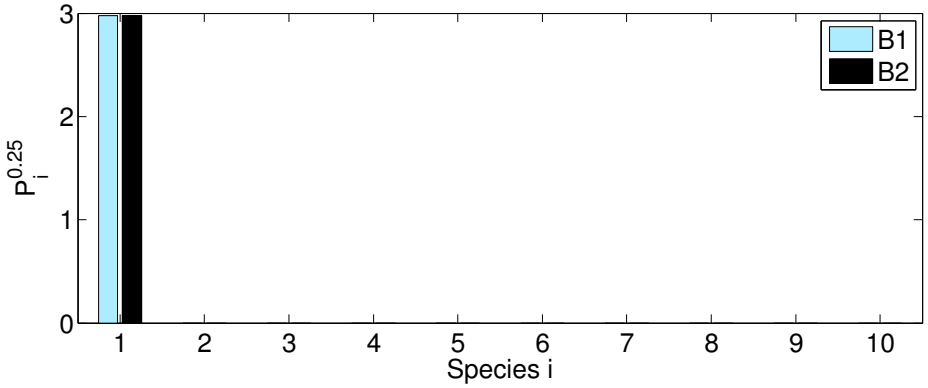

Figure 6.2: The effect of horizontal exchange between communities of different structure and nutrient utilization abilities (scenario 1; Table 6.1). The time series of species abundance, P_i, is illustrated in (a), where the exchange occurs with $\beta = 10^{-3}$ d^{-1} ($\sim T_x = 2.7$ years). Panels (b) and (c) indicate the number and time-average abundance of species over the last 2000 days of model simulation ($\frac{1}{4}$-power transformed for clear visualization of species surviving at very low concentrations) surviving in patch 1 (B1, in blue) and patch 2 (B2, in black) with $\beta = 10^{-2}$ d^{-1} ($\sim T_x = 3$ months) and $\beta = 10^{-2}$ d^{-1} ($\sim T_x = 10$ days) respectively. The exchange process begins on day 1000.

(a) Initial response to the exchange with $\beta = 5 \times 10^{-5}$ d^{-1}

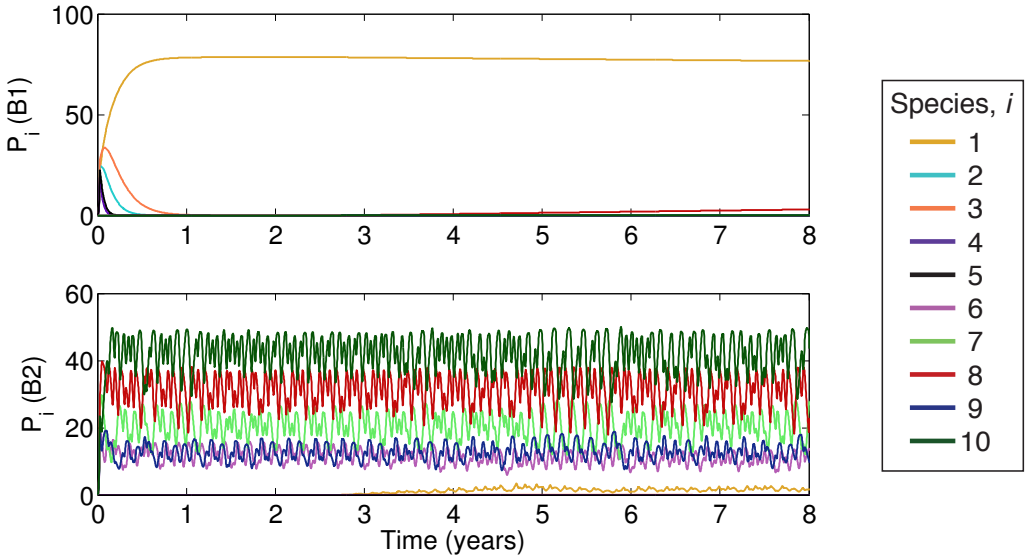

(b) Community structure 25 years after the exchange with $\beta = 10^{-5}$ d^{-1}

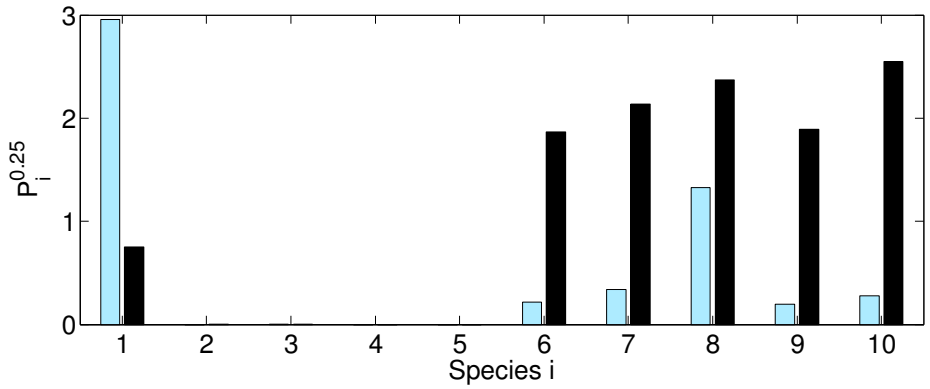

(c) Community structure 25 years after the exchange with $\beta = 10^{-4}$ d^{-1}

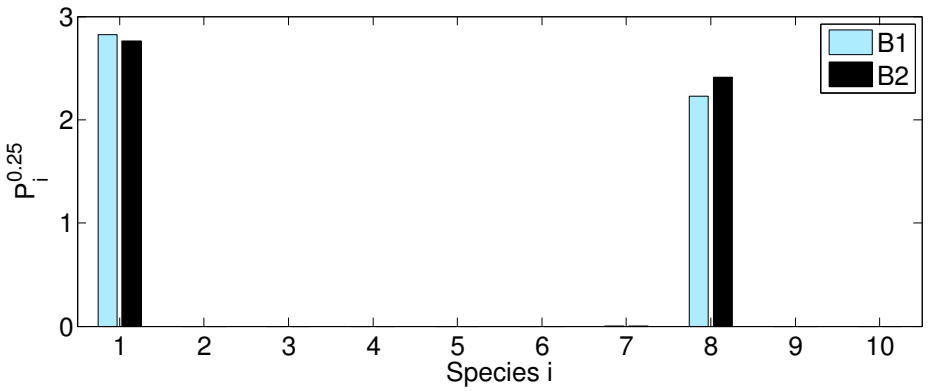

Figure 6.3: The effect of horizontal exchange between communities of different structure and nutrient utilization abilities (scenario 2; Table 6.1). The time series of species abundance, P_i, is illustrated in (a), where the exchange occurs with $\beta = 5 \times 10^{-5}$ d^{-1} ($\sim T_x = 55$ years). Panels (b) and (c) indicate the number and time-average abundance of species over the last 2000 days of model simulation ($\frac{1}{4}$-power transformed for clear visualization of species surviving at very low concentrations) surviving in patch 1 (B1, in blue) and patch 2 (B2, in black) with $\beta = 10^{-5}$ d^{-1} ($\sim T_x = 270$ years) and $\beta = 10^{-4}$ d^{-1} ($\sim T_x = 27$ years) respectively. The exchange process begins on day 1000.

(a) Initial response to the exchange with $\beta = 10^{-2}$ d^{-1}

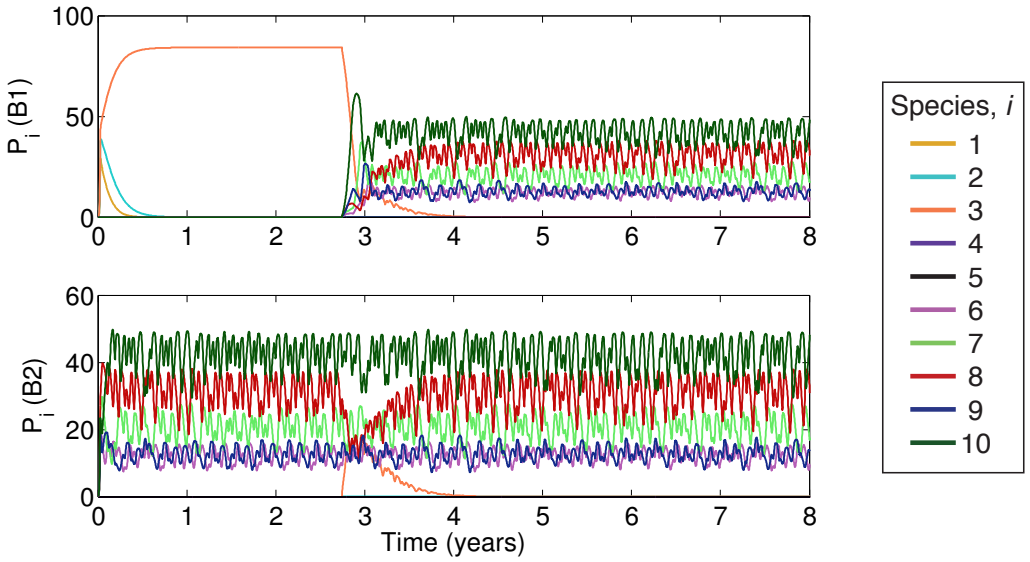

(b) Community structure 25 years after the exchange with $\beta = 10^{-8}$ d^{-1}

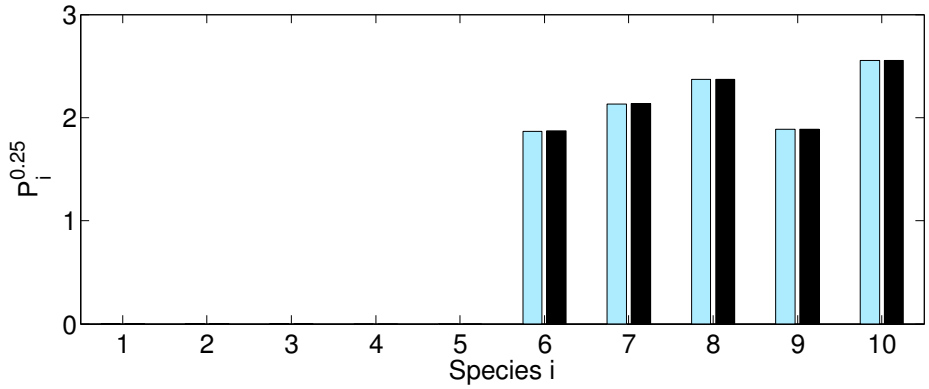

(c) Community structure 25 years after the exchange with $\beta = 1$ d^{-1}

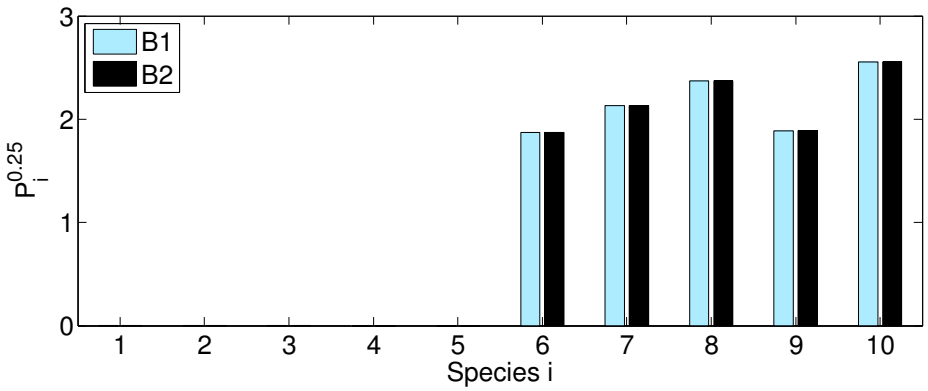

Figure 6.4: The effect of horizontal exchange between communities of different structure and nutrient utilization abilities (scenario 3; Table 6.1). The time series of species abundance, P_i, is illustrated in (a), where the exchange occurs with $\beta = 10^{-2}$ d^{-1} ($\sim T_x = 3$ months). Panels (b) and (c) indicate the number and time-average abundance of species over the last 2000 days of model simulation ($\frac{1}{4}$-power transformed for clear visualization of species surviving at very low concentrations) surviving in patch 1 (B1, in blue) and patch 2 (B2, in black) with $\beta = 10^{-8}$ d^{-1} ($\sim T_x = 270$ ky) and $\beta = 1$ d^{-1} ($\sim T_x = 1$ day) respectively. The exchange process begins on day 1000.

(a) Initial response to the exchange with $\beta = 10^{-3}$ d^{-1}

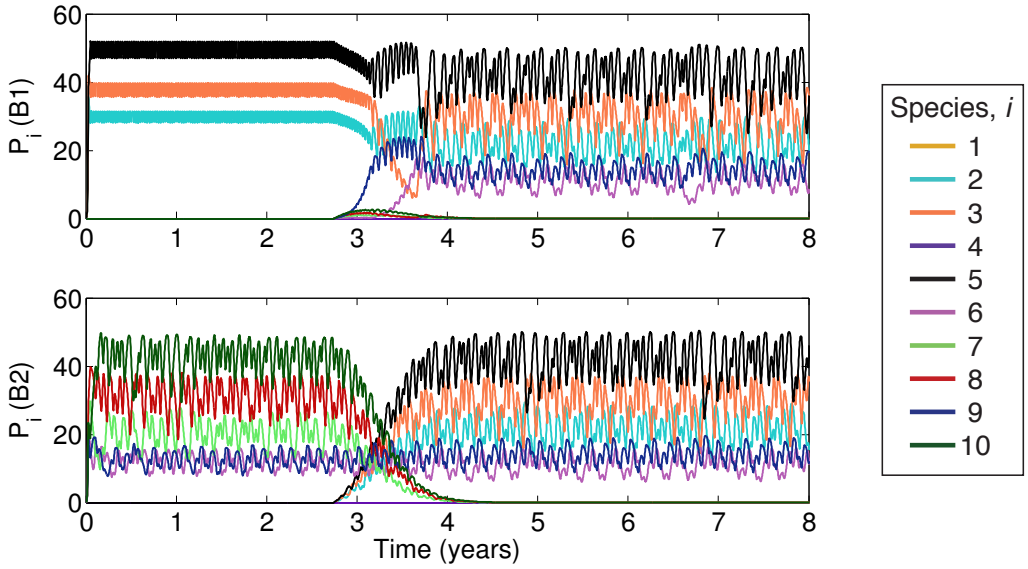

(b) Community structure 25 years after the exchange with $\beta = 10^{-8}$ d^{-1}

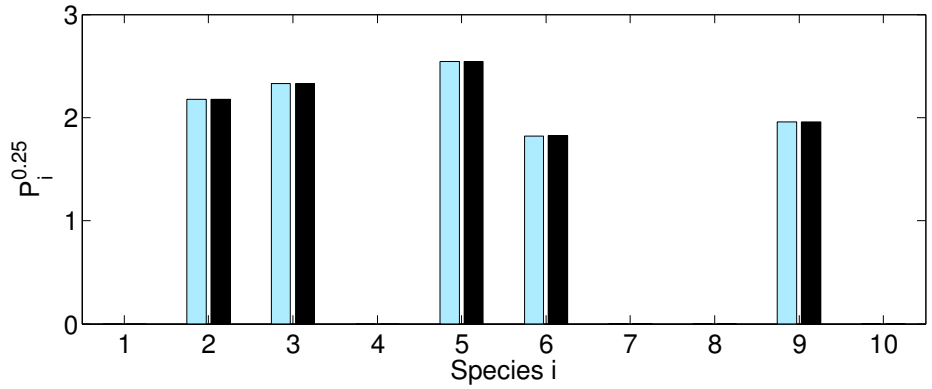

(c) Community structure 25 years after the exchange with $\beta = 1$ d^{-1}

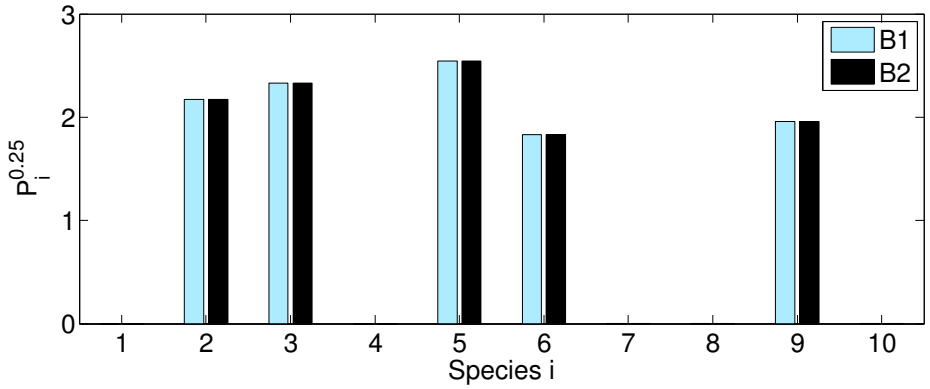

Figure 6.5: The effect of horizontal exchange between communities of different structure and nutrient utilization abilities (scenario 4; Table 6.1). The time series of species abundance, P_i, is illustrated in (a), where the exchange occurs with $\beta = 10^{-3}$ d^{-1} ($\sim T_x = 2.7$ years). Panels (b) and (c) indicate the number and time-average abundance of species over the last 2000 days of model simulation ($\frac{1}{4}$-power transformed for clear visualization of species surviving at very low concentrations) surviving in patch 1 (B1, in blue) and patch 2 (B2, in black) with $\beta = 10^{-8}$ d^{-1} ($\sim T_x = 270$ ky) and $\beta = 1$ d^{-1} ($\sim T_x = 1$ day) respectively. The exchange process begins on day 1000.

6.4 Northward advection of low-latitude communities

On larger spatial scales, there is dispersal of phytoplankton species via oceanic lateral currents. This lateral dispersion can enhance local diversity by bringing in new populations from distant locations. This study explores the role of physical transport across latitudinal gradients.

Experimental and theoretical evidence has demonstrated that small cells have an advantage when competing for nutrients due to high surface to volume ratio that leads to lower half-saturation coefficient and faster nutrient uptake (Eppley and Thomas, 1969; Aksnes and Egge, 1991; Hein et al., 1995). Lower nutrient requirement for growth allows for the smaller cells to be successful in nutrient-depleted regions (Grover, 1991). In comparison, larger cells that have a higher nutrient requirement for growth, due to a high half-saturation coefficient and slow nutrient uptake, benefit in the regions of enhanced turbulent mixing and a high nutrient availability (Eppley and Thomas, 1969; Aksnes and Egge, 1991; Margalef, 1978; Cullen and MacIntyre, 1998). For example, small *Prochlorococcus* is found to occupy the oligotrophic subtropical gyres, whilst larger dinoflagellates and diatoms flourish at higher latitudes where there is a strong seasonal nutrient supply (Margalef, 1978; Vaulot et al., 1995).

In this study, the model simulations mimic the poleward advection of the low-latitude picoplankton communities in the western boundary currents. The aim of the study is to investigate how introduction of better nutrient competitors affects the mid-latitude nanoplankton community response and local biodiversity at the mid latitudes, and how sensitive the response is to the strength of connectivity. Appropriate allometric constraints and latitudinal gradients in temperature and nutrient supply are applied.

6.4.1 Model formulation

The idealized model framework is extended to mimic physical transport processes, latitudinal variation in nutrient supply and temperature, and includes two different phytoplankton size classes, each initially dominating at a different latitude. The analysis explores how the lateral exchange of species on a regional scale affects community response. Sensitivity of the competitive outcome is investigated by modifying 3 processes that potentially inhibit the ultimate competitor: (1) the strength of the exchange through horizontal diffusion, (2) growth sensitivity to the ambient temperature through the choice of the optimum temperature, and (3) higher mortality rate implicitly representing the grazing pressure.

Connectivity between ecosystems

The model simulates the northward advection of the low-latitude community in the western boundary current, such as, the Gulf Stream, and consists of 3 interconnected chemostats (see Figure 6.6). The first well-mixed box simulates the low-latitude community at 25^oN (B1). The ecosystem, which includes biomass and nutrients, is then transported northwards at the rate α (d^{-1}) to the latitude 40^oN (B2). At the mid latitudes, B2 is advected across the basin and a two-way exchange at the rate β (d^{-1}) occurs between the advected water mass and the local ecosystem (B3).

The rate α denotes the proportion of the community transported in the western boundary current. The timescale of a northward transport in the Gulf Stream, with the current speed of 1-1.5 ms^{-1}, over 15^o of latitude is estimated to be 12-19 days. The community functioning is assumed not to be inhibited during the transport. The model simulates the transport process under two scenarios: when $\alpha = 0.25$ d^{-1} and $\alpha = 0.5$ d^{-1} sug-

gesting that 25% and 50% of the low-latitude ecosystem is transported northwards respectively.

Estimation of the horizontal, across-basin advection timescale is based on the float experiment of Bower and Rossby (1989). Bower and Rossby (1989) found that initially it took about 2 days for the float to be transported by 1^o east of the Gulf Stream at 70^oW, and a further 45 days for the float to reach 55^o W, which suggests a zonal transport timescale, T_a, of about 3 days per degree of longitude. Here, change in T_a is implemented and the timescale for the horizontal advection across the entire, 50^o-wide basin is estimated for $T_a = 150$ days. This study assumes the size of the patch $L = 100$ km and simulates the exchange for horizontal diffusivity $\kappa = 1000$ and $\kappa = 500$ m^{2}s^{-1}, which indicates the diffusion timescale of $T_x = \frac{L^2}{\kappa} = 115$ and $T_x = 230$ days and provides an estimate for the proportion of the communities exchanged per day of $\beta = 8.7 \times 10^{-3}$

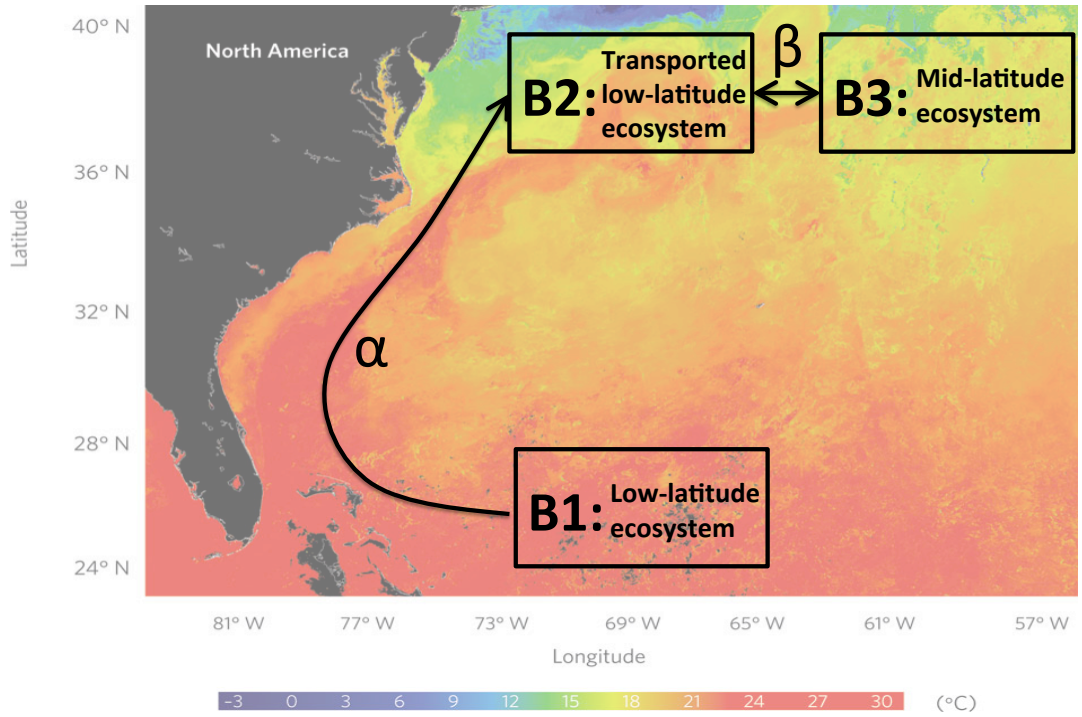

Figure 6.6: Diagram illustrating the connections between the low-latitude and mid-latitude ecosystems implemented in the model study. In the background, the remote-sensing image of the sea surface temperature in the North Atlantic reveals the pathway of the Gulf Stream (figure from Williams and Follows (2011)).

d^{-1} and $\beta = 4.3 \times 10^{-3}$ d^{-1} respectively.

The model is initialized with $n = 10$ species, where species 1-5 represent the low-latitude community transported in the western boundary current, and species 6-10 represent the local, mid-latitude community subjected to the inflow of the low-latitude species. For example, the equations for phytoplankton concentration in all 3 environments become:

$$\frac{\partial P_{B1,i}}{\partial t} = P_{B1,i}(r_i \gamma_i^N - m_i) \qquad i = 1, ..., n \tag{6.3}$$

$$\frac{\partial P_{B2,i}}{\partial t} = P_{B2,i}(r_i \gamma_i^N - m_i) + \alpha P_{B1,i} + \beta (P_{B3,i} - P_{B2,i}) \tag{6.4}$$

$$\frac{\partial P_{B3,i}}{\partial t} = P_{B3,i}(r_i \gamma_i^N - m_i) + \beta (P_{B2,i} - P_{B3,i}) \tag{6.5}$$

It is assumed that export of phytoplankton community from B1 is balanced by advection from the external source and there is no additional loss term implemented in Eq. 6.4, which allows for easier control of the initial phytoplankton community dynamics in the low latitudes.

The low-latitude patch transported to the mid latitudes, B2, undergoes horizontal diffusion as it moves across the basin. The model assumes that the population contained within the patch gradually declines until it reaches the final destination where the exchange with the local community, B3, begins. To crudely account for phytoplankton diffusion out of the patch boundaries, the concentration of lost phytoplankton is subtracted from B2 before the exchange with B3 begins:

$$P_{B2}(t) = (1 - \beta T_a)\ P_{B2}(t-1) \tag{6.6}$$

However, implementation of this process turns out of have no effect on the outcome of model simulations.

The effect of the dispersal of the low-latitude phytoplankton community, in terms of local community response and biodiversity, is investigated for the mid-latitude community at the distance ΔD_x east from the western boundary current; the transport timescale T_a is accordingly modified and ranges from 10 to 150 days (Fig. 6.7).

Implementation of environmental gradients

Nutrient concentration, N_j, varies seasonally through modifying the source S_j by a non-dimensional factor σ:

$$\frac{\partial N_j}{\partial t} = D(\sigma S_j - N_j) - \sum_{i=1}^{n} Q_{ji} r_i \gamma_i^T \gamma_i^N P_i \qquad j = 1,...,k \tag{6.7}$$

$$\sigma = 1 + 0.5\, A_{lat} \left(sin\left(\frac{2\pi t}{365\ days} \right) + 1 \right) \tag{6.8}$$

where there are $k = 5$ resources, A_{lat} is a latitude-dependent amplitude of the seasonal variation in the nutrient supply, with $A_{25} = 0.5$ and $A_{40} = 10.0$ for low- and mid-latitude environments respectively (Fig. 6.8a). For both environments nutrient supply concentration is $S_j = \frac{1}{2}\ [6, 10, 14, 4, 9]$ and the system turnover rate $D = 0.25$ d^{-1}.

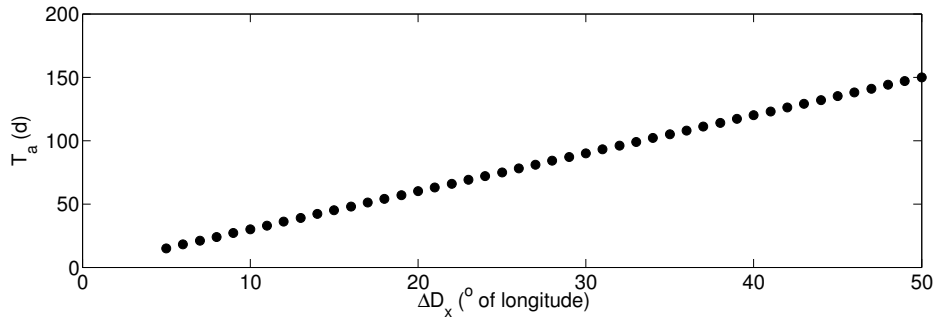

Figure 6.7: The timescale for advection across the basin, T_a, for the ecosystem transported ΔD_x east from the western boundary current. Estimates based on the float experiment of Bower and Rossby (1989).

The seasonal variation in the ambient temperature, T, is implemented in the model:

$$T(t) = T'_{lat}\ sin\left(\frac{2\pi t}{365\ days} - \frac{\pi}{2}\right) + \overline{T_{lat}} \tag{6.9}$$

where $\overline{T_{lat}}$ and T'_{lat} represent latitude-dependent annual mean temperature and seasonal departures from the mean respectively. For the low latitude environment $\overline{T_{25}} = 25\ ^{o}$C and $T'_{25} = 3\ ^{o}$C, and for mid latitudes $\overline{T_{40}} = 20\ ^{o}$C and $T'_{40} = 5\ ^{o}$C (Fig. 6.8b). The parameters controlling the seasonal cycle in the ambient temperature are estimated from the sea surface temperature re-analysis data retrieved from the European Centre for Medium-Range Weather Forecasts (ECMWF) for locations 25^{o}N 50^{o}W and 40^{o}N 50^{o}W corresponding to each environment.

(a) Seasonal nutrient supply, σS_j

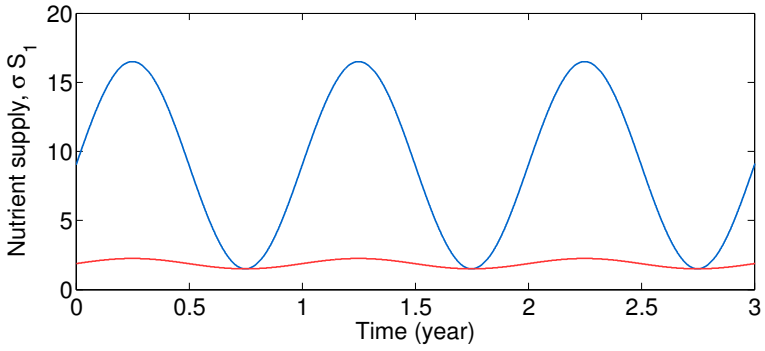

(b) Seasonal variation in ambient temperature, T

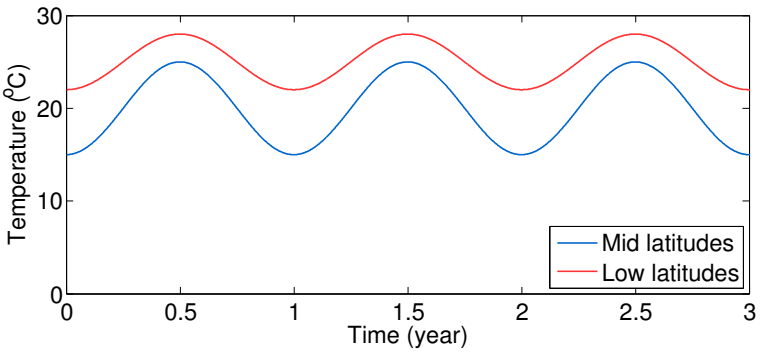

Figure 6.8: Seasonal variability in the (a) nutrient supply, σS_j, and (b) ambient temperature, T, for low-latitude (in red) and mid-latitude (in blue) environments in the ecosystem model.

Phytoplankton growth rate sensitivity to ambient temperature is implemented through modification of the maximum growth rate by a non-dimensional factor γ^T, following Follows et al. (2007):

$$\gamma^T = \frac{1}{\tau_{norm}} A^T exp[-B(T - T_{opt})^C] \tag{6.10}$$

where A, B and C regulate the form of the temperature sensitivity curve, with $A = 1.04$, $B = 3 \times 10^{-4}\ ^oC^{-1}$ and $C = 4.0$, and τ_{norm} is a normalization coefficient.

In order to investigate the effect of growth sensitivity to the ambient temperature, two scenarios are considered: (1) temperature optimum, T_{opt}, is taken as a mean annual temperature of the local environment, which is $T_{opt} = 25^oC$ for subtropical communities and $T_{opt} = 20^oC$ for mid-latitude communities, or (2) T_{opt} is chosen 2^{o}C above the local mean, thus $T_{opt} = 27^oC$ for subtropical communities and $T_{opt} = 22^oC$ for mid-latitude communities. For case (2), the growth of the picoplankton community becomes further inhibited for the mid-latitude environment.

The normalization coefficient, τ_{norm}, varies depending on the choice for T_{opt}. In case(1), $\tau_{norm} = 2.93$ and $\tau_{norm} = 2.41$ for low-latitude and mid-latitude phytoplankton community respectively. In case (2), $\tau_{norm} = 3.17$ and $\tau_{norm} = 2.61$ for low-latitude and mid-latitude phytoplankton community respectively (Fig. 6.9). The temperature sensitivity curve for phytoplankton growth, obtained with the parameters discussed above, captures the temperature range reported for marine phytoplankton from laboratory experiments (Eppley, 1972; Donk and Kilham, 1990; Moore et al., 1995). The shape of the curve is in agreement with the findings of Thomas et al. (2012) who identify that the maximum growth of phytoplankton occurs at temperatures higher than the annual mean temperature of the surrounding environment.

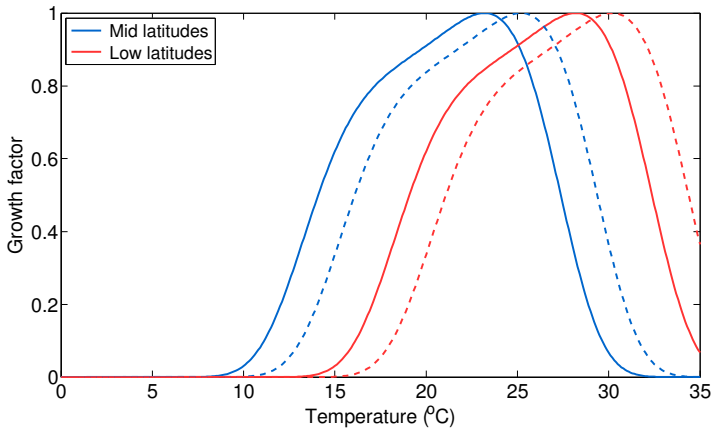

Figure 6.9: The sensitivity of phytoplankton growth to ambient temperature for low-latitude (in red) and mid-latitude (in blue) communities. Temperature sensitivity is constructed for temperature optimum, T_{opt}, specified for low-latitude and mid-latitude communities respectively: $T_{opt} = 25^o$C and $T_{opt} = 20^o$C (solid lines), or $T_{opt} = 27^o$C and $T_{opt} = 22^o$C (dashed lines).

Community structure

At the onset, the ecosystem model assumes that the low-latitude community is dominated by picophytoplankton and that nanophytoplankton dominate in the mid latitudes (Agawin et al., 2000). The mean cell size for the picoplankton community is 1 μm in diameter with cell volume $V = 0.523\ \mu\text{m}^3$, and the nanoplankton community is characterized by 10 μm cells with $V = 523.3\ \mu\text{m}^3$. The shape of the cell is assumed to be spherical so that $V = \frac{4}{3}\pi r^3$ where r is the cell radius.

Half-saturation coefficient and cell quota

In terms of estimating the half-saturation coefficients, K_{ji}, and cell quota, Q_{ji}, the allometric scaling rules are applied (Brown et al., 2004; Aksnes and Egge, 1991). The size-related traits scale with cell volume aV^b (Brown et al., 2004; Edwards et al., 2012), where a and b are constants. This approach ensures that smaller cells that grow faster are better nutrient competitors due to their low nutrient requirement (Eppley and Thomas, 1969; Aksnes and Egge, 1991; Hein et al., 1995).

Estimating the half-saturation coefficient, K_{ji}, for resource j species i, for the two considered phytoplankton size classes is based on the study of Litchman et al. (2007).

The study suggests that the half-saturation coefficient for nitrate, K_N, for marine phytoplankton species can be estimated from an allometric scaling relation $K_N = 0.17\ V^{0.27}$. For 1 μm and 10 μm cells this relation yields $K_N = 0.14$ and $K_N = 0.92$ μM respectively. The default K_{ji} matrix is then rescaled for each phytoplankton size class:

$$K_{ji} = \frac{K_N}{max(K_{default})}[K_{default}] = \frac{K_N}{0.39}\begin{pmatrix} 0.39 & 0.34 & 0.30 & 0.24 & 0.23 \\ 0.22 & 0.39 & 0.34 & 0.30 & 0.27 \\ 0.27 & 0.22 & 0.39 & 0.34 & 0.30 \\ 0.30 & 0.24 & 0.22 & 0.39 & 0.34 \\ 0.34 & 0.30 & 0.22 & 0.20 & 0.39 \end{pmatrix} \tag{6.11}$$

As in the previous section, any modification to the K_{ji} matrix resulting in different community responses is indicated by listing modifications made to the default K_{ji} matrix, $K_{default}$.

The allometric scaling for cell quota, Q_{ji}, is obtained from Marañón et al. (2013), where the minimum cell quota for nitrate, Q_N, is estimated from $Q_N = 0.034\ V^{0.84}$ pgN cell^{-1}. In order to obtain the unit conversion to $molN\ mol^{-1}C$, a scaling rule for cell carbon content is required, where $C_{cell} = 0.204\ V^{0.88}$ pgC cell^{-1} (Marañón et al., 2013). The ratio of these scaling relationships yields $Q_N = 0.17\ V^{-0.04}\ molN\ mol^{-1}C$ and provides the estimates $Q_N = 0.17$ for small and $Q_N = 0.13\ molN\ mol^{-1}C$ for larger cells, which

values are subsequently used to rescale the default Q_{ji} matrix:

$$Q_{ji} = \frac{Q_N}{max(Q_{default})}[Q_{default}] = \frac{Q_N}{0.14}\begin{pmatrix} 0.04 & 0.04 & 0.07 & 0.04 & 0.04 \\ 0.08 & 0.08 & 0.08 & 0.10 & 0.08 \\ 0.10 & 0.10 & 0.10 & 0.10 & 0.14 \\ 0.05 & 0.03 & 0.03 & 0.03 & 0.03 \\ 0.07 & 0.09 & 0.07 & 0.07 & 0.07 \end{pmatrix} \tag{6.12}$$

Maximum growth rate and mortality

Experimental measurements indicate a maximal growth within the range from 0.6 d^{-1} to 2.0 d^{-1} for picoeukaryotes (Landry et al., 1984; Glover et al., 1987; Iriarte and Purdie, 1993; Moore et al., 1995; Reckermann and Veldhuis, 1997; Mann and Chisholm, 2000; Jacquet et al., 2001; Veldhuis et al., 2005). Estimating the maximal growth rates, r_{max}, for the two different size classes in the model is challenging, as there are a limited number of studies that investigate the allometric scaling rules that can be applied to small picophytoplankton. For example, the scaling rule suggested by Edwards et al. (2012) is evaluated on cells larger than 1 μm^3, but when applied to picophytoplankton yields significantly overestimated growth rates. In contrast, implementing the allometric scaling rule obtained by Marañón et al. (2013), who incorporates small phytoplankton size classes, yields growth rates of about 0.3 d^{-1}.

For this study, the maximal growth rates for pico- and nanoplankton are taken from the model study of Ward et al. (2012), who maps the maximum growth rates as a function of cell size and verifies them against experimental estimates. The low- and mid-latitude community growth rates are characterized by $r_{max} = 1.2$ d^{-1} and $r_{max} = 0.9$ d^{-1} respectively.

Mortality rates for each phytoplankton size class are estimated based on the phytoplankton growth rates from the linear relationship identified by Calbet and Landry (2004), where $m = 0.57 r_{max} + 0.032$. This linear approximation provides $m = 0.72$ d^{-1} for small cells and $m = 0.55$ d^{-1} for large cells. This estimate for the grazing mortality for picoplankton is in accord with that obtained experimentally (Reckermann and Veldhuis, 1997; Mann and Chisholm, 2000; Veldhuis et al., 2005).

In order to investigate the potential effect of grazers on inhibiting the growth of the strongest nutrient competitors, the mortality rate for picoplankton is varied from $m = 0.72$ d^{-1} to $m = 1.02$ d^{-1}. The effect of predation is not explicitly represented here in order to remain consistent with the idealized model framework used in this thesis. Implementation of additional coupling through grazers would introduce higher complexity to the system and alter the parameterized responses of the community.

For community examples investigated in this study where chaos previously existed, implementation of the size-related trade-offs leads to the chaotic response diminishing under certain parameter choices and emerging under others. This change of response is likely due to the new parameterization changing the character of the system, which leads to chaotic regimes shifting to the different parameter regimes. Therefore, when referring to the community response generated with the default K_{ji} matrix, only the parameter values are of concern and not the response generated before the allometric traits are implemented.

6.4.2 Lateral exchange and phytoplankton competition on a regional scale

The role of physical transport processes

This section explores whether low connectivity inhibits the success of the stronger nutrient competitors from the low-latitude, oligotrophic regions. Previous experiments of a two-way exchange between phytoplankton populations suggest that introduction of the ultimate competitor at a sufficiently low concentration can prevent competitive exclusion (Mouquet and Loreau, 2003). Here, the transported concentration of the picoplankton community is controlled by the northward transport, α (d^{-1}), horizontal exchange, β (d^{-1}), and the timescale for advection across the basin, T_a. The sensitivity

of the phytoplankton community to temperature is parameterized with $T_{opt} = 25^o$C and $T_{opt} = 20^o$ for pico- and nanoplankton respectively (see Eq. 6.10).

The outcome of the phytoplankton competition in the mid latitudes proves to be insensitive to the strength of dispersal. Advection and exchange of the community at any α and β, lead to the same community structure emerging as in the scenarios of stronger population connectivity for all considered T_a. This outcome is a result of the low-latitude picoplankton community flourishing in the mid-latitude environment, and transport of the community at very low concentrations leads to the low-latitude picoplankton becoming strongly established within very short timescales and drives the local, mid-latitude nanoplankton community to extinction.

A chaotic response of the phytoplankton community persists only if the advected low-latitude picoplankton exhibits chaos. For example in Fig. 6.10, the low-latitude picoplankton community exhibiting a weakly chaotic response (with $K_{default}$) is transported north at $\alpha = 0.25$ d^{-1} and exchanged with a mid-latitude, oscillatory nanoplankton community ($K_{default\ 1,4} = 0.40$). Despite the long timescale of across-basin advection, $T_a = 150$ days, and low rates of exchange with the local nanoplankton community, $\beta = 4.3 \times 10^{-3}$ d^{-1}, the low-latitude picoplankton outcompete the local nanoplankton community and sustain the chaotic response at the mid latitudes in a form of apparent inter-annual variability (Fig. 6.10a). The maximal Lyapunov Exponent for the emergent mid-latitude community becomes $\lambda_{max} = 0.003$ d^{-1}, and indicates the ability of prediction not exceeding 1 year ($\frac{1}{\lambda_{max}} = 333$ days). If the transported picoplankton community originally exhibits regular oscillations (with $K_{default\ 1,4} = 0.40$), the nanoplankton community in the mid-latitude environment is characterized by a regular and predictable annual cycle (Fig. 6.11).

Thus, the character of the low-latitude picoplankton community is imprinted on the

mid-latitude community, unless additional curbs on their success are introduced.

The effect of temperature inhibition

This section explores the effect of picoplankton growth being inhibited by lower ambient temperatures in the mid latitudes. This sensitivity is explored by imposing a greater temperature optimum for phytoplankton growth, T_{opt}, so that picoplankton have a lower tolerance to lower temperatures, and therefore grow at a much lower rate. The aim is to explore how realistic modifications in the physiology of competing species affects the final competition outcome.

At first, $T_{opt} = 25^o$C and $T_{opt} = 20^o$ for pico- and nanoplankton are chosen respectively, under which conditions both communities should flourish in the mid-latitude summer. Nanoplankton are well adapted to low temperatures in the winter, with the growth rate inhibited to $0.6 r_{max}$, while picoplankton growth rates are significantly inhibited to $0.03 r_{max}$. Under these physiological boundary conditions picoplankton remains a superior competitor (Fig. 6.10 and 6.11).

The tolerance of phytoplankton to lower temperatures is altered by increasing their temperature optima to $T_{opt} = 27^o$C and $T_{opt} = 22^o$ for pico- and nanoplankton respectively. Now, the nanoplankton growth rate in the winter is inhibited to $0.34 r_{max}$, while the survival of the picoplankton is impeded to a much greater extend, to $0.001 r_{max}$. However, introducing these more restrained conditions for growth does not prevent the picoplankton from excluding the nanoplankton community in the mid latitudes. It is therefore concluded that higher tolerance to the local environmental conditions of modelled nanoplankton community is not sufficient to compensate for their high nutrient requirement and poor competitive abilities.

Again, the nanoplankton community at mid latitudes can exhibit chaotic response only if the transported low-latitude picoplankton community exhibits non-equilibrium dynamics, as the response of the stronger low-latitude competitors reflects on the mid-latitude community.

(a) Initial response to the exchange between communities

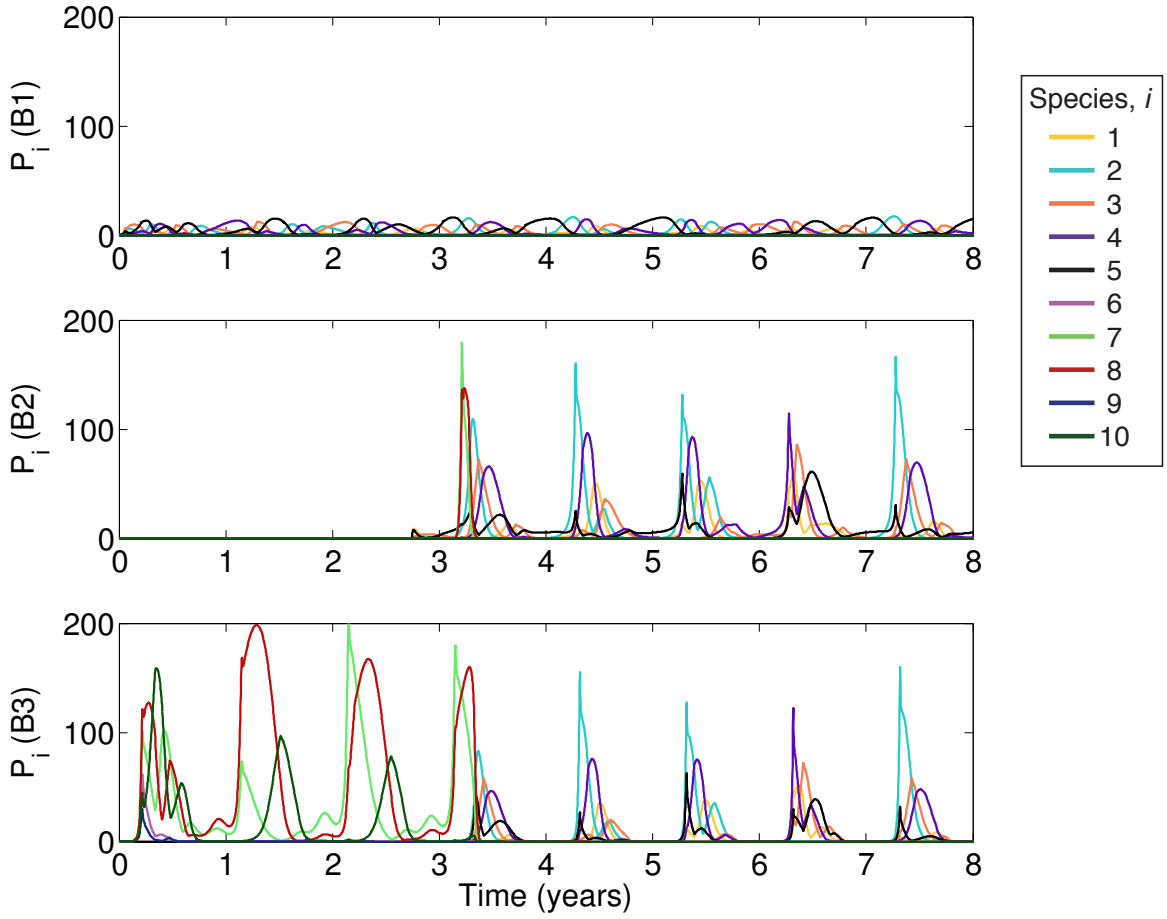

(b) Community structure 25 years after the start of the exchange

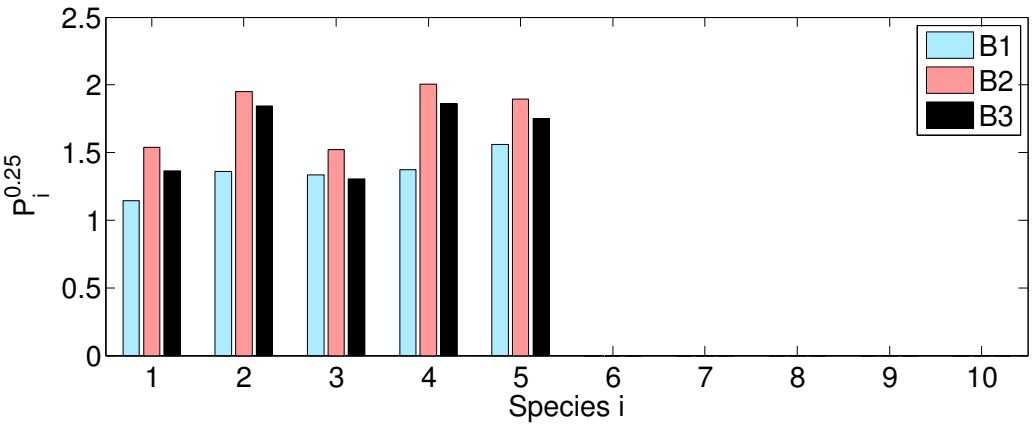

Figure 6.10: The response of the mid-latitude nanoplankton community to the advection of the low-latitude picoplankton exhibiting chaotic response: proportion of the low-latitude community (species 1-5; B1) is transported north (B2), where the exchange with the local, mid-latitude community (species 6-10; B3) occurs after 1000+T_a days. (a) The initial community response to the lateral exchange, (b) the community structure 25 years later, the abundance of particular species, P_i ($\frac{1}{4}$-power transformed), for each environment is shown in (b). Community in B1 generated with $K_{default}$ (chaos) and B3 with $K_{default\ 1,4} = 0.40$ (oscillations).

(a) Initial response to the exchange between communities

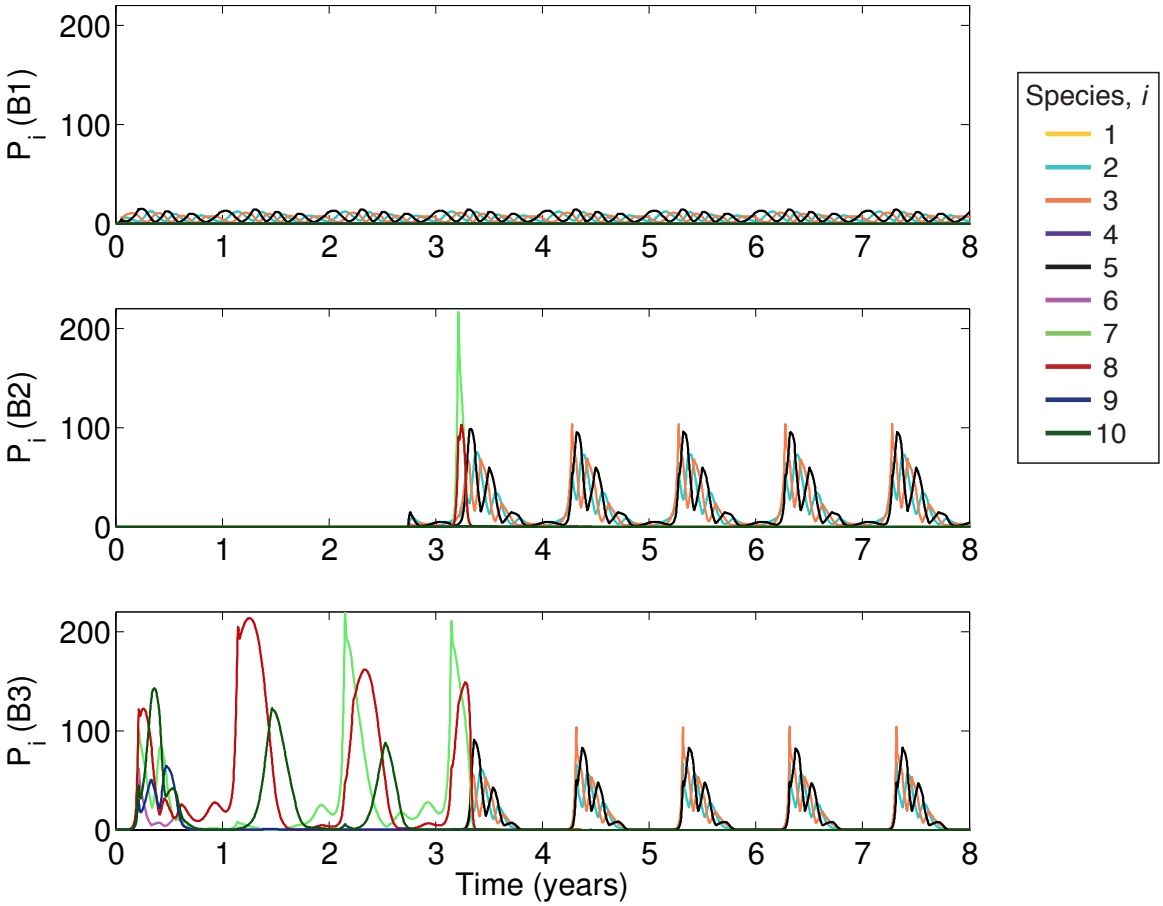

(b) Community structure 25 years after the start of the exchange

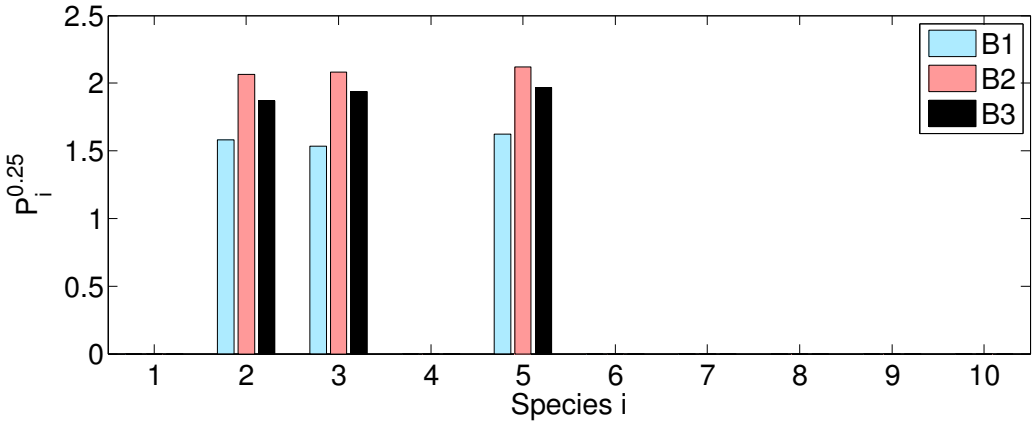

Figure 6.11: The response of the mid-latitude nanoplankton community to the advection of the low-latitude picoplankton exhibiting regular oscillations: proportion of the low-latitude community (species 1-5; B1) is transported north (B2), where the exchange with the local, mid-latitude community (species 6-10; B3) occurs after 1000+T_a days. (a) The initial community response to the lateral exchange, (b) the community structure 25 years later, the abundance of particular species, P_i ($\frac{1}{4}$-power transformed), for each environment is shown in (b). Community in B1 generated with $K_{default\ 1,4} = 0.40$ (oscillations) and B3 with $K_{default}$ (oscillations under imposed trade-offs for nanoplankton).

The influence of higher grazing pressure

The effect of increasing mortality rate of picoplankton is now considered, which decreases their competitive abilities. Microzooplankton that feed on the picoplankton community can achieve reproduction rates as high as, or exceeding, the growth rate of their prey. In comparison, nanoplankton grazers have generation timescales in the order of weeks (Riegman et al., 1993). Therefore, the grazer control prevents the picoplankton community from flourishing to a greater extend, whilst mesozooplankton grazing is less efficient due to the slower response to an increase in the prey abundance (Strom and Welschmeyer, 1991; Riegman et al., 1993; Calbet and Landry, 2004).

Enhanced mortality rate in the model simulates further amplification of the grazing pressure that is not explicitly represented in this model study. Increased loss due to predation acts to regulate the abundance of the stronger nutrient competitors, that is low-latitude picoplankton, and prevent them from dominating the mid-latitude environment.

The examples discussed so far illustrate that the mortality predicted based on the maximum growth rate of phytoplankton (Calbet and Landry, 2004) is not sufficiently strong to prevent picoplankton community from dominating the mid latitude community. The mortality rate of picoplankton is therefore further increased by imposing an offset of up to 0.3 to the initially assigned $m = 0.72$ d^{-1}. Significant shifts in the phytoplankton community structure in the mid latitudes are then diagnosed when picoplankton mortality is increased to at least $m = 0.92$ d^{-1}. Higher grazing pressure on picoplankton allows the picoplankton to be curbed and the nanoplankton species to flourish and, in a handful of cases, all of the initialized species are supported in the environment.

An example effect of the lateral exchange in Figures 6.12 and 6.13, illustrates the re-

sponse of the mid-latitude nanoplankton exhibiting chaos, generated with $K_{default\ 4,5} = 0.15$, to lateral exchange with an oscillatory community transported from the subtropics, with $K_{default}$. Note that modification of the mortality rates may lead to a change in the type of the community response, for example, $K_{default}$ with applied allometric constraints under lower picoplankton mortality ($m = 0.72$ d^{-1}; Fig. 6.10) leads to the chaotic response emerging, whilst increase picoplankton mortality leads to regular oscillations ($m = 0.92$ d^{-1}; Fig. 6.12) or competitive exclusion ($m = 1.02$ d^{-1}; Fig. 6.13).

An increase in the picoplankton mortality rates allows 2 (Fig. 6.12) and then 3 (Fig. 6.13) nanoplankton species to flourish. A chaotic response within the mid-latitude nanoplankton is sustained when the picoplankton growth is strongly inhibited with $m = 1.02$ d^{-1} (Fig. 6.13). Then, the maximal Lyapunov Exponent for the mid-latitude community is estimated for $\lambda = 0.002$ d^{-1} for community in B3, and $\lambda = 0.003$ d^{-1} in B2.

A chaotic response is not seen when picoplankton mortality is $m = 0.92$ d^{-1}, despite the observed inter-annual variability in the species abundance in the mid latitudes (Fig. 6.12). This inconsistency may indicate quasi-periodic behaviour, with multiple oscillation periods, rather than chaos itself, and suggests than a non-chaotic picoplankton community remains in control of the community response to the competition.

Therefore, higher mortality and grazing pressure of picoplankton inhibits the influx of the low-latitude community and prevents the stronger nutrient competitors from outcompeting the mid-latitude nanoplankton. If the mid-latitude nanoplankton remains the dominant community, the response originally exhibited at the mid latitudes is sustained.

(a) Initial response to the exchange between communities

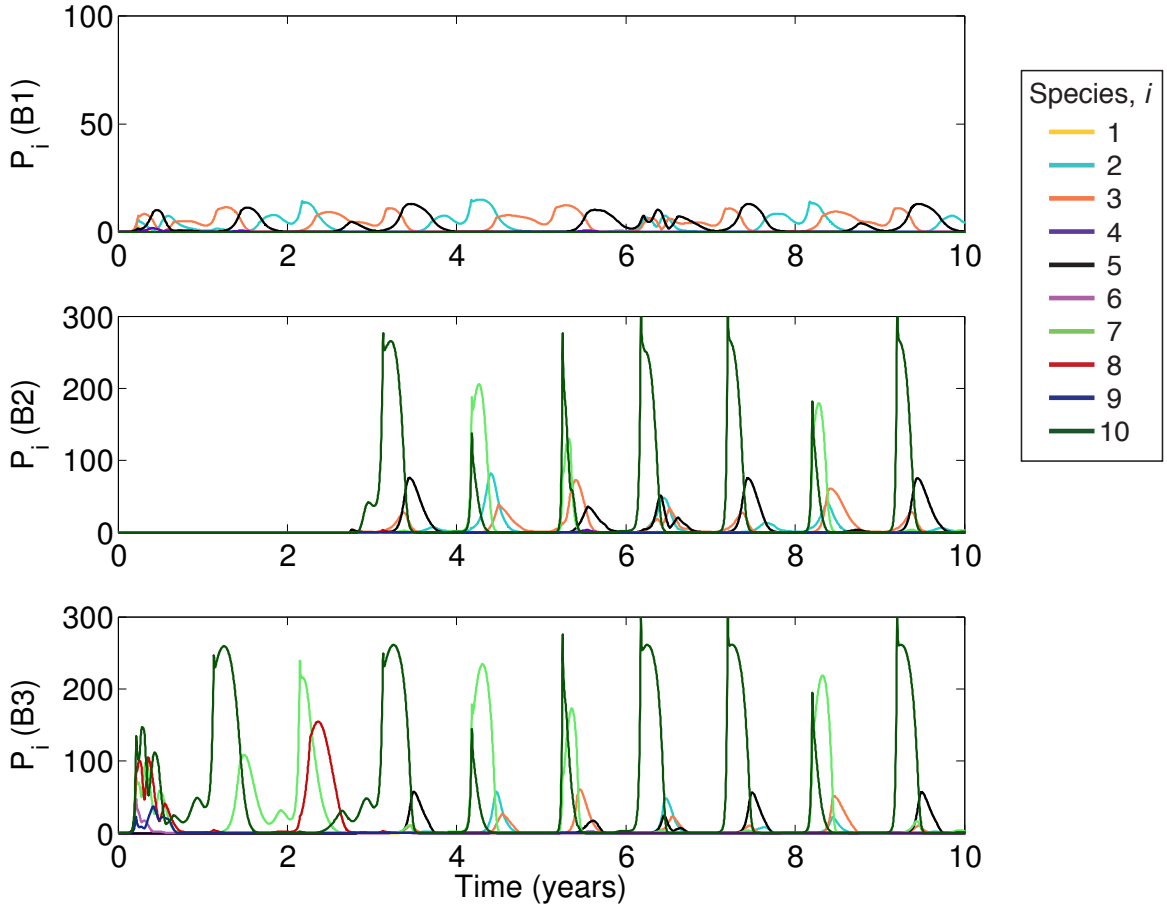

(b) Community structure 25 years after the start of the exchange

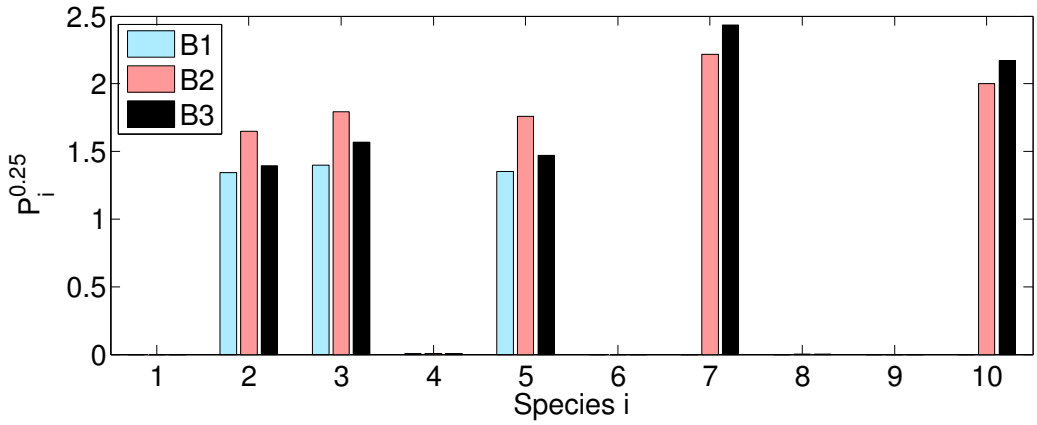

Figure 6.12: The response of the mid-latitude nanoplankton community to the advection of the low-latitude picoplankton exhibiting regular oscillations under higher mortality rate, $m = 0.92$ d^{-1}: proportion of the low-latitude community (species 1-5; B1) is transported north (B2), where the exchange with the local, mid-latitude community (species 6-10; B3) occurs after 1000+T_a days. (a) The initial community response to the lateral exchange, (b) the community structure 25 years later, the abundance of particular species, P_i ($\frac{1}{4}$-power transformed), for each environment is shown in (b). Community in B1 generated with $K_{default}$ (oscillations) and B3 with $K_{default\ 4,5} = 0.15$ (chaos).

(a) Initial response to the exchange between communities

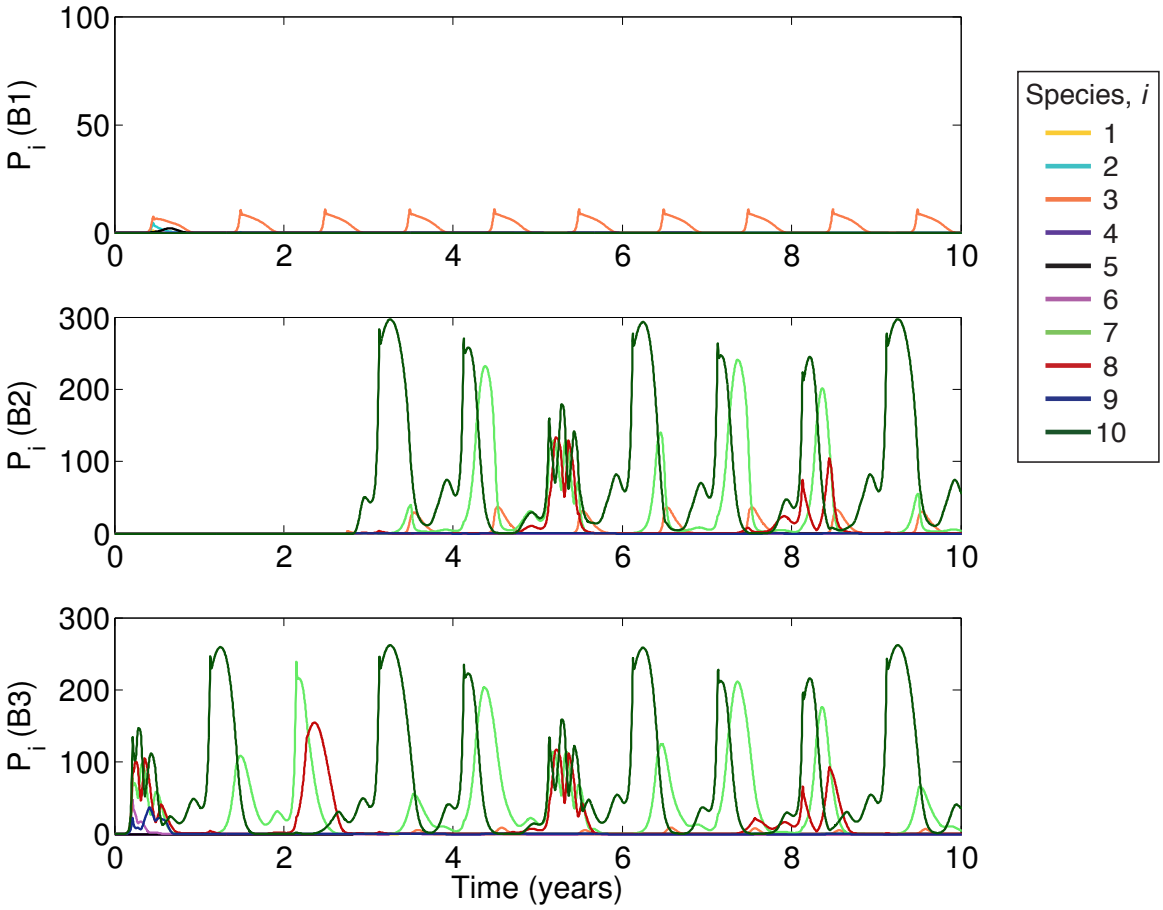

(b) Community structure 25 years after the start of the exchange

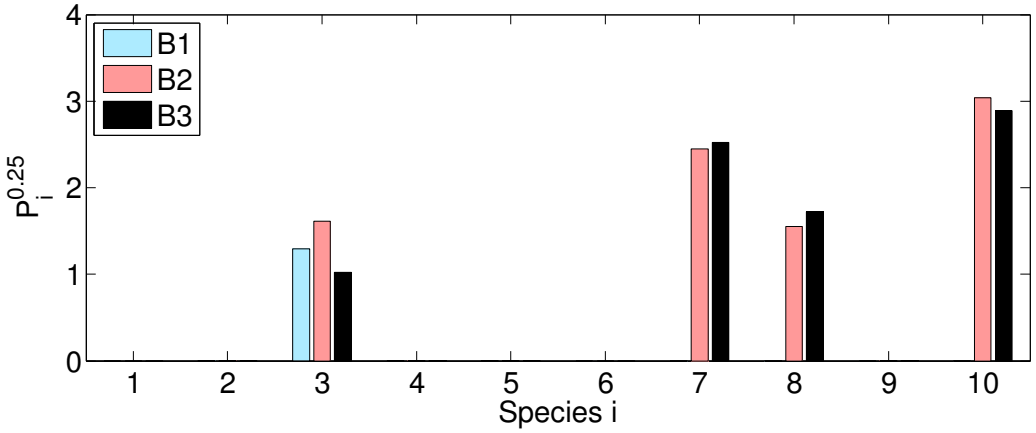

Figure 6.13: The response of the mid-latitude nanoplankton community to the advection of the low-latitude picoplankton exhibiting competitive exclusion under higher mortality rate, $m = 1.02$ d^{-1}: proportion of the low-latitude community (species 1-5; B1) is transported north (B2), where the exchange with the local, mid-latitude community (species 6-10; B3) occurs after 1000+T_a days. (a) The initial community response to the lateral exchange, (b) the community structure 25 years later, the abundance of particular species, P_i ($\frac{1}{4}$-power transformed), for each environment is shown in (b). Community in B1 generated with $K_{default}$ (competitive exclusion) and B3 with $K_{default\ 4,5} = 0.15$ (chaos).

6.5 Discussion

Chaotic behaviour that emerges in the competition of phytoplankton for nutrients has important implications for driving non-equilibrium fluctuations that facilitate the survival of greater number of species than there are resources (Allen et al., 1993; Huisman and Weissing, 1999; Huisman et al., 2001). In addition, chaotic response might enhance the inter-annual variability observed in the ecosystems subjected to the seasonal fluctuations in the physical environment (Doveri et al., 1993; Dakos et al., 2009). What differentiates this complex behaviour from irregular fluctuations driven by stochastic processes, is that chaos can be weakly predicted on short timescales and therefore the emergent inter-annual variability might be at least partially explained.

Chaotic behaviour is identified to occur for isolated marine food chains through experimental (Kooi et al., 1997; Becks et al., 2005; Benincà et al., 2008) and theoretical studies (Popova et al., 1997; Rinaldi and Solidoro, 1998; Huisman and Weissing, 2001). However, the heterogeneity in the marine environment is strongly driven by physical dispersal in a form of lateral transport and mixing processes. The connectivity between ecosystems can act to significantly modify locally established community response and lead to chaos diminishing.

In this study, the model experiments investigating the small-scale phytoplankton competition and patch dynamics find that introduction of a stronger competitor at very low concentrations prevents competitive exclusion. In such case, the local community that is already well-established regulates the abundance of the stronger competitor and the local community diversity is increased. Further increase in the rate of the exchange drives competitive exclusion. This relation between the strength of the connectivity for in-between community exchange was previously suggested by Loreau and Mouquet

(1999). However, the requirement for strength of the exchange necessary to prevent the ultimate competitor from flourishing, is rarely met in the open ocean. Sufficiently low exchange between adjacent phytoplankton patches, allowing for chaos to be sustained, would only occur in isolated environments where horizontal diffusion operates on timescales higher than 3 years.

On a larger scale, western boundary currents act to continuously transport smaller phytoplankton of lower nutrient requirements to the mid latitudes. Greater contrasts in the phytoplankton physiology introduced through allometric traits drive the competitive advantage of the low-latitude picoplankton. Even at the lowest connectivity between subtropics and the mid-latitude environment, picoplankton community can flourish and outcompete the nanoplankton, despite nanoplankton being better adapted to local temperature environment. Nanoplankton species can be sustained in their local ecosystem only when there is a higher grazing pressure on the stronger nutrient competitors.

In the context of the community response, chaotic behaviour initially generated by the phytoplankton in the mid-latitudes can persist if the nanoplankton remains dominant. However, chaotic fluctuations can be exported from the low-latitude environment as the picoplankton community flourishes and regulates the response of the local community. Otherwise, if stronger nutrient competitors exhibit regular oscillations in the subtropics, continuous lateral transport leads to chaos diminishing in the mid latitudes.

In the previous studies, continuous advection of weaker competitors was suggested to be a key process sustaining higher phytoplankton diversity (Shmida and Ellner, 1985; Loreau and Mouquet, 1999; Clayton et al., 2013). Here, continuos inflow of the low-latitude community turns out to have a negative impact on the local diversity unless the growth of picoplankton is significantly inhibited by grazing. The mass effect becomes

vital only when strong nutrient competitors have negative net growth rates and the continuous supply allows for the picoplankton community to be sustained in the mid latitudes.

Mouquet and Loreau (2003) suggested that intermediate rates of dispersal drive biodiversity on a local and regional scale. Model experiments, simulating the poleward lateral transport of better nutrient competitors in the western boundary currents, suggest that the strength of dispersal has no effect on the final community biodiversity. However, this discrepancy may be due to the strong contrasts in the species competitive abilities implemented in this study in order to differentiate between smaller and larger size classes. In addition, Mouquet and Loreau (2003) assume that species that initially occupy a particular environment, are the strongest competitors for that environment, which assumption is not made in the study presented in this chapter.

Every system depending on its complexity holds a threshold of how many species can be sustained for the model to remain stable, and addition of new species acts to reduce the stability of the system (MacArthur, 1970; Phillips, 1978). In Chapter 4, a response of the phytoplankton community to introduction of new species was investigated in a single well-mixed box. Periodic addition of random species into an idealized environment significantly weakened the stability of the system and led to a collapse of chaotic behaviour in the vast majority of model simulations, with irregular transient dynamics significantly reducing the extinction rate of species. The approach did not account for the density difference between the new community within an eddy and the resident community dominating on a regional scale, and therefore generated stronger perturbations. In this chapter, model experiments are conducted simulating a two-way exchange between two stable environments. Gradual diffusive transfer of a limited number of species leads to more stable community dynamics, where chaotic

response is more likely to be sustained. The experiments simulating patch dynamics are more representative of the physical processes controlling oceanic environments, where an introduction of a community transported within an eddy would occur slowly through a two-way exchange at the eddy boundaries.

Chaotic response of phytoplankton is an important aspect that potentially determines the predictability of the community, explains the inter-annual variability in species abundance and drives local community diversity. Whether chaos is sustained in the environment subject to the introduction of a better adapted competitor strongly depends on the contrasts in the competitive abilities. The response turns out to be highly sensitive to the strength of the connectivity between different phytoplankton communities characterised by comparable fitness. For phytoplankton species of similar size, with comparable growth and mortality rates, introduction of a strong competitor at a sufficiently low concentration acts to sustain chaotic dynamics of the local community and drives diversity. On the contrary, implementation of higher contrasts between species competitive abilities leads to chaos diminishing subject to the introduction of a strong competitor, if the grazing pressure is insufficient to inhibit the exclusion. Additionally, the chaotic response can also emerge as a result of continuous transport of phytoplankton community that reveals chaotic behaviour and displaces the local community as the competition progresses.

Bottom-up and top-down controls on phytoplankton growth are considered key factors shaping phytoplankton community size structure (Riegman et al., 1993; Cottingham, 1999; Ward et al., 2013). Latitudinal variation in phytoplankton size classes strongly follows the pattern of seasonal amplification of nutrient supply (Martin et al., 2006; Follows et al., 2007). High rates of nutrient uptake and low metabolic requirement of small phytoplankton allows them to survive at much lower nutrient concentrations than larger

cells (Eppley and Thomas, 1969; Grover, 1991) and to thrive in the nutrient-depleted areas, such as subtropical oligotrophic gyres (Agawin et al., 2000). In contrast, large cells require high amount of nutrients to maintain cell functioning and, due to the low surface area to volume ratio, they have a relatively low nutrient uptake rates (Hein et al., 1995). However, larger cells develop vacuole that serves as a nutrient reservoir utilized when ambient nutrient concentration becomes insufficient for maintaining growth. This ability acts to enhance nutrient uptake abilities of large phytoplankton and significantly improves their competitive abilities under fluctuating environment (Stolte and Riegman, 1995).

Still, for small cells, being better nutrient competitors comes at the price of inhibited net growth through higher grazing mortality. Zooplankton preferentially feed on small microbes (Calbet and Landry, 2004) and higher abundance of grazers was shown to promote the growth of larger phytoplankton (Mazumder, 1994; Cottingham, 1999). Seasonally varying grazing pressure can balance, or sometimes even exceed, the growth rate of picoplankton (Reckermann and Veldhuis, 1997; Guo et al., 2014) and allow for larger cells to flourish through utilizing excess nutrient. In addition, large cell size of phytoplankton provides a refuge from predation (Kiørboe, 1993). Small phytoplankton is grazed by protozoa that have comparable generation timescales, which allows for an instantaneous control over the prey population. Generation time of zooplankton increases with size, where different life stages control the maturity and prey preference of larger grazers. This mechanism results in a lagged numerical response of macrozooplankton to a sudden increase in the biomass of large phytoplankton, which allows the large cells to thrive due to temporarily high net growth rates.

This study outlines the pivotal role of grazers in regulating the community structure at the mid latitudes, where higher predation allows for accumulation of larger size

classes (Ward et al., 2013). The findings show that sufficient grazer control over picoplankton growth allows for different phytoplankton size classes to coexist and creates a mechanism that can sustain complex behaviour within local (mid-latitude) phytoplankton community under the invasion of better nutrient competitors. However, the study would benefit from a further investigation of the effect of dispersal on a wider range of phytoplankton communities exhibiting less profound contrasts in the species competitive abilities. The community examples discussed in this study should not be considered as representative of all possible outcomes of the phytoplankton competition for nutrients.

Model limitations and future improvements

The 3-box model implemented in the study aims to simulate the gyre circulation where better nutrient competitors, picoplankton, are being transported to the mid latitudes in the western boundary current. The model design overlooks a number of important biological and physical features implementation of which should be improved for more accurate representation of the real world processes.

Firstly, the assignment of superior nutrient utilization abilities assigned to picoplankton in the low latitudes leads to small cells outcompeting the mid-latitude species. In reality, large phytoplankton are well-established and dominate in the mid and high latitudes, which suggest that large cells have higher net growth rates and are better adapted competitors in those regions. This competitive outcome is not captured in the modelled mid-latitude environment and the biological representation of the communities, especially parameterization of the maximum growth rate, nutrient requirement and predation, needs to be re-visited.

The current physical set-up of the model poses some crucial limitations for phytoplankton community structure in the mid latitudes due to the implemented interactions between the boxes. The instantaneous coupling between the low-latitude environment, B1, and the patch advected to the mid latitudes, B2, does not account for the duration of the transport in the western boundary current and environmental variability that the community in B2 may experience. Despite a relatively low advection timescale in the western boundary current (a few weeks) a gradual decrease in the sea surface temperature and modification of the nutrient environment will affect the net growth rate of phytoplankton, which may significantly influence the concentration of the low-latitude species that reach the mid latitudes.

In addition, the phytoplankton community structure in the mid latitudes is strongly influenced by the upstream conditions, where the continuous inflow of picoplankton and no additional source of large cells inhibits competitive abilities of the mid-latitude community in B3. Therefore small phytoplankton from B1 drives the large species to extinction unless their growth rate is sufficiently inhibited to balance the inflow from B2 and prevent further expansion of the low-latitude phytoplankton.

On the consideration of the above limitations arising from the physical model configuration, a new model framework is suggested to investigate the role of physical transport on phytoplankton community dynamics (Fig. 6.14). The key modification to the model framework is implementation of the Lagrangian approach where the water column B2 is being transported all the way around the gyre: northwards in the fast-flowing, western boundary current and slowly returns south in the eastern boundary. The water column circulating around the gyre experiences an input of the low-latitude community from B1 along the southern gyre boundary and of the mid-latitude community from B3 along the northern gyre boundary.

The improved model framework retains the simplicity of the chemostat model. It accounts for variability in the transport timescales around the gyre and implements a gradual modification of the ambient environment. Finally, improved model design prevents from permanent extinction of less fit species and allows to investigate the effect of physical transport on the phytoplankton community structure and behaviour.

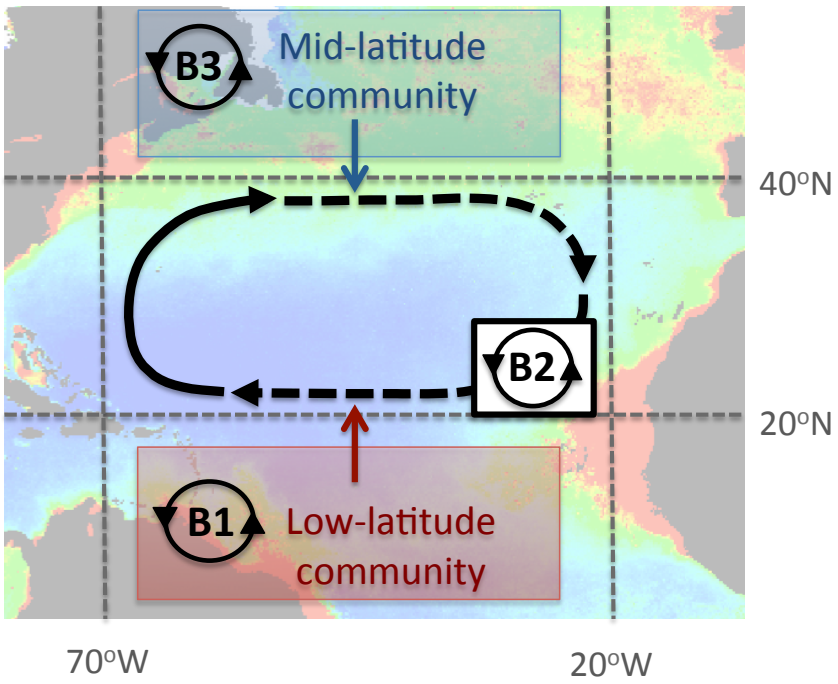

Figure 6.14: Diagram of improved 3-box model formulation for investigation of how physical transport affects phytoplankton community dynamics.

6.6 Chapter summary

This chapter explores how robust is the chaotic response subject to the lateral exchange with stronger or weaker nutrient competitors. First, idealized model experiments are used to investigate the competition outcome driven by the small-scale exchange between species of comparable physiology and cell size, dominating in the adjacent environments. Chaos can be sustained in the local environment when:

- weak competitors are introduced that gradually become extinct;
- there is a weak exchange with the strong competitor that prevents the strong competitor from flourishing and inhibits its competitive abilities;
- if the dominating community has an unoccupied niche for utilization of a particular nutrient, then a species from the weaker, chaotic community can exploit that niche.

In the second part of the study, the large-scale exchange between low-latitude picoplankton and mid-latitude nanoplankton was simulated, including plausible latitudinal gradients and allometric trade-offs. The main findings include:

- weak connectivity does not prevent picoplankton from the tropics dominating the mid-latitude ecosystem;
- the mid-latitude nanoplankton becomes displaced despite better adaptation to the local variability in the ambient temperature;
- higher mortality imposed on the tropical picoplankton community allows for nanoplankton species to be sustained in the mid-latitude environment.

As stronger nutrient competitors, tropical picoplankton flourishes and displaces the mid-latitude nanoplankton. Therefore, chaotic response among the mid-latitude nanoplankton can be sustained only if picoplankton growth is strongly inhibited through grazing pressure. Otherwise, chaos can be exported from the low-latitude ecosystem through the continuous physical transport processes.

CHAPTER 7

Synthesis

7.1 Research summary

Phytoplankton are crucial aquatic microorganisms that contribute over 50% to the global oxygen production (Field et al., 1998) and are the main drivers of the carbon export in the marine environments (Le Fèvre et al., 1998; Raven and Falkowski, 1999; Martin et al., 2006; Jackson, 2001). Marine producers are fundamental for the aquatic food webs and disturbances in their abundance can have a crucial implications for smaller grazers and fish (Flinkman et al., 1998; Frederiksen et al., 2006), or even apex predators (Le Fèvre et al., 1998).

Aquatic phytoplankton exhibit high inter-species diversity through variability in the cell size and cell traits that determine the requirement for resources and their utilization. Cell traits control the ecological niche where environmental conditions favour species survival (Follows et al., 2007; Follows and Dutkiewicz, 2011). However, not every species is successful in a particular environment due to the competition of phytoplankton for essential resources: light (Falkowski et al., 1985; Hickman et al., 2010), macronutri-

ents, such as nitrogen, phosphate and silica (Tyrrell, 1999; Moore et al., 2013), and micronutrients, such as trace metals and vitamins (Martin, 1990; Boyd et al., 2000; Saito et al., 2002). Although, weaker nutrient competitors might be expected to be excluded from the environment (Hardin, 1960; Tilman, 1977; Tilman et al., 1982), there is a great phytoplankton biodiversity where hundreds of different species coexist and compete for a handful of resources. Hutchinson (1961) first questioned why so many different phytoplankton species persist, given competition theory predicting that at equilibrium the number of species cannot exceed the number of limiting resources. He suggested that this paradox of the phytoplankton and inconsistency with competition theory is only reconciled by the phytoplankton community not being at equilibrium.

There are a variety of explanations as to why an equilibrium state for the phytoplankton community might not be achieved, possibly reflecting a response to the spatial and temporal heterogeneity in the physical environment, or instead an ecological response involving inter-species competition. Phytoplankton species typically have a doubling timescale of 2 to 5 days, and competitive exclusion might be expected to occur over the order of 10 generations, suggesting a time span for equilibrium to be reached of typically 1 to 2 months (Reynolds, 1995). On this timescale, the ocean surface boundary layer is strongly forced by the passage of atmospheric weather systems, modifying the convection and mixing within the surface boundary layer and the light received by phytoplankton. In addition, in coastal seas, the surface boundary layer is modified by the spring-neap changes in the tides. Given this temporal variability in the physical forcing, there are 2 limits leading to relatively low phytoplankton diversity: (1) if there is severe forcing, such as involving a sustained period of no light or nutrient supply followed by an onset of favourable conditions, then the phytoplankton species with the fastest growth rate dominates; and conversely, (2) persistent conditions lead to the optimal competitors flourishing for a stable environment. Hence, the maximum di-

versity in phytoplankton species is expected between these 2 limits, referred to as the intermediate disturbance hypothesis, which was applied by Connell (1978) for tropical rainforests and coral reefs, discussed for phytoplankton by Padisák (1994) and Reynolds (1995), and used to explain observed changes in the phytoplankton community for a shallow eutrophic lake (Weithoff et al., 2001). Thus, the physical forcing might induce continual temporal and spatial changes in the environment, which the phytoplankton community is continually adjusting to, such that competitive exclusion is not reached.

An alternative view to this physically induced heterogeneity is that there may be more phytoplankton variability due to inter-species competition for resources, as advocated by Huisman and Weissing (1999, 2001). Rather than a single or few species dominating as in competitive exclusion, the phytoplankton community can continually vary in the form of repeating oscillations or chaotic changes in the abundance of different species.

Deterministic chaos is characterized by irregular fluctuations where the smallest disturbance is amplified in time and affects the evolution of the system, as discussed for the atmopshere (Lorenz, 1963, 1965) and terrestrial ecosystems (Hastings et al., 1993; Ellner and Turchin, 1995). The occurrence of chaos might then have important implications within phytoplankton communities. The inter-annual variability in the phytoplankton abundance time series that is not reflected in the variability in the physical forcing (Barton et al., 2014, submitted), could be potentially explained as irregular chaotic fluctuations masked under the influence of seasonality (Doveri et al., 1993; Dakos et al., 2009), which can be predicted on short timescales. In addition, the non-equilibrium response has been suggested to have an important contribution in driving biodiversity by increasing the number of species that can coexist while competing for

a limited number of resources (Allen et al., 1993; Huisman and Weissing, 1999; Huisman et al., 2001).

There has been a number of model studies that have confirmed that chaotic behaviour is prevalent within microbial communities (Kot et al., 1992; Huisman and Weissing, 2001; Becks et al., 2005). Chaos turns out to be highly sensitive to the choices made for parameterization of modelled communities (Popova et al., 1997; Huisman and Weissing, 1999, 2001). Chaos might then only occur for a narrow range of parameters and may not be a response that is likely to occur within the real world ecosystems. In addition, the sensitivity of the response to the externally-induced variability in the physical environment has not been widely explored.

This thesis explores the sensitivity of chaotic behaviour to the externally-imposed environmental variability as well as the physiological differences of competing species. In Chapter 3, the analysis of the phytoplankton time-series data revealed that it is difficult to verify whether chaos occurs within marine microbial ecosystems due to the insufficient sampling frequency of the data. Therefore, idealized model simulations of phytoplankton competition for nutrients have been used to investigate the hypotheses stated in section 1.3.

(H1) Chaotic behaviour is an infrequent inter-species competition outcome and requires finely-tuned parameter choices.

Chaos as an internally-induced response of the phytoplankton community to the competition for nutrients can occur only if there are inter-species differences in nutrient requirements and cell structure (Chapter 4; Huisman and Weissing, 2001). This variability is to assure that species are stronger competitors for different nutrients so that

the inter-species competition leads to unstable dynamics where the ultimate competitor is not established. Modification of half-saturation coefficient for only one resource may disturb the balance and the species that becomes strongest for more than 1 resource wins. Chaotic response requires imposed species differences in both, half-saturation coefficients and cellular stoichiometric ratios represented by cell quota. If species differences are included, chaotic response can account for almost a third of possible competition outcomes, suggesting that chaos is a highly likely outcome within phytoplankton communities. This chaotic viewpoint agrees with the view that species can coexist only if they are limited by a different resource as previously suggested by Tilman (1977) who investigated different competition scenarios between two phytoplankton species using an experimental and a theoretical approach.

Chaotic response turns out to be highly sensitive to nutrient supply conditions, and in particular to the strength of nutrient feedback, referred to as nutrient relaxation. In the chemostat environment, the nutrient feedback controls how much nutrient is supplied based on the ambient nutrient concentration. Lack of the feedback leads to the accumulation of the excess nutrient, which facilitates the competitive exclusion where the winner is the strongest competitor for that nutrient.

Nutrient relaxation can be viewed as mimicking the diffusive feedback within the marine environment. The intermittent disturbances in the nutrient feedback act to diminish chaos only temporarily, with the community converging to chaotic response once again when the feedback is reinstated. The findings suggest that intermittent-weather related disturbances themselves might only on a temporary basis inhibit chaotic response. In addition, the sensitivity to the strength of the diffusive feedback may indicate the temporal character of chaotic response developing when the nutrient supply conditions are favourable. The analysis suggests that chaos would be most profound in stable or isol-

ated environments. For example, Huisman et al. (2006) suggested that chaos might occur in the deep chlorophyll maximum in the oligotrophic gyre. They used model simulations to investigate the effect of the vertical mixing on the phytoplankton competition outcome. In contrast, Popova et al. (1997) investigated the robustness of the chaotic response using a seasonally forced upper mixed layer model and found that chaos is most likely to occur in the upwelling regions with enhanced nutrient supply, where the nutrient feedback would not hold. This inconsistency may be due to the higher complexity of the marine food web incorporating three trophic levels implemented by Popova et al. (1997).

Therefore, the original hypothesis H1 remains partially valid: chaotic response exhibits a high sensitivity to the environmental conditions and strongly depends on the inter-species differences in their competitive abilities. However, in the regions where the necessary requirements are met, chaos accounts for 30% of model solutions. Therefore due to the spatial variability in the nutrient supply conditions, the occurrence of chaos would vary regionally.

(H2) Seasonal forcing facilitates a chaotic response within a phytoplankton community, and increases the likelihood of non-equilibrium dynamics.

In Chapter 5, model simulations with implemented periodic variability in the nutrient supply confirm that chaotic response can be induced as a result of imposed periodicity. The seasonal forcing itself leads to an increase in chaotic outcomes by 20%, which increases the likelihood of chaos to extend over 50% of the parameter space.

Under seasonal fluctuations, chaos would often be manifested in a form of inter-annual variability (Doveri et al., 1993; Dakos et al., 2009) as illustrated in Chapter 3. The

emerging inter-annual fluctuations are a result of frequency locking, when the phytoplankton community adjusts their internally set pace and oscillated at the frequency determined by external forcing. Seasonal variability in nutrient supply acts to temporarily enhance the strength of chaos and therefore acts to inhibit the prediction timescale, as previously suggested by Popova et al. (1997). This effect is indicated by the increase in the maximal Lyapunov Exponent in the summer under the imposed seasonal cycle. The decline in the nutrient supply from spring to autumn leads to chaotic response becoming more prevalent, which suggests that phytoplankton community becomes less predictable over summer. This relation may have crucial implications for seasonal variations in the levels of biodiversity, with highest numbers of coexisting species supported in the summer during the chaotic regime. Such temporal variability in the phytoplankton species diversity has been previously observed in freshwater lakes (Sommer, 1993) and coastal ponds (Nuccio et al., 2003), where higher biodiversity was recorded in the summer.

Therefore, my research supports the hypothesis H2 that seasonality can induce chaotic behaviour. However, the detection of chaos in highly seasonal environments may be very difficult. The study emphasizes that in order to verify whether chaos occurs within marine ecosystems, the time-series data for the concentration of specific phytoplankton taxa should be obtained from stable environments where the seasonal variability in nutrient supply is low.

(H3) Stochastic variability in forcing suppresses chaotic response in marine ecosystems.

In Chapter 5, the effect of dynamical noise was explored, where stochastic variabil-

ity in the nutrient supply was implemented to simulate weather events and enhanced mixing. This perturbation approach is relevant the applicability of the Intermediate Disturbance Hypothesis (Connell, 1978; Reynolds et al., 1993), where the theory predicts that intermediate disturbances in the resource availability prevent competitive exclusion and act to increase local diversity.

Stochastic forcing has contributed to an increase in the number of chaotic responses from 30% up to 74%, which suggests that weather-related variability leads to chaos becoming the dominant response. The emergence of chaotic model solutions may be associated with the dominant monthly frequency detected within the stochastic variability. According to the Intermediate Disturbance Hypothesis, for phytoplankton with the generation timescale of a few days, disturbance of monthly frequency is optimal for sustaining higher diversity and preventing competitive exclusion (Elliott et al., 2001). Otherwise, the positive verification of chaotic behaviour could arise as a numerical artifact of an applied method. Further extensions of the study could incorporate verification as to whether chaos detected with the numerical methods can still be detected through the direct analysis of the time series. This approach would verify whether chaotic behaviour arising from weather-related variability is a result of a numerical error.

An enhancement in community diversity occurred in 60% of model solutions where a further increase in the number of coexisting species was still possible. Changes in biodiversity and community structure were recorded for communities composed of species of contrasting nutrient requirements, as species of similar fitness would have a uniform response to externally imposed variability.

However, similarly to the effect of seasonal forcing, there is a practical caveat related to weather-related variability facilitating chaotic behaviour and detection of chaos within a

noisy time series. In Chapter 3, noise was imposed on the top of the modelled species abundance time series to investigate the ability to detect chaos from the time-series data. The analysis reveals that even small magnitude measurement noise can obscure the ability for chaos detection. Increasing the amplitude of the imposed stochastic variability suggests a weakening of the chaotic response and increased predictability timescale.

Therefore, the conducted research only partially supports the hypothesis H3: despite chaos becoming the dominant response, its detection within a noisy time series is significantly impaired. Still, as much as the weather-related variability in the nutrient supply can induce chaotic behaviour within phytoplankton communities, the potential cause may lie in the periodicity of the weather events rather than noise itself.

(H4) Physical transport processes and connectivity between different ecosystems inhibit internally-induced chaotic behaviour.

The sensitivity of the chaotic response to the lateral exchange with relatively strong or weak nutrient competitors was investigated in Chapter 6 by implementing exchange between phytoplankton communities of contrasting competitive abilities in two or three well-mixed boxes.

First, the two-way exchange was simulated between communities with comparable metabolic rates, which includes growth and mortality. The model design and parameterization of the communities simulated the small-scale exchange between adjacent patches of contrasting phytoplankton communities from the same size class. The study found that chaotic response within the local phytoplankton community could only be sustained if the exchange with the stronger nutrient competitors is sufficiently low

to sustain the contrasts in the community structure and patchiness. Only then the well-established, local phytoplankton community inhibits the ultimate competitor and prevents the competitive exclusion. Exchange with a weaker nutrient competitor does not alter the chaotic behaviour within the patch initially occupied by the local phytoplankton community.

Next, the model simulations were expanded to simulate a large-scale advection of the low-latitude picoplankton to the mid latitudes, and further exchange with the locally established nanoplankton community. Application of allometric trade-offs related to cell growth and nutrient requirements introduced more profound contrasts in the competitive abilities between modelled communities, with picoplankton flourishing in the mid latitudes and displacing the local, mid-latitude nanoplankton community. Under such scenario, chaos can only occur in the mid latitudes if the transported picoplankton community exhibits chaotic response. Otherwise, chaotic response within the nanoplankton community can only be sustained if picoplankton mortality driven by the grazing pressure is sufficiently high to prevent the stronger competitors from dominating in the mid latitudes.

Therefore, whether hypothesis H4 is valid strongly depends on the physiological contrasts between communities and the type of the response they exhibit. Dispersal can act to diminish locally-induced chaos, however, chaotic response can also be exported with the stronger nutrient competitors from distant locations. The strength of the lateral exchange can affect the competitive outcome between phytoplankton communities if they are of a comparable size, which is due to the relatively low contrasts in their competitive abilities that can be overcome by low rates of dispersal.

7.2 Limitations and future work

The research presented in this thesis explores the processes that control the outcome of phytoplankton competition for essential nutrients. The aim of the research is to establish whether chaos is a likely response and whether it can be detected within marine microbial communities. The research includes analysis of time series data and employs model simulations to explore the sensitivity of chaos to contrasts in the physiology of competing species and environmental variability.

The ecosystem model applied in the study represents an idealised chemostat that simulates the interactions between phytoplankton and nutrients. The model does not portray the true complexity of the microbial food webs and does not consider the top-down control on the phytoplankton community response through predation. However, both bottom-up and top-down controls are key factors controlling the phytoplankton community response and shaping the community structure and diversity. Higher number of trophic levels have been found to increase the frequency of chaotic dynamics (Fussmann and Heber, 2002), so that grazing pressure of zooplankton might induce chaos even when competition between phytoplankton species does not suggest a chaotic response. In contrast, higher complexity of ecosystem models have been suggested to provide a stabilizing effect on the communities and to inhibit the occurrence of chaos (Fussmann and Heber, 2002). Therefore, the research findings presented here should be viewed as addressing the question of whether chaos emerges as a consequence of inter-species competition of phytoplankton, while chaotic behaviour may also be induced or dampened by incorporating higher trophic levels. In the future work following the research presented in this thesis, I would like to implement explicit parameterization of the grazing community and further explore how the addi-

tional trophic level alters the likelihood of chaos occurring within modelled microbial communities.

In addition, in the thesis, the model simulates the phytoplankton community interactions within a well-mixed box and therefore the potential contrasts in community structure arising from the vertical structuring of the water column are not captured. The model simulations emphasize the sensitivity of chaos to the local physical conditions that control the nutrient supply, and suggest that the response might vary regionally according to the forcing. Yet, an additional constraint may be posed by the vertical gradients in light and nutrients availability, and the level of mixing across the thermocline, which drive the vertical contrasts in the community structure in the water column. For example, the model study of Huisman et al. (2006) found that phytoplankton competing for nutrients can exhibit chaotic response in the deep chlorophyll maximum in the oligotrophic gyre due to the reduced mixing and higher stability of the environment.

The analysis of the time-series data in Chapter 3 suggests that detecting chaos within marine communities is difficult to achieve due to the sparsity of data sampled at sufficiently high frequency. However, the model simulations reveal additional limitations that may arise even when sampling a time series at sufficient frequency. The accuracy of the time-series analysis techniques turns out to be highly sensitivity to the level of measurement noise and seasonality. The amplitude of the measurement noise might be reduced by applying data transformation methods, such as a logarithmic function. Still, even a low-amplitude noise can obscure the verification of chaos and lead to the underestimation of the maximal Lyapunov Exponent.

The methods applied for detecting non-linear dynamics directly from the time-series data suggest a weakening of the chaotic response with increased seasonal forcing and a failure to detect chaos in strongly seasonal environments. Thus, the ability to

detect chaos from the time-series data is inhibited as chaos becomes more 'entrained' within a stronger seasonal cycle and the statistical properties of the chaotic time series become suppressed by seasonality. In contrast, numerical implementation of the algorithm for chaos detection allows one to continuously follow the sensitivity to initial conditions and are able to capture chaotic behaviour by introducing small disturbances as the modelled ecosystem evolves.

The model simulations conducted in Chapter 5 reveal that chaotic response is enhanced in the summer, when the concentration of the available nutrient gradually declines due to a shallowing of the upper mixed layer. The temporal character of the chaotic response needs to be considered when analysing the time-series data. A phytoplankton community is able to switch to a different type of response subject to the temporal variability in the available nutrient (Becks and Arndt, 2008), and therefore chaotic behaviour that develops only over a particular time of the year, may be overlooked during the analysis of the entire time series. This feature might be a reason for the unrealistically high prediction timescales of 14 years suggested for the sea surface temperature re-analysis data obtained for the highly seasonal English Channel, in Chapter 3. Due to the design of the numerical algorithm applied in the thesis, the enhancement of the chaotic response is only detected in the strongly seasonal environment. For future work, it would be beneficial to adjust the algorithm and investigate whether the temporal character of the chaotic response is also detected for a weak seasonally-varying nutrient supply. This analysis suggests that the temporal variability in the chaotic response, where chaos is enhanced in the summer, is a characteristic for high-latitude marine ecosystems.

The research presented in this thesis emphasizes that the ability to detect chaos using the time-series analysis techniques is seriously inhibited in a strongly seasonal envir-

onment, despite the increased likelihood of chaos to occur in these regions. Therefore, the efforts to detect chaos from time-series data should be directed towards phytoplankton community in isolated regions characterized by stable community structure, such as subtropical oligotrophic gyres where seasonal species succession is less pronounced (Goericke, 1998). Following these limitations, future research investigating the extent of chaos should focus on the community dynamics in the subtropical oligotrophic gyres. While the observational time-series data in those regions is very limited, the analysis will instead be conducted using the available satellite data. The idealized model simulations of Huisman and Weissing (1999) have shown that total community biomass remains nearly constant despite the chaotic fluctuations in the abundance of modelled phytoplankton species. Therefore, future work will focus on the ocean colour satellite data that allows for differentiation of particular phytoplankton functional types and size classes.

7.3 Wider implications

Research findings presented in this thesis could be potentially criticised for being strongly model-dependent and therefore could not be considered in a wider environmental context. Indeed, quantifying the parameter space and the likelihood of different types of community responses surely is a model-specific task. The dynamics of the system strongly depends on the model formulation through interactive feedbacks, and complexity of non-linear trophic interconnections. However, the important implications of the research presented in this thesis is that chaos is a frequent dynamical response of an idealized model simulating species interactions within a single trophic level. Increasing the complexity of a system was suggested to decrease the stability of model equilibria and favour non-equilibrium dynamics (MacArthur, 1970; Phillips, 1978). Therefore, chaos as a phenomenon driving microbial communities, or even higher trophic levels, should not be excluded.

The chemostat model uses pragmatic parameter values and reproduces realistic frequency fluctuations in phytoplankton community under steady-state conditions. Chapter 5 considers perturbation frequencies characteristic of environmental variability that strongly controls microbial communities, and therefore the response of the modelled phytoplankton should be taken as an approximation of the real-world response. The findings presented in this thesis outline that the dominant environmental forcing controlling the biology of global oceans, seasonality and meteorology, act on a suitable timescales to enhance complex behaviour and drive biodiversity within phytoplankton communities. The model predicts the phytoplankton decay to occur over the timescale of 3 months to a year. In reality, this timescale may be further extended through the effect of predation, where the density-dependent grazing pressure is low for phyto-

plankton near extinction, and higher predation on the fittest species will lift the competitive pressure that drives exclusion. The decay timescale is therefore longer than, or at least comparable to, the timescale of physical transport processes such as the mesoscale eddie advection. As a result, tens of species that are periodically brought in from multiple, distant locations can be sustained in the environment and contribute to the local diversity, despite not being strong competitors in the local ecosystem.

Detection of complex behaviour within microbial community remains a challenge due to insufficient sampling and limitations related to the time-series analysis. The thesis outlines the challenges that will be faced when analysing any observational time-series data, not only of marine microbes. Still, despite the difficulties with detection, chaos could be a factor partially driving the variability in species abundance that can not be explained by externally driven fluctuations in the physical and biological environments (Barton et al., 2014).

Inter-annual fluctuations driven through competitive interactions of phytoplankton species pose crucial implications for nutrient cycling as well as higher trophic levels. Variability in phytoplankton abundance affects the uptake of atmospheric CO_2 and its subsequent removal from the surface waters (Lomas and Bates, 2004), with potentially significant implications for climate change (Cox et al., 2000). In addition, irregular fluctuations in the zooplankton abundance closely coupled to the behaviour of their planktonic prey, significantly affect the variability in the regenerated nutrient pool (Brussaard et al., 1996) and can pose important implications for fish stocks and higher trophic levels (Flinkman et al., 1998; Frederiksen et al., 2006). The coupling between phytoplankton and zooplankton can be almost instantaneous for microzooplankton or significantly delayed for macrozooplankton, depending on the generation timescales of grazers (Kiørboe, 1993). In the case of the latter size class, irregular fluctuations in

the phytoplankton abundance can pose important implications for different life stages and affect the survival abilities of the species. Variability in the abundance of primary producers is known to affect the egg production of female zooplanktoners (Corkett and McLaren, 1969; Kleppel, 1992; Hirche et al., 1997) and influence the timing and the magnitude of recruitment (Runge, 1985).

Model simulations described in this thesis are numerical investigations of population behaviour and it's sensitivity to externally-driven variability posed in the context of phytoplankton competing for inorganic nutrients. The findings can be applied to other communities, marine or terrestrial, whose functioning is controlled by the same principles, with appropriate modification of the vital rates and relative timescales of environmental disturbances. For example, generation timescale of bacterial population can be less than a quarter of a day (Becks et al., 2005). Therefore, depending on the rate of bacterial growth, it is likely that the environmental variability of weekly to monthly frequency would affect the bacterial community in a similar way seasonality controls phytoplankton with generation timescales of 3-5 days (Sommer, 1985; Reynolds et al., 1993).

Therefore, the main findings of the research presented in this thesis are:

1. In order to verify whether the irregular fluctuations in the microbial community occur due to stochastic processes or underlying chaotic behaviour, it is necessary to sample the ecosystem every 2-3 days for the minimum of 5 years.

2. Competition between species specializing in the utilization of different nutrients and with variable cellular stoichiometry can drive non-equilibrium behaviour, such as chaos and oscillations, where the ultimate competitor is not established.

3. Chaotic response of phytoplankton competing for nutrients under homogenous environmental conditions occurs in a large proportion of model solutions with randomly assigned species traits.

4. Seasonal variability in the nutrient supply acts to enhance the likelihood of chaos to occur and introduces temporal variability in the strength of the chaotic response, which is amplified during summer leading to reduced predictability then.

5. Stochastic weather events that amplify the nutrient supply to the upper ocean, act to enhance chaotic response; chaos can emerge due to the stochastic variability itself or the underling periodicity of the weather patterns.

6. Lateral exchange of species can sustain locally generated chaotic response only if weaker competitors are introduced, or when the stronger competitor is inhibited by higher grazing pressure, or when the stronger competitor is introduced at a sufficiently low concentration and it is not able to dominate over the locally-established community.

7. Chaos can be exported when the transported phytoplankton community exhibits a chaotic response and has a competitive advantage to displace the locally established community.

Bibliography

Abernathey, R., Marshall, J., Mazloff, M. and Shuckburgh, E. (2010), 'Enhancement of Mesoscale Eddy Stirring at Steering Levels in the Southern Ocean', *Journal of Physical Oceanography* **40**(1), 170–184.

Abraham, E. R. (1998), 'The generation of plankton patchiness by turbulent stirring', *Nature* **391**(6667), 577–580.

Achterberg, E. P., Moore, C. M., Henson, S. A., Steigenberger, S., Stohl, A., Eckhardt, S., Avendano, L. C., Cassidy, M., Hembury, D., Klar, J. K., Lucas, M. I., Macey, A. I., Marsay, C. M. and Ryan-Keogh, T. J. (2013), 'Natural iron fertilization by the Eyjafjallajökull volcanic eruption', *Geophysical Research Letters* **40**(5), 921–926.

Agawin, N., Duarte, C. M. and Agusti, S. (2000), 'Nutrient and temperature control of the contribution of picoplankton to phytoplankton biomass and production', *Limnology and Oceanography* **45**(3), 591–600.

Aksnes, D. L. and Egge, J. K. (1991), 'A Theoretical-Model for Nutrient-Uptake in Phytoplankton', *Marine Ecology-Progress Series* **70**(1), 65–72.

Allen, J. C., Schaffer, W. M. and Rosko, D. (1993), 'Chaos reduces species extinction by amplifying local population noise', *Nature* **364**(6434), 229–232.

Anderson, G. C. (1969), 'Subsurface chlorophyll maximum in the northeast Pacific Ocean ', *Limnology and Oceanography* **14**, 386–391.

Anderson, L. A. (1995), 'On the hydrogen and oxygen content of marine phytoplankton', *Deep Sea Research Part I* **42**(9), 1675–1680.

Armstrong, R. A. and McGehee, R. (1976), 'Coexistence of species competing for shared resources', *Theoretical Population Biology* **9**(3), 317–328.

Armstrong, R. A. and McGehee, R. (1980), 'Competitive Exclusion', *The American Naturalist* **115**(2), 151–170.

Arrigo, K. R. (2005), 'Marine microorganisms and global nutrient cycles', *Nature* **437**(7057), 349–355.

Arrigo, K. R., DiTullio, G. R., Dunbar, R. B., Robinson, D. H., VanWoert, M., Worthen, D. L. and Lizotte, M. P. (2000), 'Phytoplankton taxonomic variability in nutrient utilization and primary production in the Ross Sea', *Journal of Geophysical Research* **105**(C4), 8827.

Arrigo, K. R., Robinson, D. H., Worthen, D. L., Dunbar, R. B., DiTullio, G. R., VanWoert, M. and Lizotte, M. P. (1999), 'Phytoplankton Community Structure and the Drawdown of Nutrients and CO2 in the Southern Ocean', *Science* **283**(5400), 365–367.

Baker, A. R. (2003), 'Atmospheric deposition of nutrients to the Atlantic Ocean', *Geophysical Research Letters* **30**(24), 2296.

Baker, A. R., Weston, K., Kelly, S. D., Voss, M., Streu, P. and Cape, J. N. (2007), 'Dry and wet deposition of nutrients from the tropical Atlantic atmosphere: Links to primary productivity and nitrogen fixation', *Deep-Sea Research Part I-Oceanographic Research Papers* **54**(10), 1704–1720.

Barton, A. D., Dutkiewicz, S., Flierl, G., Bragg, J. and Follows, M. J. (2010), 'Patterns of Diversity in Marine Phytoplankton', *Science* **327**(5972), 1509–1511.

Barton, A. D., Lozier, M. S. and Williams, R. G. (2014), 'Physical controls of variability in North Atlantic phytoplankton', *Limnology and Oceanography* (submitted).

Becks, L. and Arndt, H. (2008), 'Transitions from stable equilibria to chaos, and back, in an experimental food web', *Ecology* **89**(11), 3222–3226.

Becks, L. and Arndt, H. (2013), 'Different types of synchrony in chaotic and cyclic communities', *Nature Communications* **4**, 1359–1368.

Becks, L., Hilker, F. M., Malchow, H., Jürgens, K. and Arndt, H. (2005), 'Experimental demonstration of chaos in a microbial food web', *Nature* **435**(7046), 1226–1229.

Benettin, G., Galgani, L. and Strelcyn, J.-M. (1976), 'Kolmogorov entropy and numerical experiments', *Physical Review A* **14**(6), 2338–2345.

Benincà, E., Huisman, J., Heerkloss, R., Jöhnk, K. D., Branco, P., Van Nes, E. H., Scheffer, M. and Ellner, S. P. (2008), 'Chaos in a long-term experiment with a plankton community', *Nature* **451**(7180), 822–825.

Benincà, E., Jöhnk, K. D., Heerkloss, R. and Huisman, J. (2009), 'Coupled predator-prey oscillations in a chaotic food web', *Ecology Letters* **12**(12), 1367–1378.

Berg, M. P., Kniese, J. P., Bedaux, J. J. M. and Verhoef, H. A. (1998), 'Dynamics and stratification of functional groups of micro- and mesoarthropods in the organic layer of a Scots pine forest', *Biology and Fertility of Soils* **26**(4), 268–284.

Berman-Frank, I., Cullen, J. T., Shaked, Y., Sherrell, R. M. and Falkowski, P. G. (2001), 'Iron availability, cellular iron quotas, and nitrogen fixation in Trichodesmium', *Limnology and Oceanography* **46**(6), 1249–1260.

Bertrand, E. M., Saito, M. A., Rose, J. M., Riesselman, C. R., Lohan, M. C., Noble, A. E., Lee, P. A. and DiTullio, G. R. (2007), 'Vitamin B12 and iron colimitation of

phytoplankton growth in the Ross Sea', *Limnology and Oceanography* **52**(3), 1079–1093.

Blain, S., Quéguiner, B., Armand, L., Belviso, S., Bombled, B., Bopp, L., Bowie, A., Brunet, C., Brussaard, C., Carlotti, F., Christaki, U., Corbière, A., Durand, I., Ebersbach, F., Fuda, J.-L., Garcia, N., Gerringa, L., Griffiths, B., Guigue, C., Guillerm, C., Jacquet, S., Jeandel, C., Laan, P., Lefèvre, D., Lo Monaco, C., Malits, A., Mosseri, J., Obernosterer, I., Park, Y.-H., Picheral, M., Pondaven, P., Remenyi, T., Sandroni, V., Sarthou, G., Savoye, N., Scouarnec, L., Souhaut, M., Thuiller, D., Timmermans, K., Trull, T., Uitz, J., van Beek, P., Veldhuis, M., Vincent, D., Viollier, E., Vong, L. and Wagener, T. (2007), 'Effect of natural iron fertilization on carbon sequestration in the Southern Ocean', *Nature* **446**(7139), 1070–1074.

Bopp, L., Aumont, O., Cadule, P., Alvain, S. and Gehlen, M. (2005), 'Response of diatoms distribution to global warming and potential implications: A global model study', *Geophysical Research Letters* **32**(19), L19606.

Bower, A. S. and Rossby, T. (1989), 'Evidence of Cross-Frontal Exchange Processes in the Gulf Stream Based on Isopycnal RAFOS Float Data', *Journal of Physical Oceanography* **19**(9), 1177–1190.

Boyd, P. W., Watson, A. J., Law, C. S., Abraham, E. R., Trull, T., Murdoch, R., Bakker, D. C. E., Bowie, A. R., Buesseler, K. O., Chang, H., Charette, M., Croot, P., Downing, K., Frew, R., Gall, M., Hadfield, M., Hall, J., Harvey, M., Jameson, G., LaRoche, J., Liddicoat, M., Ling, R., Maldonado, M. T., McKay, R. M., Nodder, S., Pickmere, S., Pridmore, R., Rintoul, S., Safi, K., Sutton, P., Strzepek, R., Tanneberger, K., Turner, S., Waite, A. and Zeldis, J. (2000), 'A mesoscale phytoplankton bloom in the polar Southern Ocean stimulated by iron fertilization', *Nature* **407**(6805), 695–702.

Bracco, A., Provenzale, A. and Scheuring, I. (2000), 'Mesoscale vortices and the

paradox of the plankton', *Proceedings of the Royal Society B: Biological Sciences* **267**(1454), 1795–1800.

Brown, J. H., Gillooly, J. F., Allen, A. P., Savage, V. M. and West, G. B. (2004), 'Toward a metabolic theory of ecology', *Ecology* **85**(7), 1771–1789.

Brussaard, C., Gast, G. J., Van Duyl, F. C. and Riegman, R. (1996), 'Impact of phytoplankton bloom magnitude on a pelagic microbial food web', *Marine Ecology-Progress Series* **144**, 211–221.

Cadotte, M. W. (2006), 'Dispersal and Species Diversity: A Meta-Analysis', *The American Naturalist* **167**(6), 913–924.

Calbet, A. and Landry, M. R. (2004), 'Phytoplankton growth, microzooplankton grazing, and carbon cycling in marine systems', *Limnology and Oceanography* **49**(1), 51–57.

Cardinale, B. J., Srivastava, D. S., Emmett Duffy, J., Wright, J. P., Downing, A. L., Sankaran, M. and Jouseau, C. (2006), 'Effects of biodiversity on the functioning of trophic groups and ecosystems', *Nature* **443**(7114), 989–992.

Cermeño, P., Rodríguez-Ramos, T., Dornelas, M., Figueiras, F. G., Marañón, E., Teixeira, I. G. and Vallina, S. G. (2013), 'Species richness in marine phytoplankton communities is not correlated to ecosystem productivity', *Marine Ecology-Progress Series* **488**, 1–9.

Chase, J. M., Abrams, P. A., Grover, J. P. and Diehl, S. (2002), 'The interaction between predation and competition: a review and synthesis', *Ecology* **5**, 302–315.

Clayton, S., Dutkiewicz, S., Jahn, O. and Follows, M. J. (2013), 'Dispersal, eddies, and the diversity of marine phytoplankton', *Limnology and Oceanography* **3**, 182–197.

Colijn, F. and Cadée, G. C. (2003), 'Is phytoplankton growth in the Wadden Sea light or nitrogen limited?', *Journal of Sea Research* **49**(2), 83–93.

Connell, J. H. (1978), 'Diversity in Tropical Rain Forests and Coral Reefs', *Science* **199**, 1302–1310.

Corkett, C. J. and McLaren, I. A. (1969), 'Egg production and oil storage by the copepod Pseudocalanus in the laboratory', *Journal of Experimental Marine Biology and Ecology* **3**(1), 90–105.

Costantino, R. F. (1997), 'Chaotic Dynamics in an Insect Population', *Science* **275**(5298), 389–391.

Cottingham, K. L. (1999), 'Nutrients and zooplankton as multiple stressors of phytoplankton communities: evidence from size structure', *Limnology and Oceanography* **44**, 810–827.

Cox, P. M., Betts, R. A., Jones, C. D., Spall, S. A. and Totterdell, I. J. (2000), 'Acceleration of global warming due to carbon-cycle feedbacks in a coupled climate model', *Nature* **408**(6809), 184–187.

Crutchfield, J. P., Farmer, J. D. and Huberman, B. A. (1982), 'Fluctuations and simple chaotic dynamics', *Physics Reports* **92**(2), 45–82.

Crutchfield, J. P. and Huberman, B. A. (1980), 'Fluctuations and the onset of chaos', *Physics Letters A* **77**(6), 407–410.

Cullen, J. J. and MacIntyre, J. G. (1998), Behavior, physiology and the niche of depth-regulating phytoplankton, *in* D. M. Anderson, A. D. Cembella and G. M. Hallegraeff, eds, 'Physiological Ecology of Harmful Algal Blooms', Springer-Verlag, Heidelberg.

Dakos, V., Beninca, E., van Nes, E. H., Philippart, C. J. M., Scheffer, M. and Huisman, J. (2009), 'Interannual variability in species composition explained as seasonally entrained chaos', *Proceedings of the Royal Society B: Biological Sciences* **276**(1669), 2871–2880.

de Baar, H. J. W., de Jong, J. T. M., Bakker, D. C. E., Löscher, B. M., Veth, C., Bathmann, U. and Smetacek, V. (1995), 'Importance of iron for plankton blooms and carbon dioxide drawdown in the Southern Ocean', *Nature* **373**(6513), 412–415.

Dennis, B., Desharnais, R. A., Cushing, J. M., Henson, S. M. and Costantino, R. F. (2003), 'Can noise induce chaos?', *Oikos* **102**(2), 329–339.

Descamps-Julien, B. and Gonzalez, A. (2005), 'Stable coexistance in a fluctuating environment: an experimental demonstration', *Ecology* **86**(10), 2815–2824.

Dickman, E. M., Newell, J. M., Gonzalez, M. J. and Vanni, M. J. (2008), 'Light, nutrients, and food-chain length constrain planktonic energy transfer efficiency across multiple trophic levels', *Proceedings of the National Academy of Sciences* **105**(47), 18408–18412.

Donk, E. and Kilham, S. S. (1990), 'Temperature effects on silicon- and phosphorus-limited growth and competitive interactionsamong three diatoms', *Journal of Phycology* **26**(1), 40–50.

Doveri, F., Scheffer, M., Rinaldi, S., Muratori, S. and Kuznetsov, Y. (1993), 'Seasonality and Chaos in a Plankton Fish Model', *Theoretical Population Biology* **43**(2), 159–183.

Droop, M. R. (1973), 'Some thoughts on nutrient limitation on algae', *Journal of Phycology* **9**(3), 264–272.

Ebenhöh, W. (1988), 'Coexistence of an unlimited number of algal species in a model system', *Theoretical Population Biology* **34**(2), 130–144.

Edwards, K. F., Thomas, M. K., Klausmeier, C. A. and Litchman, E. (2012), 'Allometric scaling and taxonomic variation in nutrient utilization traits and maximum growth rate of phytoplankton', *Limnology and Oceanography* **57**(2), 554–566.

Elliott, J. A., Irish, A. E. and Reynolds, C. S. (2001), 'The effects of vertical mixing on a phytoplankton community: a modelling approach to the intermediate disturbance hypothesis', *Freshwater Biology* **46**(10), 1291–1297.

Ellner, S. and Turchin, P. (1995), 'Chaos in a Noisy World: New Methods and Evidence from Time-Series Analysis', *American Naturalist* **145**(3), 343–375.

Eppley, R. W. (1972), 'Temperature and phytoplankton growth in the sea', *Fish Bull* **70**(4), 1063–1085.

Eppley, R. W. and Thomas, W. H. (1969), 'Comparison of half-saturation constants for growth and nitrate uptake of marine phytoplankton', *Journal of Phycology* **5**(4), 375–379.

Falkowski, P. G., Dubinsky, Z. and Wyman, K. (1985), 'Growth-irradiance relationships in phytoplankton.', *Limnology and Oceanography* **30**(2), 311–321.

Fasham, M. J. R., Sarmiento, J. L., Slater, R. D., Ducklow, H. W. and Williams, R. (1993), 'Ecosystem behavior at Bermuda Station "S" and ocean weather station "India": A general circulation model and observational analysis', *Global Biogeochemical Cycles* **7**(2), 379–415.

Fernández, A., Huang, S., Seston, S., Xing, J., Hickey, R., Criddle, C. and Tiedje, J. (1999), 'How Stable Is Stable? Function versus Community Composition', *Applied and Environmental Microbiology* pp. 3697–3704.

Field, C. B., Behrenfield, M. J., Randerson, J. T. and Falkowski, P. G. (1998), 'Primary Production of the Biosphere: Integrating Terrestrial and Oceanic Components', *Science* **281**(5374), 237–240.

Flinkman, J., Aro, E., Vuorinen, I. and Viitasalo, M. (1998), 'Changes in northern Baltic

zooplankton and herring nutrition from 1980s to 1990s: top-down and bottom-up processes at work', *Marine Ecology-Progress Series* **165**, 127–136.

Flöder, S. and Sommer, U. (1999), 'Diversity in planktonic communities: an experimental test of the intertmediate disturbance hypothesis', *Limnology and Oceanography* **44**(4), 1114–1119.

Follows, M. and Dutkiewicz, S. (2011), 'Modeling diverse communities of marine microbes', *Annual Review of Marine Science* **3**, 427–451.

Follows, M. J., Dutkiewicz, S., Grant, S. and Chisholm, S. W. (2007), 'Emergent Biogeography of Microbial Communities in a Model Ocean', *Science* **315**(5820), 1843–1846.

Fraser, A. I., Butterfield, D., Uncles, R., Johnes, P. and Harrod, T. R. (2000), 'Fal and Helford Special Areas of Conservation (cSAC) and the Tamar Estuaries complex cSAC/Special Protection Area (pSPA): estimation of diffuse and point-source nutrient inputs. ', *SSLRC report to the EA* .

Frederiksen, M., Edwards, M., Richardson, A. J., Halliday, N. C. and Wanless, S. (2006), 'From plankton to top predators: bottom-up control of a marine food web across four trophic levels', *Journal of Animal Ecology* **75**(6), 1259–1268.

Fussmann, G. F. and Heber, G. (2002), 'Food web complexity and chaotic population dynamics', *Ecology Letters* **5**, 394–401.

Gao, J. B., Chen, C. C., Hwang, S. K. and Liu, J. M. (1999), 'Noise-induced chaos', *International Journal of Modern Physics B* **13**(28), 3283–3305.

Gause, G. F. (1934), *The struggle for existence*, Williams and Wilkins, Baltimore.

Gemerden, H. (1974), 'Coexistence of organisms competing for the same substrate: An example among the purple sulfur bacteria', *Microbial Ecology* **1**(1), 104–119.

Gentleman, W., Leising, A., Frost, B., Strom, S. and Murray, J. (2003), 'Functional responses for zooplankton feeding on multiple resources: a review of assumptions and biological dynamics', *Deep Sea Research Part II: Topical Studies in Oceanography* **50**(22-26), 2847–2875.

Gilpin, M. E. (1979), 'Spiral Chaos in a Predator-Prey Model', *The American Naturalist* **113**(2), 306–308.

Gleason, H. A. (1917), 'The Structure and Development of the Plant Association', *Bulletin of the Torrey Botanical Club* **44**(10), 463–481.

Glover, H. E., Keller, M. D. and Spinrad, R. W. (1987), 'The effects of light quality and intensity on photosynthesis and growth of marine eukaryotic and prokaryotic phytoplankton clones', *Journal of Experimental Marine Biology and Ecology* **105**(2-3), 137–159.

Gobler, C. J., Norman, C., Panzeca, C., Taylor, G. T. and Sanudo-Wilhelmy, S. A. (2007), 'Effect of B-vitamins (B1, B12) and inorganic nutrients on algal bloom dynamics in a coastal ecosystem', *Aquatic Microbial Ecology* **49**, 181–194.

Goericke, R. (1998), 'Response of phytoplankton community structure and taxon-specific growth rates to seasonally varying physical forcing in the Sargasso Sea off Bermuda', *Limnology and Oceanography* **45**(5), 921–935.

Gonzalez-Andujar, J. L. and Perry, J. N. (1993), 'Chaos, metapopulations and dispersal', *Ecological Modelling* **65**(3-4), 255–263.

Göthlich, L. and Oschlies, A. (2012), 'Phytoplankton niche generation by interspecific stoichiometric variation', *Global Biogeochemical Cycles* **26**, GB2010.

Gottwald, G. A. and Melbourne, I. (2004), A new test for chaos in deterministic sys-

tems, *in* 'Proceedings: Mathematical, Physical and Engineering Sciences', pp. 603–611.

Gottwald, G. A. and Melbourne, I. (2009), 'On the Implementation of the 0–1 Test for Chaos', *SIAM Journal on Applied Dynamical Systems* **8**, 129–145.

Gower, J. F. R., Denman, K. L. and Holyer, R. J. (1980), 'Phytoplankton patchiness indicates the fluctuation spectrum of mesoscale oceanic structure', *Nature* **288**(5787), 157–159.

Graham, D. W., Knapp, C. W., Van Vleck, E. S., Bloor, K., Lane, T. B. and Graham, C. E. (2007), 'Experimental demonstration of chaotic instability in biological nitrification', *The ISME Journal* **1**(5), 385–393.

Grover, J. P. (1991), 'Resource Competition in a Variable Environment: Phytoplankton Growing According to the Variable-Internal-Stores Model', *American Naturalist* **138**(4), 811–835.

Guo, C., Liu, H., Zheng, L., Song, S., Chen, B. and Huang, B. (2014), 'Seasonal and spatial patterns of picophytoplankton growth, grazing and distribution in the East China Sea', *Biogeosciences* **11**(7), 1847–1862.

Habib, O. A., Tippett, R. and Murphy, K. J. (1997), 'Seasonal changes in phytoplankton community structure in relation to physico-chemical factors in Loch Lomond, Scotland', *Hydrobiologia* **350**(1/3), 63–79.

Hardin, G. (1960), 'The Competitive Exclusion Principle', *Science* **131**(3409), 1292–1297.

Harrison, W. G. and Li, W. (2007), 'Phytoplankton growth and regulation in the Labrador Sea: light and nutrient limitation', *Journal of Northwest Atlantic Fishery Science* **39**, 71–82.

Hassler, C. S., Sinoir, M., Clementson, L. A. and Butler, E. C. V. (2012), 'Exploring the Link between Micronutrients and Phytoplankton in the Southern Ocean during the 2007 Austral Summer', *Frontiers in Microbiology* **3**, 1–26.

Hastings, A. (1980), 'Disturbance, coexistence, history, and competition for space', *Theoretical Population Biology* **18**(3), 363–373.

Hastings, A. (1993), 'Complex Interactions Between Dispersal and Dynamics: Lessons From Coupled Logistic Equations', *Ecology* **74**(5), 1362.

Hastings, A., Hom, C. L., Ellner, S. and Turchin, P. (1993), 'Chaos in Ecology: Is Mother Nature a Strange Attractor?*', *Annual review of Ecological Systems* **24**, 1–33.

Hastings, A. and Powell, T. (1991), 'Chaos in a Three-Species Food Chain', *Ecology* **72**(3), 896–903.

Hegger, R., Kantz, H. and Schreiber, T. (1999), 'Practical implementation of nonlinear time series methods: The TISEAN package', *Chaos: An Interdisciplinary Journal of Nonlinear Science* **9**(2), 413–435.

Hein, M., Pedersen, M. F. and Sand-Jensen, K. (1995), 'Size-dependent nitrogen uptake in micro-and macroalgae', *Marine Ecology-Progress Series* **118**, 247–253.

Hickman, A. E., Dutkiewicz, S., Williams, R. G. and Follows, M. J. (2010), 'Modelling the effects of chromatic adaptation on phytoplankton community structure in the oligotrophic ocean', *Marine Ecology-Progress Series* **406**, 1–7.

Hirche, H. J., Meyer, U. and Niehoff, B. (1997), 'Egg production of Calanus finmarchicus : effect of temperature, food and season', *Marine Biology* **127**(4), 609–620.

Holm, N. P. and Armstrong, D. E. (1981), 'Role of nutrient limitation and competition in controlling the populations of Asterionella formosa and Microcystis aeruginosa in semicontinuous culture', *Limnology and Oceanography* **26**(4), 622–634.

Holt, R. D. and McPeek, M. A. (1996), 'Chaotic Population Dynamics Favors the Evolution of Dispersal', *The American Naturalist* **148**(4), 709–718.

Horn, H. S. and Arthur, R. H. M. (1972), 'Competition among Fugitive Species in a Harlequin Environment', *Ecology* **53**(4), 749–752.

Huisman, J., Johansson, A. M., Folmer, E. O. and Weissing, F. J. (2001), 'Towards a solution of the plankton paradox: the importance of physiology and life history', *Ecology Letters* **4**(5), 408–411.

Huisman, J., Pham Thi, N. N., Karl, D. M. and Sommeijer, B. (2006), 'Reduced mixing generates oscillations and chaos in the oceanic deep chlorophyll maximum', *Nature* **439**(7074), 322–325.

Huisman, J. and Weissing, F. J. (1999), 'Biodiversity of plankton by species oscillations and chaos', *Nature* **402**(6760), 407–410.

Huisman, J. and Weissing, F. J. (2001), 'Biological conditions for oscillations and chaos generated by multispecies competition', *Ecology* **82**(10), 2682–2695.

Hutchinson, G. E. (1961), 'The Paradox of the Plankton', *The American Journalist* **95**(882), 137–145.

Interlandi, S. and Kilham, S. S. (2001), 'Limiting resources and the regulation of diversity in phytoplankton communities', *Ecology* **82**(5), 1270–1282.

Iriarte, A. and Purdie, D. A. (1993), 'Photosynthesis and growth response of the oceanic picoplankter Pycnococcus provasolii Guillard (clone Ω48-23) (Chlorophyta) to variations in irradiance, photoperiod and temperature', *Journal of Experimental Marine Biology and Ecology* **168**(2), 239–257.

Irwin, A. J. and Oliver, M. J. (2009), 'Are ocean deserts getting larger?', *Geophysical Research Letters* **36**(18), L18609.

Jackson, G. A. (2001), 'Effect of coagulation on a model planktonic food web', *Deep-Sea Research Part I-Oceanographic Research Papers* **48**(1), 95–123.

Jackson, G. A., Waite, A. M. and Boyd, P. W. (2005), 'Role of algal aggregation in vertical carbon export during SOIREE and in other low biomass environments', *Geophysical Research Letters* **32**, L13607.

Jacquet, S., Partensky, F., Lennon, J. F. and Vaulot, D. (2001), 'Diel patterns of growth and division in marine picoplankton in culture', *Journal of Phycology* **37**(3), 357–369.

Jézéquel, V. M., Hildebrand, M. and Brzezinski, M. A. (2000), 'Silicon metabolism in diatoms: implications for growth', *Journal of Phycology* **36**, 821–840.

Kantz, H. (1994), 'A robust method to estimate the maximal Lyapunov exponent of a time series', *Physics Letters A* **185**(1), 77–87.

Kemp, W. M. and Mitsch, W. J. (1979), 'Turbulence and phytoplankton diversity: A general model of the "paradox of plankton"', *Ecological Modelling* **7**(3), 201–222.

Kiørboe, T. (1993), 'Turbulence, phytoplankton cell size, and the structure of pelagic food webs', *Advances in marine biology* **29**.

Kiørboe, T. (2011), 'How zooplankton feed: mechanisms, traits and trade-offs', *Biological reviews* **86**, 311–339.

Kiørboe, T., Saiz, E. and Viitasalo, M. (1996), 'Prey switching behaviour in the planktonic copepod *Acartia tonsa*', *Marine Ecology-Progress Series* **143**, 65–75.

Kleppel, G. S. (1992), 'Environmental regulation of feeding and egg production by Acartia tonsa off southern California', *Marine Biology* **112**(1), 57–65.

Koch, F., Marcoval, M. A., Panzeca, C., Bruland, K. W., udo Wilhelmy, S. A. S. and Go-

bler, C. J. (2011), 'The effect of vitamin B12 on phytoplankton growth and community structure in the Gulf of Alaska', *Limnology and Oceanography* **56**(3), 1023–1034.

Kooi, B. W., Boer, M. P. and Kooijman, S. A. L. M. (1997), 'Complex dynamic behaviour of autonomous microbial food chains', *Journal of Mathematical Biology* **36**(1), 24–40.

Kot, M., Sayler, G. and Schultz, T. (1992), 'Complex dynamics in a model microbial system', *Bulletin of Mathematical Biology* **54**(4), 619–648.

Lampert, W. (1989), 'The Adaptive Significance of Diel Vertical Migration of Zooplankton', *Functional Ecology* **3**(1), 21.

Landry, M. R., Haas, L. W. and Fagerness, V. L. (1984), 'Dynamics of microbial plankton communities: experiments in Kaneohe Bay, Hawaii', *Marine Ecology-Progress Series* **16**(1-2), 127–133.

Le Fèvre, J., Legendre, L. and Rivkin, R. B. (1998), 'Fluxes of biogenic carbon in the Southern Ocean: roles of large microphagous zooplankton', *Journal of Marine Systems* **17**, 325–345.

Letelier, R. M., Bidigare, R. R., Hebel, D. V., Ondrusek, M., Winn, C. D. and Karl, D. M. (1993), 'Temporal variability of phytoplankton community structure based on pigment analysis', *Limnology and Oceanography* **38**(7), 1420–1437.

Levin, S. A. (1974), 'Dispersion and population interactions', *American Naturalist* **108**(960), 207–228.

Levins, R. and Culver, D. (1971), 'Regional Coexistence of Species and Competition between Rare Species', *Proceedings of the National Academy of Sciences of the United States of America* **68**(6), 1246–1248.

Litchman, E. (1998), 'Population and community responses of phytoplankton to fluctuating light', *Oecologia* **117**(1-2), 247–257.

Litchman, E. and Klausmeier, C. A. (2008), 'Trait-Based Community Ecology of Phytoplankton', *Annual Review of Ecology and Systematics* **39**(1), 615–639.

Litchman, E., Klausmeier, C. A., Schofield, O. M. and Falkowski, P. G. (2007), 'The role of functional traits and trade-offs in structuring phytoplankton communities: scaling from cellular to ecosystem level', *Ecology Letters* **10**(12), 1170–1181.

Lomas, M. W. and Bates, N. R. (2004), 'Potential controls on interannual partitioning of organic carbon during the winter/spring phytoplankton bloom at the Bermuda Atlantic time-series study (BATS) site', *Deep-Sea Research Part I-Oceanographic Research Papers* **51**(11), 1619–1636.

Longhurst, A., Sathyendranath, S., Platt, T. and Caverhill, C. (1995), 'An estimate of global primary production in the ocean from satellite radiometer data', *Journal of Plankton Research* **17**(6), 1245–1271.

Loreau, M. and Mouquet, N. (1999), 'Immigration and the Maintenance of Local Species Diversity', *American Naturalist* **154**(4), 427–440.

Lorenz, E. N. (1963), 'Deterministic Nonperiodic Flow', *Journal of the Atmospheric Sciences* **20**, 130–141.

Lorenz, E. N. (1965), 'A study of the predictability of a 28-variable atmospheric model', *Tellus* **17**(3), 321–333.

MacArthur, R. (1970), 'Species packing and competitive equilibrium for many species', *Theoretical Population Biology* **1**, 1–11.

Mann, E. L. and Chisholm, S. W. (2000), 'Iron limits the cell division rate of Pro-

chlorococcus in the eastern equatorial Pacific', *Limnology and Oceanography* **45**(5), 1067–1076.

Marañón, E., Cermeño, P., López-Sandoval, D. C., Rodríguez-Ramos, T., Sobrino, C., Huete-Ortega, M., Blanco, J. M. and Rodríguez, J. (2013), 'Unimodal size scaling of phytoplankton growth and the size dependence of nutrient uptake and use', *Ecology Letters* **16**(3), 371–379.

Margalef, R. (1978), 'Life-forms of phytoplankton as survival alternatives in an unstable environment', *Oceanologica acta* **1**(4), 493–509.

Mariani, P., Andersen, K. H., Visser, A. W., Barton, A. D. and Kiørboe, T. (2013), 'Control of plankton seasonal succession by adaptive grazing', *Limnology and Oceanography* **58**(1), 173–184.

Marinov, I., Gnanadesikan, A., Toggweiler, J. R. and Sarmiento, J. L. (2006), 'The Southern Ocean biogeochemical divide', *Nature* **441**(7096), 964–967.

Marshall, J., Shuckburgh, E., Jones, H. and Hill, C. (2006), 'Estimates and Implications of Surface Eddy Diffusivity in the Southern Ocean Derived from Tracer Transport', *Journal of Physical Oceanography* **36**(9), 1806–1821.

Martin, A. P. (2003), 'Phytoplankton patchiness: the role of lateral stirring and mixing', *Progress in Oceanography* **57**, 125–174.

Martin, E. S., Irigoien, X., Harris, R. P., Lopez-Urrutia, A., Zubkov, M. V. and Heywood, J. L. (2006), 'Variation in the transfer of energy in marine plankton along a productivity gradient in the Atlantic Ocean', *Limnology and Oceanography* **51**(5), 2084–2091.

Martin, J. H. (1990), 'Glacial-interglacial CO 2 change: The Iron Hypothesis', *Paleoceanography* **5**(1), 1–13.

Mather, R. L., Reynolds, S. E., Wolff, G. A., Williams, R. G., Torres-Valdes, S., Woodward, E. M. S., Landolfi, A., Pan, X., Sanders, R. and Achterberg, E. P. (2008), 'Phosphorus cycling in the North and South Atlantic Ocean subtropical gyres', *Nature Geoscience* **1**(7), 439–443.

May, R. M. (1972), 'Limit Cycles in Predator-Prey Communities', *Science* **177**(4052), 900–902.

May, R. M. (1974), 'Biological populations with nonoverlapping generations: stable points, stable cycles, and chaos', *Science* **186**(4164), 645–647.

May, R. M. (1976), 'Simple mathematical models with very complicated dynamics', *Nature* **261**, 459–466.

May, R. M. and Leonard, W. J. (1975), 'Nonlinear Aspects of Competition Between Three Species', *SIAM Journal on Applied Mathematics* **29**(2), 243–253.

May, R. M. and Oster, G. F. (1976), 'Bifurcations and Dynamic Complexity in Simple Ecological Models', *American Naturalist* **110**(974), 573–599.

Mazumder, A. (1994), 'Phosphorus-Chlorophyll Relationships under Contrasting Herbivory and Thermal Stratification: Predictions and Patterns', *Canadian Journal of Fisheries and Aquatic Sciences* **51**(2), 390–400.

McCann, K., Hastings, A. and Huxel, G. R. (1998), 'Weak trophic interactions and the balance of nature', *Nature* **395**(6704), 794–798.

McCauley, E. and Murdoch, W. W. (1987), 'Cyclic and Stable Populations: Plankton as Paradigm', *American Naturalist* **129**(1), 97–121.

McGrady-Steed, J., Harris, P. M. and Morin, P. J. (1997), 'Biodiversity regulates ecosystem predictability', *Nature* **390**(6656), 162–165.

Medvinsky, A. B., Petrovskii, S. V., Tikhonov, D. A., Tikhonova, I. A., Ivanitsky, G. R., Venturino, E. and Malchow, H. (2001), 'Biological factors underlying regularity and chaos in aquatic ecosystems: Simple models of complex dynamics', *Journal of Biosciences* **26**(1), 77–108.

Michaels, A. F. and Silver, M. W. (1988), 'Primary production, sinking fluxes and the microbial food web', *Deep-Sea Research Part I-Oceanographic Research Papers* **35**(4), 473–490.

Moore, C. M., Goericke, R. and Chisholm, S. W. (1995), 'Comparative Physiology of Synechococcus and Prochlorococcus - Influence of Light and Temperature on Growth, Pigments, Fluorescence and Absorptive Properties', *Marine Ecology-Progress Series* **116**, 259–275.

Moore, C. M., Mills, M. M., Arrigo, K. R., Berman-Frank, I., Bopp, L., Boyd, P. W., Galbraith, E. D., Geider, R. J., Guieu, C., Jaccard, S. L., Jickells, T. D., La Roche, J., Lenton, T. M., Mahowald, N. M., Marañón, E., Marinov, I., Moore, J. K., Nakatsuka, T., Oschlies, A., Saito, M. A., Thingstad, T. F., Tsuda, A. and Ulloa, O. (2013), 'Processes and patterns of oceanic nutrient limitation', *Nature Geoscience* **6**(9), 701–710.

Morán, X., Urrutia, Á. L., Calvo-Diaz, A. and Li, W. (2010), 'Increasing importance of small phytoplankton in a warmer ocean', *Global Change Biology* **16**(3), 1137–1144.

Morel, F. M. M. and Price, N. M. (2003), 'The Biogeochemical Cycles of Trace Metals in the Oceans', *Science* **300**(5621), 944–947.

Mouquet, N. and Loreau, M. (2002), 'Coexistence in Metacommunities: The Regional Similarity Hypothesis', *American Naturalist* **159**(4), 420–426.

Mouquet, N. and Loreau, M. (2003), 'Community Patterns in Source-Sink Metacommunities', *American Naturalist* **162**(5), 544–557.

Nuccio, C., Melillo, C., Massi, L. and Innamorati, M. (2003), 'Phytoplankton abundance, community structure and diversity in the eutrophicated Orbetello lagoon (Tuscany) from 1995 to 2001', *Oceanologica acta* **26**(1), 15–25.

Padisák, J. (1994), 'Identification of relevant time-scales in non-equilibrium community dynamics: conclusions from phytoplankton surveys', *New Zealand Journal of Ecology* **18**(2), 169–176.

Pahlow, M. and Riebesell, U. (2000), 'Temporal Trends in Deep Ocean Redfield Ratios', *Science* **287**(5454), 831–833.

Paine, R. T. (1966), 'Food Web Complexity and Species Diversity', *American Naturalist* **100**(910), 65–75.

Palastanga, V., Van Leeuwen, P. J. and de Ruijter, W. P. M. (2006), 'A link between low-frequency mesoscale eddy variability around Madagascar and the large-scale Indian Ocean variability', *Journal of Geophysical Research* **111**, C09029.

Panzeca, C., Beck, A. J., Tovar-Sanchez, A., Segovia-Zavala, J., Taylor, G. T., Gobler, C. J. and Sañudo-Wilhelmy, S. A. (2009), 'Distributions of dissolved vitamin B12 and Co in coastal and open-ocean environments', *Estuarine, Coastal and Shelf Science* **85**(2), 223–230.

Petersen, R. (1975), 'The Paradox of the Plankton: An Equilibrium Hypothesis', *American Naturalist* **109**(965), 35–49.

Philippart, C., Cadée, G. C., van Raaphorst, W. and Riegman, R. (2000), 'Long-term phytoplankton-nutrient interactions in a shallow coastal sea: algal community struc-

ture, nutrient budgets, and denitrification potential', *Limnology and Oceanography* **45**(1), 131–144.

Phillips, O. M. (1978), 'The Equilibrium and Stability of Simple Marine Biological Systems. III. Fluctuations and Survival', *American Naturalist* **112**, 745–757.

Popova, E. E., Fasham, M. J. R., Osipov, A. V. and Ryabchenko, V. A. (1997), 'Chaotic behaviour of an ocean ecosystem model under seasonal external forcing', *Journal of Plankton Research* **19**(10), 1495–1515.

Price, P. W., Bouton, C. E., Gross, P., McPheron, B. A., Thompson, J. N. and Weis, A. E. (1980), 'Interactions Among Three Trophic Levels: Influence of Plants on Interactions Between Insect Herbivores and Natural Enemies', *Annual Review of Ecology and Systematics* **11**, 41–65.

Prowe, A. E. F., Pahlow, M., Dutkiewicz, S., Follows, M. and Oschlies, A. (2012), 'Top-down control of marine phytoplankton diversity in a global ecosystem model', *Progress in Oceanography* **101**(1), 1–13.

Ptacnik, R., Solimini, A. G., Andersen, T., Tamminen, T., Brettum, P., Lepisto, L., Willen, E. and Rekolainen, S. (2008), 'Diversity predicts stability and resource use efficiency in natural phytoplankton communities', *Proceedings of the National Academy of Sciences* **105**(13), 5134–5138.

Raven, J. A. and Falkowski, P. G. (1999), 'Oceanic sinks for atmospheric CO2', *Plant, Cell and Environment* **22**(6), 741–755.

Reckermann, M. and Veldhuis, M. (1997), 'Trophic interactions between picophytoplankton and micro-and nanozooplankton in the western Arabian Sea during the NE monsoon 1993', *Aquatic Microbial Ecology* **12**, 263–273.

Reynolds, C. (1995), 'The intermediate disturbance hypothesis and its applicability to planktonic communities: comments on the views of Padisák and Wilson', *New Zealand Journal of Ecology* **19**(2), 219–225.

Reynolds, C. S. (1984), 'Phytoplankton periodicity: the interactions of form, function and environmental variability', *Freshwater Biology* **14**(2), 111–142.

Reynolds, C. S. (1993), *Intermediate Disturbance Hypothesis in Phytoplankton Ecology*, Springer Netherlands, Dordrecht.

Reynolds, C. S., Padisák, J. and Sommer, U. (1993), 'Intermediate disturbance in the ecology of phytoplankton and the maintenance of species diversity: a synthesis', *Hydrobiologia* **249**(1-3), 183–188.

Rhee, G. and Gotham, I. (1981), 'The Effect of Environmental Factors on Phytoplankton Growth: Temperature and the Interactions of Temperature with Nutrient Limitation', *Limnology and Oceanography* **26**(4), 635–648.

Richardson, T. L., Gibson, C. E. and Heaney, S. I. (2000), 'Temperature, growth and seasonal succession of phytoplankton in Lake Baikal, Siberia', *Freshwater Biology* **44**(3), 431–440.

Richardson, T. L. and Jackson, G. A. (2007), 'Small Phytoplankton and Carbon Export from the Surface Ocean', *Science* **315**(5813), 838–840.

Richerson, P., Armstrong, R. and Goldman, C. R. (1970), 'Contemporaneous Disequilibrium, a New Hypothesis to Explain the "Paradox of the Plankton"', *Proceedings of the National Academy of Sciences* **67**(4), 1710–1714.

Riegman, R., Kuipers, B. R., Noordeloos, A. A. M. and Witte, H. J. (1993), 'Size-differential control of phytoplankton and the structure of plankton communities', *Netherlands Journal of Sea Research* **31**(3), 255–265.

Rinaldi, S. and Muratori, S. (1993), 'Conditioned chaos in seasonally perturbed predator-prey models', *Ecological Modelling* **69**, 79–97.

Rinaldi, S. and Solidoro, C. (1998), 'Chaos and Peak-to-Peak Dynamics in a Plankton–Fish Model', *Theoretical Population Biology* **54**(1), 62–77.

Ringelberg, J. (1977), 'Properties of an aquatic micro-ecosystem', *Helgoländer Wissenschaftliche Meeresuntersuchungen* **30**(1-4), 134–143.

Rosenstein, M. T., Collins, J. J. and De Luca, C. J. (1993), 'A practical method for calculating largest Lyapunov exponents from small data sets', *Physica D: Nonlinear Phenomena* **65**(1-2), 117–134.

Rosenzweig, M. L. (1971), 'Paradox of enrichment: destabilization of exploitation ecosystems in ecological time', *Science* **171**(3969), 385–387.

Rudnick, D. L. and Davis, R. E. (2003), 'Red noise and regime shifts', *Deep Sea Research Part I* **50**, 691–699.

Runge, J. A. (1985), 'Relationship of egg production of Calanus pacificus to seasonal changes in phytoplankton availability in Puget Sound, Washington.', *Limnology and Oceanography* **30**, 382–396.

Ruxton, G. D. (1994), 'Low Levels of Immigration between Chaotic Populations can Reduce System Extinctions by Inducing Asynchronous Regular Cycles', *Proceedings of the Royal Society B: Biological Sciences* **256**(1346), 189–193.

Sabin, G. and Summers, D. (1993), 'Chaos in a periodically forced predator-prey ecosystem model', *Mathematical Biosciences* **113**, 91–113.

Saito, M. A., Moffett, J. W., Chisholm, S. W. and Waterbury, J. B. (2002), 'Cobalt limitation and uptake in Prochlorococcus', *Limnology and Oceanography* **47**(7), 1629–1636.

Saiz, E. and Kiørboe, T. (1995), 'Predatory and suspension feeding of the copepod *Acartia tonsa* in turbulent environments', *Marine Ecology-Progress Series* **122**, 147–158.

Sarmiento, J. L., Slater, R., Barber, R., Bopp, L., Doney, S. C., Hirst, A. C., Kleypas, J., Matear, R., Mikolajewicz, U., Monfray, P., Soldatov, V., Spall, S. A. and Stouffer, R. (2004), 'Response of ocean ecosystems to climate warming ', *Global Biogeochemical Cycles* **18**(3), GB3003.

Schaffer, W. (1985), 'Order and Chaos in Ecological Systems', *Ecology* **66**(1), 93–106.

Scheffer, M., Rinaldi, S., Huisman, J. and Weissing, F. J. (2003), 'Why plankton communities have no equilibrium: solutions to the paradox', *Hydrobiologia* **491**(1-3), 9–18.

Schippers, P., Verschoor, A. M., Vos, M. and Mooij, W. M. (2001), 'Does "supersaturated coexistence" resolve the "paradox of the plankton"?', *Ecology Letters* **4**, 404–407.

Schouten, M. W., de Ruijter, W. P. M., van Leeuwen, P. J. and Ridderinkhof, H. (2003), 'Eddies and variability in the Mozambique Channel', *Deep Sea Research Part II: Topical Studies in Oceanography* **50**(12-13), 1987–2003.

Sharples, J., Moore, C. M., Hickman, A. E., Holligan, P. M., Tweddle, J. F., Palmer, M. R. and Simpson, J. H. (2009), 'Internal tidal mixing as a control on continental margin ecosystems', *Geophysical Research Letters* **36**(23), L23603.

Sharples, J., Tweddle, J. F., Green, J. A. M., Palmer, M. R., Kim, Y.-N., Hickman, A. E., Holligan, P. M., Moore, C. M., Rippeth, T. P. and Simpson, J. H. (2007), 'Spring-neap modulation of internal tide mixing and vertical nitrate fluxes at a shelf edge in summer', *Limnology and Oceanography* **52**(5), 1735–1747.

Shmida, A. and Ellner, S. (1985), Coexistence of plant species with similar niches, *in* 'Plant community ecology: Papers in honor of Robert H. Whittaker', Springer Netherlands, Dordrecht, pp. 275–301.

Sinoir, M., Butler, E. C. V., Bowie, A. R., Mongin, M., Nesterenko, P. N. and Hassler, C. S. (2012), 'Zinc marine biogeochemistry in seawater: a review', *Marine and Freshwater Research* **63**(7), 644–657.

Smale, S. (1976), 'On the differential equations of species in competition', *Journal of Mathematical Biology* **3**(1), 5–7.

Smayda, T. (1998), 'Patterns of variability characterizing marine phytoplankton, with examples from Narragansett Bay', *ICES Journal of Marine Science* **55**(4), 562–573.

Smith, C. L., Richards, K. J. and Fasham, M. J. R. (1996), 'The impact of meso-scale eddies on plankton dynamics in the upper ocean', *Deep-Sea Research Part I-Oceanographic Research Papers* **43**(11-12), 1807–1832.

Sommer, U. (1985), 'Comparison Between Steady State and Non-Steady State Competition: Experiments with Natural Phytoplankton', *Limnology and Oceanography* **30**(2), 335–346.

Sommer, U. (1986), 'Nitrate- and silicate-competition among antarctic phytoplankton', *Marine Biology* **91**, 345–351.

Sommer, U. (1993), 'Disturbance-diversity relationships in two lakes of similar nutrient chemistry but contrasting disturbance regimes', *Hydrobiologia* **249**(1-3), 59–65.

Sommer, U. (1995), 'An experimental test of the intermediate disturbance hypothesis using cultures of marine phytoplankton', *Limnology and Oceanography* **40**(7), 1271–1277.

Stolte, W. and Riegman, R. (1995), 'Effect of phytoplankton cell size on transient-state nitrate and ammonium uptake kinetics', *Microbiology* **141**(5), 1221–1229.

Stomp, M., Huisman, J., Mittelbach, G. G., Litchman, E. and Klausmeier, C. A. (2011), 'Large-scale biodiversity patterns in freshwater phytoplankton', *Ecology* **92**(11), 2096–2107.

Stone, L., Landan, G. and May, R. M. (1996), 'Detecting Time's Arrow: A Method for Identifying Nonlinearity and Deterministic Chaos in Time-Series Data', *Proceedings of the Royal Society B: Biological Sciences* **263**(1376), 1509–1513.

Strass, V. H. (1992), 'Chlorophyll patchiness caused by mesoscale upwelling at fronts', *Deep Sea Research Part A. Oceanographic Research Papers* **39**(1), 75–96.

Strom, S. L. and Welschmeyer, N. A. (1991), 'Pigment-specific rates of phytoplankton growth and microzooplankton grazing in the open subarctic Pacific Ocean.', *Limnology and Oceanography* **36**(1), 50–63.

Sugihara, G. and May, R. M. (1990), 'Nonlinear forecasting as a way of distinguishing chaos from measurement error in time series.', *Nature* **344**, 734–741.

Sweeney, C., Smith, W. O., Hales, B., Bidigare, R. R., Carlson, C. A., Codispoti, L. A., Gordon, L. I., Hansell, D. A., Millero, F. J., Park, M.-O. and Takahashi, T. (2000), 'Nutrient and carbon removal ratios and fluxes in the Ross Sea, Antarctica', *Deep Sea Research Part II: Topical Studies in Oceanography* **47**(15-16), 3395–3421.

Szendro, P., Vincze, G. and Szasz, A. (2001), 'Pink-noise behaviour of biosystems', *European Biophysics Journal* **30**(3), 227–231.

Talling, J. F. (1993), 'Comparative seasonal changes, and inter-annual variability and stability, in a 26-year record of total phytoplankton biomass in four English lake basins', *Hydrobiologia* **268**(2), 65–98.

Tancredi, G., Sánchez, A. and Roig, F. (2001), 'A Comparison between Methods to Compute Lyapunov Exponents', *The Astronomical Journal* **121**, 1171–1179.

Therriault, J.-C. and Platt, T. (1981), 'Environmental Control of Phytoplankton Patchiness', *Canadian Journal of Fisheries and Aquatic Sciences* **38**(6), 638–641.

Thomas, M. K., Kremer, C. T., Klausmeier, C. A. and Litchman, E. (2012), 'A Global Pattern of Thermal Adaptation in Marine Phytoplankton', *Science* **338**, 1085–1088.

Tikhonov, D. A., Enderlein, J., Malchow, H. and Medvinsky, A. B. (2001), 'Chaos and fractals in fish school motion', *Chaos, Solitons & Fractals* **12**(2), 277–288.

Tilman, D. (1977), 'Resource Competition between Plankton Algae: An Experimental and Theoretical Approach', *Ecology* **58**(2), 338–348.

Tilman, D. (1980), 'Resources: A Graphical-Mechanistic Approach to Competition and Predation', *American Naturalist* **116**(3), 362–393.

Tilman, D. (1994), 'Competition and Biodiversity in Spatially Structured Habitats', *Ecology* **75**(1), 2–16.

Tilman, D. (1999), 'The ecological consequences of changes in biodiversity: a search for general principles', *Ecology* **80**(5), 1455–1474.

Tilman, D., Kilham, S. S. and Kilham, P. (1982), 'Phytoplankton Community Ecology: The Role of Limiting Nutrients', *Annual Review of Ecology and Systematics* **13**, 349–372.

Tilman, D., Lehman, C. L. and Thomson, K. T. (1997), 'Plant diversity and ecosystem productivity: Theoretical considerations', *Proceedings of the National Academy of Sciences* **94**(5), 1857–1861.

Tilman, D., Wedin, D. and Knops, J. (1996), 'Productivity and sustainability influenced by biodiversity in grassland ecosystems', *Nature* **379**, 718–720.

Timmer, J. and König, M. (1995), 'On generating power law noise', *Astronomy and Astrophysics* **300**, 707–710.

Timms, R. M. and Moss, B. (1984), 'Prevention of growth of potentially dense phytoplankton populations by zooplankton grazing, in the presence of zooplanktivorous fish, in a shallow wetland ecosystem', *Limnology and Oceanography* **29**(3), 472–486.

Turchin, P. (1993), 'Chaos and Stability in Rodent Population Dynamics: Evidence from Non-Linear Time-Series Analysis', *Oikos* **68**(1), 167–172.

Turchin, P. and Taylor, A. D. (1992), 'Complex Dynamics in Ecological Time Series', *Ecology* **73**(1), 289–305.

Tyrrell, T. (1999), 'The relative influences of nitrogen and phosphorus on oceanic primary production', *Nature* **400**(6744), 525–531.

Vandermeer, J. (1993), 'Loose coupling of predator-prey cycles: entrainment, chaos, and intermittency in the classic MacArthur consumer-resource equations', *American Naturalist* **141**(5), 687–716.

Vandermeer, J. (2004), 'Coupled Oscillations in Food Webs: Balancing Competition and Mutualism in Simple Ecological Models', *American Naturalist* **163**(6), 857–867.

Vaulot, D., Marie, D., Olson, R. J. and Chisholm, S. W. (1995), 'Growth of Prochlorococcus, a Photosynthetic Prokaryote, in the Equatorial Pacific Ocean', *Science* **268**(5216), 1480–1482.

Vayenas, D. V. and Pavlou, S. (1999), 'Chaotic dynamics of a food web in a chemostat', *Mathematical Biosciences* **162**, 69–84.

Veldhuis, M., Timmermans, K. R., Croot, P. and van der Wagt, B. (2005), 'Picophytoplankton; a comparative study of their biochemical composition and photosynthetic properties', *Journal of Sea Research* **53**, 7–24.

Verdy, A., Follows, M. and Flierl, G. (2009), 'Optimal phytoplankton cell size in an allometric model', *Marine Ecology-Progress Series* **379**, 1–12.

Visbeck, M., Marshall, J., Haine, T. and Spall, M. (1997), 'Specification of Eddy Transfer Coefficients in Coarse-Resolution Ocean Circulation Models', *Journal of Physical Oceanography* **27**(3), 381–402.

Visser, A. W. and Fiksen, Ø. (2013), 'Optimal foraging in marine ecosystem models: selectivity, profitability and switching', *Marine Ecology-Progress Series* **473**, 91–101.

Visser, A. W., Saito, H., Saiz, E. and Kiørboe, T. (2001), 'Observations of copepod feeding and vertical distribution under natural turbulent conditions in the North Sea', *Marine Biology* **138**(5), 1011–1019.

Ward, B. A., Dutkiewicz, S. and Follows, M. J. (2013), 'Modelling spatial and temporal patterns in size-structured marine plankton communities: top–down and bottom–up controls', *Journal of Plankton Research* **36**(1), 31–47.

Ward, B. A., Dutkiewicz, S., Jahn, O. and Follows, M. (2012), 'A size-structured food-web model for the global ocean', *Limnology and Oceanography* **57**(6), 1877–1891.

Weithoff, G., Walz, N. and Gaedke, U. (2001), 'The intermediate disturbance hypothesis-species diversity or functional diversity?', *Journal of Plankton Research* **23**(10), 1147–1155.

Williams, R. G. and Follows, M. J. (2003), Physical Transport of Nutrients and the Maintenance of Biological Production, *in* M. J. Fasham, ed., 'Ocean Biogeochemistry', Springer Berlin Heidelberg, Berlin, Heidelberg, pp. 19–51.

Williams, R. G. and Follows, M. J. (2011), *Ocean Dynamics and the Carbon Cycle: Principles and Mechanisms*, Cambridge University Press.

Wolf, A., Swift, J. B., Swinney, H. L. and Vastano, J. A. (1985), 'Determining Lyapunov exponents from a time series', *Physica D: Nonlinear Phenomena* **16**(3), 285–317.

Worm, B., Barbier, E. B., Beaumont, N., Duffy, J. E., Folke, C., Halpern, B. S., Jackson, J. B. C., Lotze, H. K., Micheli, F., Palumbi, S. R., Sala, E., Selkoe, K. A., Stachowicz, J. J. and Watson, R. (2006), 'Impacts of Biodiversity Loss on Ocean Ecosystem Services', *Science* **314**(5800), 787–790.

Yachi, S. and Loreau, M. (1999), 'Biodiversity and ecosystem productivity in a fluctuating environment: The insurance hypothesis', *Proceedings of the National Academy of Sciences* **96**(4), 1463–1468.

Zaret, T. M. and Suffern, J. S. (1976), 'Vertical migration in zooplankton as a predator avoidance mechanism', *Limnology and Oceanography* **21**(6), 804–813.